ҚАЗАҚСТАН РЕСПУБЛИКАСЫ
ҒЫЛЫМ ЖӘНЕ ЖОҒАРЫ БІЛІМ МИНИСТРЛІГІ

SATBAYEV UNIVERSITY
МЕТАЛЛУРГИЯ ЖӘНЕ КЕН БАЙЫТУ ИНСТИТУТЫ

ISSN 2616-6445 (Online)
ISSN 2224-5243 (Print)
DOI 10.31643/2018/166445

Минералдық шикізаттарды кешенді пайдалану

4 (327)

Комплексное Использование Минерального Сырья

Complex Use of Mineral Resources

ҚАЗАН-ЖЕЛТОҚСАН 2023
OCTOBER DECEMBER 2023
ОКТЯБРЬ-ДЕКАБРЬ 2023

ЖЫЛЫНА 4 РЕТ ШЫҒАДЫ
QUARTERLY JOURNAL
ВЫХОДИТ 4 РАЗА В ГОД

ЖУРНАЛ 1978 ЖЫЛДАН БАСТАП ШЫҒАДЫ
JOURNAL HAS BEEN PUBLISHING SINCE 1978
ЖУРНАЛ ИЗДАЕТСЯ С 1978 ГОДА

АЛМАТЫ - 2023

Редакция мекен жайы:
Металлургия және кен байыту институты
050010, Қазақстан Республикасы, Алматы қ., Шевченко к-сі, Уәлиханов к-нің қиылысы, 29/133,
Fax. +7 (727) 298-45-03, Tel. +7-(727) 298-45-02, +7 (727) 298-45-19
E mail: journal@kims-imio.kz, product-service@kims-imio.kz
http://kims-imio.com/index.php/main

«Минералдық шикізаттарды кешенді пайдалану» журналы ғылыми жұмыстардың негізгі нәтижелерін жариялау үшін Қазақстан Республикасы Білім және ғылым министірлігінің Білім және ғылым сапасын қамтамасыз ету комитеті ұсынған ғылыми басылымдар тізіміне енгізілген.
Меншік иесі: «Металлургия және кен байыту институты» АҚ

Журнал Қазақстан Республикасының Ақпарат және коммуникация министрлігінің Байланыс, ақпараттандыру және бұқаралық ақпарат құралдары саласындағы мемлекеттік бақылау комитетінде қайта тіркелген

2016 ж. 18 қазандағы № 16180-Ж Куәлігі

Address:
Institute of Metallurgy and Ore Beneficiation
29/133 Shevchenko Street, corner of Ch. Valikhanov Street, Almaty, 050010, Kazakhstan
Fax. +7 (727) 298-45-03, Tel. +7-(727) 298-45-02, +7 (727) 298-45-19
E mail: journal@kims-imio.kz, product-service@kims-imio.kz
http://kims-imio.com/index.php/main

The Journal "Complex Use of Mineral Resources" is included in the List of publications recommended by the Committee for Control in the Sphere of Education and Science of the Ministry of Education and Science of the Republic of Kazakhstan for the publication of the main results of scientific activities.
Owner: "Institute of Metallurgy and Ore Beneficiation" JSC

The Journal was re-registered by the Committee for State Control in the Sphere of Communication, Information and Mass Media of the Ministry of Information and Communication of the Republic of Kazakhstan.

Certificate № 16180-Ж since October 18, 2016

Адрес редакции:
Институт Металлургии и Обогащения
050010, Республика Казахстан, г. Алматы, ул. Шевченко, уг. ул. Валиханова, 29/133,
Fax. +7 (727) 298-45-03, Tel. +7 (727) 298-45-02, +7 (727) 298-45-19
E mail: journal@kims-imio.kz, product-service@kims-imio.kz
http://kims-imio.com/index.php/main

Журнал «Комплексное использование минерального сырья» включен в Перечень изданий, рекомендуемых Комитетом по контролю в сфере образования и науки Министерства образования и науки Республики Казахстан для публикации основных результатов научной деятельности.
Собственник: АО «Институт металлургии и обогащения»

Журнал перерегистрирован в Комитете государственного контроля в области связи, информатизации и средств массовой информации
Министерства информации и коммуникации Республики Казахстан
Свидетельство № 16180-Ж от 18 октября 2016 г.

Crossref
DOI: 10.31643/2023/6445.34
Engineering and technology

Effect of a complex modified additive based on post-alcohol bard on the strength behavior of concrete

[1]Altynbekova A.D., [1]Lukpanov R.E., [1] Dyussembinov D.S., [1]Askerbekova A.M., [2]Gunasekaran Murali

[1] L.N. Gumilyov Eurasian National University, Astana, Kazakhstan
[2] Division of Research & Innovation, Uttaranchal University, Dehradun 248007, India

[*]Corresponding author email: kleo-14@mail.ru

Received: *September 13, 2022*
Peer-reviewed: *November 14, 2022*
Accepted: *January 30, 2023*

ABSTRACT

The article presents the third stage of the study results of a complex modified additive (CMA), in the accuracy of the influence of the variable ingredients of CMA on the strength of cement. This article shows the methodology of making samples, the selection of additive composition at different percentages of components, and the analysis of the strength behavior of the obtained results. To evaluate the changes in strength, samples were made and tested in compression and bending at 7, 14, and 28 days of normal-moist hardening. The results of the experiment showed that the addition of plasticizers (PAB) reduces the quantity of water - 35%, by increasing the strength of concrete by 20%. Compressive and bending strength results of the modified samples showed the best results, which were in the range of 42.80-63.66 MPa and 3.34-8.75 MPa, compared with the control composition. From the results of the research, the additive accelerates hardening and it was found that the additive contributes to the growth of strength, both at an early age and at the design age (28 days). The results of the experiment showed that from the standpoint of improving the qualitative characteristics of the samples, the use of plasticizers is appropriate. The use of CMA in the composition of concrete increases the strength, and therefore developed by the authors of CMA changes the structure of concrete and most importantly, increases the physical and mechanical characteristics of concrete.

Keywords: concrete, cement-sand mortar, complex modified additive, post-alcohol bard, plasticizer, hardening accelerator, bending strength, compressive strength.

	Information about authors:
Altynbekova Aliya Doszhankyzy	*Ph.D student, Department of Technology of Industrial and Civil Construction, L.N. Gumilyov Eurasian National University, 010000, st. Satbaeva 2, Astana, Kazakhstan. Email: kleo-14@mail.ru*
Lukpanov Rauan Ermagambetovich	*PhD, Professor of the Department of Technology of Industrial and Civil Construction, L.N. Gumilyov Eurasian National University, 010000, st. Satbaeva 2, Astana, Kazakhstan. Email: rauan_82@mail.ru*
Dyussembinov Duman Serikovich	*C.t.s., Assistant Professor of the Department of Technology of Industrial and Civil Construction, L.N. Gumilyov Eurasian National University, 010000, st. Satbaeva 2, Astana, Kazakhstan. Email: dusembinov@mail.ru*
Askerbekova Arailym Myrzakhankyzy	*PhD. Student, Department of Technology of Industrial and Civil Construction, L.N. Gumilyov Eurasian National University, 010000, st. Satbaeva 2, Astana, Kazakhstan. Email: aria_09.91@mail.ru*
Gunasekaran Murali	*Professor of Division of Research & Innovation, Uttaranchal University, Dehradun 248007, India. E-mail: murali_220984@yahoo.co.in*

Introduction

The main objectives of modern construction are to reduce the time required for the manufacture of concrete and reinforced concrete products and accelerate the set of s tandard concrete strengths [1]. Several articles [[2], [3], [4], [5]] discuss these problems in detail and analyze current solutions.

Nevertheless, the task of accelerating the set of standard strength of concrete and preserving its high-strength properties is relevant [6].

The basis of modern concrete technology is the creation of high-quality artificial stone,

characterized by high dispersion, a small imperfection, and structural stability. Improving the quality of concrete compositions can be achieved both through the use of chemical additives and by using local components to create a new generation of concrete, which is a very urgent task of concrete technology. New generation concrete is a high-tech, high-quality, multicomponent concrete mixes and compositions with additives that retain the required properties during operation in any conditions. The growth of multicomponent concretes is due to significant systemic effects that allow controlling the formation of the structure at all stages of the technology, ensuring the production of composites of «directional» quality, composition, structure and properties [[7], [8], [9], [10], [11], [12], [13]].

Concrete hardening can be intensified using several methods, including effective complex chemical additives [[14], [15]]. Of practical concern are multifunctional additives that act as effective plasticizers of concrete mixtures and increase the strength of concrete in the early stages of hardening [[16], [17], [18]].

Post-alcohol bard (PAB) - additives are the cheapest, suitable for all types of cement, for monolithic and precast construction from mortar and concrete, for heavy and lightweight concrete, and reinforced concrete, while increasing: strength, density, frost resistance, water resistance, durability, protection against corrosion, and improve the environment.

The aim of the research is to develop a CMA and study its influence on the physical and mechanical characteristics of cement structures. During the research a complex of laboratory tests to evaluate the physical and mechanical characteristics of samples with subsequent comparative analysis of changes in the qualitative characteristics of cement and the influence of a modifier on it has been carried out. This article provides part of the research results (third stage), on the accuracy of determining the influence of a varying mixture of CMA on the strength.

In order to achieve this goal, the following tasks were accomplished:

1. Selection of additive composition at different % ratios of its ingredients;

2. Laboratory preparation of samples of different combinations of additive components;

3. Laboratory studies of strength behavior of test samples;

4. Analysis of the obtained results.

Experimental technique

For the study were used materials that comply with the requirements and standards.

Cement. The raw materials were taken in accordance with the geographical location of the producers, and quality indicators of the material. Portland cement M400 type CEM I 42,5 H was accepted by «Kokshe-Cement» products, due to the availability of this binder.

Fine aggregate. As the fine aggregate used standard polyfractional sand (for the purity of the experiment) corresponding to the requirements of GOST 6139-2003 «Sand for testing of cement».

Modifying additive. Post-alcohol bard - PAB (main component) - ethanol production waste, meets the requirements of Technical Specifications 1110 RK 00393896-01-2003, in quantities of 2.5%, 5.0%, 7.5%, 10%, multiple of 2.5%. The product is supplied in liquid form, producer - JSC «Aydabulsky distillery». Hardening accelerant - gypsum, accelerating the process of hardening, in quantities of 1%, 1.5%, 2.0% and 2.5%, multiple of 0.5%.

The methodology of the experimental work consisted in carrying out several successive operations to create compositions, prepare mixtures, molding standard (40x40x160 mm) beam samples, and test the obtained samples on special equipment, data processing, and analysis. In the third stage, the individual influence of CMA on the strength of cement stone was studied. Compressive and bending strength was determined following GOST 30744-2001 «Cements. Test methods with polyfractional sand» at the age of 7, 14, and 28 days on the equipment Press Automatic Pilot, the total compressive load of 500 kN (50 tons). Material consumption of samples (necessary for measuring the compressive and bending strength) of cement mortar is given in Table 1.

Table 1 – Composition of samples

Number	Type	Cement, g	Sand, g	Gypsum, g	PAB, g	Caustic soda, g	Water, g
1	Type 1 Reference sample	450	1350	-	-	-	180
2	Type 2-1	445.5	1350	4.5	11.25	0.5625	168.1875
3	Type 2-2	445.5	1350	4.5	22.5	1.125	156.375
4	Type 2-3	445.5	1350	4.5	33.75	1.6875	144.5625
5	Type 2-4	445.5	1350	4.5	45	2.25	132.75
6	Type 3-1	443.25	1350	6.75	11.25	0.5625	168.1875
7	Type 3-2	443.25	1350	6.75	22.5	1.125	156.375
8	Type 3-3	443.25	1350	6.75	33.75	1.6875	144.5625
9	Type 3-4	443.25	1350	6.75	45	2.25	132.75
10	Type 4-1	441	1350	9	11.25	0.5625	168.1875
11	Type 4-2	441	1350	9	22.5	1.125	156.375
12	Type 4-3	441	1350	9	33.75	1.6875	144.5625
13	Type 4-4	441	1350	9	45	2.25	132.75
14	Type 5-1	438.75	1350	11.25	11.25	0.5625	168.1875
15	Type 5-2	438.75	1350	11.25	22.5	1.125	156.375
16	Type 5-3	438.75	1350	11.25	33.75	1.6875	144.5625
17	Type 5-4	438.75	1350	11.25	45	2.25	132.75

Results and Discussion

The selection of additives was based on the basic mechanism of action. The compound-modified additive includes gypsum, post-alcohol bard, and caustic soda (NaOH). The proposed additive has no analogs and is different in its quantitative composition of components. Application of caustic soda (NaOH index changes with the change in the quantitative index of post-alcohol bard) in combination with post-alcohol bard stabilizes its hydrogen index, approaching a neutral environment. The main plasticizing component is post-alcohol bard, which also has hydrophilic-hydrophobic properties. The influence of consumption of PAB to 10% demonstrated the expediency of this range, i.e. by optimizing the composition the maximum optimal range was determined. Earlier studies confirm the features of each component, and the complex synergistic effect is achieved [[19], [20]].

Studies have shown that concrete samples with the additive (PAB), when interacting with water, are not destroyed, indicating the effectiveness of this modifier. PAB, which is part of the complex modifier contains casein, which when interacting with the fine aggregate of concrete polymerizes, making additional contact films that improve the resistance of the material to the effects of water.

The object of the study was a cement-sand mortar at a constant w/c ratio = 0.4 based on unadded cement M400 (Kokshe-Cement) and using polyfractional sand packaged by 1350 grams. Figure 1 represented the test results of the strength of Type 1 (without additive composition) and with CMA, in the period of hardening 7, 14, and 28 days.

Figure 1 presents a diagram of the change in compressive strength of the tests as a function of curing time.

The reference samples of type 1 (without the use of additives) showed the lowest strength in all curing times (7, 14, and 28 days). The average strength points ranged from 22.11 to 40.83 MPa.

Samples of type 2-1 showed strength points higher than those of type 1 reference samples by 9.9% (7 days), 5.1% (14 days), and 4.8% (28 days), but 5.3% (7 days), 2.4% (14 days) and 4.8% (28 days) lower than those of type 2-2. The average strength points ranged from 24.3 to 42.8 MPa.

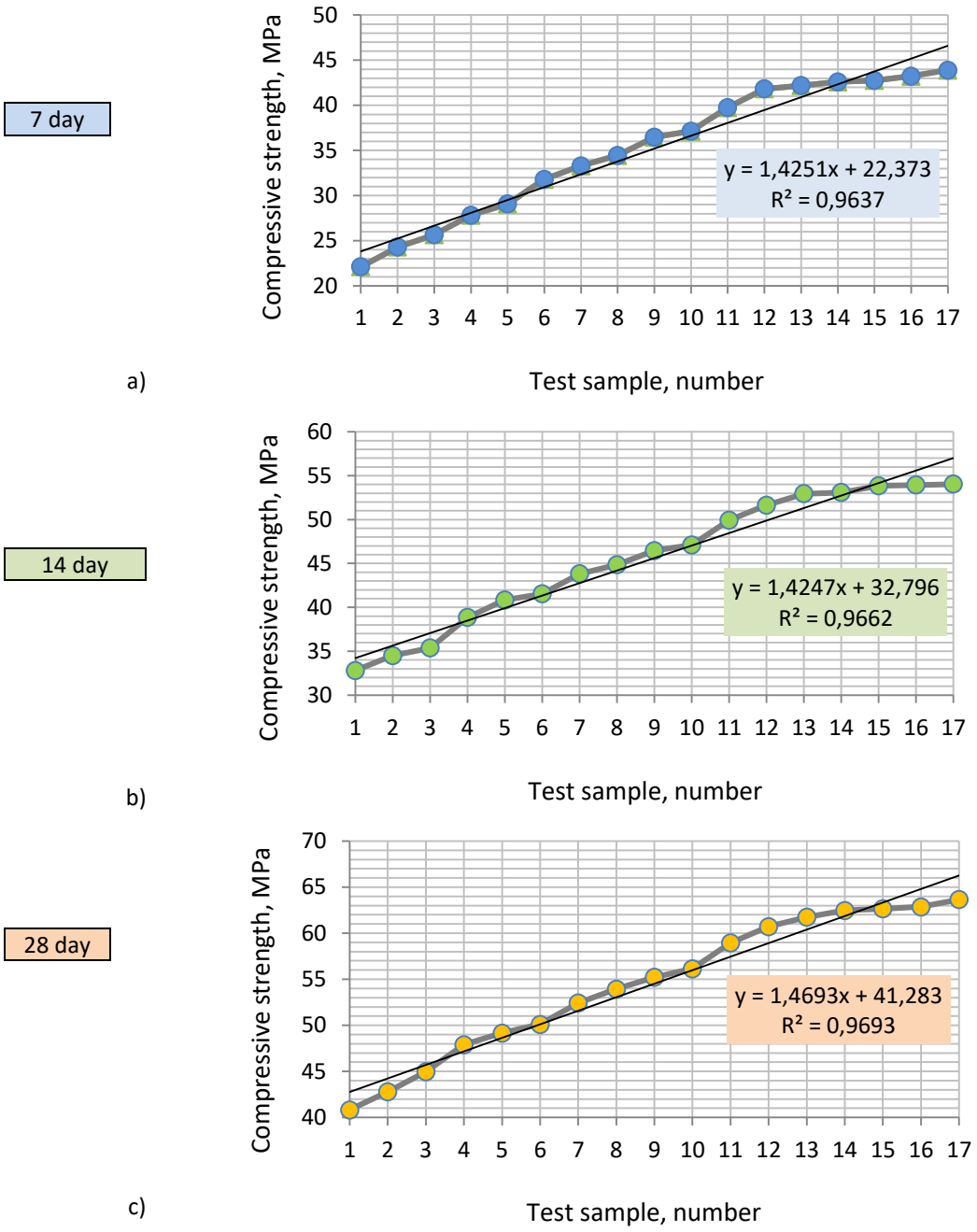

Figure 1 - Plots of growth of compressive strength of the tested samples: 7-day (a), 14-day (b), and 28 days (c)

Samples of type 2-2 showed strength points higher than those type 1 reference samples by 16.05% (7 days), 7.8% (14 days), and 10.1% (28 days), but 7.7% (7 days), 8.9% (14 days) and 6.1% (28 days) lower than those of type 2-3. The average strength points ranged from 25.66 to 44.97 MPa.

Samples of type 2-3 showed strength points higher than those type 1 reference samples by 25.8% (7 days), 18.4% (14 days), and 17.3% (28 days), but 4.2% (7 days), 4.8% (14 days) and 2.5% (28 days) lower than those of type 2-4. The average strength points ranged from 27.82 to 47.91 MPa.

Samples of type 2-4 showed strength points higher than those of type 1 reference samples by 31.4% (7 days), 24.3% (14 days), and 20.4% (28 days), but 8.5% (7 days), 1.7% (14 days) and 1.8% (28 days) lower than those of type 3-1. The average strength points ranged from 29.07 to 49.17 MPa.

Samples of type 3-1 showed strength points higher than those of type 1 reference samples by 43.8% (7 days), 26.6% (14 days), and 22.7% (28 days) but 4.4% (7 days), 5.1% (14 days) and 4.4% (28 days) lower than those of type 3-2. The average strength points ranged from 31.8 to 50.11 MPa.

Samples of type 3-2 showed strength points higher than those of type 1 reference samples by 50.5% (7 days), 33.5% (14 days), and 28.4% (28 days), but 3.3% (7 days), 2.3% (14 days) and 2.7% (28

days) lower than those of type 3-3. The average strength points ranged from 33.29 to 52.43 MPa.

Samples of type 3-3 showed strength points higher than those of type 1 reference samples by 55.8% (7 days), 36.7% (14 days), and 32.1% (28 days), but 5.5% (7 days), 3.4% (14 days) and 2.3% (28 days) lower than those of type 3-4. The average strength points ranged from 34.46 to 53.94 MPa.

Samples of type 3-4 showed strength points higher than those of type 1 reference samples by 64.9% (7 days), 41.6% (14 days), and 35.2% (28 days), but 1.8% (7 days), 1.4% (14 days) and 1.5% (28 days) lower than those of type 4-1. The average strength points ranged from 36.47 to 55.23 MPa.

Samples of type 4-1 showed strength points higher than those of type 1 reference samples by 67.9% (7 days), 43.6% (14 days), and 37.4% (28 days), but 6.5% (7 days), 5.6% (14 days) and 4.8% (28 days) lower than those of type 4-2. The average strength points ranged from 37.14 to 56.14 MPa.

Sample type 4-2 showed strength points higher than those of type 1 reference samples by 79.7% (7 days), 52.5% (14 days), and 44.4% (28 days), but 4.9% (7 days), 3.2% (14 days) and 2.8% (28 days) lower than those of type 4-3. The average strength points ranged from 39.75 to 58.96 MPa.

Sample of type 4-3 showed strength points higher than those of type 1 reference samples by 89.1% (7 days), 57.4% (14 days), and 48.7% (28 days), but 0.8% (7 days), 2.4% (14 days) and 1.6% (28 days) lower than those of type 4-4. The average strength points ranged from 41.83 to 60.72 MPa.

Samples of type 4-4 showed strength points higher than those of type 1 reference samples by 90.8% (7 days), 61.4% (14 days), and 51.2% (28 days), but 0.9% (7 days), 0.2% (14 days) and 0.2% (28 days) lower than those of type 5-1. The average strength points range from 42.19 to 61.74 MPa.

Samples of type 5-1 showed strength points highest than those of type 1 reference samples by 92.6% (7 days), 61.8% (14 days), and 53% (28 days), but 0.3% (7 days), 1.4% (14 days) and 0.2% (28 days lower than those of type 5-2. The average strength points ranged from 42.6 to 62.48 MPa.

Samples of type 5-2 showed strength points highest than those of type 1 reference samples by 93.3% (7 days), 64.1% (14 days), and 53.4% (28 days), but 1.1% (7 days), 1.4% (14 days) and 0.3% (28 days) lower than those of type 5-3. The average strength points ranged from 42.75 to 62.66 MPa.

Samples of type 5-3 showed strength points highest than those of type 1 reference samples by 95.5% (7 days), 64.4% (14 days), and 53.9% (28 days), but 1.4% (7 days), 0.1% (14 days) and 1.2% (28 days) lower than those of type 5-4. The average strength points ranged from 43.24 to 62.87 MPa.

Samples of type 5-4 showed strength points highest than those of type 1 reference samples by 98.5% (7 days), 64.7% (14 days), and 55.9% (28 days) than type 1 samples. The average strength points ranged from 43.89 to 63.66 MPa.

The analysis of the results of the conducted experiments has shown that in types 2-1 - 5-4, the compressive strength limit is within 42.8-63.66 MPa (28 days), and for the reference type 1 is 40.83 MPa, that is, this figure is 1.5 times greater than for the sample of type 1. According to the results, the hardening process occurs not only in the initial stages, but also continues to gain strength evenly in the subsequent time and to a greater extent increases the mass strength, which positively characterizes the samples with the use of CMA. It is likely that such differences in the effect on cement stone with CMA, are due to different mechanisms of action. When comparing the strength index of the sample prepared according to the sample, equal to 40.83 MPa, with the proposed compositions, which were between 42.8-63.66 MPa, it can be assumed that the samples of types 2-1 to 5-4 are of higher quality. The highest strength is observed when using the amount of additive in the amount of 2.5-7.5% of the weight of cement. This difference is explained by the modifying effect of CMA on the dispersive and morphological content of the new cement stone compounds. At the same time, the modified structure has a higher resistance to destruction.

As a consequence of the data obtained, it can be stated that the samples using CMA had a higher strength on day 7 - 24.3-43.89%; on day 14 -34.5-54.04% and on day 28 - 42.8-63.66% when compared with the reference sample. These results state that CMA increases the rate of strength gain in the early periods of hardening and contributes to high strength. Studies have shown that compositions containing 2.5 to 10% additives are the most effective, allowing for a 20% increase in the strength of the concrete. The compressive strength of such samples exceeds the value of strength without additive stone by 26.63%. The analysis of the obtained results shows that a positive effect on the kinetics of hardening has CMA on 7, 14, and 28 days of hardening, in contrast to the analog. These results state that CMA increases the rate of strength gain and contributes to high strength.

Figure 2 shows a diagram of the change in bending strength of the samples as a function of curing time. Analysis of the diagram shows that the strength of the samples increases smoothly and uniformly. Research of samples carried out with CMA increases the strength by 15-20%.

The results of behavioral studies on the bending strength of samples at 28 days of age were for:

Type 1. The test results of the reference sample were R = 5.5 MPa. The bending strength gain was 0 %.

Type 2-1. Test results of the samples with the added CMA amounted to R= 5.88 MPa. The strength gains increased by 6.9% compared to the control composition (reference sample).

Type 2-2. Test results of the samples with the added CMA amounted to R= 6.18 MPa. The strength gain increases by 12.36% compared to the control composition.

Type 2-3. Test results of the samples with the added CMA amounted to R= 6.59 MPa. The strength gain increases by 19.81% compared to the control composition.

Type 2-4. Test results of the samples with the added CMA amounted to R= 6.76 MPa. The strength gain increases by 22.9% compared to the control composition.

Type 3-1. Test results of the samples with the added CMA amounted to R= 6.89 MPa. The strength gain increases by 25.27% compared to the control composition.

Type 3-2. Test results of the samples with the added CMA amounted to R= 7.21 MPa. The strength gain increases by 31.09% compared to the control composition.

Type 3-3. Test results of the samples with the added CMA amounted to R= 7.41 MPa. The strength gain increases by 34.72% compared to the control composition.

Type 3-4. Test results of the samples with the added CMA amounted to R= 7.59 MPa. The strength gain increases by 38% compared to the control composition.

Type 4-1. Test results of the samples with the added CMA amounted to R= 7.72 MPa. The strength gain increases by 40.36% compared to the control composition.

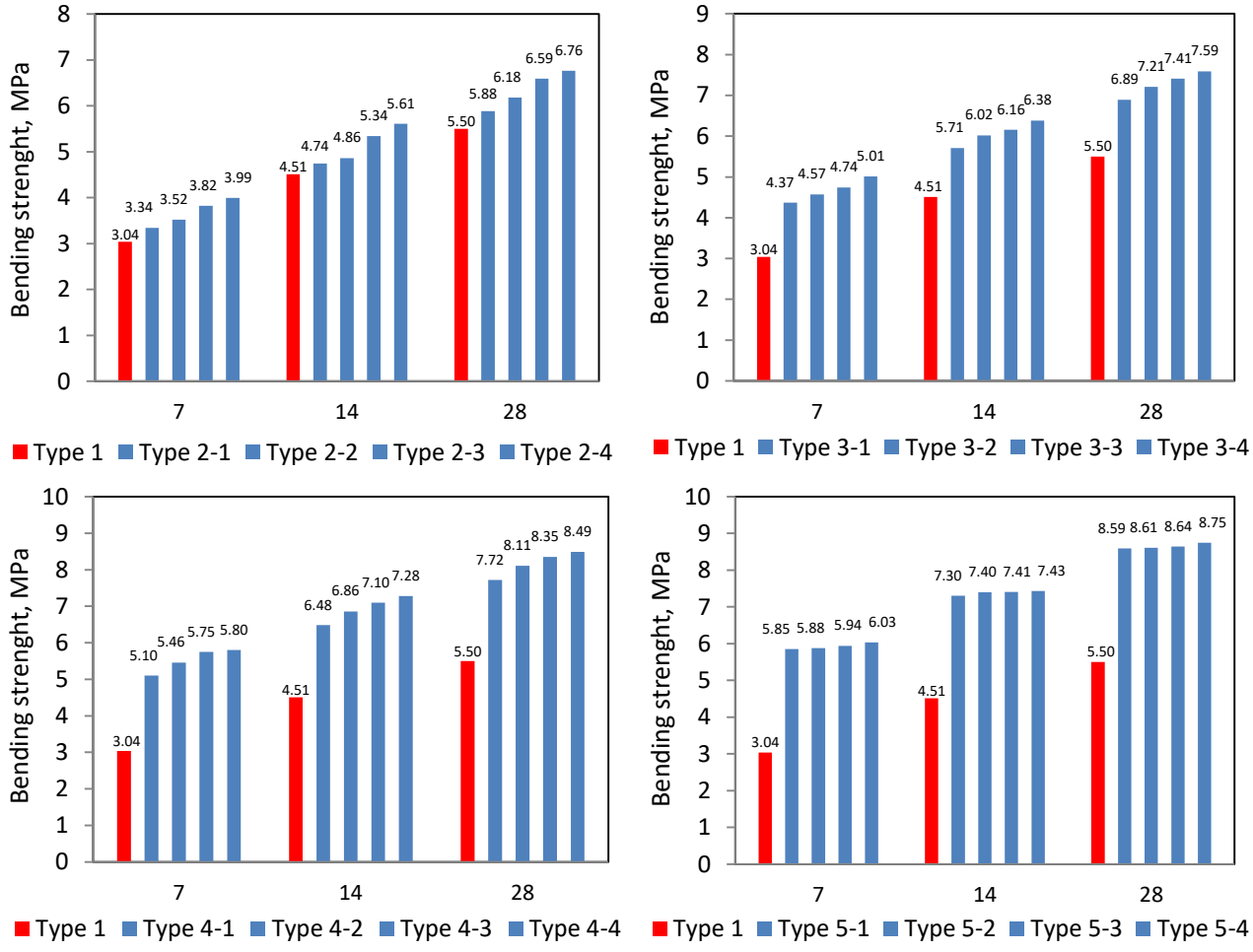

Figure 2 - Bending strength of samples at 7, 14, and 28 days

Type 4-2. Test results of the samples with the added CMA amounted to R= 8.11 MPa. The strength gain increases by 47.45% compared to the control composition.

Type 4-3. Test results of the samples with the added CMA amounted to R= 8.35 MPa. The strength gain increases by 51.81% compared to the control composition.

Type 4-4. Test results of the samples with the added CMA amounted to R= 8.49 MPa. The strength gain increases by 54.36% compared to the control composition.

Type 5-1. Test results of the samples with the added CMA amounted to R= 8.59 MPa. The strength gain increases by 56.18% compared to the control composition.

Type 5-2. Test results of the samples with the added CMA amounted to R= 8.61 MPa. The strength gain increases by 56.54% compared to the control composition.

Type 5-3. Test results of the samples with the added CMA amounted to R= 8.64 MPa. The strength gain increases by 57.09% compared to the control composition.

Type 5-4. Test results of the samples with the added CMA amounted to R= 8.75 MPa. The strength gain increases by 59.09% compared to the control composition.

The highest strength values were achieved in the compositions from 3-1 to 5-4 with an additive content of 2.5 to 7.5% of the cement weight. The highest bending strength at the age of 28 days, reaching 8.75 MPa, was obtained for the composition 5-4 (Figure 2). A slight increase in strength was observed in the bending test of beam samples made from types 5-3 and 5-4. Statistical analysis of the bending strength characteristics also showed a close relationship and relatively high convergence of individual values. In this case, the coefficient of variation does not exceed 14%; with a 95% confidence probability, the reliability coefficients do not exceed 1.17.

When the dose of CMA is increased, there is a qualitative change in the effect on strength and intensive growth of strength. In samples with different percentages of CMA (or without), the benefit of a certain amount of CMA on strength was clearly illustrated in Figures 1 and 2. During the curing process, additives have a significant effect on the bending properties of the samples, creating a strong framework in the structure, which explains the subsequent maximum increase in performance. Thus, based on the tests conducted, it was found that with the addition of CMA in the cement composition, the strength of samples tested in compression and bending, increases.

Figure 3 shows the data on the ratio of the compressive and bending strength at the age of 28 days of binders with different compositions described by the dependence $R_f = 0{,}128 \cdot R^{1{,}01}$ and characterized by the highest value of indicator R^2=0,9992, which shows a close correlation between values of compressive strength and bending strength. Thus, in terms of achieving the best results on the ratio of the compressive strength and bending strength, it is advisable to consider the composition of the binder with an additive ranging from 2.5 – 7.5% (post-alcohol bard) at a ratio of gypsum from 1 to 2%.

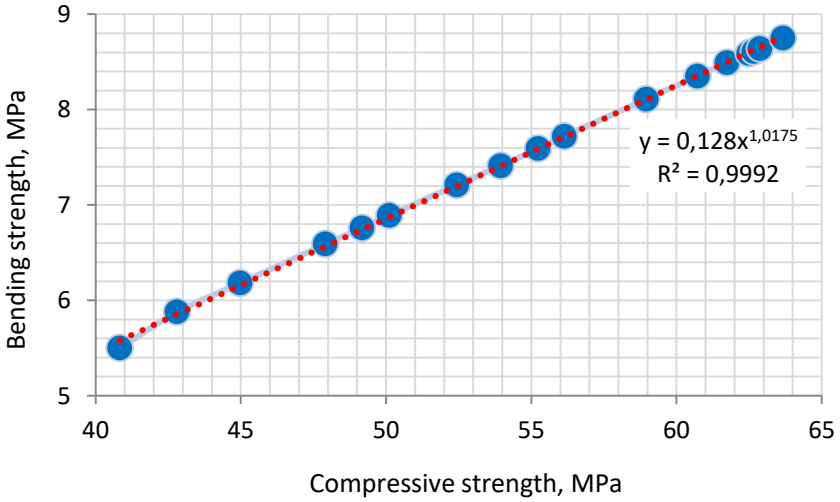

Figure 3 - Ratio of compressive and bending strengths

Conclusion

The following conclusions can be made based on the results of experimental research that the complex modified additive (CMA) shows a better water-reducing action than the composition with no additive (type 1). Based on the results of the study, the authors determined that the addition of additives reduces the quantity of water by 35%, and therefore increases the strength of the finished concrete. The results of the compression strength of the reference sample equal 40.83 MPa with the proposed compositions, which was in the range of 42.8-63.66 MPa, we can assume that the modified samples of types 2-1 - 5-4 are of higher quality. And in the case of bending strength at 28 days of age, reaching 8.75 MPa, the highest figure was obtained for the composition 5-4.

Analyzing the obtained dependencies, we can conclude that for this type of additive, the maximum effect is observed at a concentration of 2.5-7.5 % (post-alcohol bard). The additive showed an optimal positive effect, so the use of this percentage of additive is most effective in increasing the compressive and bending strength of concrete. Thus, according to the results of the research, the positive effect of CMA activation was established.

Conflict of interest. The corresponding author declares that there is no conflict of interest.

Cite this article as: Altynbekova AD, Lukpanov RE, Dyussembinov DS, Askerbekova AM, Gunasekaran Murali. Effect of a complex modified additive based on post-alcohol bard on the strength behavior of concrete. Kompleksnoe Ispolzovanie Mineralnogo Syra = Complex Use of Mineral Resources. 2023; 327(4):5-14. https://doi.org/10.31643/2023/6445.34

Спирттен кейінгі төп (барда) негізіндегі кешенді модификацияланған қоспаның бетонның беріктік сипаттамаларына әсері

[1]Алтынбекова А.Д., [1]Лукпанов Р.Е., [1]Дюсембинов Д.С., [1]Аскербекова А.М., [2]Гунасекаран Мурали

[1] Л.Н. Гумилев атындағы Еуразия ұлттық университеті, Астана, Қазақстан
[2] Зерттеу және инновация кафедрасы, Уттаранчал университеті, Дехрадун 248007, Үндістан

Мақала келді: *13 қыркүйек 2022*
Сараптамадан өтті: *14 қараша 2022*
Қабылданды: *30 қаңтар 2023*

ТҮЙІНДЕМЕ

Мақалада кешенді модификацияланған қоспаны зерттеу нәтижелерінің үшінші кезеңі, яғни осы қоспа компоненттерінің ауыспалы құрамының цементтің беріктігіне әсері келтірілген. Бұл жұмыста үлгілерді жасау әдістемесі, компоненттердің әр түрлі пайызындағы қоспаның құрамын таңдау және алынған нәтижелердің беріктік сипаттамаларының талдауы көрсетілген. Беріктіктегі өзгерістерді бағалау үшін үлгілер дайындалып, олардың 7, 14 және 28 тәулікте қалыпты ылғалдылықта қатаю кезінде қысуы мен иілуі сыналған. Тәжірибе нәтижелері көрсеткендей, қоспаларды – пластификаторларды (спирттен кейінгі төпте) қосқанда судың мөлшерін 35%-ға дейін төмендетеді, бетонның беріктігін 20%-ға арттырады. Модификацияланған үлгілердің қысу және иілу беріктігінің нәтижелері бақылау құрамымен салыстырғанда 42,80-63,66 МПа және 3,34-8,75 МПа аралығында болған ең жақсы нәтижелерді көрсетті. Зерттеу нәтижелері бойынша қоспаның қатаюы тезделеді және қоспа бетонның ерте жасында да, және жобалық жаста да (28 күн) беріктіктің өсуіне ықпал ететіні анықталды. Тәжірибе нәтижелері үлгілердің сапалық сипаттамаларын жақсарту тұрғысынан пластификаторлық қоспаларды қолдану орынды екенін көрсетті. Бетон қоспасында пластификаторларды қолдану ауыр бетонның төзімділігін және беріктігін айтарлықтай арттырады. Демек, күрделі түрлендіретін қоспаны қолдану бетонның құрылымын мақсатты түрде өзгертуге және сол арқылы физикалық-механикалық параметрлер кешенін және модификацияланған бетонның беріктігін айтарлықтай арттыруға мүмкіндік береді.

Түйін сөздер: бетон, цемент-құмның ерітіндісі, қатаю үдеткіші, спирттен кейінгі төп (барда), кешенді модификацияланған қоспа, пластификатор, иілу беріктігі, сығылу беріктігі.

Алтынбекова Алия Досжанкызы	***Авторлар туралы ақпарат:*** *PhD докторанты, «Өнеркәсіптік және азаматтық құрылыс технологиясы» кафедрасы, Л.Н. Гумилев атындағы Еуразия ұлттық университеті, 010000, Сәтбаев көшесі, 2, Астана, Қазақстан. E-mail: kleo-14@mail.ru*
Лукпанов Рауан Ермагамбетович	*PhD, «Өнеркәсіптік және азаматтық құрылыс технологиясы» кафедрасының профессорі, Л.Н. Гумилев атындағы ЕҰУ, 010000, Сәтбаев көшесі, 2, Астана, Қазақстан. Email: rauan_82@mail.ru*
Дюсембинов Думан Серикович	*Т.ғ.к., «Өнеркәсіптік және азаматтық құрылыс технологиясы» кафедрасының доценті, Л.Н. Гумилев атындағы Еуразия ұлттық университеті, 010000, Сәтбаев көшесі, 2, Астана, Қазақстан. Email: dusembinov@mail.ru*
Аскербекова Арайлым Мырзаханкызы	*PhD докторанты, «Өнеркәсіптік және азаматтық құрылыс технологиясы» кафедрасы, Л.Н. Гумилев атындағы Еуразия ұлттық университеті, 010000, Сәтбаев көшесі, 2, Астана, Қазақстан. Email: aria_09.91@mail.ru*
Гунасекаран Мурали	*Зерттеу және инновация кафедрасының профессоры, Уттаранчал университеті, Дехрадун, Үндістан. E-mail: murali_220984@yahoo.co.in*

Влияние модифицированной добавки на основе послеспиртовой барды на прочностные характеристики бетона

[1]Алтынбекова А.Д., [1]Лукпанов Р.Е., [1] Дюсембинов Д.С., [1]Аскербекова А.М., [2] Гунасекаран Мурали

[1] Евразийский национальный университет им. Л.Н. Гумилева, Астана, Казахстан
[2] Отдел исследований и инноваций, Университет Уттаранчал, Дехрадун 248007, Индия

Поступила: *13 сентября 2022*
Рецензирование: *14 ноября 2022*
Принята в печать: *30 января 2023*

АННОТАЦИЯ

В статье представлен третий этап результатов исследования комплексной модифицированной добавки (КМД), в точности влияния вариативного состава компонентов добавки на марочную прочность цемента. В данной работе показана методология выполнения образцов, подбор состава добавки при разном процентном соотношении компонентов и анализ прочностных характеристик полученных результатов. Для оценки изменений прочности были изготовлены образцы и испытаны на сжатие и изгиб в возрасте 7, 14, и 28 суток нормально-влажностного твердения. Результаты эксперимента показали, что введение добавок - пластификаторов (послеспиртовая барда) снижает количество воды до 35%, повышая прочность бетона на 20%. Результаты прочности на сжатие и изгибе модифицированных образцов показали наилучшие результаты, которые находились в диапазоне 42,80-63,66 МПа и 3,34-8,75 МПа, по сравнению с контрольным составом. Из результатов исследований добавка, ускоряет твердение и установлено, что добавка способствует росту прочности, как в раннем возрасте, так и в проектном возрасте (28 суток). Результаты эксперимента показали, что с позиций повышения качественных характеристик образцов применение пластифицирующих добавок целесообразно. Использование пластификаторов в бетонной смеси значительно повышает стойкость и долговечность тяжелого бетона. Следовательно, применение комплексной модифицирующей добавки позволяет целенаправленно изменить структуру бетона и тем самым значительно увеличить комплекс физико-механических показателей и долговечность модифицированных бетонов.

Ключевые слова: бетон, цементно-песчаный раствор, ускоритель твердения, комплексная модифицирующая добавка, послеспиртовая барда, пластификатор, прочность при изгибе, прочность на сжатие.

Алтынбекова Алия Досжанкызы	***Информация об авторах:*** *Докторант PhD, Кафедра «Технология промышленного и гражданского строительства», ЕНУ им. Л.Н.Гумилева, Астана, Казахстан. E-mail: kleo-14@mail.ru*
Лукпанов Рауан Ермагамбетович	*PhD, Профессор кафедры «Технология промышленного и гражданского строительства», ЕНУ им. Л.Н.Гумилева, 010000, ул. Сатбаева 2, Астана, Казахстан. Email: rauan_82@mail.ru*
Дюсембинов Думан Серикович	*К.т.н., Доцент кафедры «Технология промышленного и гражданского строительства», ЕНУ им. Л.Н.Гумилева, 010000, ул. Сатбаева 2, Астана, Казахстан. Email: dusembinov@mail.ru*
Аскербекова Арайлым Мырзаханкызы	*Докторант PhD, Кафедра «Технология промышленного и гражданского строительства», ЕНУ им. Л.Н.Гумилева, 010000, ул. Сатбаева 2, Астана, Казахстан. Email: aria_09.91@mail.ru*
Гунасекаран Мурали	*Профессор отдела исследований и инноваций, Университет Уттаранчал, Дехрадун, Индия. E-mail: murali_220984@yahoo.co.in*

References

[1] Ngugi HN, Mutuku RN, Gariy ZA. Effects of sand quality on compressive strength of concrete: A case of Nairobi County and Its Environs, Kenya. Open Journal of Civil Engineering. 2014; 04(03):255- 273. DOI: 10.4236/ojce.2014.43022

[2] Gora J, Piasta W. Impact of mechanical resistance of aggregate on properties of concrete. Case Studies in Construction Materials. 2020; 13:e00438. DOI: 10.1016/j.cscm.2020.e00438

[3] Hong L, Gu X, Lin F. Infl uence of aggregate surface roughness on mechanical properties of interface and concrete. Construction and Building Materials. 2014; 65:338-349. DOI: 10.1016/j.conbuildmat.2014.04.131.

[4] Kharchenko AI, Alekseev VA, Kharchenko IYa, Bazhenov DA. Structure and properties of fi ne concretes based on composite binders. Vestnik MGSU [Proceedings of Moscow State University of Civil Engineering]. 2019; 14(3):322-331. DOI: 10.22227/1997-0935.2019.3.322- 331 (in Russ.).

[5] Rakhimbaev ShM, Tolypina NM, Tolypin DA. Sravnitel'naya ustoychivost' betonov s zapolnitelyami i napolnitelyami razlichnogo sostava [Comparative stability of concrete with aggregates and fi llers of different composition]. Novosti universiteta. Stroitel'stvo [University news. Construction]. 2018; 10:13-21. DOI: 10.32683/0536-1052-2018-718-10-13-21 (in Russ.).

[6] Barannikov MV, Polyakov IV, Vinogradova LA, Polyakov VS. A multifunctional additive for heavy concretes. Vestnik MGSU. 2022; 17(6):720-726. DOI 10.22227/1997-0935.2022.6.720-726

[7] Kalashnikov VI. How to transform the old generation concrete in high-performance concretes of new generation, Concrete and reinforced concrete, Equipment, Materials, Technologies. 2012; 1:82-89

[8] Marceau S, Lespinasse F, Bellanger J, Mallet C. Microstructure and mechanical properties of polymer-modified mortars, European Journal of Environmental and Civil Engineering. 2012; 16:571-581. https://doi.org/10.1080/19648189.2012.675148

[9] Qingyu C, Wei S, Liping G, Guorong Z. Polymer-modified concrete with improved flexural toughness and mechanism analysis, Journal of Wuhan University of Technology-Materials Science Edition. 2012; 27:597-601. DOI:10.1007/s11595-012-0512-5

[10] Muhammad NZ, Keyvanfar A, Abd. Majid MZ, Shafaghat A, Mirza J. Waterproof performance of concrete: A critical review on implemented approaches, Construction and Building Materials. 2015; 101:80-90. https://doi.org/10.1016/j.conbuildmat.2015.10.048

[11] Plank J, Sakai E, Miao CW, Yu C, Hong JX. Chemical admixtures, Chemistry, applications and their impact on concrete microstructure and durability, Cement and Concrete Research. 2015; 78:81-99. DOI:10.1016/j.cemconres.2015.05.016

[12] Tian Y, Shuaifeng S, Shuguang H. Mechanical and dynamic properties of high strength concrete modified with lightweight aggregates presaturated polymer emulsion, Construction and Building Materials. 2015; 93:1151-1156

[13] Chistov YuD, Tarasov AS. Development of multi-mineral binders, Russian Chemical Journal. 2003;4:12-17

[14] Tarakanov OV, Belyakova EA, Yurova VS. Complex organomineral additives with hardening accelerator. Solid State Phenomena. 2018; 284:929-935. DOI: 10.4028/www.scientifi c.net/SSP.284.929

[15] Smirnov IR. Kompleksnyye dobavki k betonu na osnove veshchestv organicheskoy i mineral'noy prirody [Complex additives to concrete based on substances of organic and mineral nature]. Nauka i tekhnika [Science and Technique]. 2022; 21(l):57-62. DOI: 10.21122/2227-1031-2022-21-1-57-62 (in Russ.).

[16] Bessaies-Bey H, Khayat KH, Palacios M, Schmidt W, Roussel N. Viscosity modifying agents: Key components of advanced cement-based materials with adapted rheology. Cement and Concrete Research. 2022; 152:106646. DOI: 10.1016/j.cemconres.2021.106646

[17] Al-Khazraji AA. Use of plasticizers in cement concrete. Journal of Advanced Research in Dynamical and Control Systems. 2020; 12(3):599-607. DOI: 10.5373/JARDCS/V12I3/20201229.

[18] Garzón-Agudelo PA, Palacios-Alvarado W, Medina-Delgado B. Impact of plasticizers on the physical and structural properties of concrete used in constructions. Journal of Physics: Conference Series. 2021; 2046(1):012069. DOI: 10.1088/1742- 6596/2046/1/012069

[19] Altynbekova A, Lukpanov R, Dyussembinov D, Askerbekova A, Tkach E. Effect of a complex modified additive on the setting time of the cement mixture. Kompleksnoe Ispolzovanie Mineralnogo Syra = Complex Use of Mineral Resources. 2022; 325(2):29-38. https://doi.org/10.31643/2023/6445.15

[20] Altynbekova AD, Lukpanov RE, Yenkebayev SB, Dyussembinov DS, Yerzhanova NK. Bystrotverdeyushchiy udoboukladyvayemyy beton dlya proizvodstva buronabivnykh [Fast-hardening workable concrete for the production of bored]. Construction and reconstruction Construction and reconstruction [Stroitel'stvo i rekonstruktsiya Building and Reconstruction]. 2022; 2:99-111. https://doi.org/10.33979/2073-7416-2022-100-2-99-111 (In Russ.).

Crossref
DOI: 10.31643/2023/6445.35
Engineering and technology

Development of a mathematical model for a compound technological complex of vanyukov melting in order to control the material and thermal regime

[1] Mussabekov N.R., [2] Mukhanov B.K.

[1] "Institute of Automation and Information Technologies" JSC, Satbayev University, Almaty, Kazakhstan
[2] Non-profit JSC "Almaty University of Power Engineering and Telecommunications named after Gumarbek Daukeyev", Almaty, Kazakhstan

** Corresponding author email: n_mussabekov@mail.ru*

Received: *October 13, 2022*
Peer-reviewed: *November 20, 2022*
Accepted: *January 30, 2023*

ABSTRACT

This article presents a mathematical model in the form of static equations of dependencies of input and output flows based on the equations of material and heat balance for the purposes of operational planning and control of the complex technological complex of Vanyukov melting (PV). Dynamic characteristics are presented for the purpose of controlling the thermal regime based on the technology of the developed melting process with blowing from below. As a result of the study, the developed mathematical model for controlling the smelting process when calculating the material flows of the charge will allow tracking changes in the thermal state of the smelting (by the copper content in the matte). This model can quite well describe the dynamics of the state of the process, both when establishing the impacts aimed at increasing the heating of the furnace, and at reducing its heating. Based on the equations, a computer model based on the dynamic programming method in the MATLAB software package has been developed. The scientific novelty lies in the fact that for the first time, the structure of a mathematical model has been developed that describes the processes occurring in the over-tuyere zone and the sludge zone of the smelting products.

Keywords: technological complex, control system, static model, thermal regime, cooper smelting

Information about authors:

Mussabekov Nazarbek Rassulbekovich — *Master of Technical Sciences, senior lecturer of department "Automation and control", "Almaty University of Power Engineering and Telecommunications named after Gumarbek Daukeyev" Non-profit JSC, Ph.D. of the "Institute of Automation and Information Technologies " JSC, Satbayev University, Satbayev str., 22, 050013, Almaty, Kazakhstan, Email: n_mussabekov@mail.ru*

Mukhanov Bakhyt Kaskabaevich — *Candidate of technical sciences, professor of department "Automation and control", Non-profit JSC "Almaty University of Power Engineering and Telecommunications named after Gumarbek Daukeyev", Baitursynov str., 126, 050013, Almaty, Kazakhstan, Email: b.mukhanov@aues.kz*

Introduction

Smelting is one of the important processes in copper metallurgical production, in which copper and iron sulfides are oxidized to form molten matte and slag. Flash smelting and pool smelting are the main smelting technologies in copper production. [1]. Copper concentrates react with oxygen directly in the flash smelting process, which has the advantages of high productivity and automatic control. However, the flash-melting furnace requires fine and dry materials to allow fast reactions. As a result, feed preparation is required for a significant process, and dust levels are relatively higher. It has a limited ability to process scrap and other large copper-bearing materials. Bath melting is an alternative flash melting technology that involves reacting copper concentrate with oxygen in a molten bath. In [2], several technologies have been developed based on the principles of bath melting, including IsaSmelt/Ausmelt, Noranda/El Teniente, Vanyukov, and the recently developed Bottom Blowing Smelting (BBS) process. In the article [3], BBS technology has generated a lot of interest from the copper industry due to its unique processing features such as good feedstock adaptability, high oxygen utilization and thermal efficiency, and flexible performance. Articles [[4], [5]] say that in 2016, 13 BBS furnaces were built with a capacity of 1600 thousand tons of copper per year. Basic research, including slag thermodynamics and melt bath fluid dynamics, has been widely carried out in recent years to understand and support the new technology. Reviews [[6], [7]] summarize the development of the copper BBS, including its history,

features, and related basic research. The aim of the research is to develop a mathematical model of the dependence of input and output flows based on the equations of material and heat balance for the purposes of operational planning and control of the complex technological complex of Vanyukov melting.

Experimental part

The mathematical model of the Vanyukov process, developed in the framework of this study, is supposed to be used for the purposes of operational planning and management of the technological complex.

Therefore, the mathematical model of Vanyukov melting, which is supposed to be built, is selected in the class of static models based on the equations of material and heat balance for the main components of the input and output flows (copper-containing raw materials, concentrate, coal, air, oxygen, combustion gas, matte, slag, caisson temperature, exhaust gases, melt, dust, etc., released and absorbed heat) [[8], [9]].

The general structure of the model describing the process, where the input variables are the flow rates and the chemical composition of raw materials (concentrate, coal, charge, clinker), revolutions, oxygen-air mixture blowing (OAC), volumes and composition of air, oxygen, combustible gas, etc. d. and output variables of the furnace operation: quantity and composition of output products, including [10]:

- charge and content of *Cu*, *Si*, *Mg*, *S*, etc.;
- matte and its content of *Cu*, *S*, *Zn*, *P*, etc.;
- slag and its content of *CaO*, SiO_2, *MgO*, etc.;
- exhaust gases and their content of *CO*, CO_2, CH_4, N_2, O_2, etc.;
- dust and the content in it of the main components of input and output materials;
- waste (in fractions of the number of components in the input materials).

The basic equation for the relationship between the output variables of the model and the input ones is:

$$G_k^i = \sum_j^n \beta_{j/k}^i \alpha_j^i G_j \quad (1),$$

where G_k^i - is the amount of the *i*-th component in the *k*-th output product;

$\beta_{j/k}^i$ - coefficient of extraction (transition) of the *i*-th component from the *j*-th input material to the *k*-th output product;

α_j^i - the content of the *i*-th component in the *j*-th input stream (material), in fractions of units;

G_j - the amount of the *j*-th input (source) material.

The general form of equation (*1*) implies the possibility of taking into account all input material flows containing the i-th component (substance), which can be understood as a chemical element (for example, copper *Cu*, carbon *C*, etc.) and a stable compound (for example, oxides of calcium, silicon, magnesium - *CaO, SiO_2, MgO*, respectively, etc.). The choice of components *(i*), as well as the input (*j)* and output (*k*) material flows taken into account in the model, depends on the production technology and the nature of the ongoing physical and chemical processes. In this case, one can focus on metallurgical calculations of material and heat balances, which, as a rule, sufficiently reflect the current level of understanding (knowledge) of the technological features of a particular production. As a rule, the choice of component *(i*) largely depends on the respective output product: for matte, these are copper, carbon, and alloying metals; for slag - slag-forming oxides; for exhaust gases and dust - volatile and gaseous components [11].

Recovery factors used in the model ($\beta_{j/k}^i$) are widely used in metallurgical calculations. Their value is quite constant (stable) for a well-established production technology and the required accuracy of calculations performed using a mathematical model. However, for individual components to determine their content in the output products, setting the values of recovery factors requires additional calculations or the use of other calculated ratios. So the carbon content in the matte depends on the nature of the redox processes in the furnace (oxidation or carburization) [[12], [13]].

When constructing a mathematical model of the technological regime, the requirements of the material balance must be observed as for individual components:

$$\sum_{j=1}^n \alpha_j^i G_j = \sum_{k=1}^l G_k^i$$

and by the total number of input and output material flows:

$$\sum_{j=1}^n G_j = \sum_{k=1}^l G_k$$

The process of charge preparation. Calculation of the amount and composition of the charge. In the absence of experimental data and by analogy with metallurgical calculations, we believe that copper, carbon, silicon, manganese, phosphorus, and sulfur can be considered as starting materials in

the charge. After carrying out experimental studies on an operating furnace, other components of the raw materials and products of reactions occurring in the furnace can be taken into account [[14], [15]].

The general equation for determining the mass amount of components in the charge is:

$$G_{ch}^{i} = \sum_{j=1}^{n} \beta_{j/ch}^{i} \alpha_{j}^{i} G_{j}, \beta = 1$$

where j – index of initial (input) material flows – concentrates (conc1- bornite Cu_5FeS_4; conc2- chalcopyrite - $CuFeS_2$; conc3 - chalcocite - Cu_2S), fluxes (conc4 - bornite FeS_2; conc5 - quartz SiO_2; conc6 - limestone - $CaCO_3$; conc7 - magnesite $MgCO_3$)

1) The amount of copper *(Cu)* in the charge:

$$G_{ch}^{Cu}=\sum_{j=1}^{n} \alpha_{j}^{Cu} G_{j} =\alpha_{conc1}^{Cu} G_{conc1}+\alpha_{conc2}^{Cu} G_{conc2} + +\alpha_{conc3}^{Cu} G_{conc3} \approx \alpha_{ch}^{Cu} G_{ch}$$

Similarly, equations are written for calculating the number of other components in the charge, passing into it from the corresponding input material flows containing these components.

2) Total charge:

$$G_{ch}=\sum_{i} G_{ch}^{i} + G_{ch}^{ignt}$$

3) The composition of the charge, i.e. the content of individual components *(i)* is determined by the equation:

$$\alpha_{ch}^{i} = \frac{G_{ch}^{i}}{G_{ch}}$$

Melting process. Calculation of the amount and composition of the matte. The general equation for determining the mass amount of components in the charge is:

$$G_{ma}^{i}=\sum_{j=1}^{n} \beta_{j/ma}^{i} \alpha_{j}^{i} Gj \approx \beta_{in.str/ma}^{i} \alpha_{in.str/ma}^{i} G_{ma} \quad (2)$$

where *j* - is the index of input material flows coming out of the charge preparation process. When calculating the amount of matte, all materials containing the sum of copper in all forms (oxidized, sulfide, etc.) For the conditions adopted in this problem, the input copper-bearing flow is the charge (index "ch"), the production charge (index "pch"), oxygen in the blast (index "oxyg"), air (index "air"), coal (index "coal"), converter slag (index "cslg"), clinker (index "cl").

Theoretically, depending on the form of copper in each material, the recovery factors from each input material to the output product will be different. Practically by analogy with the metallurgical calculation, we can consider them the same and use the average value of the copper extraction coefficient from the matte (the last term of equation 2).

1) The amount of copper (Cu) in the matte:

$$G_{ma}^{Cu}=\sum_{j=1}^{n} \beta_{j/ma}^{Cu} \alpha_{j}^{Cu} G_{j}=\beta_{ch/ma}^{Cu} \alpha_{ch}^{Cu} G_{ch}+ \beta_{pch/ma}^{Cu} \alpha_{pch}^{Cu} G_{pch}+\beta_{cslg/ms}^{Cu} \alpha_{cslg}^{Cu} G_{cslg}+\beta_{cl/ma}^{Cu} \alpha_{cl}^{Cu} G_{cl}$$

Similarly, to equations, equations are written for calculating the number of other components in the matte passing into it from the corresponding input material flows containing these components.

In equations, the index *j* means input material flows containing the corresponding components (copper, sulfur, etc.)

4) Total amount of matte:

$$G_{ma} = \sum_{i} G_{ma}^{i}+G_{ma}^{ignm}=G_{ma}^{Cu}+G_{ma}^{Fe}+G_{ma}^{S} + G_{ma}^{Zn}+ +G_{ma}^{Pb}+G_{ma}^{ignt}$$

5) Matte composition, i.e. the content of individual components *(i*), is determined by the equation:

$$\alpha_{ma}^{i} = \frac{G_{ma}^{i}}{G_{ma}}$$

In metallurgical calculations, the composition of the matte is usually given by the content of copper and other components. In this case, the amount of matte is determined by the equation:

$$G_{ma} = G_{ma}^{Cu} \Big/ \alpha_{ma}^{Cu},$$

where $\alpha_{\text{шт}}^{Cu}$ content of copper in the matte. The amount of any component *(i*) in the matte is determined by the expression:

$$G_{ma}^{i} = G_{ma}\alpha_{ma}^{i}.$$

Melt process. Calculation of the amount and composition of slag. Components from the feedstock and products of reactions occurring in the furnace pass into the slag: oxide reduction, oxidation, slag formation, etc.

The general expression for determining the number of components in the slag is obtained from the equation:

$$G_{sl}^{i} = \sum_{j}^{n} \beta_{j/sl}^{i} \alpha_{j}^{i} G_{j} \quad (3)$$

1) The amount of calcium oxide (CaO) in the slag

$$G_{sl}^{CaO} = \sum_{j}^{n} \beta_{j/sl}^{CaO} \alpha_{j}^{CaO} G_{j} = \beta_{ma/sl}^{CaO} \alpha_{ma}^{CaO} G_{ma} + +\beta_{pma/sl}^{CaO} \alpha_{pma}^{CaO} G_{pma}+ \beta_{ksl/sl}^{CaO} \alpha_{ksl}^{Cao} G_{csl}$$

Similarly, to this equation, equations are written for calculating the amount and composition of slag of other components.

Calculation of the total amount of slag:

$$G_{sl} = G_{sl}^{CaO} + G_{sl}^{SiO_2} + G_{sl}^{Fe_2O_3} + G_{sl}^{MgO} + G_{sl}^{ignt}$$

Calculation of the quantity and composition of process off-gases. Exhaust technological gases are formed due to the blast supplied to the furnace: air (for combustion and transport of the pulverized coal mixture), oxygen, gas and gaseous products of chemical reactions of combustion, reduction, dissociation, evaporation of crystallization and ordinary moisture formed in the furnace, etc. [16].

Assuming that all input material flows are known and given the chemical reactions occurring in the furnace, it is possible to determine the mass amount of the main (accounted for) components and recalculate their content in the exhaust gases:

1) Gases from the reduction of charge oxides:

$$G^{CO} = \sum_j \beta_{j/sl}^{CO} \alpha_j^{CO} G_j$$

Thermal balance of the smelting process and the production of matte and slag in the Vanyukov furnace. The main sources of heat are (per *n* kg of charge):

1) Physical heat of the starting materials of the charge:

$$Q^{mat} = \sum_m^n M_m^{mat} \cdot C_m^{mat} \cdot T_m^{mat}$$

where Q^{mat} – heat materials;

M_m^{mat} – mass of *m*-th input material;

C_m^{mat} – the average heat capacity of the *m*-th input material;

T_m^{mat} –is the temperature of the *m*-th input (initial) material.

2) Heat of charge:

$$Q_{ch}^1 = \sum M_{ch}^{mat} \cdot C_{ch}^{mat} \cdot T_{ch}^{mat}$$

3) Converter slag heat:

$$Q_{csl}^2 = \sum M_{csl}^{mat} \cdot C_{csl}^{mat} \cdot T_{csl}^{mat}$$

4) Total physical heat of materials:

$$Q^{mat} = Q_{ch}^1 + Q_{csl}^2$$

5) Air blast heat:

$$Q_d^3 = \sum M_d^{air} \cdot C_d^{air} \cdot T_d^{air}$$

6) Heat of exothermic reactions

Exothermic reactions:

$$S + O_2 \rightarrow SO_2$$

$$CaO + SiO_2 \rightarrow Ca_2SiO_4$$

$$Fe_2O + SiO_2 \rightarrow Fe_2SiO_4$$

$$Q_{Ex} = -\sum dH_T \cdot \frac{M_{comp}}{M_m}$$

where Q_{Ex} - heat in melting;

$$Q_{Ex} = -(dH_T \cdot \frac{M_{S*O2}}{M_m} + dH_T \cdot \frac{M_L}{M_m} + dH_T \cdot \frac{M_B}{M_m})$$

where the designation L corresponds to Ca_2SiO_4, *B* - Fe_2SiO_4

7) Thermal energy due to fuel combustion (coal combustion):

$$Q_f = \sum q_f \cdot M_f$$

where q_f – the lower calorific value of fuel per working mass, kJ/kg

$$Q_f = \sum q_f \cdot M_f = q_{C_2H_8} \cdot M_{C_2H_8} + q_{C_4H_{10}} \cdot M_{C_4H_{10}}$$

where The main sources of heat consumption are (per *n* kg of charge):

The heat removed from the process products:

$$Q^{prod} = \sum_m^n M_m^{prod} \cdot C_m^{prod} \cdot T_m^{prod}$$

8) The heat of matte:

$$Q_{ma}^1 = \sum M_{ma}^{prod} \cdot C_{ma}^{prod} \cdot T_{ma}^{prod}$$

9) The heat of waste slag:

$$Q_{sl}^2 = \sum M_{sl}^{prod} \cdot C_{sl}^{prod} \cdot T_{sl}^{prod} + M_{sl}^{ign} \cdot C_{sl}^{ign} \cdot T_{sl}^{ign}$$

10) The heat of the dust:

$$Q_{dst}^3 = \sum M_{dst}^{prod} \cdot C_{dst}^{prod} \cdot T_{dst}^{prod} + M_{dst}^{ign} \cdot C_{dst}^{ign} \cdot T_{dst}^{ign}$$

11) The heat of gases:

$$Q_{gas}^4 = \sum M_{gas}^{prod} \cdot C_{gas}^{prod} \cdot T_{gas}^{prod}$$

12) Heat of endothermic processes

Endothermic reactions:

$$2CuFeS_2 \rightarrow Cu_2S + 2FeS + 0.5S_2$$

$$2Cu_5FeS_4 \rightarrow 5Cu_2S + 2FeS + 0.5S_2$$

$$FeS_2 \rightarrow FeS + 0.5S_2$$

$$Q_{endo} = -\sum dH_T \cdot \frac{M_{comp}}{M_m}$$

Thermal balance:

$$Q_{ma}^1 + Q_{ksl}^2 + Q_d^3 + Q_{Ex} + Q_f = Q_{th}^1 + Q_{sl}^2 + Q_{heat}^3 + Q_{gas}^4 + Q_{endo}$$

Development of a computer model for controlling the thermal and material regimes of the smelting process. A computer model for controlling the furnace modes is developed in MATLAB Simulink (see Figures 1-3). Figure 1 shows the general block diagram of the Vanyukov smelting process control

model for thermal and material conditions.

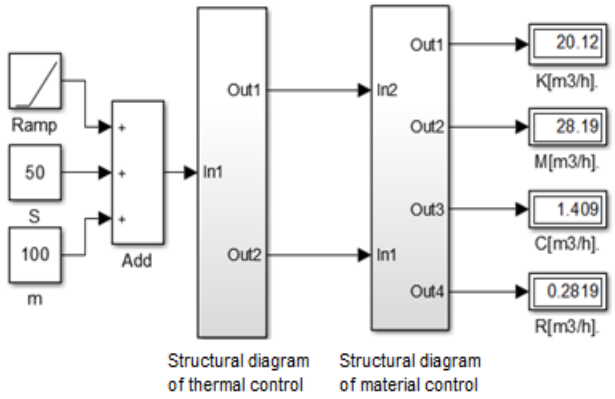

Figure 1 – Structural diagram of thermal and material control of the melting proces

As can be seen from Figure 1, the block diagram of the mathematical model consists of two subsystems: the heat balance calculation subsystem and the material balance calculation subsystem. The developed mathematical model for controlling the smelting process can quite well describe the dynamics of the state of the process, both when establishing influences aimed at increasing the heating of the furnace, and at reducing its heating.

Figures 2, 3 show: a subsystem for calculating the heat balance, which will allow, when calculating the material flows of the charge, to track changes in the thermal state of the melt (by the copper content in the matte) and the subsystems themselves for calculating the material flows of the charge. These subsystems for calculating the heat balance and material flows of the charge consist of blocks of mathematical operations and functional blocks of the Simulink Library.

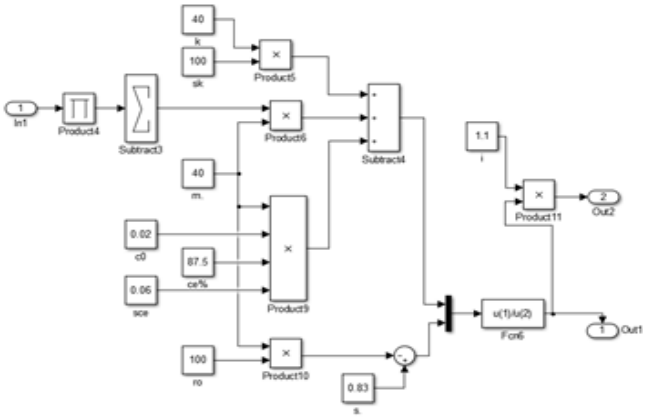

Figure 2 – Subsystem 1 for calculating the heat balance

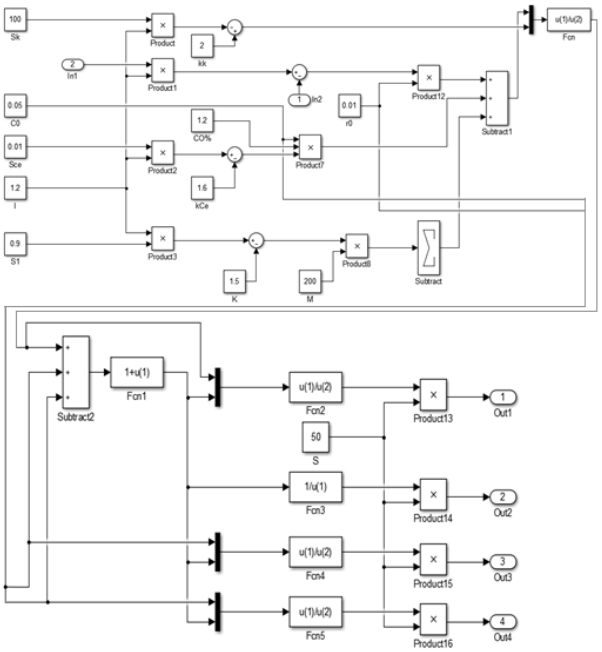

Figure 3 – Subsystem 2 for calculating the material flows of the charge

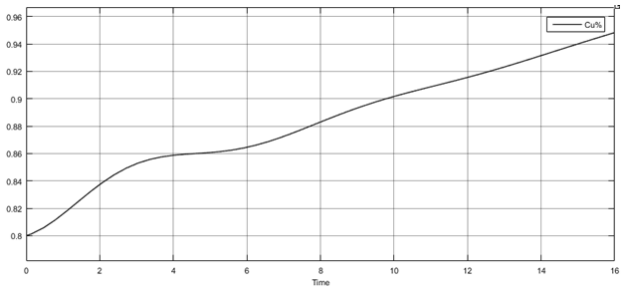

Figure 4 – Dynamics of changes in the copper content in the matte in the transition process

As can be seen from Figure 4, an oscillatory transient process in the furnace is observed if, after the disturbance is applied, it will have the opposite effect on the thermal state of the lower and upper stages of heat exchange. In this case, the overshoot value will be the greater, the more significant in magnitude and sign this difference is. The most predictable parameters affecting the copper content in the matte are changes in the matte load, blast moisture, and slag basicity.

The discussion of the results

The calculation of the dynamic characteristics of the furnace should be based on fundamental knowledge of the theory and practice of modern "autogenous" processes, as well as the general patterns of transient processes obtained using a dynamic model of the melting process [17].

The dynamic characteristics of the furnace through the various impact paths vary considerably depending on the properties of the molten raw material, and the design and operating parameters of the furnace. In this regard, it is advisable to determine the static parameters from the model, and the duration and magnitude of the delay of transient processes in the object should be related to the time of turnover of one volume of charge in the furnace [[18], [19]].

The change in the oxygen concentration in the blast and the flow of natural gas cannot be used as parameters for controlling the copper content in the matte. This is due to the variable influence of these parameters on the thermal regime of the melt. Forced regulation of natural gas flow and oxygen concentration in the blast to control the copper content in the matte can lead to results opposite to those expected [20].

Conclusion

The work carried out in this research showed the following results:

1) A mathematical model has been developed for the dependence of input and output material flows of the process of smelting copper concentrates in the Vanyukov furnace.

2) On the basis of equations of material and heat balance, the structure of a computer model has been developed for the purposes of operational planning and control of a complex technological process of melting.

3) On the basis of models it is possible to form the structure of a closed dynamic model (29-42), which takes into account both the kinetics and hydrodynamics of the processes flowing in the Vanuykov melting processes. However, creating an optimal control system is required to carry out work on identifying the model and verifying its adequacy, which requires the implementation of quite complex, lengthy, labor-intensive, and expensive studies, both the kinetics and hydrodynamics of the process.

2) Under the conditions described, it will be more efficient not to create a mathematical model of the complex process of the copper smelting process, but to develop a model for controlling this process based on the experience, knowledge, and intuition of operators-technologists working for a long time at this facility.

Conflict of interests

On behalf of all authors, the correspondent author declares that there is no conflict of interest.

Cite this article as: Mussabekov NR, Mukhanov BK. Development of a mathematical model for a compound technological complex of vanyukov melting in order to control the material and thermal regime. Kompleksnoe Ispolzovanie Mineralnogo Syra = Complex Use of Mineral Resources. 2023; 327(4):15-22. https://doi.org/10.31643/2023/6445.35

Материалдық және жылу режимін басқару мақсатында Ванюков балқытуының күрделі технологиялық кешені үшін математикалық модель әзірлеу

[1] Мусабеков Н.Р., [2] Муханов Б.К.

[1] «Автоматика және ақпараттық технологиялар институты» АҚ, Сәтбаев университеті, Алматы, Қазақстан
[2] «Ғұмарбек Дәукеев атындағы Алматы энергетика және байланыс университеті» КеАҚ, Алматы, Қазақстан

Мақала келді: *13 қазан 2022*
Сараптамадан өтті: *20 қараша 2022*
Қабылданды: *30 қаңтар 2023*

ТҮЙІНДЕМЕ

Бұл мақалада Ванюков балқымасының (ВБ) күрделі технологиялық кешенін жедел жоспарлау және басқару мақсатында материал және жылу балансының теңдеулеріне негізделген кіріс және шығыс ағындарының тәуелділіктерінің статикалық теңдеулері түріндегі математикалық модель ұсынылған. Теңдеулердің негізінде MATLAB бағдарламалық пакетіндегі динамикалық бағдарламалау әдісіне негізделген компьютерлік модель жасалды. Төменнен үрлеумен әзірленген балқыту процесінің технологиясы

негізінде жылу режимін басқару мақсатында өтпелі режимде үрлегенде оттегінің өзгеруі кезінде штейндегі мыс құрамының өзгеруінің динамикалық сипаттамалары зерттелді. Зерттеу нәтижесінде шихтаның материалды ағындарын есептеу кезінде балқыту процесін басқарудың әзірленген математикалық моделі балқытудың жылу күйіндегі өзгерістерді (штейндегі мыс мөлшері бойынша) бақылауға мүмкіндік береді. Бұл модель пешті қыздыруды арттыруға бағытталған әсерлерді орнату кезінде де, оның қызуын азайту кезінде де процестің күйінің динамикасын жақсы сипаттай алады. Ғылыми жаңалық алғаш рет балқыту өнімдерінің фурмалық және тұнба аймағында болатын процестерді сипаттайтын математикалық модель құрылымының жасалуында.

Түйін сөздер: технологиялық кешен, басқару жүйесі, статикалық модель, жылу режимі, мыс балқытуы

Авторлар туралы ақпарат:

Мусабеков Назарбек Расулбекович — *Магистр, «Автоматтандыру және басқару» кафедрасының аға оқытушысы, «Ғұмарбек Дәукеев атындағы Алматы энергетика және байланыс университеті» КеАҚ, «Автоматика және ақпараттық технологиялар институты» АҚ докторанты, 050013, Сәтбаев көш., 22, Алматы, Қазақстан, Email: n_mussabekov@mail.ru*

Муханов Бахыт Каскабаевич — *Техника ғылымдарының кандидаты, "Автоматтандыру және басқару" кафедрасының профессоры, «Ғұмарбек Дәукеев атындағы Алматы энергетика және байланыс университеті» КеАҚ, Байтурсынов көш., 126, 050013, Алматы, Казақстан, Email: b.mukhanov@aues.kz*

Разработка математической модели для сложного технологического комплекса плавки Ванюкова с целью управления материальным и тепловым режимом

[1]Мусабеков Н.Р., [2]Муханов Б.К.

[1]АО «Институт автоматики и информационных технологий», Satbayev University, Алматы, Казахстан
[2]НАО «Алматинский университет энергетики и связи имени Гумарбека Даукеева», Алматы, Казахстан

Поступила: *13 октября 2022*
Рецензирование: *20 ноября 2022*
Принята в печать: *30 ягваря 2023*

АННОТАЦИЯ

В данной статье приводится математическая модель в ввиде статических уравнений зависимостей входных и выходных потоков на основе уравнений материального и теплового баланса для целей оперативного планирования и управления сложным технологическим комплексом плавки Ванюкова (ПВ). На основе уравнений, разработана компьютерная модель, основанная на методе динамического программирования в программном комплексе MATLAB. Исследованы динамические характеристики изменения содержания меди в штейне при изменении содержания кислорода в дутье в переходном режиме с целью управления тепловым режимом на основе технологии разработанного процесса плавки с продувкой снизу. В результате исследования, разработанная математическая модель управления процессом плавки при расчете материальных потоков шихты позволит отслеживать изменения теплового состояния плавки (по содержанию меди в штейне). Данная модель достаточно хорошо может описать динамику состояния процесса как при установлении воздействий, направленных на повышение нагрева печи, так и на снижение ее нагрева. Научная новизна заключается в том, что впервые разработана структура математической модели, описывающей процессы, протекающие в надфурменной зоне и зоне отстоя продуктов плавки.

Ключевые слова: технологический комплекс, система управления, статическая модель, тепловой режим, плавка меди

Информация об авторах:

Мусабеков Назарбек Расулбекович — *Магистр технических наук, старший преподаватель кафедры «Автоматизация и управление», НАО «Алматинский университет энергетики и связи имени Гумарбека Даукеева», докторант АО «Институт автоматики и информационных технологий», «Satbayev University», 050013, ул. Сатпаева, 22, Алматы, Казахстан, Email: n_mussabekov@mail.ru*

Муханов Бахыт Каскабаевич — *Кандидат технических наук, профессор кафедры "Автоматизация и управление", НАО "Алматинский университет энергетики и связи имени Гумарбека Даукеева", ул. Байтурсынова, 126, 050013, Алматы, Казахстан, Email: b.mukhanov@aues.kz*

References

[1] Schlesinger M, Sole K, Davenport W, Alvear G. Extractive Metallurgy of Copper: 6th ed. Elsevier: Oxford; United Kingdom; Theory to practice: Pyrometallurgical industrial processes. 2021; 5:95-117

[2] Gorbunov IS. Modelirovaniye teploobmena v konechno-elementnom pakete FEMLAB: Ucheb. Posobiye [Modeling of heat transfer in the finite element package FETLAB: Proc. Allowance]. Ivanovo: NiST. 2008, 216 (in Russ.).

[3] Watt J, Kapusta J. The 2019 copper smelting survey. In Proceedings of the 58th Annual Conference of Metallurgists (COM) Hosting the 10th International Copper Conference. 18–21 August. Vancouver, BC, Canada. 2019, 595-947.

[4] Xu L, Chen M, Wang N, Gao S. Chemical wear mechanism of magnesia-chromite refractory for an oxygen bottom-blown copper-smelting furnace: A post-mortem analysis. Ceram. Int. 2021, 2908-2915. https://doi.org/10.1016/j.ceramint.2020.09.124

[5] Wang J. Copper smelting: 2019 world copper smelting data. In Proceedings of the 58th Annual Conference of Metallurgists (COM) Hosting the 10th International Copper Conference. 18–21 August. Vancouver, BC, Canada. 2019, 592-606

[6] Du X; Zhao G; Wang H. Industrial application of oxygen bottom-blowing copper smelting technology. China Nonferr. Metall. 2018; 4:4-6

[7] Mussabekov N, Ibraev A, Issayeva G, Smagulova L, Baimuldina N. Methods and tools for development a hybrid and information control systems of technological complex. News of the National Academy of Sciences of the Republic of Kazakhstan, Series of Geology and Technical Sciencesthis link is disabled. 2018; 1(427):118-126

[8] Musabekov N, Ibraev A. Mathematical description of autogenic processes of melting copper concentrates flowing in a liquid bath. Proceedings of the International Satpayev readings. The role and place of young scientists in the implementation of the new economic policy of Kazakhstan, Almaty: KazNTU. 2016; 2:79-86

[9] Suleimenov M, Kadenov S, Kadenov B. Development of a hybrid control system for agglomerated charge granulation. Engineering and Technical journal Automation Reporter. 2011; 31:5-9

[10] Mussabekov N, Ibraev A, Moldakhmetov K. Control system by technological complex on the example of the control process of copper concentrates smelting. Conference Lubelskie Dni Nauki i Biznesu WD. 2016

[11] Musabekov N, Ibrayev A, Moldakhmetov K. Razrabotka matematicheskikh modeley dlya protsessa plavki mednykh kontsentratov v pechi Vanyukova. Sbornik statey konferentsii «Evropeyskaya nauka 21 veka. 2016

[12] Musabekov N. Ibrayev A. Adilbekov M. O voprosakh razrabotki gibridnoy sistemy upravleniya tekhnologicheskim protsessom na primere upravleniya protsessami teploobmena [On the development of a hybrid process control system on the example of heat transfer process control]. DOKLADY Natsionalnoy Akademii Nauk Respubliki Kazakhstan [REPORTS of the National Academy of Sciences of the Republic of Kazakhstan]. 2016; 5:125-131 (in Russ.).

[13] Liang S. Review of oxygen bottom blowing process for copper smelting and converting. In Proceedings of the 9th International Copper Conference, Kobe, Japan. 13–16 November. 2016, 1008-1014

[14] Hellström E, Aslund J, Nielsen L. Design of an efficient algorithm for fuel-optimal look-ahead control. Control Engineering Practice. 2010; 18(11):1318-1327

[15] Wang Q, Wang Q, Tian Q, Guo X. Simulation study and industrial application of enhanced arsenic removal by regulating the proportion of concentrates in the SKS copper smelting process. Processes. 2020; 8(4):385. https://doi.org/10.3390/pr8040385

[16] Wang Q, Guo X, Tian Q, Jiang T, Chen M, Zhao B. Development and application of SKSSIM simulation software for the oxygen bottom blown copper smelting process. Metals. 2017; 7(10);431-441. https://doi.org/10.3390/met7100431 (in Chinese).

[17] Ospanov Ye, Kvyatkovskiy S, Kozhakhmetov S, Sokolovskaya L, Semenova A, Dyussebekova M, Shakhalov A. Slag heterogeneity of autogenous copper concentrates smelting. Canadian Metallurgical Quarterly, The Canadian Journal of Metallurgy and Materials Science. 2022. https://doi.org/abs/10.1080/00084433.2022.2119495

[18] Bacedoni M, Moreno-Ventas I, Ríos G. Copper Flash Smelting Process Balance Modeling. Metals. 2020; 10(9):1229-1238. https://doi.org/10.3390/met10091229

[19] Song K, Jokilaakso, A. Transport phenomena in copper bath smelting and converting processes–A review of experimental and modeling studies. Mineral Processing and Extractive Metallurgy Review. An International Journal, 2022; 43(1):107-121. https://doi.org/10.1080/08827508.2020.1806835

[20] Chenchen L, Shuhui Zh, Ran L, Qing L, Guangshi Y, Baoyong W. Thermodynamic and kinetic behaviours of copper slag carbothermal reduction process. Ironmaking & Steelmaking, Processes, Products and Applications. 2022 https://doi.org/10.1080/03019233.2022.2091726

Crossref
DOI: 10.31643/2023/6445.36
Engineering and Technology

Classification of texts on emergency situations in Almaty

[1]Andirov M.Y., [1*]Assan Zh.Zh., [2]Nopembri S., [3]Seilkhan A.M., [1]Myrzakhmetov D.E.

[1]Al-Farabi Kazakh National University, Almaty, Kazakhstan
[2]Universitas Negeri Yogyakarta, Yogyakarta, Indonesia
[3]Aktobe RSU named after K.K. Zhubanov, Aktobe, Kazakhstan

** Corresponding author email: zh.assanova98@gmail.com*

Received: *December 24, 2022*
Peer-reviewed: *January 18, 2023*
Accepted: *January 31, 2023*

ABSTRACT

Text classification is a process that includes stages and approaches for the effective classification of texts that are diverse in their structure. In this article, machine learning algorithms are implemented, such as the support vector method, logistic regression, and the k nearest neighborhood method for classifying texts collected from emergency news sites in Almaty. During the experiment, a special role was played by the data collection stage, as well as their subsequent processing. Prior to the classification of the data set, preliminary data processing was performed, which includes such steps as the removal of stop words, tokenization, stemming, lemmatization, feature extraction, and the construction of feature vectors. The data was obtained by automated collection of information from open sources using a script. Experimental results show that the classifier based on logistic regression provides the best performance results compared to other types of algorithms. The performance indicators of each algorithm were obtained, which allows us to perform a comparative analysis between them.

Keywords: machine learning, text classification, support vector machine, logistic regression, KNN, NLP, preprocessing, emergencies.

Andirov Mussa Yerezhepbayuly	*2nd year Master's student, Computer Science, Faculty of Information Technology, Al-Farabi Kazakh National University, Almaty, Kazakhstan. Email: andirov2610@gmail.com*
Assan Zhanelya Zheniskyzy	*2nd year Master's student, Computer Science, Faculty of Information Technology, Al-Farabi Kazakh National University, Almaty, Kazakhstan. Email: zh.assanova98@gmail.com*
Nopembri Soni	*Professor, Universitas Negeri Yogyakarta, Yogyakarta, Indonesia. Email: soni_nopembri@uny.ac.id*
Seilkhan Abilmansur Meiramgaliuly	*2nd year Master's student, Computer science and information technology, Faculty of Physics and Mathematics, K. Zhubanov Aktobe Regional University, Aktobe, Kazakhstan. Email: seilkhan.mansur@gmail.com*
Myrzakhmetov Dias Erlanuly	*2nd year Master's student, Computer Science, Faculty of Information Technology, Al-Farabi Kazakh National University, Almaty, Kazakhstan. Email: diko.17.04@gmail.com*

Introduction

On the Internet, the amount of data in the form of text is increasing every day, that leads to the necessity for studying and processing of this information. Basically, the texts are unstructured, but there is data that can be classified as partially structured, they include email messages, blogs and chats on social networks, articles on news sites, electronic libraries, etc. This alignment requires timely collection, monitoring and correct classification of the incoming information flow [1]. While classifying texts, the correct and fast work is required. It achieved by training on a pre-classified data-set. After training the classifier, the selected algorithm will properly categorize the provided data [2].

Science covers a large number of articles and researches based on theoretical evidences. Quite a few studies are devoted to the practical evidences of text classification. In the article [3], classification algorithms were applied on the database collected from social articles, consisting of unstructured and raw texts.

The authors used ten algorithms, five of which are based on machine learning methods, the rest are vocabulary-based. The authors came to the conclusion that almost all classifiers work correctly when classifying English texts, but when classifying foreign texts, more time and effort will be required.

The article [4] implements a classifier of a foreign language text. On a database consisting of texts in the Persian language, classification methods based on machine learning were applied. In this article, support vector, logistic regression, and k nearest neighborhood methods were used and compared. The k nearest neighborhood (KNN) method is a metric classification method based on machine learning. The selected sample is classified by calculating the distance of this object from other samples. If the distance is the minimum threshold value, the object is assigned this class. A large number of positive characteristics stand out, such as a simple theoretical basis, the ability to select metrics to increase efficiency.

Support Vector Machine is a supervised machine learning method. In this method, with the help of calculations, the optimal hyperplane is found, which divides the data set into several classes. The definition and application of this method is described in the article [5].

The logistic regression method is a supervised machine learning method. This algorithm finds the optimal hyperplane. This hyperplane will divide the test set into classes [6]. If the value of the target or target variable is of a categorical character, it is advisable to use the logistic regression algorithm. In the article [7], the authors consider the method of logistic regression largely theoretical, exactly the basic formulas for calculating the position of the hyperplane, advantages and disadvantages.

The research work [8] provides a model for classifying textual data in English. This work indicates the stages of data collection, text preprocessing, vector representation of text, as well as classification algorithms based on machine learning. Through a comparative analysis by metrics, we choose the most effective machine learning algorithm. In the article [9], the classification was carried out between unlabeled data and data with a positive class.

As a result, the authors obtained a classifier that separates the new data set into a positive and unlabeled class. The main feature of this article is the moment of selecting parameters for each algorithm separately, which gives excellent results. The work [10] represents a number of articles on the topic of text classification. The best and most significant results in this topic are indicated. When categorizing text by topic, it is necessary to highlight a number of words that are suitable for describing each class. The article [11] demonstrated the methods by which this goal is achieved. More and more information is being accumulated in social networks, and email plays an important role among them. In the article [12], such methods as SVM, classifier based on neural networks, J48, classifier based on naive Bayes are used to categorize texts received by e-mail. The data set consisted of unnormalized spam and non-spam messages. A feature of this article is that a simple classifier based on J48 showed the best results, although it is based on building a binary tree.

In the article [13], the authors noted that the main factor of correct classification is the presentation of the text. During the classification process, four methods of text representation were compared, such as phrases, RDR, key words, and N-grams. To increase the efficiency indicators, it is worth sorting out these methods and choosing the best one. Many of us notice that information on the Internet and social networks is becoming more and more personalized. The research paper [14] deals with news collected from newspapers. Thus, each person receives the information in which he is interested.

2. Materials and methods

2.1 Problem statement and data

Here considered the emergency situations of technogenic and natural character of Almaty city. Data on emergency situations were collected from the news site https://tengrinews.kz, then a data table was compiled for them.

The used dataset consists of a classification of 4 types of news about emergency situations. They are:

- Road traffic accidents are events involving vehicles, as a result of which people or environmental objects died and suffered, namely: cargo, structures, property, etc.

- Flooding is an event that carry the nature of submersion the environment as a result of a rise in the water level in a local river, sea, lake due to such causes as rain, congestion, snow.

- A fire is an event in which an uncontrolled fire occurs, which entails material damage to a person and his property.

- An earthquake is an event in which tremors and vibrations occur during various interventions in the earth's crust.

The dataset has 1712 lines and 3 columns. Each line represents specific events, and each column has different indications of those events. Each line of the data set contains the following fields:

- Data-date of news publication;
- Content-content and description of news;
- Category-category of the event.

2.2. Text classification

In the course of work the categorization of the text, several stages were performed. Figure 1 shows the general structure for categorizing emergency news articles. Depending on the goal and preferences of the performer, as well as the expected result, the steps may change, but the overall structure remains the same. As texts, documents can be selected the data from open sources or collected manually. The preprocessing step can be omitted if necessary or have a different structure.

In this study, special attention is paid to this particular stage, since the data has irrelevant elements and noise in the form of html language characters. The stages of indexing and feature selection cannot be skipped when classifying text using machine learning algorithms. The fact is that machine learning algorithms cannot accept natural language data, which leads to the need to bring the data into some numerical form to train the classifier. These stages are interconnected and perform the transformation of the text into a numerical form. Text classification algorithms can be probabilistic for example Naive Bayes, metric: k nearest neighborhood algorithm, logical: decision tree, linear: support vector machine, logistic regression, neural network-based methods: RNN, CNN.

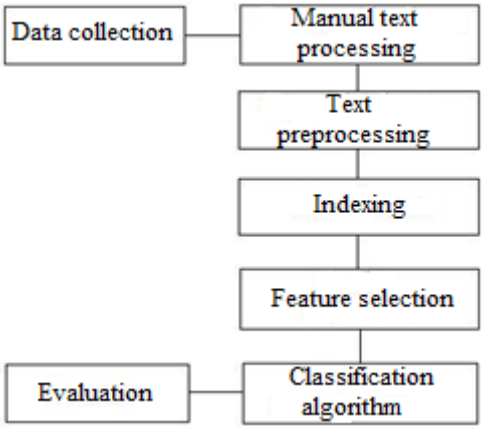

Figure 1 - Stages of text classification

2.2.1 Data collection

The website tengrinews.kz was chosen as the data source. The web scraping program is written in Python. And there are used libraries such as BeautifulSoup, requests, fake-useragent, as well as regular expressions. tengrinews.kz is a news website of Kazakhstan that publishes information about events on various topics [15]. For the classification of texts on emergency situations, the topics of traffic accidents, fire, earthquake and flood were considered. In the process, a request of the type - get was executed.

For a visual demonstration and ease of perception, a site in the Python language was designed. From the numerous sets of frameworks provided by this language, was chosen the Flask framework.

Figure 2 demonstrates a significant site for data collection. To collect identification to identify identified cases of dangerous situations. As a result, the database contains an xls file.

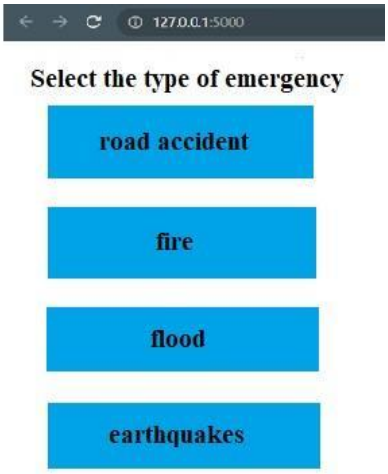

Figure 2 - Site for data collection

Table 1 provides general information about the collected database

Table 1 - Database information

Volume	6,07 MB
Number of columns	3
Number of lines (news)	1712

2.2.2 Manual processing of the text

When classifying text without manual processing, the performance indicators of the selected machine learning algorithms were low, and during the derivation of a set of features related to each category, these features did not accurately describe the category data, which prompted us to take the process of collecting data manually. Manual processing was carried out in an environment for working with spreadsheets excel. We sorted the news and filtered out irrelevant news into categories. It was necessary to collect data on other settings. As a result, the data was ready for software processing.

2.2.3 Preprocessing the dataset

Text pre-processing is a technique implemented during the initial stages of text classification systems. This stage is obligatory and may have a different structure depending on the tasks set.

Text pre-processing is the actions that must be performed when working with text in order to bring the text into a suitable form for further work. This process may change depending on the task and preferences.

- Convert text to lowercase;
- Partial or complete removal of numbers;
- Removing punctuation and punctuation marks in the text.
- Tokenization;
- Remove stop words. Such as connecting words, prepositions, conjunctions, interjections;
- Stemming;
- Lemmatization;
-Vector representation of words using CountVectorizer and TF-IDF.

When converting letters to lowercase, the ready-made language function lower () was used. Regular expressions were used to remove punctuation and punctuation marks, as well as to remove unwanted symbols and numbers. All of these manipulations on texts were placed in a function that we used repeatedly throughout the experiment. Tokenization was performed by a ready-made function, which makes it possible to quickly complete this stage. For a large amount of data, it is also necessary that the words have the initial form, which leads to the fact that the dimension decreases and the speed of the program execution increases.

Morphological analyzer pymorphy2 written in python converts words to normal form and returns the grammatical basis of words. This library is quite fast and uses the OpenCorpora dictionary. To remove stop words, we used a dictionary from the nltk library designed to perform all natural language treatment processes.

2.2.4 Indexing

Indexing is the process of converting text into numbers. Achieved using different models. For this work, the “bag of words” models was tested. As a result, the model calculated the weight of each word in the overall text. H ereinafter, indexing is necessary for the selection of features.

2.2. Feature Selection

One of the main stages in the text classification system is the stage of feature selection. In the process of performing this stage, factors such as the number of keywords, the correspondence of features to each category were taken into account. With a large number of unigrams, the system is considered ineffective. Table 2 presents the results of the work on the selection of features.

Table 2 - Unigrams and Bigrams

	fire	flood	Earthquake	road accident
Uni-gram	burn, ignition, fire, firefighter, flame	thousand, level, river, water, flood	underground, epicenter, push, magnitude, earthquake	Car crash, police, car, driver, road accident
Bigram	tremor, earthquake, magnitude			

2.3 Algorithm of classification

When performing this stage, the data is divided into test and training samples, the training data is used during the training of the algorithm, the test data is used to evaluate the efficiency of the classifier. In this work, machine learning algorithms such as k nearest neighborhood algorithm, logistic regression, and support vector machines were used to classify news about emergency situations.

2.3.1 K nearest neighbor (KNN) method

The knn algorithm consists of two stages: training and classification. During training, the algorithm remembers the vectors of each observation feature, in our case, the text, as well as the class labels of each object. It is necessary to set the parameter k, which is responsible for the number of neighborhoods required for object classification. During the stage of classifying an object for which a class label is not specified, neighborhood is determined and classification takes place based on these calculations [16].

2.3.2 Support Vector Machine (SVM*)*

Support Vector Machine is a supervised learning method that is known to be successful in a wide variety of applications. The high generalizing ability of the method makes it suitable especially for large data such as text. The principle of operation of this algorithm is to find the most correct hyperplane (line) that will divide the data into two or more classes. The algorithm receives at the input a certain set of classified data for training, after which, when

submitting unclassified texts, it outputs a class based on the separating plane [[17], [18]].

The advantages of the algorithm:

- trainability of the algorithm even with a small data set;
- the quality of the algorithm execution.

Disadvantages:

- problems in the presence of an outlier in the data;
- Difficulty in selecting parameters.

2.3.3 Logistic Regression Method (LR)

During the research work, it was decided to use multinomial logistic regression, due to the fact that the number of classes is more than two. Multinomial logistic regression is a variation of regular logistic regression, but in which the number of categories is greater than two. In our case, the number of categories in the dependent variable is four. In this algorithm, for each class in the number of the dependent variable, it is necessary to construct an equation as in binary (binary) logistic regression. One of the categories becomes the main pillar, the other categories of the dependent variable are compared with it [[19], [20]].

Advantages:

- has incremental learning.

The disadvantages of this method are similar to those of the SVM algorithm. Based on this information, these methods were selected for research and classification of texts on emergency situations.

2.5 Research data analysis

Before proceeding with the preliminary processing of a data set, it is advisable to conduct a research analysis of the data obtained. In text classification, the main problem faced by a large number of studies is the imbalance of data. This means that the data has the same amount across classes. Let's say if there are two classes and 95 ways tof processing unbalanced data. The first method assumes undersampling the majority class and resampling the minority class.

The second method implies the use of other metrics to evaluate the error, such as f1-score, recall, precision. When we analyze the data, we have indicators in the form of percentage of observations corresponding to each class. Figure 3 shows that the classes are balanced, so we did not use methods to compensate or remove the sample.

The next variable is the length of news by category, the diagram shows the distribution of length by category. From Figure 4, we can see that all four categories of emergency situations are almost the same length from 1000 to 2000 symbols. But news about a fire has a little more symbols, and news about an earthquake, on the contrary, has less symbols compared to other categories.

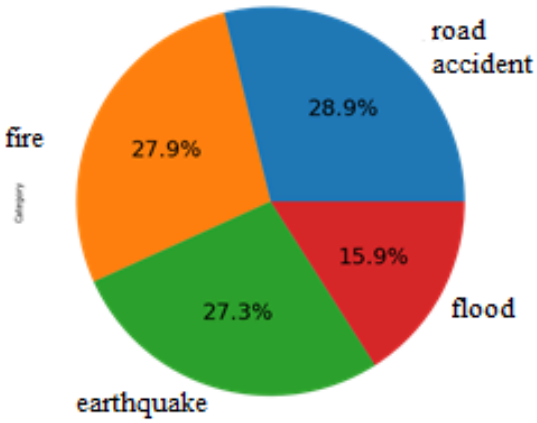

Figure 3 - Percentage of the number of news by category

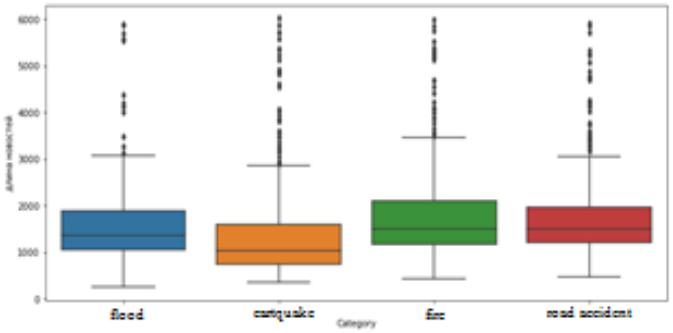

Figure 4 - Length of news by category

Results

For correct classification, it is necessary to take into account the aspects of dividing data into train and test. As practice shows, it is best to divide the data in proportions of 20% to 80% or 30% to 70%.

Data consisting of texts about emergency situations are divided in the proportions of 20-test and 80-train. Further, on this data, machine learning algorithms were used and the results of the effectiveness of each of them were provided. The k nearest neighborhood algorithm is calculated using the Euclidean distance. The number of neighborhoods affects the efficiency, so during the

experiment, their values were chosen according to high rates.

As shown in Figure 5, the classifier determined the class of the 97 texts correctly. The values 1, 1, 3 in the first line indicate that the classifier made a mistake 5 times in the course of work.

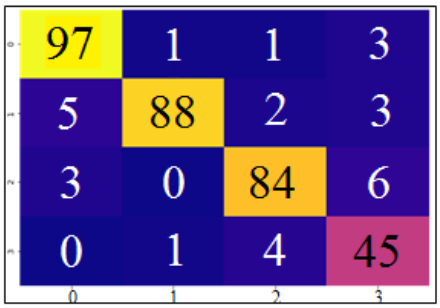

Figure 5 - KNN- confusion matrix

The metrics reflecting the efficiency of the classifier are shown in table 3. The highest indicators were obtained with the number of neighborhood equal to 8.

Table 3 - knn algorithm indicators

KNN	Accuracy	Recall	Precision	F1
6	0.92128	0.92062	0.91270	0.91517
3	0.91253	0.91021	0.90863	0.90879
8	0.93294	0.92842	0.92488	0.92597

The support vector machine, as well as the k nearest neighborhood algorithm, has reached high values. In this method, the parameter, called the core, was chosen as linear. In addition to the core, the value of the “C” parameter was adjusted, which is equal to 0.1. The effectiveness of this method was evaluated using the same quality metrics, the indicators of which are shown in Table 4.

Table 4 - Indicators of the SVM algorithm

	Accuracy	Recall	Precision	F1
SVM	0.96209	0.96179	0.95253	0.95658

In the Figure 6, you can see that the support vector classifier correctly classified 98 out of 102 texts in the first category.

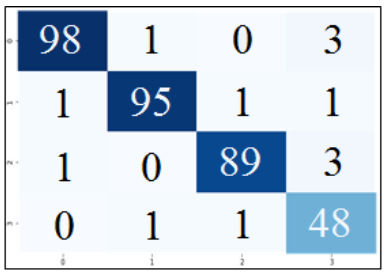

Figure 6 - SVM - confusion matrix

The results of the logistic regression method showed the highest values, which can be seen in Table 5 and the figure 7.

Table 5 - Indicators of the LR algorithm

	Accuracy	Recall	Precision	F1
Logistic Regression	0.97667	0.97452	0.97452	0.9734

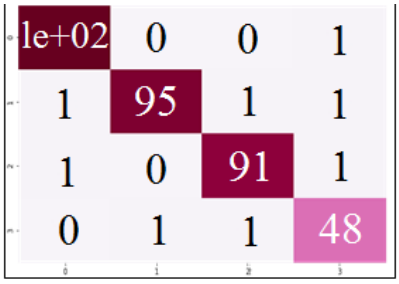

Figure 7 - LogisticRegression - confusion matrix

Conclusion

The aim of this article is to collect information about emergency situations and the subsequent classification of this data. Several methods of machine learning were chosen as algorithms.

- Data collection was carried out from the site tengrinews.kz.
- A text pre-processing process was performed, which includes the steps of clearing and converting the text to a number format.
- Before program processing, manual text processing was performed in the excel environment.
- We checked the set of features describing each category using the ''bag of words'' method.
- Comparing the methods of support vector machines, logistic regression and k nearest neighborhood , we came to the conclusion that logistic regression is in many ways superior to other machine learning algorithms. For comparison of methods, were used the metrics such as precision, f1, score, accuracy, recall.

- We compared methods such as logistic regression, k nearest neighborhood , support vector

machine. According to the result of the study, all three methods: support vector machine method, nearest neighbor method and logistic regression gave good results, but logistic regression is superior to other machine learning classification algorithms for the collected dataset. Method comparisons were achieved using metrics such as accuracy, precision, recall, f1 measure.

Conflict of interests

On behalf of all authors, the correspondent author declares that there is no conflict of interest.

Cite this article as: Kabdrakhova SS, Assan ZhZh, Nopembri S, Seilhan AM, Myrzakhmetov DE. Classification of texts on emergency situations in Almaty. Kompleksnoe Ispolzovanie Mineralnogo Syra = Complex Use of Mineral Resources. 2023; 327(4):23-31. https://doi.org/10.31643/2023/6445.36

Алматы қаласындағы төтенше жағдайлары бойынша мәтіндерді жіктеу

[1]Андиров М.Е., [1*]Асан Ж.Ж., [2]Nopembri S., [3]Сейлхан Ә.М., [1]Мырзахметов Д.Е.

[1]Әл-Фараби атындағы Қазақ ұлттық университеті, Алматы, Қазақстан
[2] Йогьякарта Мемлекеттік Университеті, Йогьякарта, Индонезия
[3]Қ.Қ.Жұбанов атындағы Ақтөбе ЕҰУ, Ақтөбе, Қазақстан

Мақала келді: *24 желтоқсан 2022*
Сараптамадан өтті: *18 қаңтар 2023*
Қабылданды: *31 қаңтар 2023*

ТҮЙІНДЕМЕ

Мәтіндерді жіктеу-бұл құрылымы бойынша әртүрлі мәтіндерді тиімді жіктеудің кезеңдері мен тәсілдерін қамтитын процесс. Бұл мақалада Алматы қаласының төтенше жағдайлар жөніндегі жаңалықтар сайттарынан жиналған мәтіндерді жіктеу үшін тірек векторлар әдісі, логистикалық регрессия, жақын көршілердің k әдісі сияқты машиналық оқыту алгоритмдері жүзеге асырылады. Тәжірибе барысында деректерді жинау кезеңі, сондай-ақ кейіннен оларды өңдеу ерекше рөл атқарды. Деректердің жиынтығын жіктеуден бұрын деректерге алдын-ала өңдеу жүргізілді, оған стоп сөздерін алып тастау, токенизация, стемминг, лемматизация, белгілерді алу, белгілердің векторларын құру сияқты қадамдар кіреді. Деректер арнайы скрипт көмегімен автоматты түрде жаңалықтар сайтынан алынды. Эксперименттік нәтижелер логистикалық регрессияға негізделген жіктеуіш алгоритмдердің басқа түрлерімен салыстырғанда ең жақсы өнімділік нәтижелерін беретінін көрсетеді. Әр алгоритмнің тиімділік көрсеткіштері алынды, бұл олардың арасында салыстырмалы талдау жасауға мүмкіндік береді.

Түйін сөздер: машиналық оқыту, мәтіндерді жіктеу, тірек векторлар әдісі, логистикалық регрессия, KNN, NLP, алдын-ала өңдеу, төтенше жағдайлар.

Авторлар туралы ақпарат:

Андиров Муса Ережепбайұлы — *Магистрант 2 курс, компьютерлік ғылымдар, ақпараттық технологиялар факультеті, әл-Фараби атындағы Қаз¥У, Алматы қ., Қазақстан. Email: andirov2610@gmail.com*

Асан Жанеля Жеңісқызы — *Магистрант 2 курс, компьютерлік ғылымдар, ақпараттық технологиялар факультеті, әл-Фараби атындағы Қаз¥У, Алматы қ., Қазақстан. Email: zh.assanova98@gmail.com*

Nopembri Soni — *Профессор, Йогьякарта Мемлекеттік Университеті, Йогьякарта, Индонезия. Email: soni_nopembri@uny.ac.id*

Сейлхан Әбілмансұр Мейрамғалиұлы — *Магистрант 2 курс, информатика және ақпараттық технологиялар, физика-математика факультеті, Қ. Жұбанов атындағы АӨУ , Ақтөбе, Қазақстан. Email: seilkhan.mansur@gmail.com*

Мырзахметов Диас Ерланұлы — *Магистрант 2 курс, компьютерлік ғылымдар, ақпараттық технологиялар факультеті, әл-Фараби атындағы Қаз¥У, Алматы қ., Қазақстан. Email: diko.17.04@gmail.com*

Классификация текстов по чрезвычайным ситуациям г. Алматы

[1]Андиров М.Е., [1*]Асан Ж.Ж., [2]Nopembri S., [3]Сейлхан А.М., [1]Мырзахметов Д.Е.

[1]Казахский национальный университет им. аль-Фараби, Алматы, Казахстан
[2]Джокьякартский государственный университет, Джокьякарта, Индонезия
[3]Актюбинский государственный университет имени К.К. Жубанова, Актобе, Казахстан

Поступила: *24 декабрь 2022*
Рецензирование: *18 января 2023*
Принята в печать: *31 января 2023*

АННОТАЦИЯ

Классификация текстов — это процесс, включающий в себя этапы и подходы для эффективной классификации разновидных по своей структуре текстов. В данной статье реализуются алгоритмы машинного обучения, такие как метод опорных векторов, логистическая регрессия, метод k ближайших соседей для классификации текстов собранных с новостных сайтов по чрезвычайным ситуациям г. Алматы. В ходе эксперимента особую роль играл этап сбора данных, а также их последующая обработка. Перед классификацией набора данных производилась предварительная обработка данных, которая включает в себя такие этапы как удаление стоп-слов, токенизация, стемминг, лемматизация, извлечение признаков, построение векторов признаков. Данные были получены с помощью автоматизированного сбора информации из открытых источников с помощью скрипта. Экспериментальные результаты показывают, что классификатор на основе логистической регрессии обеспечивает наилучшие результаты производительности по сравнению с другими видами алгоритмов. Были получены показатели эффективности каждого алгоритма, что дает нам выполнить сравнительный анализ между ними.

Ключевые слова: машинное обучение, классификация текстов, метод опорных векторов, логистическая регрессия, KNN, NLP, предобработка, чрезвычайные ситуации.

Информация об авторах:

Андиров Муса Ережепбайулы — *Магистрант 2 курс, компьютерные науки, факультет информационных технологий, КазНУ имени аль-Фараби, г. Алматы, Казахстан. Email: andirov2610@gmail.com*

Асан Жанеля Женискызы — *Магистрант 2 курс, компьютерные науки, факультет информационных технологий, КазНУ имени аль-Фараби, г. Алматы, Казахстан. Email: zh.assanova98@gmail.com*

Nopembri Soni — *Профессор Джокьякартского государственного университета, Джокьякарта, Индонезия. Email: soni_nopembri@uny.ac.id*

Сейлхан Абильмансур Мейрамгалиулы — *Магистрант 2 курс, информатика и информационные технологии, физико-математический факультет, Актюбинский РУ им. К.Жубанова, г. Актобе, Казахстан. Email: seilkhan.mansur@gmail.com*

Мырзахметов Диас Ерланулы — *Магистрант 2 курс, компьютерные науки, факультет информационных технологий, КазНУ имени аль-Фараби, г. Алматы, Казахстан. Email: diko.17.04@gmail.com*

References

[1] A Review of Machine Learning Algorithms for Text-Documents Classification. Aurangzeb Khan and Baharum Baharudin and Lam Hong Lee and Khairullah khan. JOURNAL OF ADVANCES IN INFORMATION TECHNOLOGY. 2010; 1:4-20.

[2] KNN based Machine Learning Approach for Text and Document Mining. Vishwanath Bijalwan and Vinay Kumar and Pinki Kumari and Jordan Pascual. International Journal of Database Theory and Application. 2014; 7:61-70.

[3] Krasnyansky MN, Obukhov AD, Solomatina EM, Voyakina AA. Sravnitel'nyj analiz metodov mashinnogo obucheniya dlya resheniya zadachi klassifikacii dokumentov nauchno-obrazovatel'nogo uchrezhdeniya [Comparative analysis of machine learning methods for solving the problem of classifying documents of the scientific and educational institution ques]. Vestnik VGU. 2018; 3:173-182. (in Russ.).

[4] Applying machine learning algorithms for automatic Persian text classification. Mojgan Farhoodi and Alireza Yari. International Conference on Advanced Information Management and Service. 2010; 6:318-323.

[5] Text Classification with Machine Learning Algorithms. Nasim VasfiSisi and Mohammad Reza and Feizi Derakhshi. Journal of Basic and Applied Scientific Research. 2013; 1:31-35.

[6] A Novel Active Learning Method Using SVM for Text Classification. Mohamed Goudjil and Mouloud Koudil and M. Bedda. International Journal of Automation and Computing. 2018; 15:290-298.

[7] Performance Analysis of Supervised Machine Learning Algorithms for Text Classification. Sadia Zaman Mishu and Rafiuddin SM. International Conference on Computer and Information Technology. 2016; 19:409-413.

[8] Study on SVM Compared with the other Text Classification Methods. Xiaoyu Luo. Alexandria Engineering Journal. 2021; 60:3401-3409.

[9] Text Classification Using Machine Learning Techniques. Ikonomakis, Emmanouil and Kotsiantis and Sotiris and Tampakas, V. WSEAS transactions on computers. 2005; 4:966-974.

[10] A survey of text classification algorithms. Aggarwal Charu C. and ChengXiang Zhai. Mining text data. Springer. 2012; 4:163-222.

[11] Text classification by labeling words. Liu and Bing. AAAI. 2004, 4.

[12] A Comparative Study for Email Classification, Advances and Innovations in Systems. Seongwook Youn and Dennis McLeod. Computing Sciences and Software Engineering. 2007, 387-391.

[13] Keikha, Mostafa and Razavian, Narjes and Oroumchian, Farhad and Razi, Hassan, Document Representation and Quality of Text: An Analysis, Survey of Text Mining II: Clustering, Classification, and Retrieval. 2008, 219-232.

[14] Ontolo gy-Based Classification Of News In An Electronic Newspaper. Lena Tenenboim and Bracha Shapira and Peretz Shoval. International Conference Intelligent Information and Engineering Systems. 2008.

[15] The news site is tengrinews.kz [Electronic resource]. Access mode: https://tengrinews.kz/kazakhstan_news/devushka-sportkare-sovershila-dtp-vyiezjaya-kluba-almatyi-466091/

[16] Li Qian, Hao Peng, Jianxin Li, Congying Xia, Renyu Yang, Lichao Sun, Philip S. Yu, and Lifang He. A Survey on Text Classification: From Traditional to Deep Learning. ACM Transactions on Intelligent Systems and Technology (TIST) 13. 2022; 2:1-41.
[17] Study on SVM Compared with the other Text Classification Methods. Zhijie Liu and Xueqiang Lv and Kun Liu and Shuicai Shi. 2010 Second International Workshop on Education Technology and Computer Science. 2010; 1:219-222.
[18] An Optimal SVM-Based Text Classification Algorithm. Zi-qiang Wang and Xia Sun and De-xian Zhang and Xin Li. International Conference on Machine Learning and Cybernetics. 2006; 60:1378-1381.
[19] Li Qian, Hao Peng, Jianxin Li, Congying Xia, Renyu Yang, Lichao Sun, Philip S. Yu, and Lifang He. A Survey on Text Classification: From Traditional to Deep Learning. ACM Transactions on Intelligent Systems and Technology (TIST) 13. 2022; 2:1-41.
[20] Sabri T, El Beggar O, and Kissi M. Comparative study of Arabic text classification using feature vectorization methods. Procedia Computer Science. 2022; 198:269-275.
[21] Wadud MAH, Kabir MM, Mridha MF, Ali MA, Hamid MA, and Monowar MM. How can we manage offensive text in social media-a text classification approach using LSTM-BOOST. International Journal of Information Management Data Insights. 2022; 2:100095.

Crossref
DOI: 10.31643/2023/6445.37
Engineering and technology

Investigation of the Technology of Introducing Li, Mg and Zr Alloys into Aluminum Alloy

[*1] Ablakatov I.K., [1]Ismailov M.B., [1] Mustafa L.M., [2] Sanin A.F.

[1] «National Center for Space Research and Technology» JSC, Almaty, Kazakhstan
[2] Oles Honchar Dnipro National University, Dnipro, Ukraine

** Corresponding author email: termostators@gmail.com*

Received: *August 12, 2022*
Peer-reviewed: *September 06, 2022*
Accepted: *January 31, 2023*

ABSTRACT

This article is devoted to the study of the initial phase of obtaining alloy 1420, namely, obtaining a primary material with the desired chemical composition. The effect of alloying magnesium, zirconium and lithium on the strength properties of the material. In the work, the following materials were used to obtain a cast aluminum alloy of the Al-Mg-Zr-Li system: aluminum of technical purity A0 or A5, magnesium Mg95, lithium LE-1, zirconium E100, aluminum-zirconium ligature AlZr5, aluminum-lithium ligature AlLi10. Two methods were used to introduce zirconium into the liquid Al-Mg alloy: the introduction of pure zirconium and the introduction of zirconium in the form of a ligature. Two methods were used to introduce lithium into the Al-Mg-Zr liquid alloy: the introduction of lithium in the form of a ligature and the introduction of pure lithium. Cast alloys of the Al-Mg-Zr-Li system with the following characteristics were obtained: chemical composition: Al-92.245%, Mg-5.00%, Zr-0.105%, Li-2.21%, Si-0.238%, impurities-0.202%. Mechanical properties: Brinell hardness 85 HB, microhardness 139 MPa, compressive strength 149.6 MPa, elastic modulus 12 GPa, compressive yield strength 175.2 MPa and plastic deformation modulus 0.83 GPa.

Keywords: aluminum, aluminum-lithium alloys, Al-Mg-Zr-Li, melting, casting, ligature

Ablakatov Ilyas Kabylashimuly	*Junior Researcher, National Center for Space Research and Technology JSC, Almaty, Kazakhstan. Email: termostators@gmail.com*
Ismailov Marat Bazaraliyevich	*Doctor of Engineering, Professor, Director of the Space Materials Science and Instrumentation Department under National Center for Space Research and Technology JSC, Almaty, Kazakhstan. Email: m.ismailov@gmail.com*
Mustafa Laura Moldakerimovna	*Head of the laboratory, National Center for Space Research and Technology JSC, Almaty, Kazakhstan. Email: Mustafa_laura@mail.ru*
Sanin Anatoly Fedorovich	*Doctor of Engineering, Professor. Professor of the department. Oles Honchar Dnipro National University, Dnipro, Ukraine. Email: afedsa60@gmail.com*

Introduction

Among aluminum alloys, the alloys of the Al-Li system are characterized by high strength characteristics, high corrosion resistance, and are easily amenable to any type of welding. It is known that welded aluminum structures give a significant weight advantage compared to riveted structures. For example, welded aluminum structures reduce the weight of aircraft, up to 15-25%. Earlier, in [1] were considered alloys of the Al-Li system, their types, properties, and applications. The simplest alloy 1420, as well as the possibilities of its production at Kazakhstani plants are considered in more detail. This alloy, belonging to the high-level category, has the following chemical composition: 1.9-2.3% Li; 5-6% Mg; 0.09-0.15% Zr; 0.1-0.3% Si, res. Al.

This article is devoted to the study of the initial phase of obtaining alloy 1420, namely, obtaining a primary material with the desired chemical composition. To begin with, let's consider the effect of alloying magnesium, zirconium and lithium on the strength properties of the material.

Magnesium helps to increase the strength of aluminum alloys due to the formation of a solid solution of Al-Mg, as well as by deformation hardening by riveting or cold hardening (Figure 1,2) [[2],[3]]. As can be seen in Figure 1 and 2, magnesium significantly affects the strength of aluminum. With a magnesium content of 5% (wt.) the yield strength of aluminum increases from 25

MPa to 160MPa. With a magnesium content of 2.5% (wt.) the ultimate strength increases from 180 MPa to 320 MPa with cold rolling up to 80%.

In Al-Mg alloys containing up to 6% Mg, an Al_3Mg_2 intermetallic compound is formed with a solid solution of magnesium in aluminum. An increase in the magnesium content by 1% increases the ultimate strength of the alloy by ≈ 30 MPa, and the yield strength by ≈ 20 MPa. At the same time, the relative elongation decreases slightly and is within the range of 30-35% [[4], [5]]. In addition, an increase in the magnesium content of more than 6% leads to a deterioration in the corrosion resistance of the alloy. At a temperature of 300 °C, 6.7% Mg is dissolved in the alloy. Magnesium, which has not dissolved, is in the structure and forms Al_3Mg_2, Mg_5Al_8 compounds in solid solution. This does not add additional strength, but reduces the plastic properties of the alloy. To improve the plastic properties of the alloy, the percentage of silicon and iron in it is reduced, and zirconium and titanium are added [[6], [7]].

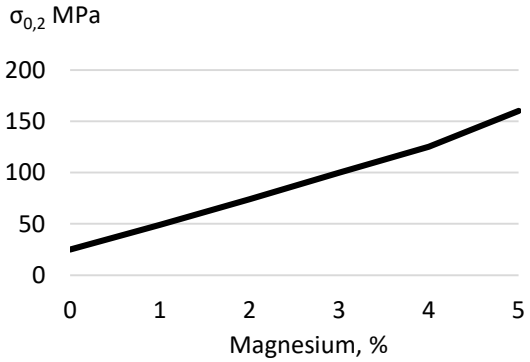

Figure 1 - The effect of magnesium on strength of aluminum alloy

The influence of lithium on the properties of Al-Mg and Al-Mg-Si alloys is given in [[8], [9], [10]]. The authors found that in the process of artificial aging, the dispersion-hardening phases of Al_3Li, Al_2MgLi and Mg_2Si are formed in the alloy. The fine phases of Al_3Li are isolated by reducing the solubility of lithium in the solid state when added to the Al-Mg alloy. The Al_2MgLi phase is formed at a high magnesium content >4%. The main hardening in Al-Mg and Al-Mg-Si alloys occurs precisely due to the Al_3Li and Al_2MgLi phases. Also, the Al_2MgLi phase improves the corrosion resistance of the alloy itself.

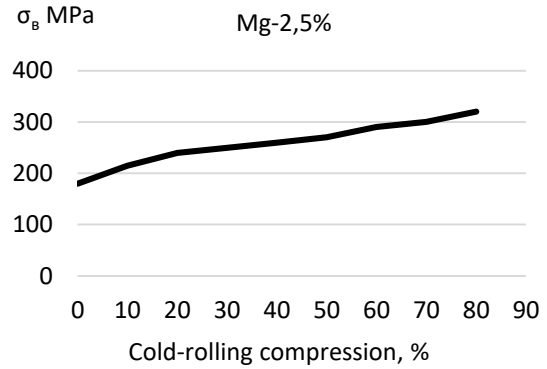

Figure 2 - The effect of deformation on strength of aluminum alloy

The authors Shamas ud Din, Hasan Bin Awais [[11], [12]] investigated the effect of lithium on the properties of Al-Mg-Si alloys. The research results showed (Figure 3, 4) that when lithium is introduced up to 3%, the strength limit of Al-Mg-Si alloys increases from 60 MPa to 350 MPa and when lithium is introduced up to 2%, the microhardness increases from 50 HV in the cast state to 90 HV in the aged state.

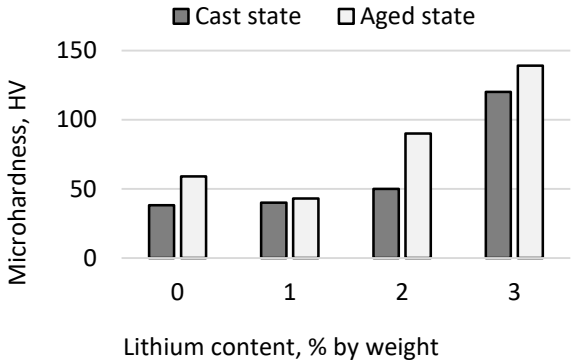

Figure 3 - The effect of lithium on the microhardness of Al-Mg-Si alloys

It is known [1] that the addition of 1% lithium reduces the density of the alloy by 3% and increases the modulus of elasticity by 6%. For example, Figures 5 and 6 show the effects of lithium, magnesium, and zirconium content on Young's modulus and aluminum density. With an increase in the lithium content to 1%, the density of aluminum decreases from 2690 mg/cm^3 to 2600 mg/cm^3 and the Young's modulus increases from 66-67 GPa to 70-71 GPa [[13],[14]]. With a lithium content of up to 1.8%, the aluminum alloy has a low resistance to stress corrosion, and at 1.9% the alloy becomes resistant to corrosion cracking. With a lithium content of 1.9-

2.0%, the tensile strength and yield strength increases, but the plastic properties decrease. A further increase in the lithium content from 2.1 to 2.3% contributes to an increase in looseness and the appearance of cracks [[15], [16]]. As can be seen, lithium is the most effective alloying element, which significantly increases the Young's modulus and reduces the density of aluminum.

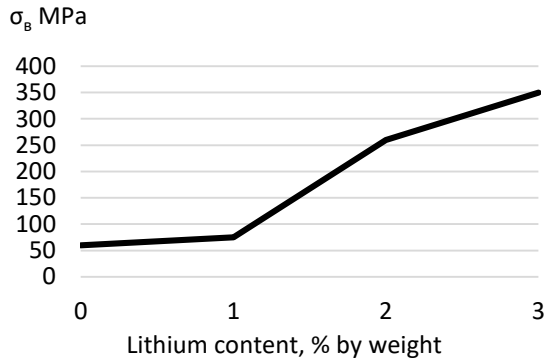

Figure 4 - The effect of lithium on the strength of Al-Mg-Si alloys

Zirconium forms with aluminum and lithium a composite intermetallic Al_3Zr–Al_3Li, which improves the ductility of the alloy. In aluminum alloys, the Al_3Zr phase is used as a grain shredder, which improves the impact strength [[17], 18], [19], [20]].

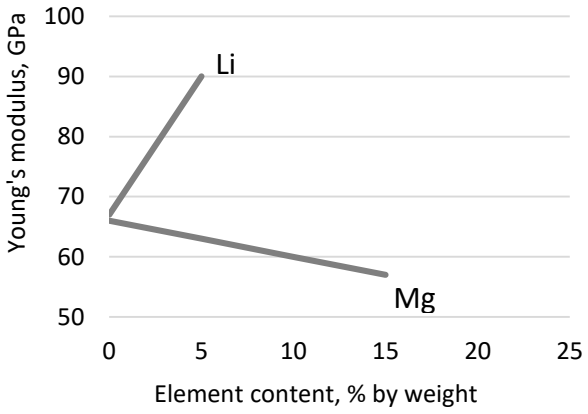

Figure 5 - Effect of alloying elements on Young's modulus

Thus, in this paper, the methods of alloying lithium, magnesium and zirconium into aluminum are considered. Difficulties in this work are associated with the processes of introducing zirconium and especially lithium into the liquid-alloy. Information on the technology of obtaining alloy 1420 is not disclosed in open literature sources, since this alloy with a strength of $\sigma_B \geq 415$ MPa falls under the export control regime of goods and technologies for missile, dual-use and nuclear purposes.

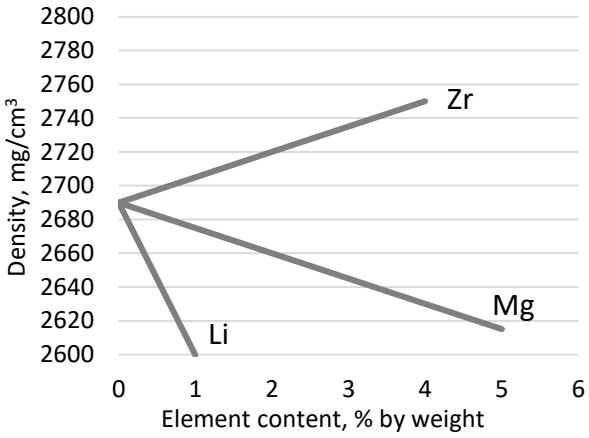

Figure 6 - Effect of alloying elements on aluminum density

The experimental part

To obtain the aluminum alloy of the Al-Mg-Zr-Li system, melting and casting were carried out in a vacuum induction furnace UIPV-0.001 (JSC "IMiO", Almaty). The unit is equipped with various mechanisms and devices that load metal into the crucible, electromagnetic mixing, casting into molds, measuring the liquid-alloy temperature and pressure in the chamber. The maximum heating temperature of the furnace reaches 2000 ^{0} C, the residual pressure is 100 Pa. The entire process of melting, aging, alloying, casting and cooling takes place in a vacuum or in an argon atmosphere.

To determine the chemical composition and study the microstructure of samples, samples with a diameter of 40 mm and a height of 15 mm were cut from cast bars. The samples were cut at the Brilliant 221 unit. The cut samples were ground and polished on a Rubin 500 - Sahpir 320e machine using sanding papers and polishing suspensions from 15 microns to 1 microns. To identify the structure, the surface of the samples was etched with 10% nitric acid solution and 30% hydrofluoric acid solution. The microstructure of the polished and etched samples was studied using a Zeiss Axiovert 200 Mat optical microscope. The chemical composition was studied using an X-ray fluorescence semi-quantitative spectrometer Axios 1kW PANalytical (JSC "IMiO"), an atomic emission spectrometer Optima 8300 DV (JSC

"IMiO") and an electron probe chemical analyzer Joel Superprobe 733 (Institute of Geological Sciences named after K. I. Satpayev). To study the mechanical properties, compression tests were carried out on Shimadzu AG testing machine (JSC "IMiO"), Brinell hardness on the HBV-30A hardness tester (JSC "IMiO") and microhardness on the PMT-3 microhardometer (JSC "National Center for Space Research and Technology"). For compression tests, cylindrical samples were manufactured according to GOST 25.503-97 with dimensions of 40/60 mm. To determine the Brinell hardness, samples were made according to GOST 9012-59 with the extrusion of a 2 mm ball of hardened steel up to 10 prints with a load of 5 kgf. To determine the microhardness, the samples were made according to GOST 9450-76 with the extrusion of a diamond pyramid up to 30 prints with a load of 10 g. The phase composition of the samples was determined using an X-ray diffractometer DRON-3. Polished samples in the form of square plates with dimensions of 10/10/1 mm were prepared for the study.

In the work, the following materials were used to obtain a cast aluminum alloy of Al-Mg-Zr-Li system: aluminum of technical purity A0 or A5, magnesium Mg95, lithium LE-1, zirconium E100, aluminum-zirconium ligature AlZr5, aluminum-lithium ligature AlLi10. The composition of the charge materials from which the cast alloys of the Al-Mg-Zr and Al-Mg-Zr-Li systems were smelted is shown in Table 1.

Two methods were used to introduce zirconium into the Al-Mg liquid-alloy: the introduction of pure zirconium (series No. 1) and the introduction of zirconium in the form of a ligature (series No. 2). Two methods were used to introduce lithium into the Al-Mg-Zr liquid-alloy: the introduction of lithium in the form of a ligature (series No. 3) and the introduction of pure lithium (series No. 4). All series of experiments are given below:

Experiment Series No. 1. Aluminum A0, magnesium Mg95 and zirconium E100 were used to produce the Al-Mg-Zr liquid-alloy. Aluminum and zirconium charge was simultaneously introduced into the crucible. Since the melting point of zirconium is higher than the melting point of aluminum, melting was carried out in a vacuum of 100 Pa at a temperature of 800 ^{0} C, then kept for 5 minutes and cooled to 700 ^{0} C, after which argon was injected to prevent magnesium evaporation and magnesium was injected. After that, the melt was kept for 5, 10, 20 minutes and cast into a graphite mold. Cooled in the chamber.

Experiment Series No. 2. Aluminum A5, magnesium, and zirconium ligature AlZr5 were used to produce the Al-Mg-Zr liquid-alloy. Aluminum and zirconium ligature were simultaneously loaded into the crucible, melted in a vacuum of 100 Pa at a temperature of 800 ^{0}C. At this temperature, they were kept for 5 minutes, after which the liquid-alloy was cooled to 700 ^{0}C, then argon was injected and a magnesium charge materials were introduced. After that, the liquid-alloy was kept for 5, 10, 20 minutes at a temperature of 700 ^{0}C. Then the liquid-alloy was poured into graphite molds and cooled in the chamber.

Experiment Series No. 3. Aluminum A5, magnesium Mg95, zirconium ligature AlZr5, lithium ligature AlLi10 were used to produce the Al-Mg-Zr-Li liquid-alloy. Aluminum, lithium ligature and zirconium ligature were melted at a temperature of 700 ^{0}C in an argon medium, then a magnesium suspension was introduced and kept for 5, 10 or 20 minutes at the same temperature. After that, the finished liquid-alloy was poured into a graphite mold and cooled inside the chamber.

Experiment Series No. 4. Aluminum A5, magnesium Mg95, lithium LE-1 and zirconium ligature AlZr5 were used to produce the Al-Mg-Zr-Li liquid-alloy. Aluminum, lithium and zirconium ligature were melted at a temperature of 700 ^{0}C in an argon medium and a magnesium charge materials were added, then kept for 5, 10 or 20 minutes at a temperature of 700 ^{0}C in an argon atmosphere. After that, the finished liquid-alloy was poured into a graphite mold and cooled inside the chamber.

Results of the experiment series No. 1-4

The chemical composition of the obtained cast samples of Al-Mg-Zr-Li with different sequences of magnesium, lithium, AlZr5 and AlLi10 ligatures is shown in Table 2.

As can be seen from Table 2, the samples obtained in Series No. 1 contain a significant silicon content of 0.269-0.346% and other impurities of 0.735-0.78%. The use of A0 grade aluminum with a high impurity content does not give the desired result in terms of purity of the chemical composition, the total impurity content of which reaches up to 1.14%. The impurity content of more

Table 1 - Elemental composition of the charge materials in a series of experiments

Samples of charge materials of a series of experiments	Elemental composition of the charge materials, % by weight.					
	Al	***Mg***	***Zr***	***AlZr5 (Zr-5%)***	***Li***	***AlLi10 (Li-10%)***
1	93.58	6.3	0.12	-	-	-
2	91.3	6.3	-	2.4	-	-
3	91.38	5.3	-	2.4	2.2	-
4	70.3	5.3	-	2.4	-	22

Table 2 - Chemical composition of Al-Mg-Zr and Al-Mg-Zr-Li samples

Experiment series	Exposure time, min.	Elemental composition, %					
		Al	***Mg***	***Zr***	***Li***	***Si***	***Impurities***
No.1. Al +Zr+ Mg	5	91.828	6.238	0.122	-	0.346	0.735
	10	92.76	6.034	0.124	-	0.344	0.76
	20	92.687	5.987	0.123	-	0.269	0.78
No.2. Al +AlZr5 + Mg	5	93.044	6.138	0.107	-	0.203	0.24
	10	93.285	6.023	0.102	-	0.212	0.24
	20	93.372	5.733	0.105	-	0.201	0.22
No.3. Al-Mg+ AlZr5 + AlLi10	5	92.545	4.74	0.112	2.2	0.231	0.178
	10	92.577	4.69	0.108	2.16	0.232	0.207
	20	92.656	4.63	0.094	2.18	0.241	0.162
No.4. Al-Mg + AlZr5 + Li	5	92.245	5.00	0.105	2.21	0.238	0.202
	10	92.443	4.87	0.101	2.1	0.235	0.210
	20	92.588	4.73	0.098	2.14	0.250	0.183

than 1% negatively affects the mechanical properties of the alloy. Therefore, in the subsequent series of experiments, a cleaner grade A5 aluminum was used. In the whole series of experiments, a decrease in the magnesium content is observed with an increase in the exposure time from 5 to 20 minutes. The zirconium content in series No. 1, 2 and 4 is kept in the range of 0.098-0.124%, which corresponds to the specified amount of suspension for alloying. In series No. 3, the magnesium content of the samples sharply decreases from the specified 5.3% to 4.63-4.74%, zirconium from 0.12% to 0.094-0.112%. The decrease in magnesium in all series of experiments is explained by the fact that magnesium is an active element and over 560 ^{0}C interacts with oxygen, which remains after pumping in a vacuum chamber and is present in the composition of the injected argon. The chemical composition of the alloy obtained in the experiment series No. 4 with an exposure time of 5 minutes is optimal, since the chemical composition is close to the specified content of the charge materials components and contains fewer impurities.

The microstructures of the Al-Mg-Zr and Al-Mg-Zr-Li samples obtained with a Zeiss Axiovert 200 Mat optical microscope are shown in Figures 7 and 8.

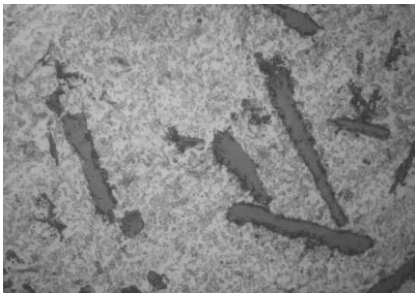

Figure 7 – Microstructures of the Al-Mg-Zr alloys (magnification x200). Series No. 1.

Figure 8 – Microstructures of the Al-Mg-Zr alloys (magnification x200). Series No. 2.

As can be seen in Figure 7, the samples of Al-Mg-Zr series No. 1 consists of Al, a solid solution of Mg in Al and an intermetallic Al_3Mg_2. The alloy also contains a large number of clusters of primary crystals in the form of needle plates. The separation of primary Al_3Zr crystals from the liquid-alloy in the studied temperature range of 700-800 °C is most likely due to the heterogeneity of the liquid-alloy, which is confirmed by the uneven separation of particles in the form of clusters whose sizes reached more than 100 microns (Figure 7). Thus, in the course of research, it was found that as parameters for melting and casting bars from the alloys of the Al-Mg-Zr system, it is advisable to use zirconium ligature instead of metal pieces of zirconium, since zirconium in this case dissolves in the aluminum liquid-alloy and separation of smaller primary crystals of $Al_3Zr \leq 100$ microns occurs (Figure 8). Introduction of zirconium ligature into the aluminum liquid-alloy is an optimal choice when melting the alloy, because the zirconium ligature is evenly and faster distributed over the entire volume of the liquid-alloy compared to metallic zirconium, as evidenced by the analysis of the micrograph of the Al-Mg-Zr alloy from series No. 2. In this regard, in subsequent experiments of series No. 3 and No. 4, a zirconium ligature was used to introduce zirconium into the liquid-alloy.

The following phases are present in the microstructure of the Al-Mg-Zr-Li alloys of series No. 3 and No. 4: Al, Mg solid solution in Al, Al_3Mg_2, Al_3Zr. As can be seen in Figure 9, the Al-Mg-Zr-Li alloy has a dendritic structure with many different inclusions. As it turned out, these inclusions appeared when the AlLi10 ligature was added.

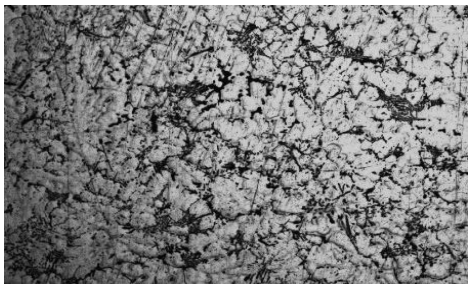

Figure 9 – Microstructures of the Al-Mg-Zr-Li alloys (magnification x200). Series No. 3

As is already known, lithium is coated with an oxide film at room temperature. The introduction of such a ligature into the aluminum liquid-alloy leads to the appearance of many oxide films. These captives complicate the merging into the mold and fall into the cast bar. Lithium could also react with hydrogen (present in argon) at 500-700 ^{0}C, with iron and silicon (present in aluminum) at 600-700 ^{0}C and with carbon (graphite cast). When composing the charge materials, it is recommended to exclude the use of AlLi10 ligatures.

As can be seen in Figure 10, in the structure of the Al-Mg-Zr-Li alloy of series No. 4 there are also Al phases, Mg solid solution in Al, Al_3Mg_2, Al_3Zr. The multitude of phases makes it difficult to visually identify each phase, including the lithium phases that are present in the alloy.

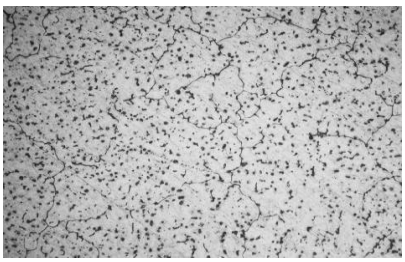

Figure 10 – Microstructures of the Al-Mg-Zr-Li alloys (magnification x200). Series No. 4

To determine the phases with lithium, an additional X-ray diffractometric analysis was performed on a DRON-3 diffractometer. The results of the phase analysis are shown in Figure 11.

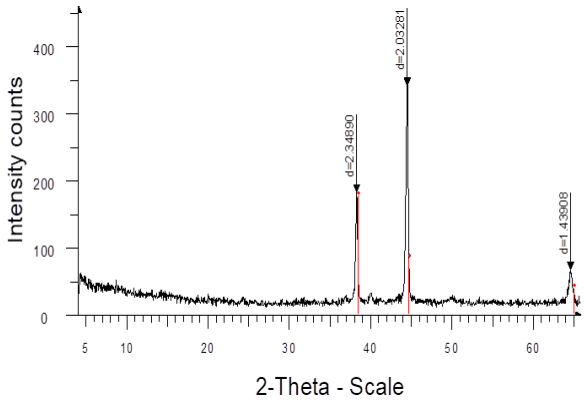

Figure 11 – Diffractogram of the presence of phases of aluminum with lithium

Peak d=2.03281 corresponds to 100% aluminum content, peak d=2.34890 has an atomic content of 53.3% aluminum and 46.7% lithium. This atomic ratio corresponds to the AlLi phase. The peak d=1.43908 has an atomic content of 19.5% aluminum and 80.5% lithium. This atomic ratio corresponds to the phase Al_4Li_9.

Table 3 – Mechanical properties of Al-Mg-Zr and Al-Mg-Zr-Li alloy

No.	**1**	**2**	**3**	**4**
Alloy	***Al +Zr + Mg***	***Al +AlZr5 + Mg***	***Al-Mg + AlZr5 + AlLi10***	***Al-Mg + AlZr5 + Li***
Brinell hardness , HB	80.0	82.14	69.1	85.0
Microhardness, MPa	148	154	97.2	139
Compression elastic limit $\sigma_{0.05}$, MPa	69.8	138.7	99.5	149.6
Modulus of elasticity, E_1, GPa	3.5	10.5	9.5	12
Modulus of plastic deformation, E2, GPa	1.1	1.2	0.9	0.83
Yield strength at compression $\sigma_{0.2}$, MPa	77.22	164.5	119	175.2
Deformation at 500 MPa, %	31	20	32.6	20

Compression, hardness and microhardness tests were carried out to study the mechanical properties of the samples. The results of the mechanical properties of alloys of the Al-Mg-Zr and Al-Mg-Zr-Li systems are shown in Table 3.

As can be seen from Table 3, Al-Mg-Zr alloys of series No. 2, compared with alloys of series No. 1, show an increase in all characteristics: Brinell hardness from 80 to 82.14 HB, microhardness from 148 to 154 MPa, compressive strength from 69.8 to 138.7 MPa, modulus of elasticity from 3.5 to 10.5 GPa, modulus of plastic deformation from 1.1 to 1.2 GPa, yield strength under compression from 77.22 to 164.5 MPa. Such indicators are achieved due to the uniform distribution of zirconium in the liquid-alloy by introducing zirconium ligature instead of metallic zirconium.

Al-Mg-Zr-Li alloys of series No. 4 compared with alloys of series No. 3 showed an increase in Brinell hardness from 69.1 to 85 HB, microhardness from 97.2 to 139 MPa, compressive strength from 99.5 to 149.6 MPa, elastic modulus from 9.5 to 12 GPa, compressive yield strength from 119 up to 175.2 MPa and with a slight decrease in plastic deformation modulus from 0.9 to 0.83 GPa. As noted earlier, the introduction of the AlLi10 ligature negatively affects the mechanical properties of the Al-Mg-Zr-Li alloy. It is advisable to use lithium in its pure form.

Conclusions

Cast alloys of the Al-Mg-Zr-Li system with the following characteristics were obtained:

- chemical composition: Al-92.245%, Mg-5.00%, Zr-0.105%, Li-2.21%, Si-0.238%, impurities-0.202%

- mechanical properties: Brinell hardness 85 HB, microhardness 139 MPa, compressive strength 149.6 MPa, elastic modulus 12 GPa, compressive yield strength 175.2 MPa and plastic deformation modulus 0.83 GPa.

- production technology: melting aluminum, lithium and AlZr5 ligatures at a temperature of 700 ^{0}C in an argon medium, then adding a magnesium sample to the liquid-alloy and holding for 5 minutes at a temperature of 700 ^{0}C in an argon atmosphere. Draining the finished liquid-alloy into the graphite cast and cooling inside the chamber.

Conflict of interest. On behalf of all the authors, the correspondent author declares that there is no conflict of interest.

Gratitude. This study is funded by the Science Committee of the Ministry of Education and Science of the Republic of Kazakhstan (Grant № 00037/GF)", where 00037/GF (№ 00037/ГФ) is the IRN of the project.

Cite this article as: Ablakatov IK, Ismailov MB, Mustafa LM, Sanin AF. Investigation of the Technology of Introducing Li, Mg and Zr Alloys into Aluminum Alloy. Kompleksnoe Ispolzovanie Mineralnogo Syra = Complex Use of Mineral Resources. 2023; 327(4):32-40. https://doi.org/10.31643/2023/6445.37

Легірлеуші Li, Mg және Zr металдарын алюминий қорытпасына енгізу технологиясын зерттеу

[1] Аблакатов И.К., [1] Исмаилов М.Б., [1] Мұстафа Л.М., [2] Санин А.Ф.

[1] «Ұлттық ғарыштық зерттеулер мен технологиялар орталығы» АҚ, Алматы, Қазақстан
[2] Олеся Гончар атындағы Ұлттық университет, Днепр, Украина

Мақала келді: *12 тамыз 2022*
Сараптамадан өтті: *06 қыркүйек 2022*
Қабылданды: *31 қаңтар 2023*

ТҮЙІНДЕМЕ

Al-Mg-Zr-li жүйесінің келесі сипаттамалары бар құйма қорытпалары алынды: химиялық құрамы: Al-92,245%, Mg-5,00%, Zr-0,105%, Li-2,21%, Si-0,238%, қоспалар-0,202%. Механикалық қасиеттері: 85 НВ Бринелл қаттылығы, 139 МПа микроқаттылығы, 149,6 МПа қысу серпімділік шегі, 12 ГПа серпімділік модулі, 175,2 МПа қысу кезінде аққыштық шегі және 0,83 гПа пластикалық деформация модулі. Алу технологиясы: аргонның ортасында 700^0с температурада алюминий, литий және $AlZr_5$ лигатурасын балқыту, содан кейін балқымаға магнийдің нақты мөлшерін қосу және аргон атмосферасында 700^0с температурада 5 минут ұстау. Дайын балқыманы графит құймасына ағызып, камера ішінде салқындату. Al-Mg-Zr-Li жүйесінің алюминий қорытпасын алу үшін балқыту және құю УИПВ-0,001 вакуумдық индукциялық пеште ("ИМиО" АҚ, Алматы) жүргізілді. Бұл мақала 1420 қорытпасын алудың бастапқы кезеңін зерттеуге, атап айтқанда қажетті химиялық құрамы бар бастапқы материалды алуға және магний, цирконий және литий легірлеушілерінің материалдың беріктік қасиеттеріне әсеріне арналған.

Түйін сөздер: алюминий, алюминий-литий қорытпалары, Al-Mg-Zr-Li, балқыту, құю, лигатура

Аблакатов Ілияс Қабылашымұлы — *Кіші ғылыми қызметкер," Ұлттық ғарыштық зерттеулер мен технологиялар орталығы " АҚ, Алматы, Қазақстан. Email: termostators@gmail.com*

Исмаилов Марат Базаралыұлы — *Техника ғылымдарының докторы, профессор, ғарыштық материалтану және аспап жасау департаментінің директоры, "Ұлттық ғарыштық зерттеу және технологиялар орталығы" АҚ, Алматы, Қазақстан. Email: m.ismailov@gmail.com*

Мұстафа Лаура Молдакерімқызы — *"Ұлттық ғарыштық зерттеулер және технологиялар орталығы" АҚ зертхана меңгерушісі, Алматы, Қазақстан. Email: Mustafa_laura@mail.ru*

Санин Анатолий Федорович — *Техника ғылымдарының докторы, профессор. Кафедра профессоры. Олеся Гончар атындағы Ұлттық университет, Днепр, Украина. Email: afedsa60@gmail.com*

Исследование технологии введения в алюминиевый сплав легирующих Li, Mg и Zr

[1] Аблакатов И.К., [1] Исмаилов М.Б., [1] Мустафа Л.М., [2] Санин А.Ф.

[1] АО «Национальный центр космических исследовании и технологии», Алматы, Казахстан
[2] Днепровский национальный университет имени Олеся Гончара, Днепр, Украина

Поступила: *12 августа 2022*
Рецензирование: *06 сентября 2022*
Принята в печать: *31 января 2023*

АННОТАЦИЯ

Получены литые сплавы системы Al-Mg-Zr-Li со следующими характеристиками: химический состав: Al-92,245%, Mg-5,00%, Zr-0,105%, Li-2,21%, Si-0,238%, примеси-0,202%. Механические свойства: твердость по Бринеллю 85 НВ, микротвердость 139 МПа, предел упругости при сжатии 149,6 МПа, модуль упругости 12 ГПа, предел текучести при сжатии 175,2 МПа и модуль пластической деформации 0,83 ГПа. Технология получения: плавка алюминия, лития и $AlZr_5$ лигатуры при температуре 700^0С в среде аргона, затем добавление навески магния в расплав и выдержка в течении 5 минут при температуре 700^0С в атмосфере аргона. Слив готового расплава в графитовую изложницу и охлаждение внутри камеры. Для получения алюминиевого сплава системы Al-Mg-Zr-Li плавка и литье проводились в вакуумной индукционной печи УИПВ-0,001 (АО «ИМиО», Алматы). Настоящая статья посвящена исследованию начальной фазы получения сплава 1420, а именно получению первичного материала с нужным химическим составом, влиянию легирующих магния, циркония и лития на прочностные свойства материала.

Ключевые слова: алюминий**,** алюминий-литиевые сплавы, Al-Mg-Zr-Li, плавка, литье, лигатура

Аблакатов Ильяс Кабылашимулы	*Младший научный сотрудник, АО «Национальный центр космических исследовании и технологии», Алматы, Казахстан. Email: termostators@gmail.com*
Исмаилов Марат Базаралиевич	*Доктор технических наук, профессор, директор департамента космического материаловедения и приборостроения, АО «Национальный центр космических исследовании и технологии», Алматы, Казахстан. Email: m.ismailov@gmail.com*
Мустафа Лаура Молдакеримовна	*Заведующий лабораторией АО "Национальный центр космических исследований и технологий", Алматы, Казахстан. Email: Mustafa_laura@mail.ru*
Санин Анатолий Федорович	*Доктор технических наук, профессор. Профессор кафедры. Днепровский национальный университет имени Олеся Гончара, Днепр, Украина. Email: afedsa60@gmail.com*

References

[1] Ablakatov IK, Baiserikov BM, Ismailov MB, Nurgozhin MR. Aluminum-lithium alloys: types, properties, application, and production technologies. Overview. Complex Use of Mineral Resources. 2022; 323(4):5-14. ISSN-L 2616-6445, ISSN 2224-5243. https://doi.org/10.31643/2022/6445.34

[2] Uprochnenie alyuminiya: 3 mekhanizma [Aluminum hardening: 3 mechanisms]. Electron resource. URL: https://aluminium-guide.com/uprochnenie-alyuminiya/ (accessed 10 October 2022).

[3] Parker BA, Lim JH. Microstructure development during the deformation of aluminium-magnesium alloys. Journal of materials processing technology. 1996; 60:563-566. http://dx.doi.org/10.1016/0924-0136(96)02387-4

[4] Alyuminievye splavy [Aluminum alloys]. Electron resource. URL: https://ru.wikipedia.org/wiki/Алюминиевые_сплавы. (accessed 10 October 2022).

[5] Duan Y, Qian J, Xiao D. Effect of Sc and Er additions on superplastic ductilities in Al-Mg-Mn-Zr alloy. Journal of central south university. 2016; 26(6):1283-1292. http://dx.doi.org/10.1007/s11771-016-3178-x

[6] Litejnye alyuminievye splavy [Foundry aluminum alloys]. (Electron resource). URL: https://promexcut.ru/litejnyie-alyuminievyie-splavyi (accessed 10 October 2022).

[7] Gancarz T, Jourdan J. Physicochemical properties of Al, Al-Mg and Al-Mg-Zn alloys. Journal of molecular liquids. 2018; 249:470-476. http://dx.doi.org/10.1016/j.molliq.2017.11.061

[8] Huaguan L, Yubing H, Yiwei X. Reinforcement effects of aluminum – lithium alloy on the mechanical properties of novel fiber metal laminate. Composites Part B. 2015; 82:72-77. http://dx.doi.org/10.1016/j.compositesb.2015.08.013

[9] Thomas D, Alireza V, Justin L. Aluminium Lithium Alloys. Fundamentals of Aluminium Metallurgy. 2018; 387-438. https://doi.org/10.1016/B978-0-08-102063-0.00011-4

[10] Trudonoshin AI. Izuchenie struktury litejnyh splavov sistemy Al-Mg-Si, legirovannyh litiem [Study of the structure of lithium–doped cast alloys of the Al–Mg-Si system.]. Physics of metals and metallology, 2020; 7:771-778. https://doi.org/10.31857/S0015323020070116 (in Russ.)

[11] Shamas D, Hasan BA. Effect of Li addition on microstrusture and mechanical properties of Al-Mg-Si alloy. Int. J. Mater. Res. 2014; 105:770-777. ISSN 1862-5282. https://doi.org/10.3139/146.111089

[12] Mortsell EA, Marioara CD. The effects and behaviour of Li and Cu alloying agents in lean Al-Mg-Si alloys. 2017; 699:235-242. https://doi.org/10.1016/j.jallcom.2016.12.273

[13] Ali AA, Yong X, Xunzhong G, Shi HZh, Yan M, Dayong Ch. Strengthening mechanisms, deformation behavior, and anisotropic mechanical properties of Al-Li alloys: A review. Journal of Advanced Research. 2018; 10:49-67. https://doi.org/10.1016/j.jare.2017.12.004

[14] Yang X, Xiong B. Effect of Li content on ageing precipitation behavior of Al-Mg-Si alloy. Cailiao gongcheng-journal of materials engineering. 2021; 49(6):100-108. https://doi.org/ 10.11868/j.issn.1001-4381.2020.000794

[15] Litij [Lithium]. (Electron resource). URL: https://ru.wikipedia.org/wiki/Литий (accessed 10 October 2022).

[16] Trudonoshyn O. Studying the Structure of Al-Mg-Si Casting Alloys Doped by Lithium. Physics of metals and metallography. 2020; 121(7):701-707. https://doi.org/10.1134/S0031918X2007011X

[17] Augustyn-PJ, Adrian H, Rzadkosz S, Choroszyński M. Structure and Mechanical Properties of Al-Li Alloys as Cast. Archives of Foundry Engineering. 2013; 13(2):5-10. ISSN (1897-3310). https://doi.org/10.2478/afe-2013-0027

[18] Zhang Y, Gao H, Kuai Y. Effects of Y additions on the precipitation and recrystallization of Al-Zr alloys. Materials characterization. 2013; 86:1-8. https://doi.org/10.1016/j.matchar.2013.09.004

[19] Zhang X, Liu W. Effect of processing parameters on quench sensitivity of an AA7050 sheet. Materials science and engineering a-structural materials properties microstructure and processing. 2011; 528:795-802. https://doi.org/10.1016/j.msea.2010.07.033

[20] Jia Zh, Couzinie JPh. Precipitation behaviour of Al3Zr precipitate in Al-Cu-Zr and Al-Cu-Zr-Ti-V alloys. Transactions of nonferrous metals society of china. 2012; 22:1860-1865. https://doi.org/10.1016/S1003-6326(11)61398-8

Crossref
DOI: 10.31643/2023/6445.38
Engineering and technology

A Study of Superpave Design Gyrations for High Traffic Surface Mixtures

[1*]Kosparmakova S.A., [2]Azlan M.N., [3]Fischer D.E.

[1]L.N. Gumilyov Eurasian National University, Nur-Sultan, Kazakhstan
[2]University Pendidikan Sultan Idris, Malaysia
[3]Satbayev University; Institute of Metallurgy and Beneficiation, Almaty, Kazakhstan

[*]Corresponding author email: smartsam0509@gmail.com

Received: *November 18, 2022*
Peer-reviewed: *December 23, 2022*
Accepted: *January 31, 2023*

ABSTRACT
The methodology of the research that was used to evaluate the comparative results of surface mixes with a nominal maximum aggregate size of 12.5mm is presented in this paper. Also presented are the recommended Ndes values for C-level and D-level mixes, which are designed to handle traffic levels of 3-30 Million and greater than 30 Million ESALs, respectively. In order to determine the amount of asphalt that was present, asphalt concrete mixes were fabricated utilizing the Superpave design process at Ndes levels of 50, 75, 100, and 125 gyrations. Using the Asphalt Mixture Performance Tester instrument, we were able to determine the dynamic modulus (E*) at the design asphalt content for a number of different gyration levels. The E* data and related binder properties were used as input in the AASHTO Darwin-ME software to anticipate the rutting and fatigue performance of the mixtures. This was accomplished by assuming a model pavement section and appropriate traffic levels. In order to determine which Ndes are most appropriate, relative performance indicators for rutting and fatigue have been developed and plotted against asphalt content. The Ndes value of 85 gyrations was found to be ideal for both surface mixes after extensive research.

Keywords: Relative performance; Asphalt concrete mixtures; Superpave; Design gyrations; Fatigue cracking; Rutting;

Information about authors:

Kosparmakova Samal Akhmetaly — *Ph.D. Student, Department of Technology of Industrial and Civil Construction, L.N. Gumilyov Eurasian National University, 010000, Kazhymukhan Munaytpasov Street 13, Nur-Sultan, Kazakhstan. Email: smartsam0509@gmail.com*

Azlan M.N. — *Physics Department, Faculty of Science and Mathematics, Universiti Pendidikan Sultan Idris, Tanjung Malim, Perak, 35900, Malaysia. Email: azlanmn@fsmt.upsi.edu.my*

Fischer Dametken — *Doctor, JSC "Institute of Metallurgy and Ore Beneficiation", st. Shevchenko, 29/133, 050010, Almaty, Kazakhstan. Email: damishka3004@gmail.com*

1. Introduction

The number of design gyrations (N_{des}) is a critical element in the Superpave asphalt concrete mix design procedure. The selection of Ndes is based on total traffic, during service life of the pavement, which is indicated in ESALs. Asphalt concrete mixtures for higher traffic volumes are compacted to higher Ndes because a denser mix resists rutting better. However, this results in a reduced design asphalt content, which reduces the mix's fatigue performance. As a result, a performance-oriented strategy to determining N_{des} that maximizes mix performance in terms of both rutting and fatigue cracking was devised [1].

The Superpave mix design approach, created as part of the Strategic Highway Research Program, combines into the design process performance-related design parameters, environmental variables, load factors, and material characterization. The requirements created for the mix design process are intended to improve the performance of asphalt pavement structures by decreasing rutting, thermal cracking, and fatigue cracking [2].

The Superpave method employs a volumetric technique in which the aggregate gradation and optimal asphalt content are determined by examining the mix's air void proportion and other volumetric features. The gyration levels are established by the anticipated total traffic in Equivalent Single-Axle Loads (ESALs) over the pavement's anticipated service life (Prowell & Brown, 2007). According to the current Superpave specifications for characterization of asphalt concrete mix materials, rutting resistance is measured for the asphalt binder using the G*/sinδ parameter and fatigue cracking resistance is measured using the G*sinδ parameter, where G* is the complex shear modulus of the asphalt binder and represents the phase angle δ. In addition to the volumetric requirements, these characteristics can be utilized to develop a mixture that performs well in the field in

terms of rutting and fatigue cracking [2].

However, the mix's performance is not expressly considered during the design phase. This is owing to the fact that the design method determines only the aggregate structure and the matching asphalt content required to produce 4% air voids, without any extra mix performance characterization [3]. Consequently, numerous State Highway Agencies have implemented additional specification requirements based on performance tests, such as the Hamburg Wheel Tracking Device (HWTD) and Asphalt Pavement Analyzer (APA), to assess the rutting potential of asphalt concrete mixtures [4].

As a result of their robust aggregate skeletons, superpave mixtures often display adequate rutting resistance. In addition, mixtures that meet the approval criteria of wheel tracking device testing, as stated previously, exhibit enhanced field rutting performance. To ensure a high rutting performance, the asphalt percentage of the mix is decreased, resulting in a comparatively drier mixture with less plastic flow of the asphalt binder. The decreased asphalt percentage, however, causes an increase in fatigue cracking, which is becoming a frequent issue, particularly in relatively young pavements that are 5-7 years old (Maupin, 2003). In order to obtain an acceptable mixture, it is required to enhance the fatigue cracking resistance without compromising the rutting resistance [[3], [4], [5], 6], [7]].

Both fatigue cracking and rutting are load-related distresses that result from a loss of structural integrity in the asphalt concrete layer. Rutting can also be caused by potholes. Rutting in the asphalt layer is assessed in terms of millimeters (or inches) of deformation, whereas fatigue cracking in a flexible pavement is quantified in terms of the percentage of cracking that has occurred per unit area. During the process of optimization, it is not possible to make a direct comparison against the number of design gyrations because of differences in the methods used to measure the degree of the two types of distress. The mixture provides the maximum performance possible against fatigue cracking at the Ndes level that is lowest, and it provides the maximum performance possible against rutting at the Ndes level that is highest [8].

Locking point (Prowell & Brown, 2007, Hornbeck, 2008) and Ndes level reduction are two common strategies for optimizing mix performance (Hornbeck, 2008, Aschenbrenner & Harmelink, 2002). Locking point correlates laboratory mix density to ultimate field density, but weakly (Prowell & Brown, 2007). The laboratory-field density correlation ignored aggregate type, gradation, and angularity, which affected the locking point. Christensen and Bonaquist (2006) used the Ndes reduction strategy to show that rutting performance rose by 25% with one level of compactive effort (25 gyrations) and fatigue performance decreased by 20% [[1], [2], [8], [9]].

Prowell and Brown (2007), Hornbeck (2008), and Button, Chowdhury and Bhasas (2009) examined how compactive effort affects rutting and fatigue cracking (2006). Superpave mixtures' rutting and fatigue performance was tested at various Ndes levels in the Ndes level reduction approach. Asphalt content was adjusted to match a 4% air void content for four Ndes levels—50, 75, 100, and 125 gyrations—proposed by the NCHRP for different traffic loads (Prowell & Brown, 2007) [[3], [10]].

The aims of the study were to:

1. Evaluate the sensitivity of asphalt volumetric properties to varying levels of design gyrations;

2. Determine the optimal design gyrations for asphalt pavements.

3. Determine the effect of changes in N_{des} on the stiffness and performance characteristics of the mix by comparing the fatigue and rutting performance anticipated by the mechanistic-empirical design approach for a typical pavement segment.

4. Recommend N_{des} values for surface mixes S12.5C and S12.5D.

On the basis of the volumetric design approach, there are two methods for enhancing fatigue cracking resistance:

1. Increasing the relative density objective for a given number of design gyrations by increasing the asphalt composition of the design.

2. Reducing the amount of design gyrations while keeping a 4% air void design content in the mix.

This research utilized the second method to enhance rutting and fatigue performance because increasing the desired relative density has the potential to cause performance issues, particularly with soft binders (Prowell & Brown, 2007) [[1], [3], [11]]. For the design gyration optimal number determination, asphalt concrete mixes were prepared at various Ndes levels, and their performance was characterized. Mix design, performance testing, and evaluation are described in depth in the sections that follow.

2. Experimental technique

2.1 Design Gyrations Optimum Number Determining Method.

For fatigue and rutting, relative performance indicators were constructed using a control or base level that indicates the maximum performance of the mixture. Performance is defined as the number of ESALs required to attain failure for a given distress,

where failure limits are specified as 10% cracking of the entire fatigue place and 6.35 mm permanent deformation of AC layer for rutting [[12], [13], [14]]. The control fatigue performance, $P_{Fatigue}$, will be clear at 50 gyartions fatigue life measurement, as the mix design results in a higher asphalt content, which makes the asphalt concrete layer more flexible and therefore more resistant to fatigue cracking. Similarly, the control rutting performance $P_{Rutting}$ will be determined by cycles number to failure for a mixture intended for 125 gyrations, as a higher amount of compaction results in increased rutting resistance [[15], [16]]. Therefore, relative performance is computed using Equation (1) for fatigue cracking and Equation (2) for rutting (Button, Chowdhury, and Bhassa, 2006):

$$RP_{Fatigue} = \frac{P_{Fatigue,N_{des}=i}}{P_{Fatigue,N_{des}=50}}$$

$$RP_{Rutting} = \frac{P_{Rutting,N_{des}=i}}{P_{Rutting,N_{des}=125}}$$

Where, $P_{FatigueNdes=I}$ is the estimated fatigue life and $P_{FatigueNdes=I}$ is the estimated rutting life for the mix designed using "i" number of design gyrations. $RP_{Fatigue}$ is equal to 1 at 50 gyrations of Ndes and diminishes as Ndes increases. RPRutting is 1 at Ndes of 125 gyrations and decreases as Ndes decreases. The examination of relative performance data involved graphing relative performance values expressed as a percentage versus asphalt content. Instead of design gyrations, the asphalt content was chosen as the independent variable in this study since it is more logical to relate performance to a mix attribute. By graphing the relative performance values against the asphalt content and locating the intersection of the curves, the optimal asphalt content was identified. The best Ndes was found by plotting the number of gyrations versus the asphalt composition [[17], [18]].

State highway agencies' performance test methodologies can be utilized to validate mix performance, thereby enhancing the mix design process. In evaluating mix performance, these test methods are not based on fundamental material properties (measurement of real material reaction to an applied stress or strain) and do not account for variations in mix design factors such as asphalt content variation. Additionally, these experiments are undertaken at temperatures unique to the mix type, and the effect of aggregate gradation is not assessed adequately (Prowell & Brown, 2007, Watson, Moore, Heartsill, Jared & Wu, 2008). As a key material property, the dynamic modulus of the asphalt concrete mix was employed to evaluate mix performance in this study. The AMPT was used to measure the dynamic modulus, and the DARWin-ME program was used to forecast the rutting and fatigue performance of the mixes at different design gyration levels [[19], [20], [21], [22]].

2.2 Superpave Mix Design Criteria for Surface Mixes

The surface mixes are often designed on 9.5mm and 12.5mm NMAS (nominal maximum aggregate size). Based on traffic level (design number of ESALs), surface mixes are further classified as (0.3 Million for A), (0.3 - 3 Million for B), (3 - 30 Million for C), and (>30 Million for D). S12.5C mixes are compacted to 75 gyrations and S12.5D mixes are compacted to 100 gyrations Superpave requirements [[21], [23]]. Notably, the drop in N_{des} levels on NCHRP-recommended C and D mixes, respectively, have gyration values of 100 and 125, is not based on mix performance, which was the objective of this study.

This article recommends a change of Superpave mix design requirements for S12.5C and S12.5D mixes, which are utilized in surface courses intended for traffic intensities in excess of 3 Million ESALs. As recommended, the performance grade of asphalt binder PG 70-22 was used in the S12.5C blend, while PG 76-22 was used in the S12.5D blend.

3. Results and Discussion

3.1 Design and Modification of Superpave Mixes for Different N_{DES} Levels

Through the utilization of the Superpave mix design procedure, the two mixtures S12.5 C and S12.5 D were developed. Calculations were made to determine the asphalt content based on 4% air voids at N_{des} levels of 75 gyrations for S12.5C mix and 100 gyrations for S12.5D mix. By performing volumetric back-calculations of specimen heights at a given asphalt content and making use of the theoretical maximum specific gravity (Gmm) of the mix in conjunction with the asphalt content, we were able to determine the asphalt content that was necessary to generate 4% air voids at N_{des} levels of 50, 75, 100, and 125 gyrations. This was accomplished by using the asphalt content as the input variable (Pb). The mix volumetrics for S12.5C and S12.5D mixes are displayed in Table 1 at a variety of different N_{des} values. The statistics show the average of three different specimens that were compressed to the number of gyrations that was requested for each N_{des}.

Table 1. Design of Superpave Mix Volumetric Properties

N_{des} Mix Properties	S12.5C				S12.5D			
Design Gyrations Number (N_{des})	50	75	100	125	50	75	100	125
Total Mix Asphalt Content %	5.71	5.41	5..20	5.03	5.47	5.18	4.97	4.81
Bulk Specific Gravity, Gmb	2.358	2.463	2.458	2.451	2.432	2.442	2.449	2.455
Max.Specific Gravity, Gmm	2.451	2.458	2.463	2.469	2.438	2.452	2.457	2.465
Total Mix Air Voids, %	3.8	4.3	3.7	4.3	4.3	4.1	4.2	4.1
Voids in Mineral Agg.(VMA), %	16.4	16.3	15.5	15.6	17.2	16.5	16.2	15.7
Voids Filled w/binder (VFA), %	76.9	73.8	75.8	72.4	75.2	75.2	73.9	74.1

3.2. Testing and Development of E* Mastercurves for Dynamic Modulus

The Asphalt Mixture Performance Tester (AMPT) was used to conduct the dynamic modulus was determined using the Asphalt Mixture Performance Tester and the AASHTO TP79-09 Standard Method of Test for Determining the Dynamic Modulus and Flow Number for Hot Mix Asphalt (HMA) (AMPT). 150 mm in diameter Superpave gyratory specimens compressed with a height of 178 mm. A test specimen with a 100 mm diameter and a 150 + 2.5 mm height was made by coring and sawing the compacted samples; the desired air void content for the cored test specimen was 4 + 0.5%. Three temperatures and three frequencies were used in the experiment: 4, 20, and 40 degrees Celsius. Table 2 displays the E* (Pa) values for the two mixtures. Using the dynamic modulus values acquired at the three test temperatures and three test frequencies, a non-linear optimization approach given in AASHTO PP61-09 was utilized to produce an E* master curve.

Standard Method for the Development of Dynamic Modulus Master Curves for Hot Mix Asphalt (HMA) Using the Asphalt Mixture Performance Tester [Standard Method for the Development of Dynamic Modulus Master Curves for Hot Mix Asphalt (HMA)] (AMPT) [24].

Since the stiffness of an asphalt concrete mix is measured by its dynamic modulus, it stands to reason that a mix compacted at a higher Ndes level, with its lower asphalt content and greater stiffness, should have a larger dynamic modulus. Figure 1 shows that this shape may be detected in the E* master curves of both mixtures.

Table 2. Test Results of Dynamic Modulus (Pa)

Temp. (°C)	Freq. (Hz)	S12.5C Mix, N_{des}				S12.5D Mix, N_{des}			
		50	75	100	125	50	75	100	125
4	10	1.83E10	1.97E10	2.07E10	2.19E10	1.85E10	1.91E10	1.97E10	2.06E10
	1	1.42E10	1.62E10	1.71E10	1.79E10	1.46E10	1.54E10	1.58E10	1.65E10
	0.1	1.02E10	1.24E10	1.34E10	1.38E10	1.08E10	1.18E10	1.19E10	1.25E10
20	10	8.47E09	1.01E10	1.12E10	1.16E10	8.78E09	9.63E09	9.66E09	1.01E10
	1	5.11E09	6.51E09	7.39E09	7.39E09	5.41E09	6.19E09	6.23E09	6.49E09
	0.1	2.69E09	3.78E09	4.45E09	4.42E09	3.05E09	3.57E09	3.69E09	3.85E09
40	10	2.27E09	3.01E09	3.46E09	3.52E09	2.34E09	2.81E09	2.95E09	3.02E09
	1	9.87E08	1.39E09	1.63E09	1.66E09	1.07E09	1.31E09	1.39E09	1.49E09
	0.1	4.76E08	6.69E08	7.68E08	8.08E08	5.54E08	6.97E08	6.71E08	8.16E08

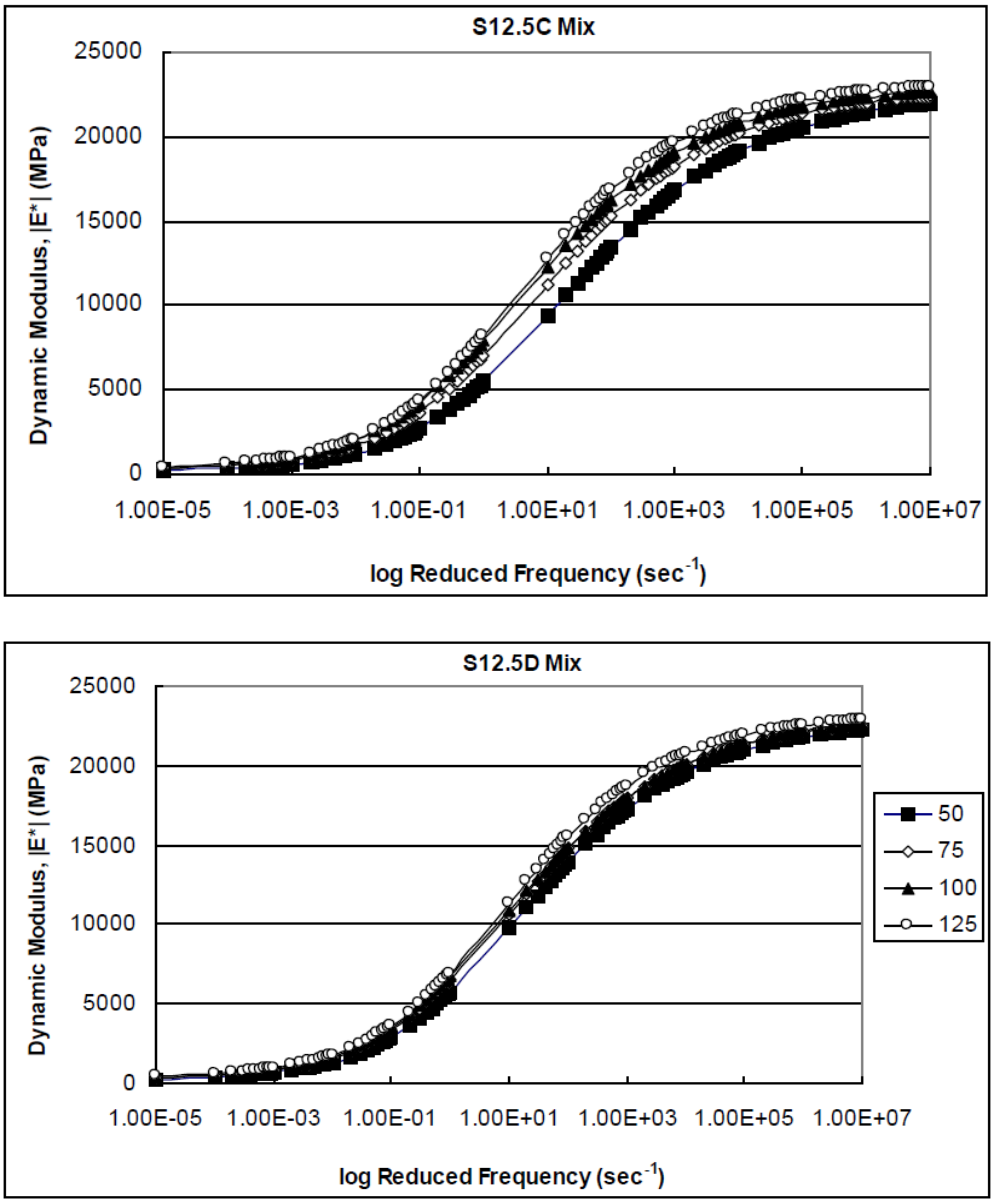

Figure 1. E* Mastercurves for Various N_{des} Levels, Reference Temperature 20°C

3.3 Prediction of Pavement Performance Using DARWin-ME Design Guide Software

The dynamic modulus (E*) is a crucial parameter that correlates material attributes to fatigue cracking and rutting performance and is used in the mechanical-empirical pavement design technique to define asphalt concrete mixes. The fatigue and rutting performances of the mixtures were investigated using the DARWin-ME design guide, the most recent edition of NCHRP 1-37A Mechanistic-Empirical Pavement Design Guide, which has recently been selected as the industry's key instrument for pavement design and performance prediction. The analysis made use of model pavement sections, which are routinely used by some specifications for planning asphalt concrete pavements where C and D mixes are required. There were three distinct parts to the pavement's structure:

Part1: Asphalt concrete surface course, thickness: 7.5 centimeters, air void content: 8%

Part2: Crushed stone base course, 25 cm (S12.5C) and 38 cm (S12.5D) thick, 163 MPa modulus.

Part3: Subgrade AASHTO classification A-7-5 (clay), modulus - 46 MPa

Table 3 presents the predicted fatigue and rutting performance, together with the relative performance values at different gyration levels.

Table 3. Estimated Levels of Rutting and Fatigue Performance in Comparison to Their Relative Values

Mix Type	Number of Gyrations, N_{des}	Asphalt Content, %	$P_{Fatigue}$ (ESALs)	$P_{Rutting}$ (ESALs)	$RP_{Fatigue}$, %	$RP_{Rutting}$, %
S12.5C	50	5.61	2.25E06	1.78E06	100	68
	75	5.31	2.17E06	2.27E06	96	86
	100	5.10	2.08E06	2.54E06	92	96
	125	5.01	1.94E06	2.65E06	85	100
S12.5D	50	5.17	3.98E06	3.50E06	100	84
	75	5.08	3.54E06	3.94E06	89	95
	100	4.87	3.23E06	3.98E06	81	96
	125	4.71	2.85E04	4.20E06	73	100

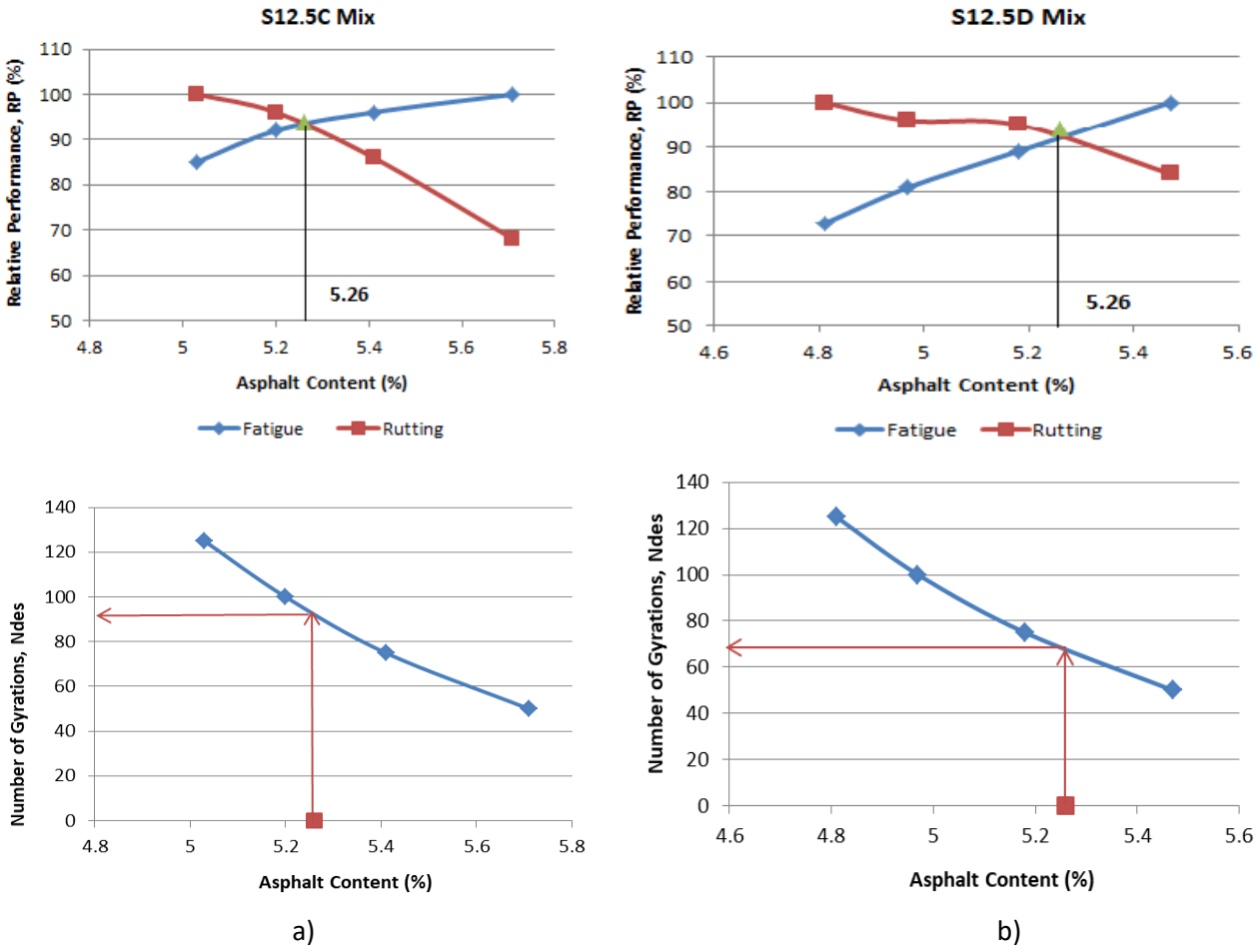

Figure 2 - Optimal N_{des} estimation from Relative Performance and Asphalt Content Graphs

3.4 An Analysis of the Relative Performance Data and a Suggested Change to the N_{des}

Figures 2(a) and 2(b) show relative fatigue and rutting performance versus asphalt content for S12.5C and S12.5D mixtures, respectively, using the approach stated in Section 1.2. Figures 2(a) and 2(b) show the relationship between the asphalt content and the total number of design gyrations for each of the two mixtures, respectively. A total of 95

gyrations was determined to be the optimum N_{des} value for S12.5C mix based on the relative performance curves, which is higher than the current some specification of 75 gyrations. This improves durability against rutting but lowers its resilience against fatigue cracking. Compared to the current some specification of 100 gyrations, the determined optimal N_{des} value for S12.5D mix was 72 gyrations, which results in increased fatigue cracking resistance. But since the mixture is used in surface courses made to support traffic loads greater than 30 Million ESALs, optimizing its rutting performance is crucial.

Thus, in order to find practically usable values that optimize both distresses, a more in-depth investigation of the relative performance at values other than the anticipated optimums was conducted. It's worth noting that in an attempt to increase the longevity of Superpave mixes, the N_{des} values currently used by various specifications were arbitrarily reduced from the original Superpave N_{des} table.

It was determined that 95 rotations were necessary to achieve optimum performance from the S12.5C blend. It can be seen from the difference in the slopes of the rutting and fatigue relative performance curves in Figure 2(a) that the variation in rutting performance with gyration number is larger than the variation in fatigue cracking performance. Accordingly, raising N_{des} has a bigger impact on enhancing rutting than lowering fatigue resistance. For example, if you set N_{des} to 85 gyrations, you'll see a loss of 2% in fatigue performance and an increase of 5% in rutting. The overall binder weight drops by 2% as a result of the drop in asphalt composition from 5.45% to 5.36%. This results in a N_{des} value of 85 gyrations for the 12.5C mixture. The suggested value of 85 gyrations has real-world implications for rutting resistance and cost savings via reduced asphalt binder usage.

Based on the relative performance research, 72 gyrations was shown to be the optimal N_{des} for the S12.5D mix. The current NCDOT N_{des} value for this mix is 100, although increasing the design asphalt content will increase the pavement's flexibility.

However, the rutting must also be optimized for design traffic reasons. Accordingly, it is suggested that the N_{des} level for this mixture be lowered to 85 gyrations. As the N_{des} climbs to 85 gyrations, fatigue performance improves by 6%, while rutting resistance drops by 2%. Asphalt with 85 gyrations has a higher total binder weight of 5.13%, up from 4.87%.

4. Conclusions

The optimal asphalt concentration decreased as the Ndes level to which specimens were compacted grew, as shown by the mix design results for several countries' surface mixes S12.5C and S12.5D. The modulus of the mixture at different temperatures and frequencies increases with an increase in Ndes, as evidenced by the trend in E* master curves from AMPT testing. These results corroborate the theory behind this work, which suggests that increasing the Ndes during the mix design phase will require less binder, leading to a more rigid final product.

For the S12.5C mix, the optimum Ndes was calculated to be 95 gyrations, while the optimum Ndes for the S12.5D mix was calculated to be 72 gyrations. We used the rutting and fatigue performance data to calculate relative values for the optimal Ndes values that resulted and for the values recommended by the National Cooperative Highway Research Program. Two primary criteria were used to provide guidelines for ideal Ndes:

– Using a lower Ndes has a negative impact on rutting performance, but has a positive impact on pavement life compared to fatigue life.

– The economic benefits of utilizing less asphalt binder in the mix and the decrease in fatigue life that results from adopting a higher Ndes are considered and balanced. As a proportion of the asphalt binder required for mix design, the asphalt content decrease is calculated.

For both S12.5C and S12.5D mixes, the optimal Ndes value is 85 gyrations.

Conflict of interest. On behalf of all the authors, the correspondent author states that there is no conflict of interest.

Cite this article as: Kosparmakova SA, Azlan MN, Fischer DE. A Study of Superpave Design Gyrations for High Traffic Surface Mixtures. Kompleksnoe Ispolzovanie Mineralnogo Syra = Complex Use of Mineral Resources. 2023; 327(4):41-49. https://doi.org/10.31643/2023/6445.38

Қарқынды қозғалыс беттерінің Superpave қоспаларына арналған жобалық гиратор тербелісін зерттеу

[1]Коспармакова С.А., [2]Азлан М.Н., [3]Фишер Д.Е.

[1] Л.Н. Гумилев атындағы Еуразия ұлттық университеті, Нұр-Сұлтан, Қазақстан
[2]Сұлтан Ыдырыс атындағы білім беру университеті, Малайзия
[3]Металлургия және кен байыту институты; Сәтбаев Университеті, Алматы, Қазақстан

Мақала келді: *18 қараша 2022*
Сараптамадан өтті: *23 желтоқсан 2022*
Қабылданды: *31 қаңтар 2023*

ТҮЙІНДЕМЕ

Бұл жұмыста номиналды максималды толтырғыш мөлшері 12,5 мм болатын беттік қоспалардың салыстырмалы нәтижелерін бағалау үшін пайдаланылған зерттеу әдістемесі берілген. Сондай-ақ, сәйкесінше 3-30 миллион және 30 миллионнан астам ESAL трафик деңгейлерін өңдеуге арналған C-деңгейі және D-деңгейлі қоспалар үшін ұсынылған Ndes мәндері көлтірілген. Асфальттың бар мөлшерін анықтау үшін 50, 75, 100 және 125 айналу Ndes деңгейлерінде Superpave жобалау процесін қолдана отырып, асфальтбетон қоспалары дайындалды. Asphalt Mixture Performance Tester құралын пайдалана отырып, біз әртүрлі айналу деңгейлері үшін асфальттың жобалық құрамындағы динамикалық модульді (E*) анықтай алдық. E* деректері мен байланыстырғыштың сәйкес қасиеттері AASHTO Darwin-ME бағдарламалық жасақтамасында қоспалардың екіге бөлінуі мен тозу өнімділігін болжау үшін кіріс ретінде пайдаланылды. Бұл үлгі тротуар учаскесін және тиісті қозғалыс деңгейлерін болжау арқылы орындалды. Қай Ndes ең қолайлы екенін анықтау үшін асфальттың құрамына қатысты ойықтар мен тозуының салыстырмалы өнімділік көрсеткіштері әзірленді және графигі жасалды. 85 айналымдық Ndes мәні ауқымды зерттеулерден кейін екі беттік қоспалар үшін де өте қолайлы болатыны анықталды.

Түйін сөздер: Салыстырмалы сипаттамалары; асфальтбетон қоспалары; Superpave; гиратор мөлшері; жабынның сынуы; дөңгелек ізінің пайда болуы.

Авторлар туралы ақпарат:

Коспармакова Самал Ахметалыевна — *PhD докторанты, «Өнеркәсіптік және азаматтық құрылыс технологиясы» кафедрасы, Л.Н. Гумилев атындағы Еуразия ұлттық университеті, Нұр-Сұлтан, Қазақстан. Email: smartsam0509@gmail.com*

Азлан М.Н. — *физика кафедрасы, жаратылыстану-математика факультеті, Университет Пендидикан Сұлтан Идрис, Танджунг Малим, Перак, 35900, Малайзия. Email: azlanmn@fsmt.upsi.edu.my;*

Фишер Дәметкен Еділовна — *Доктор, "Металлургия және кен байыту институты" АҚ, Шевченко көш., 29/133, 050010, Алматы, Қазақстан.*

Исследование проектных колебаний гиратора для смесей Superpave с интенсивным движением поверхностей

[1]Коспармакова С.А., [2]Азлан М.Н., [3]Фишер Д.Е.

[1] Евразийский национальный университет им. Л.Н. Гумилева, Нур-Султан, Казахстан
[2]Образовательный университет Султана Идриса, Малайзия
[3]Институт металлургии и обогащения; Сатпаев Университет, Алматы, Казахстан

Поступила: *18 ноября 2022*
Рецензирование: *23 декабря 2022*
Принята в печать: *31 января 2023*

АННОТАЦИЯ

В статье представлена методика исследования, которая использовалась для оценки сравнительных результатов поверхностных смесей с номинальным максимальным размером заполнителя 12,5 мм. Также представлены рекомендуемые значения Ndes для смесей уровней C и D, которые предназначены для обработки уровней трафика 3-30 миллионов и более 30 миллионов ESAL соответственно. Чтобы определить количество присутствующего асфальта, были изготовлены асфальтобетонные смеси с использованием процесса проектирования Superpave на уровнях Ndes 50, 75, 100 и 125 оборотов. Используя прибор для определения характеристик асфальтобетонной смеси, мы смогли определить динамический модуль (E*) при расчетном содержании асфальта для ряда различных уровней гирации. Данные E* и соответствующие свойства вяжущего были использованы в качестве входных данных в программном обеспечении AASHTO Darwin-ME для прогнозирования колейности и усталостных характеристик смесей. Это было достигнуто за счет модели участка дорожного покрытия и соответствующих уровней трафика. Для того, чтобы определить, какие Ndes являются наиболее подходящими, были разработаны и нанесены на график относительные показатели колейности и усталости в зависимости от содержания асфальта. После обширных исследований было установлено, что значение Ndes, равное 85 оборотам, идеально подходит для обеих поверхностных смесей.

	Ключевые слова: Относительные характеристики; асфальтобетонные смеси; Superpave; количество гиратора; усталостное растрескивание; колееобразование.
Коспармакова Самал Ахметалыевна	***Информация об авторах:*** *Докторант PhD, Кафедра «Технология промышленного и гражданского строительства», ЕНУ им. Л.Н.Гумилева, Нур-Султан, Казахстан. Email: smartsam0509@gmail.com*
Азлан М.Н.	*Кафедра физики, факультет естественных наук и математики Университета Пендидикан Султан Идрис, Танджунг Малим, Перак, 35900, Малайзия. Email: azlanmn@fsmt.upsi.edu.my*
Фишер Даметкен Едиловна	*Доктор, АО «Институт металлургии и обогащения», ул. Шевченко, 29/133, 050010, Алматы, Казахстан. E-mail: damishka3004@gmail.com*

References

[1] Prowel BD, Brown ER. Superpave Mix Design: Veryfing Gyration Levels in the Ndeign table, NCHRP Report 573. National Cooperative Highway Research Program, Washington D.C. 2007.

[2] Hombeck NC. Effect of Compaction Effort on Superpave Surface Course Materials, Masters Thesis. West Virginia University. 2008.

[3] Superpave Mix Design. Asphalt Institute Superpave Series. (SP-2), 3rd Edition, 2013; 2.

[4] Performance Graded Asphalt Binder Specification and Testing. Superpave Series No. 1 (SP-1). Third Edition, Asphalt Institute, Inc., 2003: 1-59.

[5] Huber G, Wielinski J, Campbell Ch, Padgett J, Rowe G, Beeson M, Cho S. Superpav5: Relationship of in-place air voids and asphalt binder aging. Asphalt Paving Technology: Association of Asphalt Paving Technologists-Proceedings of the Technical Sessions. 2019; 88:183-220.

[6] Mirbaha B, Abdi A, Zarei M, and Zarei A. "Experimental determination of the optimum percentage of asphalt mixtures reinforced with Nano-carbon black and polyester fiber industries," Engineering Solid Mechanics. 2017; 5:285-292.

[7] Ying H, Elseifi MA, Mohammad LN, and Hassan MM. "Heterogeneous Finite-Element Modeling of the Dynamic Complex Modulus Test of Asphalt Mixture Using X-ray Computed Tomography," Journal of Materials in Civil Engineering. 2013; 26: 04014052.

[8] Aliha M, and Fattahi Amirdehi H. "Fracture toughness prediction using Weibull statistical method for asphalt mixtures containing different air void contents," Fatigue & Fracture of Engineering Materials & Structures. 2016.

[9] Jong-Sub Lee, Jin-Hwan Kim, Oh-Sun Kwon, Byung-Duk Lee. Asphalt binder performance grading of North Korea for Superpave asphalt mix-design. International Journal of Pavement Research and Technology. Edition. 2018; 11(6):647-654.

[10] Duarte Gabriel MacÊdo, Faxina Adalberto Leandro. Low-Temperature and Fatigue Properties of Asphalt Binders Modified with Crumb Rubber from Discarded Tires and Recycled Low-Density Polyethylene. Journal of Materials in Civil Engineering. Edition. 2022; 34(9).

[11] Mirsayar M, Razmi A, and Berto F. "Tangential strain-based criteria for mixed-mode I/II fracture toughness of cement concrete," Fatigue & Fracture of Engineering Materials & Structures. 2018; 41:129-137.

[12] Tutu KA, Ntramah S, Tuffour YA. Superpave performance graded asphalt binder selection for asphalt mixture design in Ghana. Scientific African. 2022; 17. DOI: 10.1016/j.sciaf.2022.e01348

[13] Da Silva TO, Pitanga HN, Rodrigues MHR, Rezende JP, Marques GL. Study of the mechanical behavior of asphalt mixtures in terms of creep and Superpave compaction parameters. Acta Scientiarum – Technology. 2022; 16. DOI:10.4025/actascitechnol.v45i1.60212

[14] Razmi A, and Mirsayar M. "Fracture resistance of asphalt concrete modified with crumb rubber at low temperatures," International Journal of Pavement Research and Technology. 2017.

[15] Mirsayar M. "On the low temperature mixed mode fracture analysis of asphalt binder–Theories and experiments," Engineering Fracture Mechanics. 2017; 186:181-194.

[16] Aliha M, Fazaeli H, Aghajani S, and Nejad FM. "Effect of temperature and air void on mixed mode fracture toughness of modified asphalt mixtures," Construction and Building Materials. 2015; 95:545-555.

[17] Gao Y, Hou K, Jia Y, Wei Z, Wang S, Li Z, Ding F, Gong X. Variability evaluation of gradation for asphalt mixture in asphalt pavement construction. Autom. Constr. 2021; 128:103742.

[18] Yue Y, Abdelsalam M, Khater A, Ghazy M. A comparative life cycle assessment of asphalt mixtures modified with a novel composite of diatomite powder and lignin fiber. Constr. Build. Mater. 2022; 323:126608.

[19] Khater A, Luo D, Abdelsalam M, Yue Y, Hou Y, Ghazy M. Laboratory evaluation of asphalt mixture performance using composite admixtures of lignin and glass fibers. Appl. Sci. 2021; 11:364.

[20] Lv Q, Huang W, Zheng M, Sadek H, Zhang Y, Yan C. Influence of gradation on asphalt mix rutting resistance measured by Hamburg Wheel Tracking test. Constr. Build. Mater. 2020; 238:117674.

[21] Zhang Y, Luo X, Onifade I, Huang X, Lytton RL, Birgisson B. Mechanical evaluation of aggregate gradation to characterize load carrying capacity and rutting resistance of asphalt mixtures. Constr. Build. Mater. 2019; 205:499-510.

[22] Wang DY, Kan L, Xu C. Evaluation of rutting resistance on asphalt mixture based on aggregate contact characteristics. South China Univ. Technol. Nat. Sci. Ed. 2012; 40:121-126.

[23] Husain NM, Karim MR, Mahmud HB, Koting S. Effects of aggregate gradation on the physical properties of semiflexible pavement. Adv. Mater. Sci. Eng. 2014, 529305.

[24] Moghaddam TB, Mohamed RK, Mahrez A. A review on fatigue and rutting performance of asphalt mixes. Sci. Res. Essays. 2011; 6:670-682.

Crossref
DOI: 10.31643/2023/6445.39
Earth sciences

Optimizing the contours of open pit mining with the use of mining and geological information systems and technologies

[1] Tyo S.G., [2*]Zeitinova Sh.B.

[1]E4-Capital LLC, Almaty, Kazakhstan
[2]Abylkas Saginov Karaganda Technical University, Karaganda, Kazakhstan

** Corresponding authors email: zeitinova_rmpi@mail.ru*

Received: *October 17, 2022*
Peer-reviewed: *January 12, 2023*
Accepted: *February 2, 2023*

ABSTRACT

This article studies optimization of open pit mining using mining and geological information systems and technologies. The aim of the study is to develop an algorithm of optimizing the contour of an open pit using a mining and geological information system. The Lerch-Grossman algorithm has been applied using the Whittle program. Justification for changing the contour of an open pit based on the opening scheme, geometric characteristics and special technical and economic parameters of the blocks has been proposed. This proposal provides increasing the production efficiency and reducing capital and operating costs during the development of the deposit. The authors have come to the conclusion that the functionality of updated mining and geological information systems helps to take into account market conditions when designing the main parameters of an open pit and to make the right decision at the stage of preparing a deposit for development and while optimizing the existing open pit contour.

Keywords: open pit mining, iron ore, mining efficiency, open pit contour, mining operations, information technology, geotechnologies

Information about authors:

Tyo Sergey *Senior Mining engineer, (MPONEN, MAusIMM), «E4-Capital» LLC, Almaty, Republic of Kazakhstan. Email: Sergey.Tyo@yandex.ru*

Zeitinova Sholpan Bekzhigitovna *Ph.D., senior lecturer, Abylkas Saginov Karaganda Technical University, Ave. Nursultan Nazarbayev, 56/2, 100027, Karaganda, Kazakhstan. Email: zeitinova_rmpi@mail.ru*

Introduction

With the development and improvement of information and computing equipment in the twentieth century, innovative technologies gradually began to be introduced into mining. Today, the largest part of narrow information technologies is used for certain enlarged areas: as mining and geological information systems (hereinafter MGIS), information resource bases, dispatch systems, etc [[1], [2]]. The advantages of informatization of the methods and tools used at a modern mining enterprise are obvious:

- accelerating the processes due to automation of routine operations;

- improving safety and control over mining operations;

- improving the accuracy of calculations in terms of estimating reserves, forecast and completed scope of work, establishing the boundaries of dangerous zones;

- optimizing business processes of a mining enterprise with increasing the economic efficiency [3].

The effectiveness of the open pit mining of a particular deposit depends on the decision made by the engineer at the open pit design stage. Here an important point establishing the contours of the operational excavation. Various indicators affect the boundaries of a pit, from the life of the mine and the productivity of the pit itself, to the economic parameters, including profitability of the project and return on direct investment [4]. A positive effect is achieved with involving balance reserves in the development and decreasing the volume of overburden.

Initially, optimization measures to identify open pit contours were carried out using highly specialized programs that helped establishing the

parameters of the optimal excavation contour. With improving the existing deposit modeling technologies and design automation, the process of determining the boundaries of the open pit was supplemented by the use of a set of software. As a result, separate programs have been developed for planning mining operations and designing optimal pit boundaries.

Such programs have become the basis for the development and testing of mining and geological information systems focused on solving problems in terms of optimization and design measures [5, p. 81], as well as planning and comprehensively supporting all the mining cycles [6, p. 46].

Due to the volatility of overburden and minerals, the optimal contour of deep pits used for haulage berms changes periodically. This hypothesis is confirmed by such researchers of ore deposits, such as E. Appianing and D. Mireku-Gyimah, who substantiated that increasing the volume of overburden in the final contour by 16 % entailed decreasing the mass fraction of ore by 20 % depending on the contour. The result is a 26 % reduction in profits [[7], [8]].

Researchers have paid much attention to the issue of eliminating this shortcoming in mining planning. Thus, a number of researchers [[9], [10], [11], [12], [13]] believe that when optimizing, it is important to take into account the opening scheme, to introduce changes in the slope angle of the open-pit wall with haulage berms placed on it, into the calculations. Such a solution will make it possible to model the optimal open pit with its corners in accordance with the design contour. It should be noted that this technique has a number of disadvantages:

1. Minimizing the depth of the design contour. As a result, the obtained estimate will be 7-20 % lower than that of the contour modeled without taking into account the slope angle of the pit wall.

2. Absence of rationale for the optimality of the selected solution. The trajectory of the opening workings, that is, the places where the sites will be located in the future is not taken into account.

From the point of view of the scientific substantiation of the project's effectiveness, it should be taken into account that a high level of its implementation is assigned if there is a discrepancy between the values of the optimal and final contour of the deposit of no more than 10 % [14, p. 39].

In practice, the situation looks somewhat different. The design engineer seeks to find a compromise between leaving a part of the mineral reserves and cutting in additional volumes of overburden.

Optimization information systems allow calculating quickly and easily the optimal contours of an open pit. The economic justification for the use of MGIS is caused by the minimization of labor costs and identification of the open pit boundaries with maximum efficiency. The universality of this approach is characterized by the ability to take into account the time component when discounting cash flows using the software. All the tools meet the requirements of the present-day economy and can be used for a comprehensive assessment of the project investment attractiveness [[15], [16], [17]].

As part of the use of this software product, high accuracy and reliability of models are ensured, which allows considering the calculated volume values as universal parameters for the statistical analysis of the obtained mathematical models [18].

Methods

Block models of deposits form the basis of innovative programs with optimization tools for establishing the boundaries of an open pit [[19], [20]]. To form their layout, the entire area is divided into specific blocks, the size of which depends on many factors: geometric characteristics of the ore body, dispersion of qualitative values in the contours of the mineralization area, the ledge predicted height, special parameters of the exploration system, the mining unit used. For each block, its own economically justified estimate is calculated.

Thus, the economic performance of a particular block is determined by subtracting from the income received from the sale of minerals in this sector all the costs of extraction and dressing. This formula also takes into account the volumetric characteristics of a particular block, the physical and mechanical components of the rock, the volume of the useful component, the percentage of loss during production, and others. The economic assessment can take both positive and negative values, which are determined by the content of the useful component and the amount of overburden in the block.

In the classic version, the formula for calculating the economic valuation is the difference between non-operating income and total production costs until the end product is received. To calculate such costs (Rj), the following formula is used:

$$Rj = \sum_{i=1}^{i} Wi * ki * (Zi + (1 - Qi) * Pi * (Ri + Z^0_i)), \quad (1)$$

where Zi is the total costs for the extraction of the i-material in the block (characterized by variability for different types of ores and host rocks);

Ri is the total costs for mining and processing of the i-material;

ki is the specific weight of the i-material;

Pi is diluting the material of the i-th type;

Qi is losses of the i-type material in the course of the block mining;

Wi is the material volume in the block;

Z^0_i is the cost for processing the material of the specific i-th type.

The formula can be upgraded by adding additional variables to account for costs, such as logistics costs, the sale of a useful component, and production tax.

In addition to the above factors, updated software products can take into account other parameters, including mining conditions, restrictions, and additional features for calculating the most accurate results.

In the course of optimization measures, it is necessary to take into account the general slope angle of the pit wall reflecting or not reflecting the ramps in the pit. Software packages are endowed with wide functionality that allows setting different values for different areas both in-depth and in the plan, for example, local zones with different slope angles can be effectively distinguished using wireframe models of lithological differences or coordinates of this area. The use of such methods is justified by taking into account the geomechanical and hydrogeological conditions of mining operations.

Additional functionality of the MGIS is to assess the sensitivity of the investment project to changes in cost parameters, such as prices for mineral resources and their forecast. This goal is achieved by applying a yield adjustment factor. This indicator should be multiplied by the price of each useful component that is set during optimization. For forecasting, a range of coefficient values and an increment step for performing calculations are determined.

It is also possible to set limiters to include or conversely exclude specific areas from optimization. So, if there are industrial and administrative buildings on the surface, as well as mining facilities, these areas can be removed from the calculation of the optimal contour of the pit. There also can be set boundaries of the allotment to form the optimal pit shell.

The calculated optimal contour is the surface reflecting the outer boundaries of the blocks in each section. Despite the fact that the general angles of the pit walls are taken into account in their formation, the slope angle on each ledge is not taken into account. To identify the general angle, there is practiced introducing additional blocks in the corresponding area.

The proposed algorithm for forming the contour of a pit includes a number of successive stages:

1. Identifying the optimal open pit shell using a block model of deposit design. The result is a digital model of the open pit surface and the establishment of economic estimates for each block by analyzing the technical and economic characteristics. To improve the position of the trench route, both the optimal contour of the pit and the block model are used simultaneously.

2. Pit tracing is carried out taking into account the specified coordinates (beginning and exit to the daylight surface) of the opening workings. When calculating, many factors are taken into account: the direction of the cargo flow, the productivity, the presence of mining facilities on the surface, the terrain, and others. Then, the optimal location of the opening workings in relation to the contour of the quarry is revealed.

3. Modeling the final contour of the site with a system of opening workings. To display the ledge edge line on horizontal plans, the economic estimates of the model blocks and their sizes, as well as the established boundaries within the optimal open-pit shell are taken into account. In this situation, the key design goal is to obtain the maximum economic evaluation of the blocks included in the block model within the final contour of the open pit.

Results

Figure 1 shows the optimal contour of the open pit of the Benkala iron ore deposit obtained as part of the design using information systems based on the optimal shell and the concept of substantiating the final contours. As part of the design, the Whittle MGIS has been used (Figure 1).

The ledge crest lines have been made using the developed technique based on the optimal pit

contour. To do this, the starting point of the route has been set and the position of the opening workings has been optimized with further calculations of the value of the blocks involved in the construction of this trajectory. As a result, the track moved to the surface due to the variability of the pit horizons at the endpoint of the exit. Despite ensuring the track structure's safety, the entry point to the lower horizon had to be moved. This is a forced measure to preserve the designed exit points from the open pit. These measures made it possible to reduce the depth of the contour by 6 meters compared to the initial data.

a)

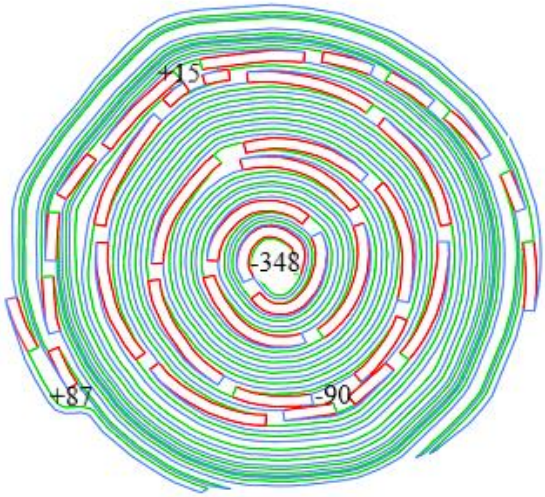

a) the open pit contour option from Benkala

b)

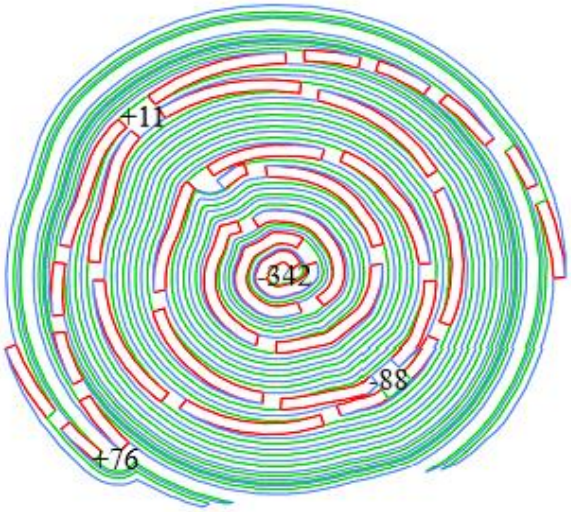

b) the open pit contour from the authors

Figure 1 – Modeling the contour of the open pit at the Benkala deposit

Discussion of results

The comparative analysis according to the parameters of the design contour of option a), presented by Benkala, and option b) modeled by the authors showed decreasing the volume of overburden by 9.59 %, and the volume of ore by 4.01 %. The average content of the useful component increased by 0.7 %. It should be noted that characteristics of the general angle of the open pit remained unchanged, and its final depth became less by 6 meters, which is also a positive characteristic.

Decreasing the overburden and ore volumes relative to option a) caused reducing the deposit mining period by 6 months. In general, decreasing the volume of overburden led to decreasing the volume of related work after reaching the design capacity, which made it possible to reduce the vehicle fleet for mining the deposit.

Figure 2 shows the comparative cost analysis for both options.

a)

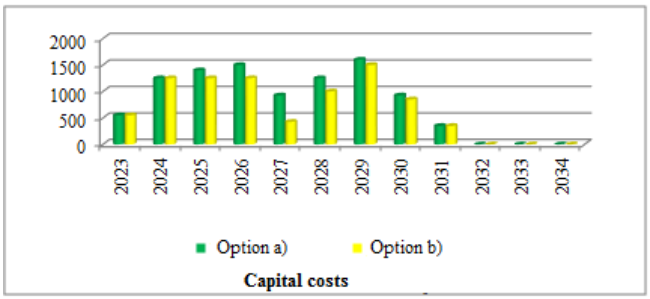

b)

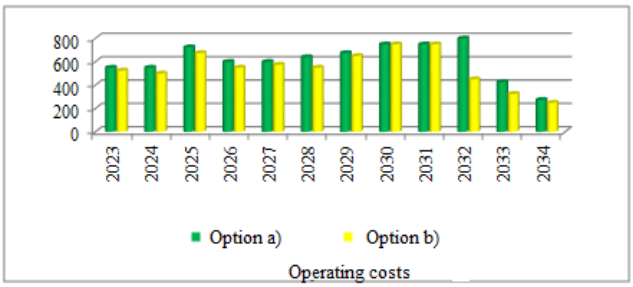

Figure 2 – Costs for the deposit development by the options of the open pit contours, mln.tg.

The reduction of the rock mass in the developed open pit and the distribution of the released volumes made it possible to reduce the company's vehicle fleet by 3 vehicles. This optimization measure led to reducing the capital costs in the authors' option b) compared to the Benkala option a).

There is an observed slight decreasing the volume of operating costs after the field reaches its

design capacity. As a result, the volumes of rock mass were redistributed over the years. During the pit completion period, which should take place in 2032-2034, there is predicted the maximum difference between the operating costs of the two options for the pit contours (the peak falls in 2032).

The investment attractiveness of the proposed option is evidenced by the indicators of net discounted income (+7.48 % compared to the Benkala option), net profit (+1.81 %), and internal rate of return (+4.81 %).

Conclusions

The results of technical and economic calculations allow drawing the following conclusions:

1. When using the pit contour option proposed by the authors, the investment attractiveness of the project increases, it is evidenced by higher rates of the net present value.

2. Current financial ratios and indicators are higher for the proposed option, which also ensures stable resistance to possible risks.

The results obtained and the economic justification allows stating that the proposed method using the Whittle MGIS is effective for the development of iron ore deposits with deep open pits.

Mining and geological information systems based on optimization tools for determining the contour of an open pit are actively used by mining enterprises in designing the work for reconstructing and open pit mining. In the absence of techniques for optimizing the boundaries of open pits, the gross profit from the extraction of rocks is reduced.

The developed method of identifying open pit boundaries takes into account the opening scheme and allows designing the contour in advance, which is especially important for maintaining high technical and economic indicators of the mining enterprise.

Conflict of interest. On behalf of all authors, the corresponding author declares that there is no conflict of interest.

Gratitude. The authors thank the anonymous peer-reviewers whose insightful comments helped to improve this article in profound ways.

Cite this article as: Tyo SG, Zeitinova ShB. Optimizing the contours of open pit mining with the use of mining and geological information systems and technologies. Kompleksnoe Ispolzovanie Mineralnogo Syra = Complex Use of Mineral Resources. 2023; 327(4):50-56. https://doi.org/10.31643/2023/6445.39

Тау-кен-геологиялық ақпараттық жүйелер мен технологиялардың көмегімен ашық тау-кен жұмыстарының контурларын оңтайландыру

[1]Тё С.Г., [2]Зейтинова Ш.Б.

[1]«E4-Capital» ЖШС, Алматы, Қазақстан
[2]Әбілқас Сағынов атындағы Қарағанды техникалық университеті, Қарағанды, Қазақстан

Мақала келді: *17 қазан 2022*
Сараптамадан өтті: *12 қаңтар 2023*
Қабылданды: *02 ақпан 2023*

ТҮЙІНДЕМЕ

Бұл мақалада тау-кен-геологиялық ақпараттық жүйелер мен технологиялардың көмегімен ашық тау-кен жұмыстарын оңтайландыру зерттелді. Зерттеудің мақсаты – тау-кен геологиялық ақпараттық жүйесін қолдана отырып, карьер контурын оңтайландыру алгоритмін жасау. Whittle бағдарламасының көмегімен Лерч-Гроссман алгоритмі қолданылды. Карьер контурын ашу схемасына, геометриялық сипаттамаларға және блоктардың арнайы техникалық-экономикалық параметрлеріне сүйене отырып өзгерту негіздемесі ұсынылған. Бұл ұсыныс кен орнын игеру кезінде өндіру тиімділігін арттырады және күрделі және пайдалану шығындарын қысқартады. Авторлар, қазіргі заманғы ТКГАЖ функционалдығы карьердің негізгі параметрлерін жобалау кезінде нарықтық жағдайларды ескеруге және кен орнын игеруге дайындау кезеңінде және қолданыстағы карьер контурын оңтайландыру кезінде дұрыс шешім қабылдауға көмектеседі деген қорытындыға келді.

Түйін сөздер: ашық тау-кен өндірісі, темір кені, өндіру тиімділігі, карьер контуры, тау-кен жұмыстары, ақпараттық технологиялар, геотехнологиялар.

Тё Сергей Геннадьевич	***Авторлар туралы ақпарат:*** *Аға тау-кен инженері, (MPONEN, MAusIMM), «E4-Capital» ЖШС, Алматы, Қазақстан. Email: Sergey.Tyo@yandex.ru*
Зейтинова Шолпан Бекжигитовна	*PhD докторы, аға оқытушы, Әбілқас Сағынов атындағы Қарағанды техникалық университет, Н.Назарбаев даңғылы, 56/2, 100027, Қарағанды, Қазақстан. Email: zeitinova_rmpi@mail.ru*

Оптимизация контуров открытых горных работ с помощью горно-геологических информационных систем, технологий

[1]Тё С.Г., [2]Зейтинова Ш.Б.

[1]ТОО «E4-Capital», Алматы, Казахстан

[2] Карагандинский технический университет имени Абылкаса Сагинова, Караганда, Казахстан

Поступила: *17 октября 2022*
Рецензирование: *12 января 2023*
Принята в печать*: 02 февраля 2023*

АННОТАЦИЯ

В настоящей статье исследуется оптимизация открытых горных работ с помощью горно-геологических информационных систем и технологий. Целью исследования является разработка алгоритма оптимизации контура карьера с помощью горно-геологической информационной системы. Применен алгоритм Лерча-Гроссмана с помощью программы Whittle. Предложено обоснование изменения контура карьера исходя из схемы вскрытия, геометрических характеристик и специальных технико-экономических параметров блоков. Данное предложение обеспечивает повышение эффективности добычи и сокращение капитальных и эксплуатационных затрат при отработке месторождения. Авторы пришли к выводу, что функционал современных ГГИС помогает учитывать рыночные условия при проектировании основных параметров карьера и принять правильное решение на этапе подготовке месторождения к разработке и при и оптимизации имеющегося контура карьера.

Ключевые слова: открытая добыча, железная руда, эффективность добычи, контур карьера, горные работы, информационные технологии, геотехнологии.

Тё Сергей Геннадьевич	***Информация об авторах:*** *Старший горный инженер (MPONEN, MAusIMM), ТОО «E4-Capital», Алматы, Казахстан Email: Sergey.Tyo@yandex.ru*
Зейтинова Шолпан Бекжигитовна	*Доктор PhD, ст.преподаватель, Карагандинский технический университет имени Абылкаса Сагинова, пр.Н.Назарбаева, 56/2, 100027, Караганда, Казахстан. Email: zeitinova_rmpi@mail.ru*

References

[1] Ordabekova AZh. Geoinformatsionnoye modelirovaniye karyerov [Geoinformation modeling of quarries]. Uchebnoye posobiye. Almaty: KazNTU. 2014. (in Russ.).

[2] Enrique Jelvez, Nelson Morales, Julian M. Ortiz. Stochastic Final Pit Limits: An Efficient Frontier Analysis under Geological Uncertainty in the Open-Pit Mining Industry. Mathematics. 2022; 10*(*1):100. https://doi.org/10.3390/math10010100

[3] Lagos G, Espinoza D, Moreno E, Amaya J. Robust planning for an open-pit mining problem under ore-grade uncertainty. Electron Notes Discrete Math. 2011; 37:15-20. https://doi.org/10.1016/j.endm.2011.05.004

[4] Sarykalin S, Serraino G, Uryasev S. Value-at-Risk vs. Conditional Value-at-Risk in Risk Management and Optimization. In State-of-the-Art Decision-Making Tools in the Information-Intensive Age. Chen Z L, Raghavan S, Gray P, Greenberg HJ. Eds. INFORMS: Catonsville, MD, USA. 2008, 270-294. ISBN 978-1-877640-23-0. https://doi.org/10.1287/educ.1080.0052

[5]Nagovitsyn OV. Kontseptsiya i metody formirovaniya gorno-geologicheskoy informatsionnoy sistemy [The concept and methods of formation of the mining and geological information system]: GIS MINEFRAME: diss... dokt. tekhnicheskikh nauk: 25.00.35. Apatity. 2018. (in Russ.).

[6]Baymuldin MM, Bakhtybayev NB. Analiz vozmozhnostey sushchestvuyushchikh gorno-geologicheskikh informatsionnykh system [Analysis of the capabilities of existing mining and geological information systems]. Rekultivatsiya vyrabotannogo prostranstva: problemy i perspektivy. 2020, 46-49. https://elibrary.ru/item.asp?id=42733772. (in Russ.).

[7]Appianing E, Mireku-Gyimah D. Open Pit Optimisation and Design. Accra: George Grant University of Mines and Technology. 2016,89.
https://www.researchgate.net/publication/312653068_Open_Pit_Optimisation_and_Design_A_Stepwise_Approach

[8]Akisa DM. and Mireku-Gyimah D. Application of Surpac and Whittle Software in Open Pit Optimisation and Design. Ghana Mining Journal. 2015; 15(1):35-43. https://www.ajol.info/index.php/gm/article/view/119495

[9] Rakishev BR, Moldabayev SK. Modernizirovannyye tekhnologii gornykh rabot na karyerakh Kazakhstana [Upgraded technologies of mining operations at the quarries of Kazakhstan]. Forum gornyakov - materialy mezhdunarodnoy konferentsii. Dnepropetrovsk. 3–6 oktyabrya. 2012; 3:13-20. http://ir.nmu.org.ua/jspui/bitstream/123456789/150321/1/13-20.pdf (in Russ.).

[10] Moldabayev SK. Optimizatsiya razvitiya rabochey zony na krutykh bortakh deystvuyushchikh i stroyashchikhsya karyerov Kazakhstana [Optimization of the development of the working area on the steep sides of existing and under construction quarries in Kazakhstan]. Sbornik nauchnykh trudov Natsionalnogo gornogo universiteta. Dnepr: NGU. 2017; 50:69-78. http://ir.nmu.org.ua/handle/123456789/151330 (in Russ.).

[11] Kuznetsov DV, Kosolapov LI. Optimizatsiya parametrov tekhnologicheskikh kompleksov rudnykh karyerov [Optimization of parameters of technological complexes of ore pits]. monografiya. Krasnoyarsk: Sibirskiy federalnyy universitet. 2020, 188. (in Russ.).

[12] Nemova NA, Reznik AV, Karpov VN. O modelirovanii geomekhanicheskikh protsessov na mestorozhdeniyakh v usloviyakh tsifrovoy transformatsii gornodobyvayushchikh predpriyatiy [On modeling geomechanical processes at deposits in the conditions of digital transformation of mining enterprises]. Interekspo Geo-Sibir. 2021; 2(3):332-341. DOI: 10.33764/2618-981X-2021-2-3-332-341 (in Russ.).

[13] Nemova NA, Gavrilov VL. O geomekhanicheskom modelirovanii pri vedenii gornykh rabot na Elginskom mestorozhdenii [About geomechanical modeling during mining operations at the Elginsky field]. Interekspo Geo-Sibir. 2020; 2(1):117-128. DOI: 10.33764/2618-981X-2020-2-117-128. (in Russ.).

[14] Anistratov Yu I. Spravochnik po otkrytym gornym rabotam [Handbook of Open-pit mining]. 2-e izd. dop. M.: NTTs "Gornoye delo". 2019, 239. (in Russ.).

[15] Bruno Tomasi Kuckartz, Rodrigo Lemos Peroni. NPV analysis of multiple surface constraints for pit expansion scenarios under geological uncertainty. Mining REM. 2019; 72(2):293-300. https://doi.org/10.1590/0370-44672017720113

[16] Elkington T, Durham R. Integrated open pit pushback selection and production capacity optimization. Journal of Mining Science. 2011; 47:177-190. https://doi.org/10.1134/S1062739147020055

[17] Ben-Awuah Eugene, Richter Otto, Elkington Tarrant, Pourrahimian Yashar. Strategic mining options optimization: Open pit mining, underground mining or both. International Journal of Mining Science and Technology. 2016; 26(6):1065-1071. http://dx.doi.org/10.1016%2Fj.ijmst.2016.09.015

[18] Canessa G, Moreno E, Pagnoncelli BK. The Risk-Averse Ultimate Pit Problem. Optim. 2021; 22:2655-2678.

[19] Hochbaum DS, Chen A. Performance Analysis and Best Implementations of Old and New Algorithms for the Open-Pit Mining Problem. Oper. Res. 2000; 48:894-914. https://doi.org/10.1287/opre.48.6.894.12392

[20] Rakhmangulov A, Burmistrov K, OsintsevN. Selection of Open-Pit Mining and Technical System's Sustainable Development Strategies Based on MCDM. Sustainability. 2022; 14:8003. https://doi.org/10.3390/su14138003

Crossref
DOI: 10.31643/2023/6445.40
Earth sciences

Studies of the thermal stability of briquettes based on microsilica

[1]Baisanov A.S., [1*]Vorobkalo N.R., [1]Makhambetov Ye.N., [1]Mynzhasar Ye.A., [2]Zulfiadi Zulhan

[1]Zh.Abishev Chemical-Metallurgical Institute, Karaganda, Kazakhstan
[2]Bandung Institute of Technology, Bandung, West Java, Indonesia

[*]Corresponding author email: nina.timirbaeva23@gmail.com

Received: *December 10, 2022*
Peer-reviewed: *January 16, 2023*
Accepted: *February 21, 2023*

ABSTRACT

The object of study in this work is microsilica. Microsilica is a pulverized technogenic waste generated during the smelting of technical silicon in industries. The intended use of this material is to obtain the highest quality grades of technical silicon in the end result without the use of expensive quartz. Microsilica is a finely dispersed powder, the direct processing (without preliminary preparation) of which into technical silicon is impossible in ore-thermal furnaces. That requires the manufacture of high-strength briquettes based on it, meeting all the requirements for raw materials for ore-thermal furnaces. In this paper, the authors present the results of a study of the thermal stability of microsilica-based briquettes in order to optimize the physicochemical properties of the resulting briquettes. The tested microsilica briquettes with various carbonaceous reducing agents (screenings of coke of thermo-oxidative coking, screenings of charcoal, etc.) were obtained on a large-scale laboratory roller briquetting press ZZXM-4. The evaluation of the thermal stability of the briquettes was carried out according to the method in which the resulting briquettes are subjected to thermal shock followed by abrasion on a special drum. The thermal resistance of a briquette is defined as the ratio of the weight of the main body of the briquette after the abrasion test to the sum of the weight of the main body and the crumbled material. The dependence of thermal stability on the granulometric composition of briquettes was also determined. The optimal granulometric composition was determined, with which the briquettes have satisfactory thermal stability. Thus, the most technologically advanced granulometric composition of the briquetting charge for reduction smelting in an ore-thermal furnace was established. It is best to use briquettes with granulometric compositions of the appropriate ratio of fractions 0-1; 1-3; 3-5 mm with the following proportions 35/35/30 and 60/20/15, as well as briquettes with particle size distribution within these ranges of variation.

Keywords: thermal stability, briquettes, microsilica, silicon briquettes, briquetting, silicon waste.

Information about authors:

Baisanov Alibek Sailaubaevich — *Candidate of Technical Sciences, Professor, Head of the Laboratory of Pyrometallurgical Processes, Zh.Abishev Chemical and Metallurgical Institute, Ermekova str., 63, 100009, Karaganda, Kazakhstan. Email: alibekbaisanov@mail.ru*

Vorobkalo Nina Ruslanovna — *Master of Technical Sciences, Junior Researcher of the Laboratory of Pyrometallurgical Processes, Zh.Abishev Chemical and Metallurgical Institute, Ermekova str., 63, 100009, Karaganda, Kazakhstan. Email: nina.timirbaeva23@gmail.com*

Makhambetov Yerbolat Nysanalyuly — *PhD, Head of the Laboratory of Ferroalloys and recovery processes, Zh.Abishev Chemical and Metallurgical Institute, Ermekova str., 63, 100009, Karaganda, Kazakhstan. Email: m.ye.n@mail.ru*

Mynzhasar Yesmurat Amangalievich — *Master of Technical Sciences, Junior Researcher of the Laboratory of Pyrometallurgical Processes, Zh.Abishev Chemical and Metallurgical Institute, Ermekova str., 63, 100009, Karaganda, Kazakhstan. Email: ye.myngzhassar@gmail.com*

Zulfiadi Zulhan — *Dr.-Ing., Lecturer/Researcher of Department of Metallurgical Engineering, Faculty of Mining and Petroleum Engineering, Bandung Institute of Technology, Indonesia. Email: zulfiadi.zulhan@gmail.com*

Introduction

Due to the widespread use of silicon in various fields of industry, a lot of work is currently underway to optimize the technological process of its production [1]. An important problem of the technological process of production of technical silicon in the conditions of Tau-KenTemir LLP is the formation of a large amount of microsilica. Under the conditions of Tau-KenTemir LLP, when smelting one ton of technical silicon according to standard technology using vein quartz with a carbonaceous reducer, one ton of microsilica is captured by gas cleaning systems, with 65-70% extraction of silicon

into metal [[2], [3]]. Such average annual technical and economic indicators significantly worsen the economics of production, which not only highlights the problem of the lack of technological solutions for the processing/utilization of microsilica but also creates an environmental problem associated with the storage of technogenic waste [[4], [5], [6], [7]]. This fact indicates the need for a number of research works to find a competent utilization of microsilica. It should also be noted that developments are underway around the world to improve existing and create new methods for involving finely dispersed raw materials in metallurgical processing [[8], [9]], including in the production of technical silicon.

Microsilica is an ultra-disperse material consisting of spherical particles, obtained in the process of cleaning the exhaust gases of furnaces in the production of technical silicon [10]. In the world, only a small part of these wastes has found application for the manufacture of building concrete mixtures [[11], [12]]. In turn, microsilica can be a significant quality source of raw materials for the production of technical silicon. This material in the bulk consists of a valuable component - silicon dioxide and the number of harmful impurities is not high, so it is important to use microsilica as a raw material for the production of silicon and its alloys.

Utilization and use of pulverized waste in the form of microsilica should be considered as an important direction in saving material resources [[13], [14], [15]]. The use of microsilica for the production of silicon is complicated by the fact that it is in a finely dispersed form [[16], [17], [18]], and does not meet the requirements for charge materials for smelting in ore-thermal furnaces. Therefore, it is required to develop an optimal mode of agglomeration of this material to obtain high-strength briquettes. This should be taken into account when developing a new resource-saving technology for smelting crystalline silicon using microsilica. Briquetting is considered the most effective method of agglomeration for metallurgical production due to the possibility of agglomeration of raw materials of wide-size classes in almost any ratio and any chemical composition, as well as the ergonomics of the process.

Currently, there is no state regulatory and technical base that regulates the requirements for briquettes as an element of the technological process. In this connection, the resulting briquettes in terms of their chemical composition, geometric dimensions (size), and strength must meet the requirements and features of the technological process in which they are supposed to be used. Since the chemical composition and size of briquettes are set before briquetting, one of the important characteristics of the quality of briquettes is their thermal stability. Heat resistance is characterized by the preservation of the shape of briquettes when they are kept for 3 minutes at a temperature above 600 °C.

The authors of this work, in order to optimize the process of microsilica briquetting for the smelting of technical silicon, for the first time among previous studies, took into account the factor of thermal stability of briquettes. This factor has never been taken into account before. The lack of this experience often led to the disintegration of briquettes when loaded onto the top of an ore-thermal furnace. Therefore, a negative attitude towards the possibility of using briquettes based on finely dispersed quartz materials as a feedstock in the smelting of technical silicon has firmly entrenched in the silicon industry.

Experimental part

High-strength briquettes based on microsilica with various carbonaceous reducing agents (screenings of coke of thermo-oxidative coking, screenings of charcoal, etc.) were obtained on a large laboratory briquetting press ZZXM-4. By achieving close contact in the briquette between microsilica silicon oxides and solid carbon of carbonaceous reducing agents, the most favorable conditions for the reduction and smelting of silicon are achieved. In this case, it becomes possible to involve scarce low-ash carbonaceous reducing agents as fine fractions reducing agents. The liquid glass was used as a binder. The optimal consumption of liquid glass per ton of charge mixture was established - 0.067 t / t at a charge moisture content of 8%. The resulting briquettes were subjected to natural drying at a temperature of 18-24 ^{0}C during the day.

Until now, with the use of briquette raw materials, not only in the production of silicon but in many electrothermal industries, little attention has been paid to the thermal stability index of briquettes. Many researchers only qualitatively described the fact of scattering of briquettes when they hit the top of an ore-thermal furnace as a result of a sharp change in temperature [[19], [20]].

To optimize the process of smelting technical silicon from briquette mono-charge, the authors of this work carried out studies to determine the thermal stability of briquettes obtained from microsilica and carbonaceous reducing agents. Here

a method for the quantitative description of this property is proposed. This method (technique) for quartz was proposed by SMS Demag (Germany) [21].

According to this technique, quartz samples with a fraction of 20 - 30 mm are placed in a crucible and kept at 1300°C for one hour. The sample is taken out and cooled to room temperature. A fraction of + 20 mm is taken and placed in a drum with a diameter of 200 mm, a depth of 100 mm with four 17 mm ribs on the side. The drum is rotated 80 times at a rotation speed of about 40 rpm. Next, the sample is sieved on 20, 10, 4, and 2 mm sieves, and a granulometric curve is built. The temperature resistance is evaluated according to the reference curves - figure 1, developed by SMS Demag.

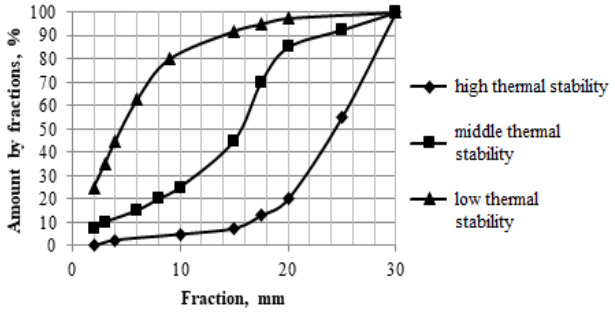

Figure 1 - Particle-size curves for assessing the thermal stability of quartz raw materials

In this work, the evaluation of the thermal stability of briquettes was carried out by a similar method, with the difference that the briquettes after thermal shock and the subsequent abrasion test were not subjected to screening, but the fraction of fines that crumbled as a result of the test relative to the main body of the briquette was estimated. The thermal shock was carried out at a temperature of 900 0C with exposure for 1 hour. After testing for abrasion on a special drum, the main body of the briquette is weighed, and the material that has fallen off the surface of the briquette during the test is collected and weighed. The thermal resistance of a briquette is defined as the ratio of the weight of the main body of the briquette after the abrasion test to the sum of the weight of the main body and the crumbled material.

It should be especially noted that the achievement of the highest thermal stability is achieved by optimizing the drying mode. Two options for removing moisture from the briquette were considered. In the first version, the briquettes were dried in a laboratory oven at a temperature of 250-2700C with high intensity and forced air blowing of the furnace space for 30 minutes from the initial moisture content of 20-25% to the residual moisture content of 1-2%. The second option is closer to practical implementation in industrial production and includes three stages. In the first stage, wet briquettes from the briquetting press are kept under natural drying conditions for about 24 hours until a residual moisture content of about 12-18%. This is necessary in order to be able to reload wet briquettes using special equipment and load them into bunkers without significant destruction of the briquette structure. Next, the briquettes are loaded into a chamber-type oven with natural air circulation in the oven space, where the briquettes are dried to a residual moisture content of 10-12% for 8 hours. After that, dried briquettes should gain strength within 5-7 days. In this case, the residual external humidity of the briquette will be about 5%. Part of the moisture in the process of setting the briquette will turn into a crystalline form.

Results and discussion

Table 1 presents the results of the thermal stability of briquettes of various compositions at various stages of the drying process, as well as in different variants of its implementation. As can be seen from the table, the final thermal strength of the briquettes is higher when drying according to the second option. In this regard, when assessing the impact of the granulometric composition of the briquette mixture and the briquetting force on the physicochemical properties of the briquettes, the data obtained as a result of the three-stage method of drying the briquettes were taken

Figure 2 shows graphs of the thermal strength of briquettes for different types of granulometric composition of the briquette charge. Analyzing the data presented in Figure 2, it should be noted that all dependencies, except for the dependence for fine mixtures, pass through a maximum. Reducing the proportion of fine fractions from 60 to 35% provides a slight shift of the maximum towards greater optimal briquetting forces from 300 to 370 kgf/cm^2. This achieves a large value of thermal stability of the briquettes - about 90%. Further reduction of fines fraction 0-1 mm in the charge to 15% leads to a sharp deterioration in the conditions of briquetting and requires an increase in effort at optimal heat resistance up to 780 kgf/cm^2. Optimum thermal

stability under these conditions is reduced to 65%. When finely dispersed mixtures are used in the process of briquetting, the thermal strength of the briquettes sharply increases to a force of 300 kgf/cm^2. After this value, the growth rate decreases significantly. The dependence in this area has a monotonically increasing character up to a force value of 880 kgf/cm2. The value of thermal strength at this force is quite high, but does not exceed the option with a fine fraction of 35%. Thus, from the point of view of the thermal strength of the briquette, the optimal ratio of fractions is 0-1; 1-3; 3-5 mm in proportions 35/35/30.

Table 1 - Comparative analysis of thermal stability of briquettes, % at various stages of the drying process

Briquette composition	Drying stage			
	Drying 24 hours up to 12-18%	Drying in a chamber furnace - 8 hours up to 10-12%	Drying - 5-7 days up to 5%	Quick furnace dry 30 minutes
Special coke - 40% Microsilica - 60%	40	58	75	50
Charcoal - 10% Special coke – 20% Microsilica - 70%	32	40	82	48

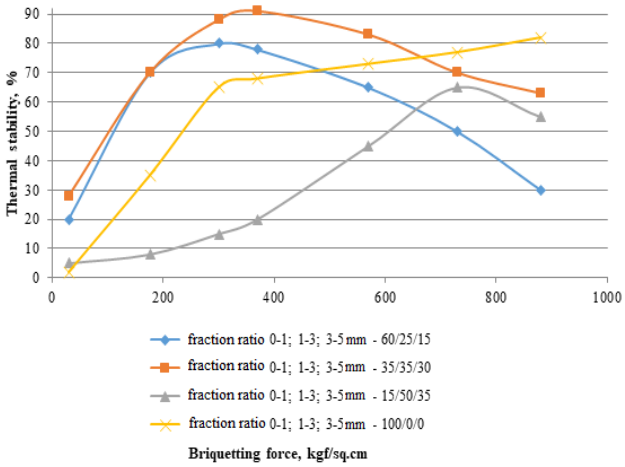

Figure 2 - The dependence of the thermal stability of briquettes on the briquetting force and particle size distribution of the briquetting charge

The presence of particles of different pore diameters in the briquette improves the gas permeability of the layer of reaction products due to the formation of macrocavities in the body of the briquette during the gasification of carbon inclusions. The negative point in this is a decrease in the thermal stability of briquettes with content of particles with a diameter of 1-3 and 1-5 mm increased by more than 30%. The briquettes subjected to the thermal stability test, formed from a charge, including microsilica, screenings of quartz, and screenings of oxidative thermocoking coke with a particle size ratio close to optimal, acquire a specific macrostructure, shown in Figure 3. They can be identified by the presence of macrocavities (pores) on the body of the briquette, the solid body of the briquette is microsilica, white inclusions are quartz, black are coke screenings.

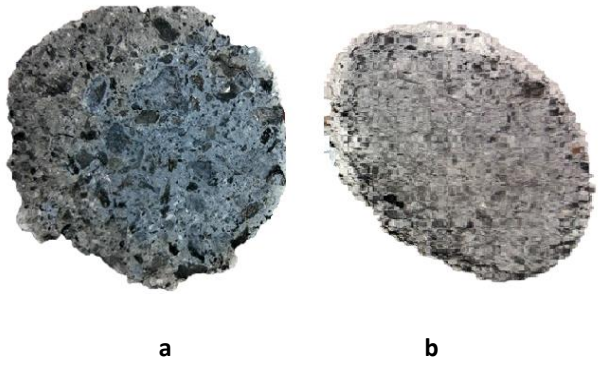

a **b**

Figure 3 - Macrostructure on the fracture of a briquette of fractions 0-1; 1-3; 3-5 mm at a ratio of 35/35/30 (a - briquette at a pressure of 175 kgf / cm^2; b - briquette at a pressure of 300 kgf / cm^2)

Conclusions

Thus, the most technologically advanced granulometric composition of the briquetting charge for reduction smelting in an ore-thermal furnace was established. It is best to use briquettes with granulometric compositions of the appropriate ratio of fractions 0-1; 1-3; 3-5 mm with the following proportions 35/35/30 and 60/20/15, as well as briquettes with particle size distribution within these ranges of variation. A briquette with a finer fractional composition is characterized by greater thermal stability, which is undesirable when smelted in ore-thermal furnaces. Less fine briquette shows the opposite characteristics. Which of the factors is

more significant can be determined as a result of the use of these briquettes in ore-thermal smelting.

It is also worth noting that in all cases the high thermal stability was combined with the high mechanical strength of the briquette. Therefore, this indicator was not studied in this work.

Source of financing. This work was carried out as part of a study funded by the Science Committee of the Ministry of Science and Higher Education of the Republic of Kazakhstan (grant no. AP14870218).

Conflict of interest. The corresponding author declares that there is no conflict of interest.

Cite this article as: Baisanov AS, Vorobkalo NR, Makhambetov YeN, Mynzhasar YeA, Zulfiadi Zulhan. Studies of the thermal stability of briquettes based on microsilica. Kompleksnoe Ispolzovanie Mineralnogo Syra = Complex Use of Mineral Resources. 2023; 327(4):57-63. https://doi.org/10.31643/2023/6445.40

Микрокремнезем негізіндегі брикеттердің термиялық беріктігін зерттеу

[1]Байсанов А.С., [1*]Воробкало Н.Р., [1]Махамбетов Е.Н., [1]Мыңжасар Е.А., [2]Zulfiadi Zulhan

[1]Ж.Әбішев атындағы химия-металлургия институты, Караганда Қазақстан
[2]Бандунг технологиялық институты, Бандунг, Батыс Ява, Индонезия

Мақала келді: *10 желтоқсан 2022*
Сараптамадан өтті: *16 қаңтар 2023*
Қабылданды: *21 ақпан 2023*

ТҮЙІНДЕМЕ

Осы жұмыстағы зерттеу объектісі микрокремнезем - өндірістерде техникалық кремнийді балқыту кезінде пайда болатын шаң тәрізді техногендік қалдықтар болып табылады. Бұл материалды болжамды пайдалану-қымбат кварцты пайдаланбай, техникалық кремнийдің ең жоғары сапалы брендтерін алу. Микрокремнеземді қайта өңдеу проблемасы микрокремнеземнің кенді-термиялық пештерде техникалық кремнийге тікелей өңдеу (алдын ала дайындықсыз) мүмкін болмайтын ұсақ дисперсті ұнтақ болып табылатындығына байланысты. Бұл кенді-термиялық пештерге арналған шикізат материалдарына қойылатын барлық талаптарды қанағаттандыратын оның негізінде жоғары беріктігі бар брикеттерді дайындауды талап етеді. Бұл жұмыста авторлар алынған брикеттердің физика-химиялық қасиеттерін оңтайландыру мақсатында микрокремнезем негізіндегі брикеттердің термиялық тұрақтылығын зерттеу нәтижелерін ұсынды. Әр түрлі көміртекті тотықсыздандырғыштары бар сыналатын микрокремнезем брикеттері (Термо тотықтырғыш кокстеу коксы, көмір скринингі және т.б.) ZZXM-4 ірі зертханалық роликті брикеттеу прессінде алынды. Брикеттердің термиялық беріктігін бағалау әдістеме бойынша жүргізілді, онда алынған брикеттер термиялық соққыға ұшырайды, содан кейін оларды арнайы барабанда тоздырады. Брикеттің термиялық тұрақтылығы абразивті сынақтан кейінгі брикеттің негізгі дене салмағының және құлаған материалдың қосындысына қатынасы ретінде анықталады. Сондай-ақ, термиялық тұрақтылықтың брикеттердің гранулометриялық құрамына тәуелділігі анықталған болатын. Брикеттердің қанағаттанарлық термиялық төзімділігі бар оңтайлы гранулометриялық құрамы анықталды. Егер брикеттелген шихтаның ең технологиялық гранулометриялық құрамын таңдаса, онда 0-1; 1-3; 3-5 мм фракцияларының тиісті қатынасы бар түйіршікті құрамы бар брикеттер сәйкесінше 35/35/30 және 60/20/15 пропорцияларында, сондай-ақ осы вариация шегінде түйіршікті құрамы бар брикеттер кенді-термиялық пеште тотықсыздандырғыш балқу үшін жақсырақ екенін атап өтуге болады.

Түйін сөздер: термиялық төзімділік, брикеттер, микрокремнезем, кремний брикеттері, брикеттеу, кремний қалдықтары

Авторлар туралы ақпарат:

Байсанов Алибек Сайлаубаевич — *Техника ғылымдарының кандидаты, профессор, пирометаллургиялық процестер зертханасының меңгерушісі, Ж.Әбішев атындағы химико-металлургиялық институт, Ермеков көшесі, 63, 100009, Қарағанды қ., Қазақстан. Email: alibekbaisanov@mail.ru*

Воробкало Нина Руслановна — *Техника ғылымдарының магистрі, пирометаллургиялық процестер зертханасының кіші ғылыми қызметкері, Ж.Әбішев атындағы химико-металлургиялық институт, Ермеков көшесі, 63, 100009, Қарағанды қ., Қазақстан. Email: nina.timirbaeva23@gmail.com*

Махамбетов Ерболат Нысаналыулы — *PhD, ферроқорытпалар және қалпына келтіру процестері зертханасының меңгерушісі, Ж.Әбішев атындағы химико-металлургиялық институт, Ермеков көшесі, 63, 100009, Қарағанды қ., Қазақстан. Email: m.ye.n@mail.ru*

Мыңжасар Есмұрат Аманғалиұлы — *Техника ғылымдарының магистрі, пирометаллургиялық процестер зертханасының кіші ғылыми қызметкері, Ж.Әбішев атындағы химико-металлургиялық институт, Ермеков көшесі, 63, 100009, Қарағанды қ., Қазақстан. Email: ye.myngzhassar@gmail.com*

Zulfiadi Zulhan — *Техника ғылымдарының докторы,Бандунг технологиялық институтының тау-кен ісі және мұнай инженериясы факультетінің металлургиялық машина жасау кафедрасының оқытушысы / зерттеушісі, Индонезия. Email: zulfiadi.zulhan@gmail.com*

Исследования термической стойкости брикетов на основе микрокремнезема

[1] Байсанов А.С., [1*]Воробкало Н.Р., [1]Махамбетов Е.Н., [1]Мыңжасар Е.А., [2]Zulfiadi Zulhan

[1]Химико-металлургический институт им. Ж. Абишева, Караганда Қазақстан
[2]Бандунгский технологический институт, Бандунг, Западная Ява, Индонезия

Поступила: *10 декабря 2022*
Рецензирование: *16 января 2023*
Принята в печать: *21 февраля 2023*

АННОТАЦИЯ

Объектом исследования в настоящей работе является микрокремнезем - пылевидный техногенный отход, образующийся при выплавке технического кремния на производствах. Предполагаемое использование данного материла - получение в конечном результате наиболее высококачественных марок технического кремния без использования дорогостоящего кварца. Проблема переработки микрокремнезема связана с тем, что микрокремнезем представляет собой мелкодисперсный порошок, непосредственная переработка (без предварительной подготовки) которого на технический кремний невозможна в рудно-термических печах. Что требует изготовления высокопрочных брикетов на его основе, удовлетворяющих всем требованиям, предъявляемым к сырьевым материалам для рудно-термических печей. В данной работе авторами представлены результаты исследования термической стойкости брикетов на основе микрокремнезема с целью оптимизации физико-химических свойств получаемых брикетов. Испытываемые брикеты из микрокремнезема с различными углеродистыми восстановителями (отсевы кокса термоокислительного коксования, отсевы древесного угля и др.) были получены на крупно-лабораторном валковом брикетировочном прессе ZZXM-4. Оценку термической стойкости брикетов выполняли по методике, в которой полученные брикеты подвергаются термическому удару с последующим их истиранием на специальном барабане. Термическая стойкость брикета определяется как отношение веса основного тела брикета после испытания на истираемость к сумме веса основного тела и осыпавшегося материала. Также была определена зависимость термической стойкости от гранулометрического состава брикетов. Определен оптимальный гранулометрический состав, с которым брикеты обладают удовлетворительной термической стойкостью. Если выбирать наиболее технологичный гранулометрический состав брикетированной шихты, то можно отметить, что лучше подходят к восстановительной плавке в рудно-термической печи брикеты с гранулометрическими составами соответствующим соотношением фракций 0-1; 1-3; 3-5 мм в следующих пропорциях 35/35/30 и 60/20/15 соответственно, а также брикеты с гранулометрическим составом в этих пределах варьирования.

Ключевые слова: термическая стойкость, брикеты, микрокремнезем, кремниевые брикеты, брикетирование, кремниевые отходы

Информация об авторах:

Байсанов Алибек Сайлаубаевич — *Кандидат технических наук, профессор, заведующий лабораторией пирометаллургических процессов, Химико-металлургический институт им. Ж. Абишева, ул. Ермекова, 63, 100009, г. Караганда, Казахстан. Email: alibekbaisanov@mail.ru*

Воробкало Нина Руслановна — *Магистр технических наук, младший научный сотрудник лаборатории пирометаллургических процессов, Химико-металлургический институт им. Ж. Абишева, ул. Ермекова, 63, 100009, г. Караганда, Казахстан. Email: nina.timirbaeva23@gmail.com*

Махамбетов Ерболат Нысаналыулы — *PhD, заведующий лабораторией ферросплавов и процессов восстановления, Химико-металлургический институт им. Ж.Абишева, ул. Ермекова, 63, 100009, г. Караганда, Казахстан. Email: m.ye.n@mail.ru*

Мыңжасар Есмұрат Аманғалиұлы — *Магистр технических наук, младший научный сотрудник лаборатории пирометаллургических процессов, Химико-металлургический институт им. Ж. Абишева, ул. Ермекова, 63, 100009, г. Караганда, Казахстан. Email: ye.myngzhassar@gmail.com*

Zulfiadi Zulhan — *Доктор технических наук, преподаватель/исследователь кафедры металлургического машиностроения факультета горного дела и нефтяной инженерии Бандунгского технологического института, Индонезия. Email: zulfiadi.zulhan@gmail.com*

References

[1] Protopopov A, Protopopov M, Suleimenov E, Aimenov Z, Altynbekov R. Study of silicon production process in ore-smelting furnace and optimization of technological process. Kompleksnoe Ispolzovanie Mineralnogo Syra = Complex Use of Mineral Resources. 2022, 326(3):68-80. https://doi.org/10.31643/2023/6445.30

[2] Data of LLP Tauken Temir (Electron resource) 2022. (Access date: 12.11.2022), URL: http://www.tks-temir.kz/

[3] Nikolay Zobnin, Torgovets Anatoliy, Pikalova Irina, Yussupova Yuliya, Atakishiyev Sergey. Influence of Thermal Stability of Quartz and the Particle Size distribution of Burden Materials on the Process of Electrothermal Smelting of Metallurgical Silicon. Oriental Journal of Chemistry. 2018; 34:1120-1125. http://dx.doi.org/10.13005/ojc/340265

[4] Glazev M, Bazhin V. On the recycling and use of microsilica in the oil industry. E3S Web of Conferences. 2021, 266. https://doi.org/10.1051/e3sconf/202126602010

[5] Freitas L, Magrini A. Waste Management in Industrial Construction: Investigating Contributions from Industrial Ecology. Sustainability. 2017; 9(7):1251. https://doi.org/10.3390/su9071251

[6] Dvořáček J, Vodzinský V, Domaracká L. Industrial Wastes and Economics of their Utilization. Metalurgija. 2006; 45(2):141-143. https://hrcak.srce.hr/6527

[7] Yi Zhong, Sun Heng, Wan Jian, Li Chao. A New Process for Highly Effective Utilization of Industrial Solid Wastes — Sialite Technology. Advanced Materials Research. 2009; 66:210-213. https://doi.org/10.4028/www.scientific.net/AMR.66.210

[8] Li Y, Zhang J, Liu Z, et al. Reduction Mechanism of Iron Oxide Briquettes by Carbonaceous Materials Extracted from Blast Furnace Dust. Metallurgical and Materials Transactions B: Process Metallurgy and Materials Processing Science. 2019; 50(5): 2296-2303. https://doi.org/10.1007/s11663-019-01628-7

[9] Snyman M, Snyman N. Improved ultrafine coal dewatering using different layering configurations and particle size combinations. Journal of the Southern African Institute of Mining and Metallurgy. 2019, 119. https://doi.org/10.17159/2411-9717/2019/v119n3a10

[10] Bruno M. An investigation of microsilica by thermoanalytical methods. Thermochimica Acta. 1998; 318(1-2):125-129.

[11] Ahmad Subhan, Umar A, Masood Amjad, Nayeem Mohammad. Performance of self-compacting concrete at room and after elevated temperature incorporating Silica fume. Advances in concrete construction. 2019; 7:31-37. https://doi.org/10.12989/acc.2019.7.1.031

[12] Mater J. Guide for the use of silica fume in concrete. ACI. 1995; 92(4):437-440.

[13] Zakharov SV, Vasiliev KO, Yermolovich E V. Assessment of environmental friendliness of the use of silicon production waste. School of postgraduate students of the All-Russian scientific conference. Irkutsk. 2017, 16-20.

[14] Bernd F. Microsilica-characterization of a unique additive. IIBCC 2006 - Sao Paulo, Brazil. October 15 – 18. 2006; 10.

[15] Elkin KS. Production of metallic silicon in Russia — state and prospects. "Non-ferrous metals and minerals 2014": materials of the sixth international congress. 16-19 September 2014, Krasnoyarsk. 2014.

[16] Dubenskiy MS, Kargin A A. Mikrokremnezem - otkhod ili sovremennaya dobavka? [Microsilica is a waste or a modern additive?]. Vestnik Kuzbasskogo gosudarstvennogo tekhnicheskogo universiteta [Bulletin of the Kuzbass State Technical University]. 2012; 1(89):119-120. (In Russ.).

[17] Szelag M. Development of cracking patterns in modified cement matrix with microsilica. Materials. 2018; 11(10):1928. https://doi.org/10.3390/ma11101928

[18] Kuz'min MP, Larionov LM, Paul K. Chu. New Methods of Obtaining Al–Si Alloys Using Amorphous Microsilica. International Journal of Metalcasting. 2019; 14:207-217.

[19] Ozhogin VV. Osnovy teorii i tekhnologii briketirovaniya izmelchennogo metallurgicheskogo syria: monografiya. Mariupol: PGTU (Fundamentals of the theory and technology of briquetting shredded metallurgical raw materials: monograph. Mariupol: PSTU). 2010, 442.

[20] Ravich BM. Briketirovaniye v tsvetnoy i chernoy metallurgii [Briquetting in non-ferrous and ferrous metallurgy]. D. M.: «Metallurgiya». 1975, 356.

[21] Degel R, Fröhling Ch, Kalisch M, Hecker E. Oterdoom H. Innovative electric smelter solutions of the SMS group for the silicon industry. The Fourteenth International Ferroalloys Congress Energy efficiency and environmental friendlinessare the future of the global Ferroalloy industry. 2015; 4:122-132.

Crossref
DOI: 10.31643/2023/6445.41
Metallurgy

A review of recovery technologies of rare and rare earth metals from wastes generated in titanium and magnesium production

[1]Toishybek A.M., [1*]Baigenzhenov O.S., [2]Turan M.D., [3]Kurbanova B., [1]Merkibayev Y.S.

[1] Satbayev University, Almaty, Kazakhstan
[2] Firat University, Elazig, Turkey
[3]Nazarbayev University, Astana, Kazakhstan

[*]Corresponding author email: o.baigenzhenov@satbayev.university

Received: *December 04, 2022*
Peer-reviewed: *January 23, 2023*
Accepted: *February 22, 2023*

ABSTRACT

It is acknowledged that titanium and magnesium production wastes pollute the environment, which in the sequence they create an environmental hazard for soils, groundwater and vegetation. Meanwhile, these wastes can be considered secondary resources of rare and rare earth metals. In recent years, the processing of industrial waste has been a new trend for the extraction of rare and rare earth metals, which can partially cover the demand in case of their disposal. This article is devoted to a review of the available literature and articles on the extraction of rare metals from titanium-magnesium production waste using various processing methods. Methods of their utilization are discussed with an emphasis on the extraction of rare and rare earth metals. This review considered waste processing technologies of various pyrometallurgical and hydrometallurgical processes. Technological schemes of various leaching and extraction processes were presented to give a holistic view of waste processing and extraction of rare metals contained in them. In general, the article contains an overview of the works published on the extraction of rare metals, such as REE (rare earth elements), niobium, tantalum and vanadium.

***Keywords*:** titanium wastes, rare metals, niobium, vanadium, scandium, rare earth elements, leaching, chlorination

Information about authors:

Toishybek Azamat Magauiyauly — *PhD student, Non-commercial joint-stock company "Satbayev University", the department "Metallurgical processes, heat engineering and technology of special materials", st. Satpaeva 22, 050000, Almaty, Kazakhstan, E-mail: A.Toishybek@stud.satbayev.university*

Baigenzhenov Omirserik Sabyrzhanovich — *Doctor PhD, Assoc. Professor, Non-commercial joint-stock company "Satbayev University", the department "Metallurgical processes, heat engineering and technology of special materials", st. Satpaeva 22, 050000, Almaty, Kazakhstan, E-mail: o.baigenzhenov@satbayev.university*

Turan Mehmet Deniz — *Professor, Doctor PhD, Firat University, Engineering Faculty, Metallurgical and Materials Engineering, Elazig, Turkey, E-mail: mdturan@firat.edu.tr*

Kurbanova Bayan — *Researcher, Nazarbayev University, Department of Physics, School of Sciences and Humanities, ave. Kabanbay Batyra 53, 010000 Astana, Kazakhstan, E-mail: bayan.kurbanova@nu.edu.kz*

Merkibayev Yerik Serikuly — *PhD student, Non-commercial joint-stock company "Satbayev University", the department "Metallurgical processes, heat engineering and technology of special materials", st. Satpaeva 22, 050000, Almaty, Kazakhstan, E-mail: y.merkibayev@satbayev.university*

Introduction

Rapid industrialization has influenced the demand for rare metals, in particular titanium and titanium-bearing materials. Titanium is used for different branches of the car industry, aerospace, doping, petroleum engineering, and chemical processing. However, during the recovery of titanium-bearing raw materials, there are massive amounts of waste generated. These wastes are sent to special landfills or sludge storage facilities and they pose a significant danger to the environment, polluting soils and natural waters. Because they are released into the atmosphere and acidic industrial wastewater is discharged into water streams. It is widely known that for the recovery of titanium, the Kroll process is

commonly used. As a result, various residues, especially such as titanium chloride residues, electrolytes, sludge, and gases, residues are formed consisting of chlorides, and oxychlorides of rare metals [1].

The complex recovery of waste in titanium production has long been considered one of the most pressing issues. The waste contains various valuable components and rare metals. Considering that reserves of rare metals are concentrated in the surface layer of waste, in turn, it affects the fall in the cost of production of rare metals. Niobium, tantalum and scandium oxides with a total content of 0.6-1.5% are found in titanium production waste [2].

It is acknowledged that the Kroll method based on magnesium thermal reduction is used for processing titanium concentrates. Therefore, a large amount of waste is formed. For the process of producing 1 ton of titanium, about 2 tons of chloride waste are formed. In this regard, there is a need to neutralize chloride residues [3]. Various chloride wastes (used electrolytes, melts, sludge) are thrown into waste landfills and are harmful to the environment because they are not used as raw materials. In the production of titanium tetrachloride, titanium-containing slag is used, which contains a significant amount of rare metals-Nb, Ta, Sc, V, Zr, etc. In addition, in large quantities, the additives Fe, K, Na, Ca, Na, and Mg are irretrievably lost. During chlorination, most of these impurities are converted into chlorides and oxychlorides, and due to their physicochemical properties, they are concentrated in individual semi-products and production waste. This leads to high chlorine consumption, additional costs and environmental pollution [[4], [5]].

Sludge and waste are stored in special warehouses and landfills at titanium-magnesium plants. In turn, waste storage is an expensive service, as well as in the event of an increase in the norms of the maximum permissible concentration (MPC) in accumulated waste and the enterprise will face fines and sanctions. [6].

The purpose and objective of the review are to highlight existing technologies for processing wastes that are generated in titanium and magnesium production, as well as the survey of methods of recovery rare and rare earth metals from them.

Recovery of Nb and Ta from titanium wastes. Niobium (Nb) and tantalum (Ta) are rare metals and the qualities of both metals make them critical raw materials. In nature, tantalum and niobium are most often found together. In deposits, as in the earth's crust, the concentration of Nb is usually an order of magnitude higher than Ta. It is worth noting that niobium itself has a high affinity for titanium which in turn it affects the formation of a wide range of niobium minerals with titanium. In addition to this, these two mineral groups (titanoniobates and tantaloniobates) are regarded as economically viable options for niobium recovery. Owing to this fact, titanium raw materials and waste, by-products are considered one of the sources of niobium production [7].

The chemical composition of spent titanium chlorinator melts is presented in Table 1 [8].

According to Table 1, the content of niobium in spent melt of titanium chlorinators (SMTC) is on average 0.025-0.030%, which is a good indicator, given that rare metals are concentrated in a scattered form. Another important feature of niobium is its large smear on titanium and its ability to heterovalent isomorphism. This affects the formation of niobium impurities and the formation of niobium compounds in titanium minerals. This means that the higher the concentration of titanium in raw materials and waste, the higher the niobium impurities [[9], [10]]. The importance of niobium and tantalum lies in their internal properties such as corrosion resistance, conductivity, high electrical capacity and biocompatibility. Both metals have similar chemical and physical properties, which makes them easier to separate and clean. However, their content in the Earth's crust is very low, Nb-0.002%, Ta-0.0002% [11]. Such limited availability requires the processing of secondary raw materials containing Ta and Nb, including titanium-magnesium waste, as well as metal waste and intermediates.

Recovery of pure titanium is a complex and technically difficult process; as crude titanium ore can not be recovered directly from its natural form. Therefore, raw titanium ore is processed by the Kroll method. As a result, titanium tetrachloride is formed, which in turn is used for obtaining titanium dioxide (TiO_2) pigment and titanium sponge. The titanium tetrachloride ($TiCl_4$) contains substantial amounts of niobium, tantalum and scandium due to accompanying elements in titanium ore [12]. These rare metals can not be recovered by traditional methods because the slurry contains $TiCl_4$.

Xiang et al. [13] developed a process flow sheet (figure 1) for recovering niobium concentrate from

$TiCl_4$ slurry residue by evaporation and acid leaching (HCl). According to their research, titanium tetrachloride ($TiCl_4$), niobium concentrate and solution of aluminium chloride ($AlCl_3$) were recovered separately. The authors first evaporated the slurry at 200°C for 60 minutes. As a result, around 98% of titanium was recovered from the slurry. Then, they leached the residue with HCl (concentration -2.1 mol/l, L/S ratio of 6:1, T-80°C, t-60 minutes) and washed it with an ammonia solution (2 mol/l, L/S ratio of 4:1 ml/g, t-30 minutes, at room temperature). Their results after filtration indicated that Nb concentrate content with Nb-53,40% and Ta-5,57% was obtained.

In other studies, the authors investigated the recovery of niobium from chloride residues generated from the chlorination of titanium slags [[14], [15]]. In order to recover two-stage leaching process was suggested. The technological scheme of two-stage leaching is shown in Figure 2 [15]. For the first stage of leaching, water is used, whereas 4.0 M of HCl (Hydrochloric acid) is used in the second stage. The leaching process was carried out at 25°C, with an S:L ratio of 1:4 and a mixing speed of 400 rpm. Cation exchange sorbents such as Purolite-C104 and KU-2-8H were used for the sorption of niobium from the leaching process solution. After the leaching process with water, the pulp was sent to the filtration process to separate the pregnant leach solution and the niobium-rich cake. Then, the leaching solution was sent to the processes of obtaining scandium and carnallite. When using Purolite-C104 ion exchange resin, the sorption efficiency of niobium from solution with the concentration of 2 g/l was around 71.0 % (0.071 g/g) in 3.5 hours. Meanwhile, in terms of KU-2-8 H ion exchange resin, this indicator was about 89.0 % (0.089 g/g).

Table 1 - Chemical composition of spent titanium chlorinator melt [8].

Composition	Content, %	Composition	Content, %	Composition	Content, %
TiO_2	1-2	$MgCl_2$	6-12	$MgCl_2$	4.5-5,0
SiO_2	4-7	$CaCl_2$	3-4,5	Cr_{total}	0.8-1.55
C	3-6	$FeCl_2$	10-12	Nb_2O_5	0.025-0.030
Sc_2O_3	0.01-0.03	$FeCl_3$	1-3	Ta_2O_5	0.005-0.006
$AlCl_3$	5-6	KCl	22-47	Cl^-	45-50
V_2O_5	0.01-0.45	NaCl	14-18		

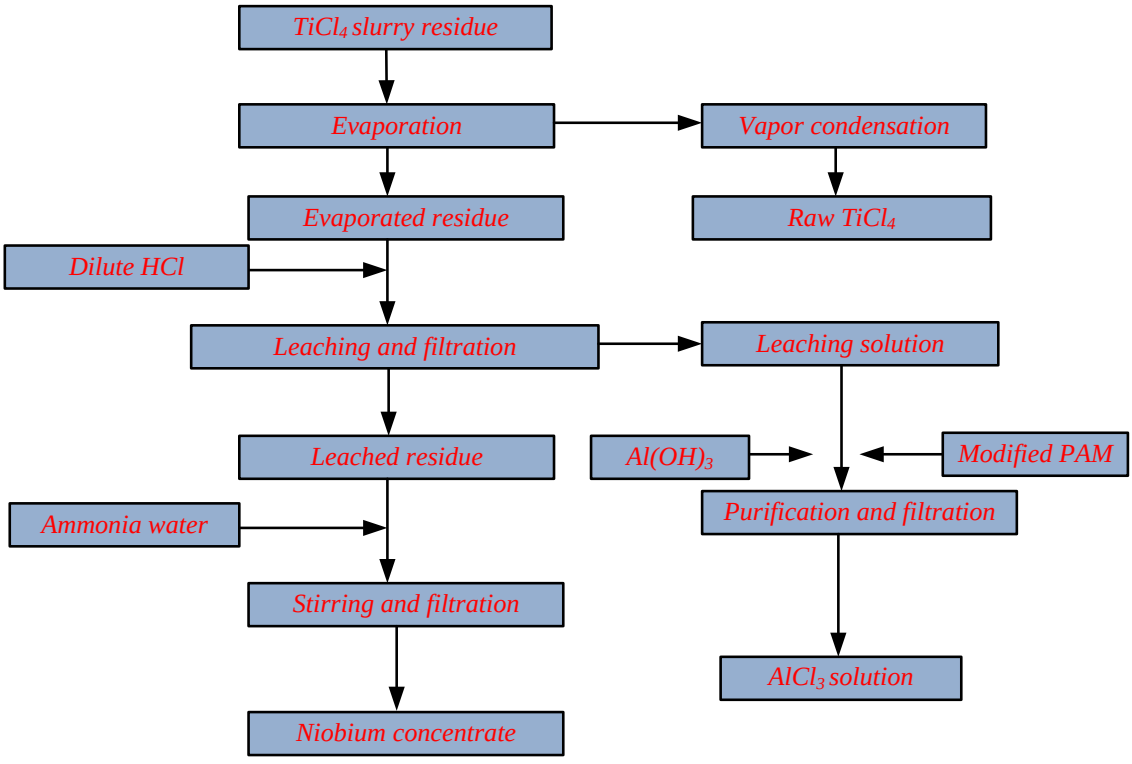

Figure 1 - Technological flow sheet of metal recovery from $TiCl_4$ slurry residue [13].

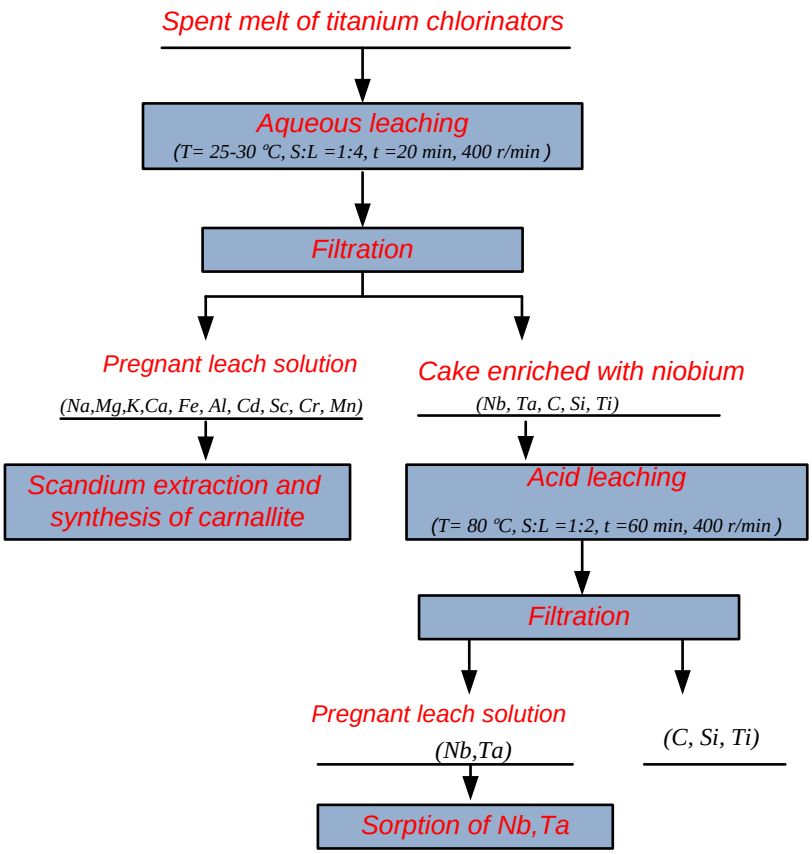

Figure 2 - Flow sheet of the two-stage leaching process [15].

Recovery of V from titanium wastes. Ilmenite ore commonly contains titanium, iron, and vanadium. Most of the vanadium passes into titanium slag, during the reduction melting of ilmenite concentrate. Throughout, the chlorination of titanium slag, about 70% of vanadium is concentrated in technical $TiCl_4$ mainly in the form of $VOCl_3$ and partially VCl_4. The presence of vanadium in titanium sponge significantly deteriorates the quality of titanium [[16], [17]].

Purification of titanium tetrachloride from impurities is a key stage in the production of titanium sponges. Because $TiCl_4$ contains a significant amount of impurities in the dissolved state and in the form of a fine mechanical suspension. For example, $SiCl_4$, $VOCl_3$, VCl_4, CCl_4, $SOCl_2$ and other chloride solutions are mixed with $TiCl_4$ in all ratios. As a result, it leads to the form of a continuous series of solutions that is a hindrance to further processing Titanium tetrachloride is purified from impurities in various ways, such as sedimentation, filtration, rectification, and distillation [18].

These wastes as a form of pulp represent a mixture of $TiCl_4$, $TiCl_3$, and $AlCl_3$. When mixing pulps of lower chlorides with titanium tetrachloride titanium trichloride interacts with vanadium oxytrichloride and converts it into an insoluble form of $VOCl_2$. The precipitate containing $VOCl_2$ is sent to the extraction of vanadium [[19], [20]].

Sidorenko et al. proposed (figure 3) [21] vanadium recovery by the method of liming aluminium vanadium cake with further processing of lime cake. The authors suggested washing lime cake with water. After that, the compounds of vanadium, aluminium and titanium passed into the dechlorinated cake and the chloride ions and the main part of calcium into the solution. The dechlorinated cake is easier to treat during oxidative roasting without adding special additives. The optimal temperature for roasting was between 700-750°C. After roasting, the cinder was leached by soda between 70-80°C. Hence, vanadium pentoxide is converted into the soluble form of $NaVO_3$. Whereas, insoluble compounds formed the cake that contained aluminium and titanium.

The concentration of the soda solution fluctuated in the range of 33-100 g/dm^3, and the leaching time was between 1-4 hours. According to the authors, evidence leaching proceeded better in denser pulps. The highest degree of vanadium extraction was observed at a solution concentration

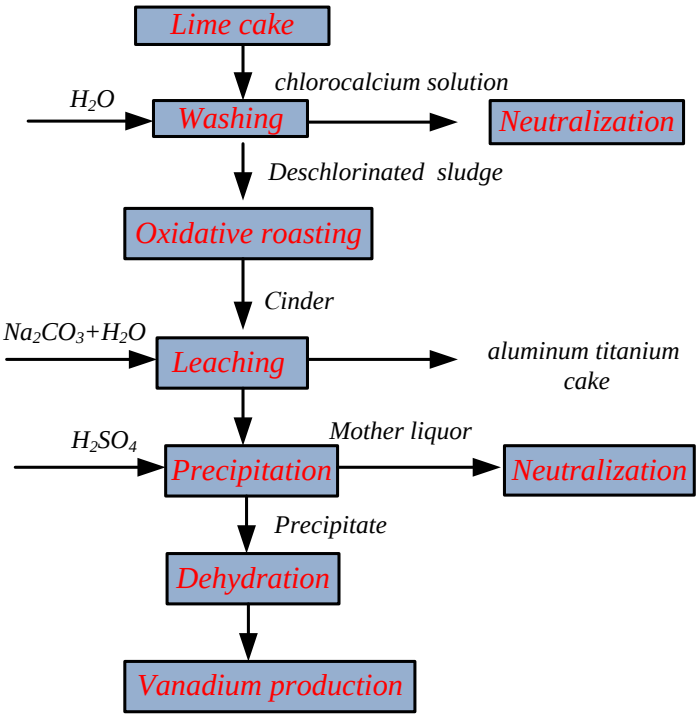

Figure 3 - Technological flow sheet for recovery vanadium from lime cake [21].

of 50 g/dm^3. An increase in the leaching time at this concentration led to an increase in the degree of extraction of vanadium from 90 to 96.5%.

Recovery of REEs from titanium wastes. Rare earth elements (REEs) are a group of 17 elements, including scandium (Sc), yttrium (Y) and 15 lanthanides [22]. REEs are almost not mined from primary ore deposits, because of their economic feasibility and effectiveness. Owing to this, the urgent demand has prompted many organizations to evaluate alternative sources of REE [[23], [24]].

As elucidated above, Sc is a less abundant element and it is a related group of REE. According to the latest works, scandium recovery from secondary sources has been accelerated from different by-products (tailings, waste acids, and solid residues, residue streams) in the production of other metals including REE, titanium, aluminium, iron ore, and uranium [[25], [26], [27], [28], [29], [30]].

Scandium is the solid residue generated in Titanium dioxide (TiO_2) production [31]. Titanium-bearing ores contain high content of scandium and are the most important resource for their extraction [[32], [33]]. For instance, in China, the ilmenite ores on average contain 0.002-0.004 Scandium oxide (Sc_2O_3) [34]. Scandium resources are accessible in the form of liquid wastes of TiO_2 pigment production, and industrial production volume is estimated to be 8.4 million tons around the world [35].

One of the resources of scandium is hydrolyzed sulfuric acid, which is generated in the production of titanium dioxide [[36], [37]]. The authors studied the separation and recovery of Sc and Ti from the hydrolyzed sulfuric acid waste of titanium dioxide [32] by using the solvent extraction method. This method is based on using a mixed solution of Na_3PO_4 and H_2O_2 to selectively scrub titanium over scandium from the loaded organic solution bearing scandium and titanium. Then, NaOH solution (4 mol/l) is added to strip scandium from the scrubbed solution. Authors, scandium stripping was 93% and after elaboration results, the final product of scandium was 83,9%.

E. Mikeli et al. studied [38] the absorption process of scandium by ion-exchange resins from acidic iron chloride solution ($FeCl_2$) that generated th titanium industry. The authors used two types of exchange resins VP OC 1026 and TP 260 respectively. Among them, VP OC 1026 was more suitable for Scandium extraction and column capacity was 1.46 mg/ml in the experimental conditions. This study also demonstrated the presence of Zr, V, and Ti in the initial solution as they coextracted both resins tests. These metals have more capacity values in the loaded resins,

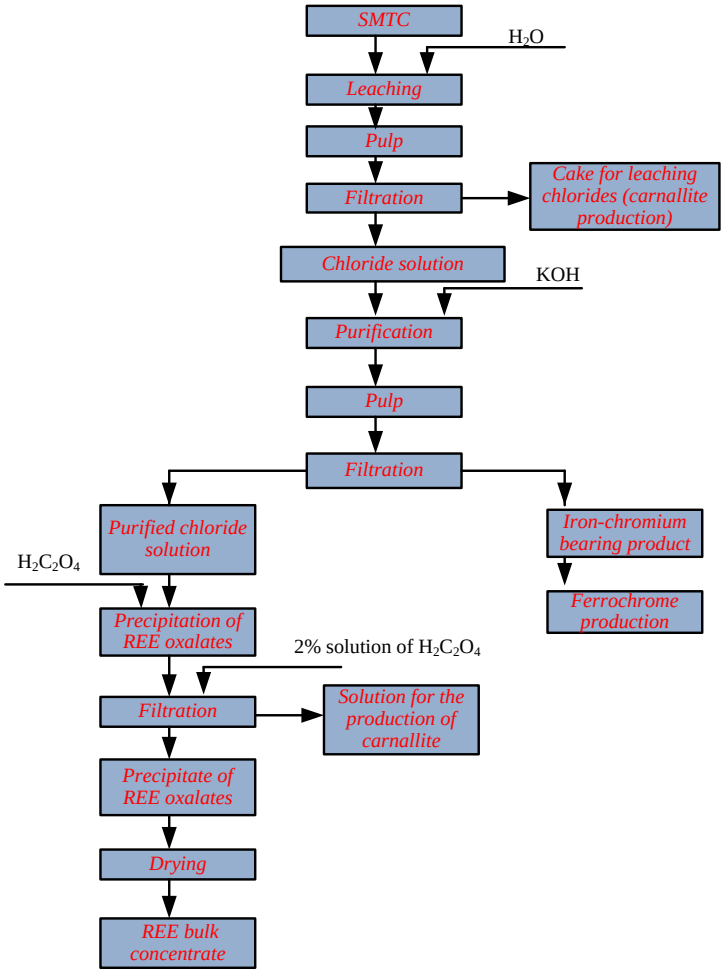

Figure 4 - Technological flow sheet of recovery concentrate of REE from spent melt of titanium chlorinators (SMTC) [40].

however, particularly in VP OC 1026, an improvement in Sc concentration was better than the other metals. It demonstrated that VP OC 1026 resin showed a higher affinity for Sc.

From the commercial perspective, the composition of the rare earth elements in the spent melt of titanium chlorinators (SMTC) is attractive, as the proportion of dysprosium is 57%, neodymium 8%, and cerium is 13% [[39], [40]]. The authors of this work [41] studied the recovery of REE concentrate from SMTC. Thus, the authors proposed technological flow sheet recovery of REE concentrate from SMTC (figure 4). The results of chemical analysis showed that the content of REE oxalates was 96.0%, while the overall content of the main impurities such as barium and iron oxalates accounted for 3.1%. The recovery of rare-earth elements from REE from SMTC into the bulk concentrate reached 66% [42].

Conclusion

Rare metals are widely used in many strategic industry objects. Rare metals are generally found in ores of other metals as concomitant elements and recovered from their slurries and residues. Different metallurgical processes of niobium, vanadium and REEs recovery from titanium and magnesium production, such as spent titanium chloride wastes, titanium dioxide wastes, tailings, and residues are reviewed. Specifically, niobium and tantalum are mainly concentrated in the spent melt of titanium chlorinators (SMTC), sludge, whereas, scandium also is concentrated in SMTC. When it comes to vanadium, it is mainly concentrated in aluminium vanadium cake. Considering, the rare metals and rare earth elements distribution and content, titanium industry residues might be prospective rare metal resources. According to the literature survey,

hydrometallurgical methods such as ion exchange, solvent extraction, and leaching are now applicable for the recovery of rare metals from wastes, slurries, and residues, but most of them have not found their method for effective application in the industry. In summary, despite the aforementioned challenges requiring further research, the recovery of rare metals from titanium waste continues to show significant prospects for the foreseeable future.

Cite this article as: Toishybek AM, Baigenzhenov OS, Turan MD, Kurbanova B, Merkibayev YS. A review of recovery technologies of rare and rare earth metals from wastes generated in titanium and magnesium production. Kompleksnoe Ispolzovanie Mineralnogo Syra = Complex Use of Mineral Resources. 2023; 327(4):64-73. https://doi.org/10.31643/2023/6445.41

Титан және магний өндірісінің қалдықтарын қайта өңдеу арқылы сирек және сирек жер металдарын алу технологияларына шолу

[1]Тойшыбек А.М., [1*]Байгенженов О.С., [2]Туран М.Д., [3]Құрбанова Б., [1]Меркібаев Е.С.

[1]Сәтбаев университеті, Алматы, Қазақстан
[2] Фырат Университеті, Элязыг,Турция
[3] Назарбаев университеті, Астана, Қазақстан

Мақала келді: *04 желтоқсан 2022*
Сараптамадан өтті: *23 қаңтар 2023*
Қабылданды: *22 ақпан 2023*

ТҮЙІНДЕМЕ

Титан және магний өндірісінің қалдықтары қоршаған ортаны ластап, экологиялық қауіп тудыратыны белгілі. Бұның салдарынан, топырақ, жер асты сулары мен өсімдіктер зардап шегеді. Сонымен қатар, бұл қалдықтарды сирек кездесетін және сирек жер элементтерінің (СЖЭ) қайталама ресурстары ретінде қарастыруға болады. Соңғы жылдары техногендік өнеркәсіптік қалдықтарды қайта өңдеу сирек кездесетін және сирек жер элементтерін (СЖЭ) алудың жаңа тенденциясы болып табылады. Бұл мақала әртүрлі өңдеу әдістерін қолдана отырып, титан және магний өндірісінің қалдықтарынан сирек металдарды алу туралы әдебиеттер мен мақалаларға шолу жасауға арналған. Мақалада сирек және сирек кездесетін элементтерді (СЖЭ) алуға баса назар аудара отырып, оларды кәдеге жарату жолдары талқыланады. Жоғарыда келтірілген қайта өңдеу технологиялары әртүрлі пирометаллургиялық және гидрометаллургиялық процестерді қамтиды. Қалдықтарды қайта өңдеу және құрамындағы сирек металдарды алу туралы тұтас түсінік беру үшін әртүрлі шаймалау, сорбция және экстракция процестерінің технологиялық сызбалары ұсынылды. Тұтастай алғанда, мақалада СЖЭ, ниобий, тантал және ванадий сияқты сирек металдарды алу жұмыстарына шолу көрсетілген.

***Түйін сөздер*:** титан қалдықтары, сирек металдар, ниобий, ванадий, сирек жер металдар, шаймалау, хлорлау

Авторлар туралы ақпарат:

Тойшыбек Азамат Мағауияұлы — *Ph.D. докторант, «Сәтбаев университеті», «Металлургиялық процестер, жылу техникасы және арнайы материалдар технологиясы» кафедрасы, Алматы, Қазақстан, E-mail: A.Toishybek@stud.satbayev.university*

Байгенженов Омирсерик Сабыржанович — *Doctor Ph.D., қауымд.проф. «Сәтбаев университеті», «Металлургиялық процестер, жылу техникасы және арнайы материалдар технологиясы» кафедрасы, Алматы, Қазақстан, E-mail: o.baigenzhenov@satbayev.university*

Туран Мехмет Дениз — *Doctor Ph.D., проф. «Фырат университеті», «Металлургия және материалтану» кафедрасы, Элязыг, Туркия, E-mail: mdturan@firat.edu.tr*

Құрбанова Баян — *Зерттеуші, Назарбаев университеті, Жаратылыстану, әлеуметтік және гуманитарлық ғылымдар мектебі, «Физика» кафедрасы, Астана, Қазақстан, E-mail: bayan.kurbanova@nu.edu.kz*

Меркібаев Ерік Серікұлы — *Ph.D. докторант, Сәтбаев университеті, «Металлургиялық процестер, жылу техникасы және арнайы материалдар технологиясы» кафедрасы, Алматы, Қазақстан, E-mail: y.merkibayev@satbayev.university*

Обзор по технологиям переработки отходов титаномагниевого производства и извлечению редких и редкоземельных металлов

[1]Тойшыбек А.М., [1*]Байгенженов О.С., [2]Туран М.Д., [3]Курбанова Б., [1]Меркибаев Е.С

[1]Satbayev University, Алматы, Казахстан
[2]Университет Фырат, Элязыг, Турция
[3]Nazarbayev University, Астана, Казахстан

Поступила: *04 декабря 2022*
Рецензирование: *23 января 2023*
Принята в печать: *22 февраля 2023*

АННОТАЦИЯ

Известно, что отходы титаномагниевого производства загрязняют окружающую природную среду, создавая экологическую опасность: страдают почвы, и грунтовые воды и растительность. В то же время эти отходы могут быть рассмотрены в качестве вторичных ресурсов редких и редкоземельных металлов. Последние годы переработка техногенных промышленных отходов является новой тенденцией для извлечения редких и редкоземельных металлов, которые могут частично покрыть спрос в случае их утилизации. Данная статья посвящена обзору имеющих литературы и статей по извлечению редких металлов из отходов титаномагниевого производства с использованием различных способов переработки. Обсуждаются способы их утилизации с акцентом на извлечение редких и редкоземельных металлов. Приведенные технологии переработки отходов включают различные пирометаллургические и гидрометаллургические процессы. Были представлены технологические схемы различных процессов выщелачивания и извлечения, чтобы дать целостное представление о переработке отходов и извлечении содержашихся в них редких металлов. В целом, в статье содержится обзор опубликованных работ по извлечению редких металлов, таких как РЗЭ, ниобий, тантал и ванадий.

Ключевые слова: титановые отходы, редкие металлы, ниобий, ванадий, редкоземельные элементы , выщелачивание, хлорирование

Информация об авторах:

Тойшыбек Азамат Мағауияұлы — *Ph.D. докторант, Satbayev University, кафедра «Металлургические процессы, теплотехника и технология специальных материалов», Алматы, Казахстан, E-mail: A.Toishybek@stud.satbayev.university*

Байгенженов Омирсерик Сабыржанович — *Доктор Ph.D., ассоц. профессор, Satbayev University, кафедра «Металлургические процессы, теплотехника и технология специальных материалов», Алматы, Казахстан, E-mail: o.baigenzhenov@satbayev.university*

Туран Мехмет Дениз — *Доктор Ph.D., профессор, Firat University, факультет Инженерия, кафедра «Металлургия и материаловедение», Элязыг, Турция, E-mail: mdturan@firat.edu.tr*

Баян Курбанова — *Исследователь, Nazarbayev University, Школа естественных, социальных и гуманитарных наук, кафедра «Физики», Астана, Казахстан, E-mail: bayan.kurbanova@nu.edu.kz*

Меркибаев Ерик Серикулы — *Ph.D. докторант, Satbayev University, кафедра «Металлургические процессы, теплотехника и технология специальных материалов», Алматы, Казахстан, E-mail: y.merkibayev@satbayev.university*

References

[1]Wensheng Z, Zhaowu Z, Chu YC. A literature review of titanium metallurgical processes. Hydrometallurgy. 2011; 108(3-4):177-188. ISSN 0304-386X, https://doi.org/10.1016/j.hydromet.2011.04.005.

[2]Baybekov MK, Popov VD, Cheprasov IM. Proizvodstvo chetyrekhkhloristogo titana [Production of titanium tetrachloride]. Moscow: Metallurgy. 2nd edition. 1987, 128. (in Russ.).

[3]Nguyen TH, Lee MS. A review on the recovery of titanium dioxide from Ilmenite ores by direct leaching technologies. Mineral Processing and Extractive Metallurgy Review. 2018, 1-17. doi:10.1080/08827508.2018.1502668

[4]Perks C, Mudd G. Titanium, zirconium resources and production: A state of the art literature review. Ore Geology Reviews. 2019; 107:629-646.

[5]Maldybayev G, Naimanbaev M, Shadrunova I, Lokhova N, Sharipov R. Study of soda effect on the sintering process of low titanium slag, Journal of Chemical Technology and Metallurgy. 2018; 53(3):564-571

[6]Yessengaziyev AM, Ultarakova AA, Burns PC. Fluoroammonium method for processing of cake from leaching of titanium-magnesium production sludge. Kompleksnoe Ispolzovanie Mineralnogo Syra = Complex Use of Mineral Resources. 2022; 320(1):67-74. https://doi.org/10.31643/2022/6445.08

[7]Ultarakova A, Kenzhaliyev B, Onayev M, Yessengaziyev A, Kasymzhanov K. Investigations of waste sludge of titanium production and its leaching by nitric acid. 19th International Multidisciplinary Scientific Geoconference & Expo SGEM 2019, Albena. 2019, 861-868.

[8]Khudaibergenov TE. Titanomagnievoe proizvodstvo. Tekhnologiya pererabotki promproduktov iotkhodov: Ucheb. nauch. izd. dlya Vuzov. Almaty: IPF S&K. 1996, 178.

[9] Volodin V, Tuleushev Y, Kenzhaliyev B, Trebukhov S. Thermal degradation of hard alloys of the niobiumcadmium system at low pressure. Kompleksnoe Ispolzovanie Mineralnogo Syra = Complex Use of Mineral Resources. 2020; 312(1):41-47. https://doi.org/10.31643/2020/6445.05

[10] Sarsembekov TK, Chepushtanova TA. Distribution of niobium and vanadium in titanium tetrachloride production middlings. Tsvetnye Metally. 2022; 8:55-60. DOI: 10.17580/tsm.2022.08.07

[11] Abundance of elements in the earth's crust and in the sea, CRC Handbook of Chemistry and Physics, 97th edition. 2016-2017, 14-17.

[12] Wang XW, Wang MY, Xiang XY, Gong SC, and Zhao, YR. Recovery of $TiCl_4$ from precipitation slime by spray drying. Titanium Industry Progress. 2012; 29(5):36-38.

[13] Xiang X, Wang X, Xia W, and Yin J. Metal recovery from $TiCl_4$ slurry by evaporation and acid leaching. The Southern African Insitute of Mining and Metallurgy. http://dx.doi.org/10.17159/2411- 9717/85-192-1/2019

[14] Khabiyev A, Baigenzhenov O, Korganbayeva Zh. Toishybek A, Chepushtanova T, Orynbayev B. Niobium (V) recovery from leaching solution of titanium wastes: kinetic studies. Metalurgija. 2022; 61(3-4).

[15] Baigenzhenov OS, Toishybek AM, Khabiyev AT, Aimbetova IO, Dagubayeva AT. Tïtan öndirisiniñ qaldıqtarınan nïobïydi katïon almaswşı sorbentter kömegimen bölip alw [Recovery of niobium from wastes generated in titanium production by cation exchange sorbents]. Kompleksnoe Ispolzovanie Mineralnogo Syra = Complex Use of Mineral Resources. 2021; 3(318):97-103. (In Kazakh). https://doi.org/10.31643/2021/6445.33

[16] Nasimifar A, Mehrabani JV. A review on the extraction of vanadium pentoxide from primary, secondary, and co-product sources. International Journal of Mining and Geo-Engineering. 2022; 56(4):361-382.

[17] Gilligan R, Nikoloski AN. The extraction of vanadium from titanomagnetites and other sources. Minerals Engineering. 2020; 146:106106.

[18] Gunjko IM, Egorov SG, SidorenkoSA, Chervonyj IF. O vozmoznosti izvlechenija vanadija iz produktov kaskadno-rektifikacionnoj tehnologii [The possibility of extracting vanadium from cascaded products distillation technology]. Journal of Zaporozhye State University. 2012, 71-75. (in Russ.).

[19] Gunjko IM, Egorov SG. Izvlechenie pentaoxsida vanadija iz othodov tetrahlorida titana razlichnimi metodami [The extraction of vanadium pentoxide from waste of titanium tetrachloride by various methods] Science Rise. 2015; 4(2(9)):7-11. (in Russ.).

[20] Dorda IYu, Overchenko IE, Shkurin BN. i dr. Promyshlennye ispytanija novogo reagenta dlja himicheskoj ochistki tehnicheskogo tetrahlorida titana ot vanadija s ocenkoj kachestva titana gubchatogo [Industrial test new reagent for chemical cleaning from vanadium to the assessment of quality of titanium sponge of technical titanium tetrachloride]. Report on implementation of research works. 2011, 104-109. (in Russ.).

[21] Sidorenko SA, Nesterenko TN, Litvinova EN. Izvlechenie vanadija iz hloridnyh othodov titanovogo proizvodstva [Vanadium extraction from chloride waste of titanium production]. Journal of Zaporozhye State University. 2009; 38-42. (in Russ.).

[22] Jena BC, Dresler W, & Reilly IG. Extraction of titanium, vanadium and iron from titanomagnetite deposits at pipestone lake, Manitoba, Canada. Minerals Engineering. 1995; 8(1-2):159-168. doi:10.1016/0892-6875(94)00110-x

[23] Balaram, V. Rare earth elements: A review of applications, occurrence, exploration, analysis, recycling, and environmental impact.Geosci. Front. 2019; 10:1285-1303.

[24] Botelho Junior AB, Espinosa DCR, Vaughan J, Tenório JAS. Recovery of scandium from various sources: A critical review of the state of the art and future prospects. Miner. Eng. 2021; 172:107148.

[25] Sariev O, Dossekenov M, Kelamanov B, Abdirashit A. High-carbon ferromanganese smelting on high-base slags. Kompleksnoe Ispolzovanie Mineralnogo Syra = Complex Use of Mineral Resources. 2020; 315(4):63-73. https://doi.org/10.31643/2020/6445.38

[26] Daminescu D, Duteanu, N, Ciopec M, Negrea A, Negrea P, Neme¸s NS, Berbecea A, Dobra G, Iliev S, Cotet L, et al. Scandium Recovery from Aqueous Solution by Adsorption Processes in Low-Temperature-Activated Alumina Products. Int. J. Mol. Sci. 2022; 23:10142. https://doi.org/ 10.3390/ijms231710142

[27] Zhang Y, Zhao H, Sun M, Zhang Y, Meng X, Zhang L, Lv X, Davaasambuu S, Qiu G. Scandium extraction from silicates by hydrometallurgical process at normal pressure and temperature. J. Mater. Res. Technol. 2020; 9:709-717.

[28] Chen Y, Ma S, Ning S, Zhong Y, Wang X, Fujita T, Wei Y. Highly efficient recovery and purification of scandium from the waste sulfuric acid solution from titanium dioxide production by solvent extraction. J. Environ. Chem. Eng. 2021; 9:106226.

[29] Koizhanova AK, Kenzhaliyev BK, Kamalov EM, Erdenova MB, Magomedov DR, Abdyldaev NN. Research of Gold Extraction Technology from Technogenic Raw Material. News of the National Academy of Sciences of the Republic of Kazakhstan: Series Chemistry and Technology. 2020; 439(1):95-101. https://doi.org/10.32014/2020.2518-1491.12

[30] Jha AR. Rare Earth Materials: Properties and Applications. 1st ed. CRC Press. 2014. https://doi.org/10.1201/b17045Bc

[31] Wang W, Pranolo Y, & Cheng CY. Metallurgical processes for scandium recovery from various resources: A review. Hydrometallurgy. 2011; 108(1-2):100-108. doi:10.1016/j.hydromet.2011.03.001

[32] Li Y, Li Q, Zhang G, Zeng L, Cao Z, Guan W, & Wang L. Separation and recovery of scandium and titanium from spent sulfuric acid solution from the titanium dioxide production process. Hydrometallurgy. 2018; 178:1-6. doi: 10.1016/j.hydromet.2018.01.019

[33] Gao LK, Rao B, Dai HX, Hong Z, & Xie HY. Separation and Extraction of Scandium and Titanium from a Refractory Anatase Lixivium by Solvent Extraction with D2EHPA and Primary Amine N1923. Journal of Chemical Engineering of Japan. 2019; 52(11):822-828. doi:10.1252/jcej.18we347 B

[34] Chen Z. The Determination of Microamounts of Scandium in Vanadous Titanomagnetite. Mining and Metallurgical Engineering. 1990; 10:54-56.

[35] Gambogi J. USGS Minerals Information: Titanium and Titanium Dioxide. Online. U.S. Geological Survey, National Minerals Information Center: Reston, VA, USA. 2021.

[36] U.S. patent no. 6,530,987. Auer G, Lailach G, Meisen U, Schuy W. and Julius U. Washington, DC: U.S. patent and trademark office. Opubl. 2003.

[37] Xu SQ, Li SQ. Review of the extractive metallurgy of scandium in China 1978-1991. Hydrometallurgy. 1996; 42(3):337-343.

[38] Mikeli E, Marinos D, Toli A, Pilichou A, Balomenos E, Panias D. Use of Ion-Exchange Resins to Adsorb Scandium from Titanium Industry's Chloride Acidic Solution at Ambient Temperature. Metals. 2022; 12(5):864. https://doi.org/10.3390/met12050864

[39] Kenzhaliyev OB, Ilmaliyev ZB, Tsekhovoy AF, Kassymova GK. Conditions to facilitate commercialization of R & D in case of Kazakhstan, Technology in Society. 2021; 67:101792. https://doi.org/10.1016/j.techsoc.2021.101792

[40] Ultarakova AA, Lokhova NG, Naymanbayev MA, Baltabekova ZhA, Alzhanbayeva NSh. Razrabotka kompleksnoy tekhnologii pererabotki otkhodov titanomagniyevogo proizvodstva [Development of a comprehensive technology for waste processing of titanium magnesium production]. Materialy shestoy mezhd. nauch. praktich. konf. «GEOTEKhNOLOGIYa-2013: Problemy i puti innovatsionnogo razvitiya gornodobyvayushchey promyshlennosti [Materials of the Sixth Int.scientific-practical.Conf. GEOTECHNOLOGY-2013: Problems and ways of innovative development of the mining industry.] Institut gornogo dela im. D.A. Kunayeva. Almaty. 2013, 351-355. (in Russ).

[41] Mamutova AT, Ultarakova AA, Kuldeev EI, Yessengaziyev AM. Sovremennoe sostoyanie I predlagaemye resheniya problem pererabotki khloridnykh otkhodov titano-magnievogo proizvodstva [Modern condition and proposed solutions for propessing chloride waste processes of titanium-magnesium production] Kompleksnoe Ispolzovanie Mineralnogo Syra = Complex Use of Mineral Resources. 2018; 4:173-180. https://doi.org/10.31643/2018/6445.44. (in Russ).

[42] Yessengaziyev AM, Ultarakova AA, Uldakhanov OH. Calcium nitrate generating out of nitrogen-acid solutions after breaking up slurries of titanium production. Kompleksnoe Ispolzovanie Mineralnogo Syra = Complex Use of Mineral Resources. 2019; 4:74-81. https://doi.org/10.31643/2019/6445.40

Crossref
DOI: 10.31643/2023/6445.42
Metallurgy

Electrothermal processing of chrysotile-asbestos wastes with production of ferroalloy and extraction of magnesium into the gas phase

[1]Akylbekov Ye.Ye., [1*]Shevko V.M., [2]Aitkulov D.K.,[1]Karataeva G.E.

[1]M. Auezov South Kazakhstan University, Shymkent, Kazakhstan
[2]National Center on complex processing of mineral raw materials of the Republic of Kazakhstan, Almaty, Kazakhstan

**Corresponding author email: shevkovm@mail.ru*

Received: *November 23, 2022*
Peer-reviewed: *January 24, 2023*
Accepted: *February 22, 2023*

ABSTRACT

The article presents the results of an experimental study on the processing of wastes from chrysotile-asbestos production at Kostanay Minerals JSC. An electrothermal technology for the extraction of magnesium and siliceous ferroalloy from the chrysotile-asbestos wastes is proposed. The influence of the amount of coke and steel shavings on the technological parameters of the obtained alloys is determined. The results of derivatographic and SEM analyses of the chrysotile-asbestos waste samples are presented. The studies included planning experiments using the second-order rotatable designs (Box-Hunter plans), graphical optimization of technological parameters, and electric melting of a charge in a graphite crucible using a single-electrode arc furnace. Adequate regression equations were obtained explaining the effect of the amount of coke and steel shavings added to the chrysotile-asbestos waste on the extraction degree of silicon into the alloy and the silicon concentration in the alloy. By the electric melting of the charge, high-quality FS25 grade ferrosilicon with a silicon content of 24.4-29.2% and FS45 grade ferrosilicon with a silicon content of 41.6-45% were obtained. It was established that FS45 grade ferrosilicon with the extraction degree of silicon into the alloy from 75 to 85.4% is formed in the presence of 33.6-38% of coke and 16-20.8% of steel shavings. FS25 grade ferrosilicon is formed in the presence of 30-38% of coke and 29.4-40% of steel shavings; the extraction degree of silicon is 68.6-73.8%.

Keywords: chrysotile-asbestos waste, coke, steel shavings, rotatable planning, electric smelting, arc furnace, ferrosilicon

Information about authors:

Akylbekov Yerbol Yergaliuly — *Doctoral student of the Department of Silicate technology and metallurgy of M. Auezov South Kazakhstan University, Tauke Khan Avenue, 5, 160002, Shymkent, Kazakhstan. E-mail: e.akylbekov@bk.ru*

Shevko Viktor Mikhailovich — *Doctor of technical sciences, Professor of the Department of Silicate Technology and Metallurgy of M. Auezov South Kazakhstan University, Tauke Khan Avenue, 5, 160002, Shymkent, Kazakhstan. E-mail: shevkovm@mail.ru*

Aitkulov Dosmurat Kyzylbievich — *Doctor of technical sciences, professor, director of scientific research of National Center on complex processing of mineral raw materials of the Republic of Kazakhstan, Zhandosov st., 67, 050036, Almaty, Kazakhstan. E-mail: aitkulov_dk@mail.ru*

Karatayeva Gulnara Yergeshovna — *candidate of technical sciences, associate professor of the Department of Silicate Technology and Metallurgy of M. Auezov South Kazakhstan University.Tauke Khan Avenue, 5, 160002, Shymkent, Kazakhstan. E-mail: karataevage@mail.ru*

Introduction

Kazakhstan is among the top three leaders in the world in the extraction and processing of chrysotile ores. In accordance with [1], the Zhetikara deposit located in the Kostanay region ranks fifth in the world in terms of chrysotile-asbestos reserves. Chrysotile-asbestos production from ores of this deposit is organized at Kostanay Minerals JSC. Up to 5 million tons of chrysotile-asbestos are extracted annually at Kostanay Minerals JSC [2].

When enriching 1 ton of the chrysotile-asbestos ore by the dry gravity method [3], 0.92 tons of wastes are formed, which contain 39.45-40.25% of MgO, 36.0-38.67% of SiO_2, 2.8-4.89% of Fe_2O_3, 1.98-3.18% of FeO, 1.03-1.31% of Al_2O_3, 0.16-0.24% of NiO, 0.025-0.77% of Cr_2O_3, 0.75-1.96% of CaO, 0.3-0.46% of CO_2, 0.12-0.48 of SO_3, 11.48-13.67% of loss on ignition, 0.1-0.15% of others (TiO_2, MnO,

K_2O, Na_2O) [[4], [5], [6]]. Thus, the main components in the wastes are MgO and SiO_2 [[7], [8], [9]]. 1.16 million tons of magnesium, 0.73 million tons of silicon, and 9.0 thousand tons of nickel are annually lost at Kostanay Minerals JSC. There are some methods of chrysotile-asbestos waste processing using acid leaching [[10], [11]]. The disadvantage of these methods is their multi-stage. For example, according to [10], the production of magnesium from serpentinite includes grinding the waste, leaching with HCl, separating the solution from the precipitate, purifying and concentrating the solution, obtaining synthetic carnallite, its multi-stage dehydration to obtain magnesium chloride raw materials for electrolysis, electrolysis to obtain magnesium and chlorine. We propose an electrothermal technology for magnesium and siliceous ferroalloy production from chrysotile-asbestos wastes with fewer stages compared to the hydrometallurgical method.

Initial materials. Research Methodology

According to [[12], [13]], chrysotile-asbestos wastes contain serpentine ($3MgO*2SiO_2*2H_2O$) – 57%, talc ($3MgO*4SiO_2*H_2O$) – 17%, brucite ($Mg(OH)_2$) – 9%, forsterite (Mg_2SiO_4) – 6-7%, magnesium, and iron oxides (MgO, FeO, Fe_2O_3) – 8-9%. DTA and SEM analyses of a chrysotile-asbestos waste sample, performed with using a derivatograph Q-1500D (DEMO) and a scanning electron microscope, are shown in Figures 1 and 2.

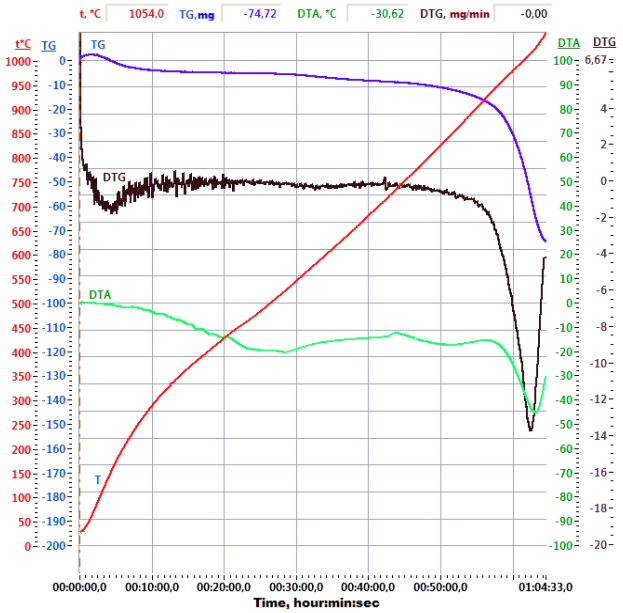

Figure 1 – Derivatogram of the chrysotile-asbestos waste

It is seen that the weight loss of the chrysotile-asbestos waste is 12.5%. According to the SEM analysis, the initial waste sample contained 46.0% of MgO, 35.8% of SiO_2, 2.4% of Al_2O_3, 0.9% of Na_2O, 1.5% of K_2O, 0.9% of CaO, 1.2% of Fe_2O_3, 1.4% of ZnO, 1.0% of PbO, 0.3% of MnO, 10% of others. For melting, the chrysotile-asbestos waste sample was used calcined at 800°C for 30 minutes; its composition was 50% of MgO, 38.9% of SiO_2, 2.7% of Al_2O_3, 1% of Na_2O, 1.6% of K_2O, 1% of CaO, 1.3% of Fe_2O_3, 1.5% of ZnO, 1.1% of PbO, 0.3% of NiO, and 0.1% of Cr_2O_3. Coke was used produced on the West Siberian Metallurgical Plant and contained 88.2% of solid carbon, 1.5% of volatiles, 1.2% of S, 9.1% of ash (including 4.5% of SiO_2, 2.3% of Al_2O_3, 1.5% of Fe_2O_3, 0.5 of ∑ (CaO and MgO), 0.1% of others. Steel shavings contained 98.2% of Fe, 1.1% of C, 0.3% of Si, 0.2% of Mn, and 0.2% of others.

I

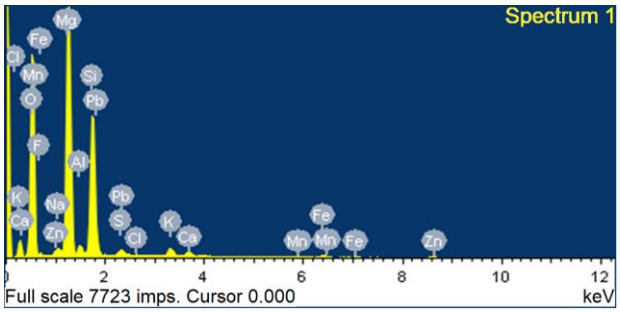

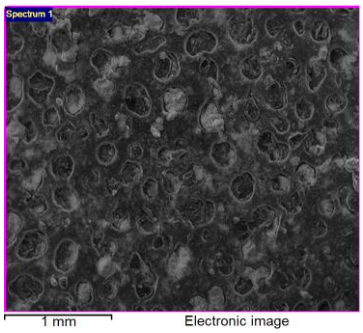

II

Element	O	F	Na	Mg	Al	Si	S
Weight %	46.63	1.25	0.74	27.61	1.25	16.77	0.6
Element	Cl	K	Ca	Mn	Fe	Zn	Pb
Weight %	0.15	1.22	0.64	0.27	0.85	1.1	0.93

I - spectrogram, II - elemental composition

Figure 2- SEM analysis of the chrysotile-asbestos waste

The studies included electric melting using a single-electrode arc furnace, shown in Figure 3.

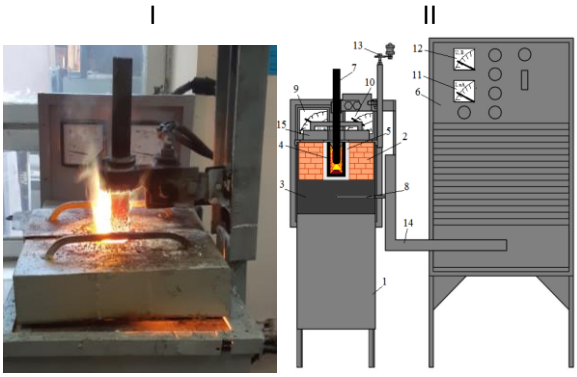

1 – furnace shell, 2 – chromium-magnesite lining,
3 – coal-graphite hearth, 4 – graphite crucible,
5 – coal-graphite layer, 6 – transformer TDZF-1002,
7 – graphite electrode, 8 – lower current lead,
9-12 – control ammeters and voltmeters,
13 – electrode movement mechanism, 14 – flexible part of a low-voltage circuit, 15 – furnace cover
I – melting the charge, II – furnace with transformer

Figure 3 – Single-electrode arc furnace

The electric melting of the charge was carried out in a single-electrode arc furnace (up to 15 kVA power) lined with chromium-magnesite bricks. The bottom electrode was made of a graphite block. A graphite crucible (d = 6 cm, h = 12 cm) was placed on the hearth. The furnace in the upper part was closed with a removable cover with holes for placing a graphite electrode with a diameter of 3 cm and a gas outlet. The crucible was preliminarily heated by electric arc for 20-25 min. After that, the first portion of the charge (200-250 g) was loaded into the crucible. It was melted for 3-6 minutes. Then, every 4-6 minutes, 200-250 g portions of the charge were loaded in the crucible. During 1 experiment, 1500-2000 g of the charge was melted. Occasionally, the temperature at the outlet of gases from the furnace was measured with a GM2200 pyrometer and the temperature of the outer graphite crucible surface at the reaction zone level was measured with a tungsten-rhenium thermocouple. The temperature under the furnace cover during the melting period was 900-1050°C, and the temperature by the crucible wall was 1750-1850°C. During the melting period, the current strength was 350-400A, and the voltage was 30-35V. Electricity was supplied to the furnace from transformer TDZF-1002. The required power was maintained by a thyristor regulator. After the electric melting, the furnace was cooled for 6-7 hours. The graphite crucible was removed from the furnace and broken. The resulting ferroalloy was weighed and analyzed by the atomic absorption method on the AAS-1 instrument (Germany) to determine the metals' content. The ferroalloy density was determined by the pycnometer method according to [14]. Then, based on the density according to [15], the silicon content in the alloy was determined. Some alloys were analyzed by means of a scanning microscope (ASS-1N).

To determine the optimal parameters of the process, the second-order rotatable designs (Box-Hunter plans) were used [16]. To establish the regression equations for changing the optimization parameters, the technique [17] was used, and to construct the volumetric and horizontal images of the optimization parameters, the technique [18] was used. The optimal parameters were determined by combining the horizontal images in one figure. This method was described by us in articles [[19], [20], [21], [22]].

Research results

Table 1 shows the planning matrix and research results. During the research, the effect of the coke (K) and steel shavings (St) amount (in % of the chrysotile-asbestos waste weight) on the extraction degree of silicon into the alloy (α_{Si}) and the silicon concentration in the alloy (C_{Si}, %) was studied.

Table 1 – Planning matrix and research results

№	Variables				Technological parameters	
	Coded view		*Natural view*			
	X1	*X2*	*Coke, %*	*Steel shavings, %*	*C_{Si},%*	*α_{Si}, %*
1	+	+	43.7	36.5	21.0	56.6
2	-	+	32.3	36.5	26.3	70.9
3	+	-	43.7	19.5	37.0	69.3
4	-	-	32.3	19.5	39.0	73.0
5	1.41	0	46	28	25.6	57.9
6	-1.41	0	30	28	30.8	69.7
7	0	1.41	38	40	27.5	78.0
8	0	-1.41	38	16	45.3	76.2
9	0	0	38	28	34.3	79.5
10	0	0	38	28	35.0	79.8
11	0	0	38	28	34.6	80.0
12	0	0	38	28	35.4	80.4
13	0	0	38	28	35.8	80.6

Using the data from Table 1, we found the regression equations according to the method [17]:

$$\alpha Si=-361.43+22.47\cdot K+3.6St-0.272\cdot K^2-0.03\cdot St^2+3.6\cdot K\cdot St; \quad (1)$$

$$CSi=-1313.17+8.999\cdot K-0.392\cdot St-0.116\cdot K^2+0.004\cdot St^2-0.017\cdot K\cdot St. \quad (2)$$

Based on equations 1 and 2, according to [18], the volumetric and horizontal images of αSi and $C_{Si(alloy)}$=f(K, St) were constructed (Figure 4).

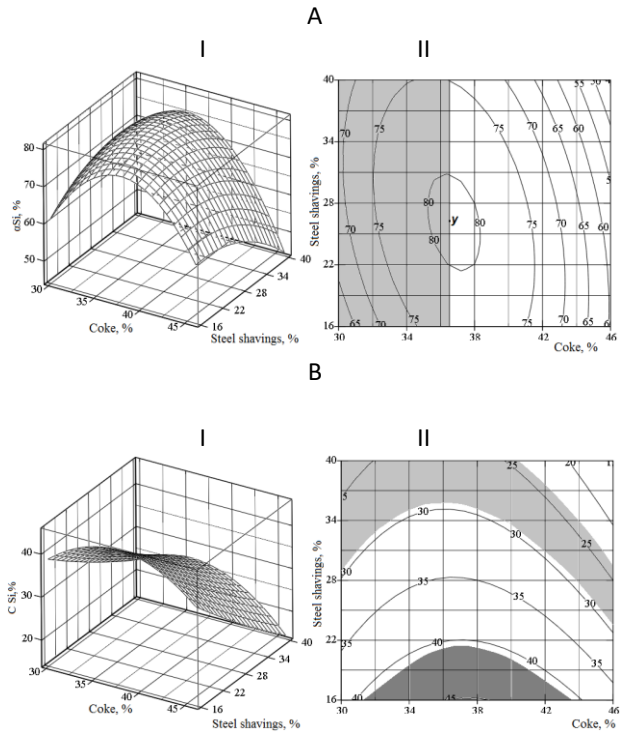

I - volumetric image, II - planar image

Figure 4 – Effect of coke and steel shavings on the extraction degree of silicon into the alloy (A) and the silicon concentration in the alloy (B)

It can be seen that the surface of αSi(alloy) = f(K, St) has an extremal view with a maximum (α_{Si}=84.5%) at 37.0% of coke and 26.5% of steel shavings. The extremal view of the surface is due to the fact that at 36-38% excess coke (when αSi(alloy) decreases), the electrical conductivity of the furnace bath increases. To maintain the required current, the electrodes together with the arc are moved to the upper horizons of the bath. The reaction zone also moves up. The throat is heated, and the filter layer of the charge decreases. As a result, the loss of silicon with gaseous SiO increases and αSi(alloy) decreases. It is seen that αSi varies from 45 to 84.5% (x and y points). αSi(alloy) from 64.6 to 84.5% is achieved at 30-37.0% of coke and 30-40% of steel shavings (shaded area of Figure 4 (I)). The silicon concentration in the alloy varies from 23.4 to 45.1%. FS45 grade ferrosilicon was formed at a small amount (<22%) of steel shavings in a large range of coke (from 32 to 42.5% of coke (shaded area of Figure 4 (II)). In the case of 30-46% of coke and and increased amount of steel shavings (from 23 to 40%), FS25 grade ferrosilicon was formed (shaded area of Figure 4 (B)).

To determine the optimal conditions, the planar α_{Si} and C_{Si} images were combined (Figure 5). The values of technological parameters at the boundary points of the obtained ferroalloys are shown in Table 2.

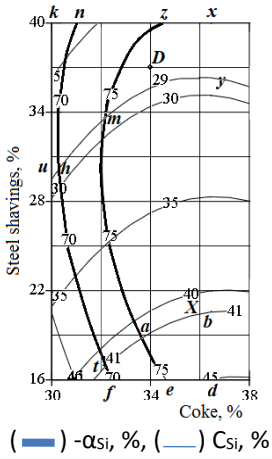

Figure 5 – Combined information about α_{Si} and C_{Si}

Table 2 – Technological parameters at the points of Figure 5

Point in Figure 5	Technological parameter			
	Coke, %	*Steel shavings, %*	*α_{Si}, %*	*C_{Si}, %*
t	32.3	16.8	70.0	41.0
a	33.6	18.7	75.0	41.0
b	38.0	20.6	79.0	41.0
d	38.0	16.0	76.6	45.0
e	34.4	16.0	75.0	44.7
f	32.5	16.0	70.0	41.4
u	30.0	29.4	69.4	29.0
K	30.0	40.0	68.6	32.4
n	30.9	40.0	70.0	34.1
z	34.4	40.0	75.3	25.9
x	36.2	40.0	75.0	25.4
y	36.2	35.6	76.7	29.0
m	32.2	32.5	75.0	29.0
h	30.3	30.4	70.0	29.0

In view of the fact that when the amount of coke is >36-38%, the right side of the Figure 5 surface is practically the same as the left (with a large amount of coke), it is advisable to consider the left side of the figure.

Based on Figure 5 and Table 2, it is possible to determine the optimal technological parameters for obtaining ferrosilicon of FS45 and FS25 grades [23] with different extraction of Si into the alloy. So, for α_{Si}≥75%, FS45 with C_{Si} = 41-45% is formed in the region *abde* (33.69-36.2% of coke and 16-20.8% of steel shavings). For α_{Si} from 70 to 75%, FS45 ferrosilicon with C_{Si} = 41-44.7% is formed in the region *ftac* at 32.3-34.4% of coke and 16-18.7% of steel shavings. FS25 ferrosilicon with αSi(alloy) ≥75% and C_{Si} = 26.7-29% is formed in the region *mzxy* at 32.2-38% of coke and 32.5-40% of steel shavings. FS25 ferrosilicon is also formed in the region *hnzm*. However, in this area, α_{Si} decreases to 70%. In this case, the amount of coke can be changed from 30.3 to 34.4% and the number of steel shavings from 30.4 to 40%.

Figure 6 shows the ferroalloys obtained from two charge compositions: 1st charge – 58% of chrysotile waste, 22% of steel shavings, and 20% of coke; 2nd charge – 63% of chrysotile waste, 23% of coke, and 14% of steel shavings.

I II

I – ferroalloy obtained from the 1st charge, II – ferroalloy obtained from the 2nd charge

Figure 6 – Photos of resulting ferroalloys

The silicon content in the alloy was determined based on its density (P, g/cm^3) by the pycnometric method according to the equation:

C_{Si}= 252.405-101.849*P+18.209*P^2-1.213*P^3[15] (3)

Density of the first ferroalloy was 6.4 g/cm^3, and dencity of the second one – 5.47 g/cm^3. The silicon content in the first alloy was:

CSi=252.405-101.849·6.4+18.209·6.42--1.213·6.43 = 24.4% (4)

and in the second alloy:

CSi = 252.405-101.849·5.47+18.209·5.472--1.213·5.473 = 41.6% (5)

The SEM analysis of the first alloy is represented in Figure 7.

I

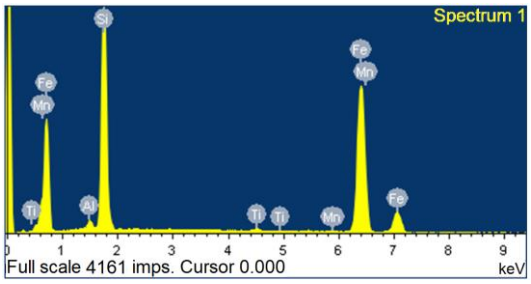

II

Element	Al	Si	Ti	Mn	Fe
Weight %	1.21	29.25	0.45	0.31	68.78

I - spectrogram, II - elemental composition

Figure 7 – SEM-analysis of the alloy

It is seen that the alloy produced from the first charge composition contains 29.2% of silicon. Judging by the silicon content, in accordance with [23], the produced alloys correspond to ferrosilicon of FS25 and FS45 grades. The obtained ferroalloys do not contain magnesium. The extraction degree of magnesium into the gas phase was at least 92-98%. The rest of magnesium (2-8%) passed into the slag. For the condensation of magnesium from the gas phase, it is recommended to use the Magneterm method [24].

Conclusion

The results obtained during the electric melting of chrysotile-asbestos waste allow us to draw the following conclusions:

- FS45 grade ferrosilicon with the silicon extraction degree from 75 to 85.4% is formed in the presence of 33.6-38% of coke and 16-20.8% of steel shavings;
- FS25 grade ferrosilicon with the silicon extraction degree from 68.6 to 73.8% is formed in the presence of 30-38% of coke and 29.4-40% of steel shavings;
- the main amount of magnesium (92-98%) passes into the gas phase; the resulting ferroalloys do not contain magnesium.

Cite this article as: Akylbekov YeYe, Shevko VM, Aitkulov DK, Karataeva GE. Electrothermal processing of chrysotile-asbestos wastes with magnesium extraction and ferroalloy production. Kompleksnoe Ispolzovanie Mineralnogo Syra = Complex Use of Mineral Resources. 2023; 327(4):74-81. https://doi.org/10.31643/2023/6445.42

Ферроқорытпа алу және газ фазасына магний алу арқылы хризотил-асбест өндірісінің қалдықтарын электротермиялық өңдеу

[1]Ақылбеков Е.Е., [1*]Шевко В.М., [2]Айткулов Д.К. [1]Каратаева Г.Е.

[1]М.Әуезов атындағы Оңтүстік Қазақстан университеті, Шымкент, Қазақстан
[2]Қазақстан Республикасының минералдық шикізатты кешенді қайта өңдеу жөніндегі ұлттық орталығы, Алматы, Қазақстан

Мақала келді: *23 қараша 2022*
Сараптамадан өтті: *24 қаңтар 2023*
Қабылданды: *22 ақпан 2023*

ТҮЙІНДЕМЕ

Мақалада «Қостанай минералдары» АҚ хризотил-асбест өндірісінің қалдықтарын қайта өңдеу бойынша эксперименттік зерттеулердің нәтижелері келтірілген. Хризотил-асбест өндірісінің қалдықтарынан магний мен кремнийлі ферроқорытпаны алудың электротермиялық технологиясы ұсынылды. Алынған қорытпалардың технологиялық параметрлеріне кокс пен болат жоңқалары мөлшерінің әсері анықталды. Хризотил-асбест өндірісінің қалдықтарын талдаудың дериватограммасы мен растрлық электронды микроскопиясы ұсынылған. Зерттеулер екінші ретті айналмалы жоспарларды (Бокс-Хантер жоспары) қолдана отырып, эксперименттерді жоспарлау әдісімен жүргізілді, технологиялық параметрлерді графикалық оңтайландыру және бір электродты доғалы пешті қолдана отырып, графитті тигельде электр балқыту. Хризотил-асбест қалдықтарының массасынан кремнийді қорытпаға алу дәрежесіне және кремний қорытпасындағы концентрацияға кокс пен болат жоңқалары мөлшерінің әсер етуінің барабар регрессия теңдеулері алынды. Шихтаны электрмен балқыту арқылы құрамында 24,4-29,2% кремнийі бар ФС25 маркалы сұрыпты ферросилиций және 41,6-45% кремнийі бар ФС45 маркалы ферросилиций алынды. ФС45 маркалы Ферросилиций оған өту дәрежесі 75-тен 85,4% - ға дейін Si 33,6-38% кокс және 16-20,8% болат жоңқаларының қатысуымен түзіледі. ФС25 маркалы Ферросилиций, оған өту дәрежесі 68,6-73,8% кремний 30-38% кокс және 29,4-40% болат жоңқалары кезінде түзіледі.

Түйін сөздер: хризотил-асбест қалдықтары, кокс, болат жоңқалары, айналмалы жоспарлау, электр балқыту, доға пеші, ферросилиций

Авторлар туралы ақпарат:

Ақылбеков Ербол Ерғалиұлы — *Силикат технологиясы және металлургия кафедрасының докторанты, М.Әуезов атындағы Оңтүстік Қазақстан университеті, Тәуке хан даңғылы, 5, 160002. Шымкент, Қазақстан. E-mail: e.akylbekov@bk.ru*

Шевко Виктор Михайлович — *Техника ғылымдарының докторы, Силикат технологиясы және металлургия кафедрасының профессоры, М.Әуезов атындағы Оңтүстік Қазақстан университеті, Тәуке хан даңғылы, 5, 160002. Шымкент, Қазақстан. E-mail: shevkovm@mail.ru*

Айткулов Досмурат Қызылбиевич — *Техника ғылымдарының докторы, профессор, Қазақстан Республикасының минералдық шикізатты кешенді қайта өңдеу ұлттық орталығының ғылыми-зерттеу бөлімінің директоры, Жандосов к-сі, 67, 050036, Алматы, Қазақстан. E-mail: aitkulov_dk@mail.ru*

Каратаева Гульнара Ергешовна — *Техника ғылымдарының кандидаты, Силикат технологиясы және металлургия кафедрасының доценті, М.Әуезов атындағы Оңтүстік Қазақстан университеті, Тәуке хан даңғылы, 5, 160002, Шымкент, Қазақстан . E-mail: karataevage@mail.ru*

Электротермическая переработка отходов хризотил-асбестового производства с получением ферросплава и извлечением магния в газовую фазу

[1]Акылбеков Е.Е., [1*]Шевко В.М., [2]Айткулов Д.К. [1] Каратаева Г.Е.

[1] Южно-Казахстанский университет имени М. Ауэзова, Шымкент, Казахстан
[2] Национальный центр покомплексной переработки минерального сырья Республики Казахстан, Алматы, Казахстан

Поступила: *23 ноября 2022*
Рецензирование: *24 января 2023*
Принята в печать: *22 февраля 2023*

АННОТАЦИЯ

В статье приводятся результаты экспериментальных исследования по переработке отходов хризотил-асбестового производства АО «Костанайские минералы». Предложена электротермическая технология извлечения магния и кремнистого ферросплава из отходов хризотил-асбестового производства. Определены влияние количества кокса и стальной стружки на технологические параметры полученных сплавов. Представлены дериватограмма и растровая электронная микроскопия анализа проб отходов хризотил-асбестового производства. Исследования проводились методом планирования экспериментов с использованием рототабельных планов второго порядка (план Бокса-Хантера) с исследующей графической оптимизацией технологических параметров и электроплавкой шихты в графитовом тигле с использованием одноэлектродной дуговой печи. Получены адекватные уравнения регрессий влияния количества кокса и стальной стружки от массы хризотил-асбестовых отходов на степень извлечения кремния в сплав и концентрацию в сплаве кремния. Электроплавкой шихты получен сортовой ферросилиций марок ФС25 с содержанием кремния 24,4-29,2% и ФС45 с содержанием кремния 41,6-45%. Ферросилиций марки ФС45 со степенью перехода в него от 75 до 85,4% Si образуется в присутствии 33,6-38% кокса и 16-20,8% стальной стружки. Ферросилиций марки ФС25 со степенью перехода в него 68,6-73,8% кремния образуется при 30-38% кокса и 29,4-40% стальной стружки.

Ключевые слова: хризотил-асбестовые отходы, кокс, стальная стружка, рототабельное планирование, электроплавка, дуговая печь, ферросилиций.

Информация об авторах:

Акылбеков Ербол Ергалиулы — *Докторант кафедры «Технологии силикатов и металлургия» Южно-Казахстанский университет им. М. Ауэзова, проспект Тауке хана, 5, 160002, Шымкент, Казахстан, E-mail: e.akylbekov@bk.ru*

Шевко Виктор Михайлович — *Доктор технических наук, профессор кафедры «Технологии силикатов и металлургия»Южно-Казахстанского университета имени М. Ауэзова, проспект Тауке Хана, 5, 160002, Шымкент, Казахстан, E-mail: shevkovm@mail.ru*

Айткулов Досмурат Қызылбиевич — *Доктор технических наук, профессор, научный руководитель Национального центра комплексной переработки минерального сырья Республики Казахстан, Жандосова, 67 050036, Алматы, Казахстан, E-mail: aitkulov_dk@mail.ru*

Каратаева Гульнара Ергешовна — *Кандидат технических наук, ассоциированный профессор, доцент кафедры «Технологии силикатов и металлургия» Южно-Казахстанского университета им. М. Ауэзова, проспект Тауке Хана, 5, 160002, Шымкент, Казахстан, E-mail: karataevage@mail.ru*

References

[1] Satimbekova AB, Bekaulova AA, Dikanbayeva AK, Auyeshov AP, Umirzakhov NU, Idrisheva ZhK. Pererabotka otkhodov proizvodstva khrizotil-asbesta kak faktor ekologicheskoy bezopasnosti okruzhayushchey sredy [Recycling of chrysotile-asbestos production waste as a factor in environmental safety]. Vestnik vostochno-kazakhstanskogo gosudarstvennogo tekhnicheskogo universiteta im. D. Serikbayeva =Bulletin of the D. Serikbaev East Kazakhstan State Technical University, 2019; 1: 173-177. (in Russ.).

[2] Waste utilization technology of chrysotile-asbestos production by sulfuric acid method with obtaining commercial magnesium products in the form of sulphate, oxide and metal. http://www.cmrp.kz/index.php?option=com_content&task=view&id=351&pop=1&page=0&Itemid=0&lang=en, (Accessed on 30 October 2022).

[3] Altynbasova KZh, Kozlovskaya YeA, Ybray KB. Issledovaniye vozmozhnosti izvlecheniya nikelya iz otkhodov proizvodstva khrizotil-asbesta mestorozhdeniya Zhetygora [Study of the possibility of extracting nickel from the waste products of the chrysotile-asbestos production at the Zhetygora deposit]. Almaty: Satpaev University. 2020, 45. (in Russ.).

[4] Dzhafarov NN. Khrizotil-asbest Kazakhstana [Chrysotile-asbestos of Kazakhstan]. Almaty: RIO VAK RK. 2000, 180. (in Russ.).

[5] Zhalgasuly N, Cherniy GM, Razumova OB, Ismailova AA. Tekhnologiya sozdaniya rastitel'nogo pokrova na tekhnogennykh obrazovaniyakh [Technology of creation of vegetation cover on technogenic formations]. Nauchno-tekhnicheskoye obespecheniye gornogo proizvodstva: Trudy Instituta gornogo delaim. D.A. Kunayeva [Scientific and technical support of mining: Proceedings of the D. A. Kunaev Institute of Mining]. Almaty, 2014; 85:192-198. (in Russ.).

[6] Alshanov RA. Kazakhstan na mirovom mineral'no-syr'yevom rynke: problemy i ikh resheniye : analiz i prognoz [Kazakhstan in the world mineral market: problems and their solution: analysis and forecast]. Almaty: Print-S. 2005, 422. (in Russ.).

[7] Aueshov AP, Satimbekova AB, Arynov KT, Dikanbaeva AK, Bekaulova AA. Environmental and Technological Aspects of Acid Treatment of Serpentinite Waste from Chrysotile Asbestos Mining and Processing. International Journal of Engineering Research and Technology. 2020; 13:12-15. https://doi.org/10.37624/IJERT/13.6.2020.1215-1219

[8] Auyeshov A, Satimbekova A, Arynov K, Bekaulova A, Yeskibayeva S, Idrisheva Z. Environmentally friendly and resource-saving technology for disposal of dusty asbestos-containing wastes and production of magnesium salts. ARPN Journal of Engineering and Applied Sciences. 2021; 16(9):987-990.

[9] Baigenzhenov OS, Kozlov VA, Luganov VA, Mishra B, Shayahmetova RA, Aimbetova IO. Complex processing of wastes generated in chrysotile asbestos production. Mineral Processing and Extractive Metallurgy Review. 2015; 36(4):242-248. https://doi.org/10.1080/08827508.2014.955610

[10] Pat. 2244044 RU. The method of obtaining magnesium chloride hexahydrate. Pensky A, Gladkova L, Shudinov N. Publ. 10.01.2005.

[11] Koizhanova AK, Kenzhaliyev BK, Kamalov EM, Erdenova MB, Magomedov DR, Abdyldaev NN. Research of Gold Extraction Technology from Technogenic Raw Material. News of the National Academy of Sciences of the Republic of Kazakhstan: Series Chemistry and Technology. 2020; 439(1):95-101. https://doi.org/10.32014/2020.2518-1491.12

[12] Biryukova AA, Tikhonova TA, Merkibayev YeS, Khabas TA, Pogrebenkov VM. Sintez kordiyeritomullitovoy keramiki s zadannym fazovym sostavom na osnove syr'ya Kazakhstana [Synthesis of cordierite-mullite ceramics with a given phase composition based on raw materials from Kazakhstan]. Kompleksnoe Ispolzovanie Mineralnogo Syra = Complex Use of Mineral Resources. 2016; 2:88-94. (in Russ.).

[13] Spasiano D, Pirozzi F. Treatments of asbestos containing wastes. Journal of Environmental Management. 2017; 204:82-91. https://doi.org/10.1016/j.jenvman.2017.08.038

[14] State standard 22524-77. Piknometry steklyannyye Tekhnicheskiye trebovaniya i usloviya postavki [Glass pycnometers Technical requirements and terms of delivery]. Moscow: Standartinform. 2011. (in Russ.).

[15] Shevko VM, Amanov DD, Karatayeva GYe, Aytkulov DK. Kinetika polucheniya kompleksnogo ferrosplava iz kremniy–alyuminiysoderzhashchey opoki [Kinetics of obtaining a complex ferroalloy from a silicon-aluminum-containing flask] International Journal of Applied and Fundamental Research. 2016; 10(2):194-196. (in Russ.).

[16] Akhnazarova SL, Kafarov VV. Metody optimizacii eksperimenta v himicheskoj promyshlennosti [Experiment Optimization Methods in the Chemical Industry]. Moscow: High school. 1985, 327. (inRuss.).

[17] Inkov AM, Tapalov T, Umbetov UU, Hu Wen Tsen V, Akhmetova KT, Dyakova ET. Optimization methods: e-book. Shymkent: SKGU. 2003.

[18] Ochkov VF. Mathcad 14 dlyastudentov, inzhenerov i konstruktorov [Mathcad 14 for students, engineers and designers]. St. Petersburg: BHV-Petersburg. 2009, 512. (in Russ.).

[19] Shevko VM, Karataeva GE, Tuleev MA, Badikova AD, Amanov DD, AbzhanovaAS. Complex electrothermal processing of an oxide zinc-containing ore of the Shaymerden deposit. Physicochemical Problems of Mineral Processing. 2018; 54(3):955-964. https://doi.org/10.5277/ppmp1897

[20] Shevko VM, Mirkayev NK, Aitkulov DK. Electrothermal production of ferroalloy from tripoli. Kompleksnoe Ispolzovanie Mineralnogo Syra = Complex Use of Mineral Resources. 2023; 324(1):50-56. https://doi.org/10.31643/2023/6445.07

[21] Shevko VM, Badikova AD, Tuleev MA, Karataeva GE. Kinetics of extraction of the silicon, aluminum and calcium of the basalt from the Daubaba deposit. Kompleksnoe Ispolzovanie Mineralnogo Syra = Complex Use of Mineral Resources. 2019; 2:83-89 https://doi.org/10.31643/2019/6445.20

[22] Shevko VM, Akylbekov YY, Karataeva GY, Badikova AD. Recycling of chrysotile-Asbestos production waste. Metallurgical Research and Technology. 2022; 119(4):410. https://doi.org/10.1051/metal/2022050

[23] State standard 1415-93. Ferrosilitsiy. Tekhnicheskiye trebovaniya i usloviya postavki [Ferrosilicon. Technical requirements and terms of delivery]. Moscow: Standartinform. 2011, 19. (in Russ.).

[24] Utkin NI. Proizvodstvo tsvetnykh metallov [Production of non-ferrous metals]. Moscow: Intermet Inzhiniring. 2004, 442. (in Russ.).

Crossref
DOI: 10.31643/2023/6445.43
Metallurgy

Pre-activation of nepheline before the enrichment

[1*]Akhmadiyeva N.K., [1]Abdulvaliyev R.A., [2]Akcil A., [1]Manapova A.I.

[1] Institute of Metallurgy and Ore Beneficiation, Satbayev University, Almaty, Kazakhstan
[2]Suleyman Demirel University, Isparta, Turkey

** Corresponding author email: n.akhmadiyeva@satbayev.university*

Received: *December 20, 2022*
Peer-reviewed: *January 22, 2023*
Accepted: *February 27, 2023*

ABSTRACT

Due to limited reserves of bauxite, nepheline can be used in the industrial production of alumina in Kazakhstan. The most promising deposit is the nepheline syenites of the Kubasadyr deposit. Currently, there is no effective technology for processing nepheline ores. High energy intensity, capital intensity, and significant emissions into the atmosphere are the main drawbacks of the conventional technology of nepheline ore processing by the sintering method. Efficient hydrochemical processing of nepheline requires pre-enrichment with the separation of a part of silica. According to the existing technology of chemical enrichment in an alkaline solution at a temperature of 280°C, the silica extraction degree is no more than 36%. A pre-roasting at 500°C is used to increase the extraction rate of silica and this process permits an increase in the extraction rate to 65%. The paper presents the results of the chemical activation of nepheline syenites in a solution of sodium hydrogen carbonate. The optimum conditions of activation are determined. Activation at a temperature of 280 °C resulted in a change in the phase composition of the feedstock and increases the degree of silica extraction up to 65.5%. The results obtained showed the possibility in principle of using hydrochemical enrichment technology for the resulting high-quality nepheline concentrate and replacing the energy-intensive roasting process.

Keywords: nepheline, enrichment, preliminary activation, silica, alumina.

Information about authors:

Akhmadiyeva Nazym Kanatovna — *Ph.D. Researcher of the alumina and aluminium laboratory of the Institute of Metallurgy and Ore Beneficiation, Satbayev University, Shevchenko str., 29/133, 050010, Almaty, Kazakhstan. Email: n.akhmadiyeva@satbayev.university; naz-ank@inbox.ru*

Abdulvaliyev Rinat Abdulvaliyev — *Candidate of Technical Sciences, head of the laboratory of alumina and aluminium of the Institute of Metallurgy and Ore Beneficiation, Satbayev University, Shevchenko str., 29/133, 050010, Almaty, Kazakhstan. Email: rin-abd@inbox.ru*

Ata Akcil — *PhD, Professor, Head of the Mineral-Metal Recovery and Recycling MMR&R Research Group, Mineral Processing Division, Department of Mining Engineering, SDU, TR32260, Isparta, Turkey. Email: ataakcil1@gmail.com*

Manapova Alfiyam Ilyaevna — *Master of Technical Sciences, junior researcher of the laboratory of alumina and aluminium of the Institute of Metallurgy and Ore Beneficiation, Satbayev University, Shevchenko str., 29/133, 050010, Almaty, Kazakhstan. Email: alfiya_0603@mail.ru*

Introduction

The global aluminium industry is growing dynamically and is one of the leaders in the production of construction materials [[1]], [[2]].

The traditional source of aluminium is bauxite. However, their quality reserves are limited and the currently known reserves will be exhausted within the next 20 years and the reserve base will be adequate for not more than 25 years [3]. This has led to a search for alternative sources. Aluminosilicate minerals such as kaolins or nepheline and others can be considered as such [[4]], [5], [6], [7], [8], [9], [[10]].

Nepheline is processed in the world only in Russia, Canada, and Norway [11].

Large accumulations of non-bauxite aluminium raw materials have been identified in Kazakhstan. These are high alumina minerals: nepheline of alkaline, ultrabasic and granitoid rocks. There are three main varieties of rocks rich in nepheline: nepheline rocks of alkaline or ultrabasic massifs, nepheline-leucite rocks of alkaline-basic massifs, and nepheline syenites of massifs of alkaline granitoids [12].

Several dozens of nepheline rock massifs are known in different regions of Kazakhstan:

- Kosistek in Western Kazakhstan;

- Yesil, Kentassk, Derzhavinsk, Karsakpai, and Shynsai in Central Kazakhstan;
- Irisu, Mashat, Badam, Kulandinsk in Southern Kazakhstan;
- Semeytausk in Eastern Kazakhstan.

The geological reserves of alumina raw materials at the above deposits are huge and counted in billions of tonnes of complex ores, by category C2 - over 500 million tonnes. At the present stage of exploration, the largest, well-studied is the Yesilsk massif of the Kubasadyr nepheline-leucite syenite deposit, which is represented by two sections: Ashchilisai and Taskuduk. The intrusive is located in a large deeply eroded caldera of an Early Devonian stratovolcano, confined to the intersection of two deep faults of northwest and northeast directions. The host rocks are metasomatically reworked nepheline syenites [12].

Reserves of alumina raw materials in category C2 total 239 million tons in two areas, but there is no production of their processing. To organize the production of nepheline processing in Kazakhstan, it is necessary to develop an effective technology that takes into account the peculiarities of the mineral composition of raw materials.

The information used to define industrial mineral quality relates to consumer specifications: minimum SiO_2, maximum Fe_2O_3, or whiteness, among others [13].

Sintering or hydrochemical methods can be used for nepheline processing. Sintering nepheline with limestone at 1200 ^oC decomposes it to form sodium and potassium aluminates and a two-calcium silicate. However, this process is very energy and capital-intensive.

Potentially, the processing of 1 million tons of ore could produce 150 thousand tons of alumina on existing technologies, by the way, to get 1,7 million tons of cement, 70 thousand tons of soda, and 100 thousand tons of sulphuric potash. The production requires 2.5M tonnes of limestone, with capital costs of about $1bn.

There have been studies of nepheline sintering at lower temperatures, e.g. sintering with an excess 5–10 % of sodium carbonate at 760–880 °C for 1.0–1.5 h. Such processes would provide high Al extraction, and the high energy consumption and CO_2 footprint that derive from the thermal treatment step are of great concern [14].

Given the negative attitudes in the world towards the sintering process due to high carbonate emissions into the atmosphere, hydrochemical technologies are preferable.

In the hydrochemical process, the nepheline is decomposed by an alkaline solution in the presence of lime in autoclaves at a temperature of 280^oC. Under these conditions, sodium and potassium aluminates pass into the solution and silica remains in precipitation in the form of sodium-calcium hydro silicate. High aluminium recovery is achieved at Na_2O content in the solution of 400-500 g/dm^3.

The hydrochemical method is characterized by a high alkali turnover, which predetermines a considerable heat consumption for solvent evaporation. However, in contrast to the sintering process specific material losses of solutions and heat consumption per tonne of Al_2O_3 do not depend much on the solid phase (SiO_2 + CaO), i.e. on the silicon ratio of raw materials (SiO_2: Al_2O_3). During sintering, the specific fuel consumption per tonne of Al_2O_3 is almost proportional to the silicon ratio. This implies that the hydrochemical process is of interest for processing alkaline silica-rich aluminosilicate rocks and the profitability of production should increase as the quality of aluminosilicate raw materials deteriorates.

Nepheline syenite is also processed by acid treatment [15].

There are also technologies of combining the hydrochemical method with chemical enrichment, roasting, and others [[16], [17]].

Chemical enrichment of nepheline is used to reduce its silica content, leading to a reduction in the flow of raw materials for further processing in alumina production.

Chemical enrichment is carried out in an alkaline solution containing 240 g/dm^3 Na_2O at a temperature of 280^oC and a duration of 40 minutes [16]. Under these conditions, the degree of silica extraction into the solution of 38.6% was obtained. To increase of efficiency of chemical enrichment offered to carry out preliminary activation of nepheline by roasting with the steam-air mixture at a temperature of 500^oC [17]. As a result, the degree of silica extraction is increased to 60.0-65.0%. However, roasting is an energy-intensive process.

In the conducted research to increase the efficiency of the enrichment process, the possibility of pre-chemical activation of nepheline syenites of the Kubasadyr deposit in a solution of sodium hydrogen carbonate has been studied.

Preliminary chemical activation of raw materials in a solution of sodium hydrogen carbonate leads to a change in the phase composition, which will allow for obtaining higher values for further processing [[18]], [19], [20].

Preliminary chemical activation was tested in the processing of low-quality gibbsite-kaolinite [18], waste products [19], and semi-products of ferrochrome production [20], and ash and showed high results.

Experimental part

X-ray fluorescence analysis of the chemical composition was carried out on a Venus 200-wave dispersion spectrometer (PANalytical B.V., Holland).

Chemical analysis was performed on an optical emission spectrometer with inductively coupled plasma Optima 2000 DV (USA, Perkin Elmer).

Semi-quantitative X-ray phase analysis was carried out on the D8 Advance diffractometer (BRUKER) using Cu-K_α radiation at an accelerating voltage of 36 kV, current 25 mA.

Chemical activation of nepheline syenites was carried out in a solution containing 120 g/dm^3 $NaHCO_3$ at an L: S ratio of 3 and a temperature range of 120 - 280 ^{o} using a thermostatically controlled unit with 6 autoclaves rotating through the head, with a working volume of 250 cm^3 and activation time 90 minutes. The maximum sodium hydrogen carbonate content in the solution was 120 g/dm^3, taking into account its solubility limit.

Chemical enrichment was carried out in an alkaline solution containing 240 g/dm^3 Na_2O at a temperature of 280^{o}C and a duration of 40 minutes.

Results and discussion

Physical and chemical studies of the material composition of nepheline syenites of the Kubasadyr deposit were carried out.

Chemical composition of the initial sample, mass %: Al_2O_3 – 17,77; SiO_2 – 48,37; Fe_2O_3 – 3,18; CaO – 2,89; Na_2O – 4,24; K_2O – 5,34; MgO – 0,34; Cl – 0,3.

The phase composition of the initial sample is shown in figure 1 and table 1.

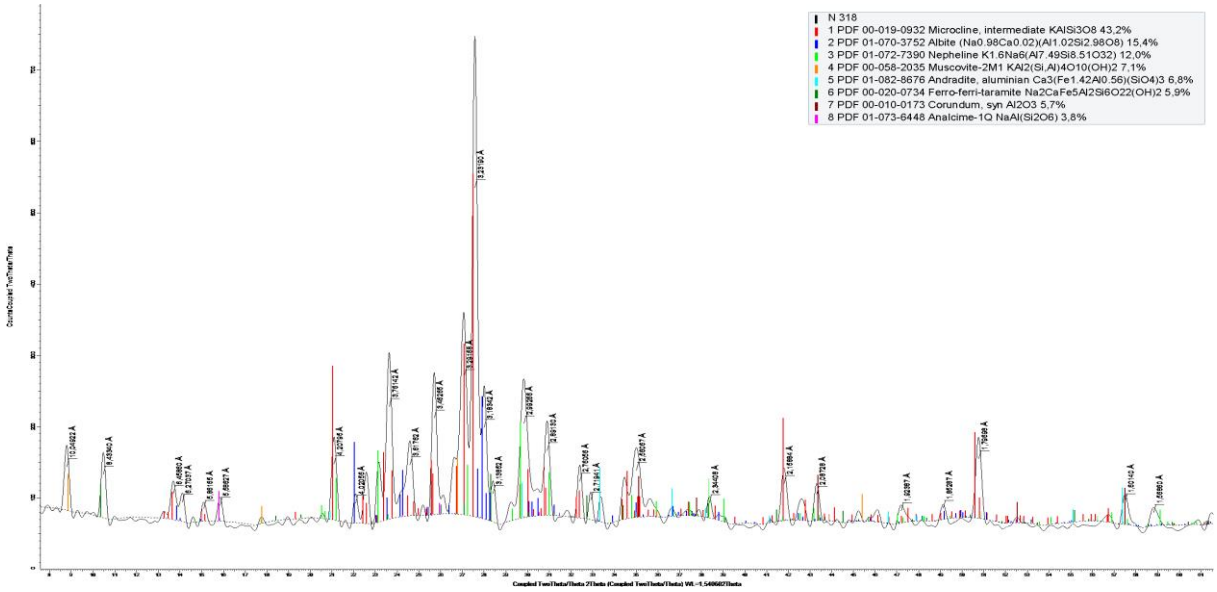

Figure 1 - X-ray diffraction pattern of nepheline

Table 1 – Phase composition of nepheline

Composition		
Components	Components	%
Microcline	$KAlSi_3O_8$	43.2
Albite	$(Na_{0.98}Ca_{0.02})(Al_{1.0}2Si_{2.98}O_8)$	15.4
Nepheline	$K_{1.6}Na_6(Al_{7.49}Si_{8.51}O_{32})$	12.0
Muscovite-	$KAl_2(Si,Al)_4O_{10}(OH)_2$	7.1
Andradite,	$Ca_3(Fe_{1.42}Al0_{.56})(SiO_4)_3$	6.8
Ferro-ferri-taramite	$Na_2CaFe_5Al_2Si_6O_{22}(OH)_2$	5.9
Corundum,	Al_2O_3	5.7
Analcime-1Q	$NaAl(Si_2O_6)$	3.8

Table 2 - Phase composition of nepheline syenite samples depending on the temperature of chemical activation

Activation temperature, °C	Composition		
	Components	Formula	%
120	Microcline, intermediate	$KAlSi_3O_8$	40.1
	Albite	$(Na_{0.98}Ca_{0.02})(Al_{1.02}Si_{2.98}O_8)$	17.5
	Nepheline	$K_{1.6}Na_6(Al_{7.49}Si_{8.51}O_{32})$	13.1
	Corundum, syn	Al_2O_3	7.7
	Andradite, aluminian	$Ca_3(Fe_{1.42}Al0_{.56})(SiO_4)_3$	3.8
	Ferro-ferri-taramite	$Na_2CaFe_5Al_2Si_6O_{22}(OH)_2$	6.9
	Muscovite-2M1	$KAl_2(Si,Al)_4O_{10}(OH)_2$	6.6
	Analcime-1Q	$NaAl(Si_2O_6)$	4.4
150	Microcline, intermediate	$KAlSi_3O_8$	34.6
	Albite	$(Na_{0.98}Ca_{0.02})(Al_{1.02}Si_{2.98}O_8)$	18.8
	Nepheline	$K_{1.6}Na_6(Al_{7.49}Si_{8.51}O_{32})$	16.3
	Ferro-ferri-taramite	$Na_2CaFe_5Al_2Si_6O_{22}(OH)_2$	7.0
	Corundum, syn	Al_2O_3	6.9
	Muscovite-2M1	$KAl_2(Si,Al)_4O_{10}(OH)_2$	6.4
	Analcime-1Q	$NaAl(Si_2O_6)$	6.3
	Andradite, aluminian	$Ca_3(Fe_{1.42}Al_{0.56})(SiO_4)_3$	3.8
200	Microcline, intermediate	$KAlSi_3O_8$	33.4
	Albite	$(Na_{0.98}Ca_{0.02})(Al_{1.02}Si2.98O_8)$	18.2
	Nepheline	$K_{1.6}Na_6(Al_{7.49}Si8_{.51}O_{32})$	15.7
	Andradite, aluminian	$Ca_3(Fe_{1.42}Al_{0.56})(SiO_4)3$	4.2
	Ferro-ferri-taramite	$Na_2CaFe_5Al_2Si_6O_{22}(OH)_2$	6.8
	Corundum, syn	Al_2O_3	6.7
	Muscovite-2M1	$KAl_2(Si,Al)_4O_{10}(OH)_2$	6.1
	Analcime-1Q	$NaAl(Si_2O_6)$	6.1
280	Albite	$Na_{0.986}Al_{1.005}Si_{2.995}O_8$	31.5
	Microcline, intermediate	$KAlSi_3O_8$	15.3
	Nepheline	$NaAlSiO_4$	14.1
	Calcium iron(II) Aluminum oxide	$Ca_4Fe_{1.5}Al_{17.67}O_{32}$	13.1
	hydrosodalite, hexasodium	$Na_6(AlSiO_4)_6(H_2O)_8$	9.8
	Calcium Iron Oxide	$Ca_2Fe_2O_{5.12}$	7.3
	Ferro-tschermakite	$Ca_2Fe_3Al_2(Si_6Al_2)O_{22}(OH)_2$	6.6
	Analcime-1Q	$NaAl(Si_2O_6)$	2.3

The phase composition of nepheline syenite samples depending on the temperature of chemical activation is presented in table 2.

During chemical activation depending on the temperature, there were changes in the phase composition of nepheline syenites: almost three times less microcline content; two times more albite content, hydro sodalite, calcium-iron oxide and analcite phases were formed, and the andradite and corundum phases disappeared (figure 2).

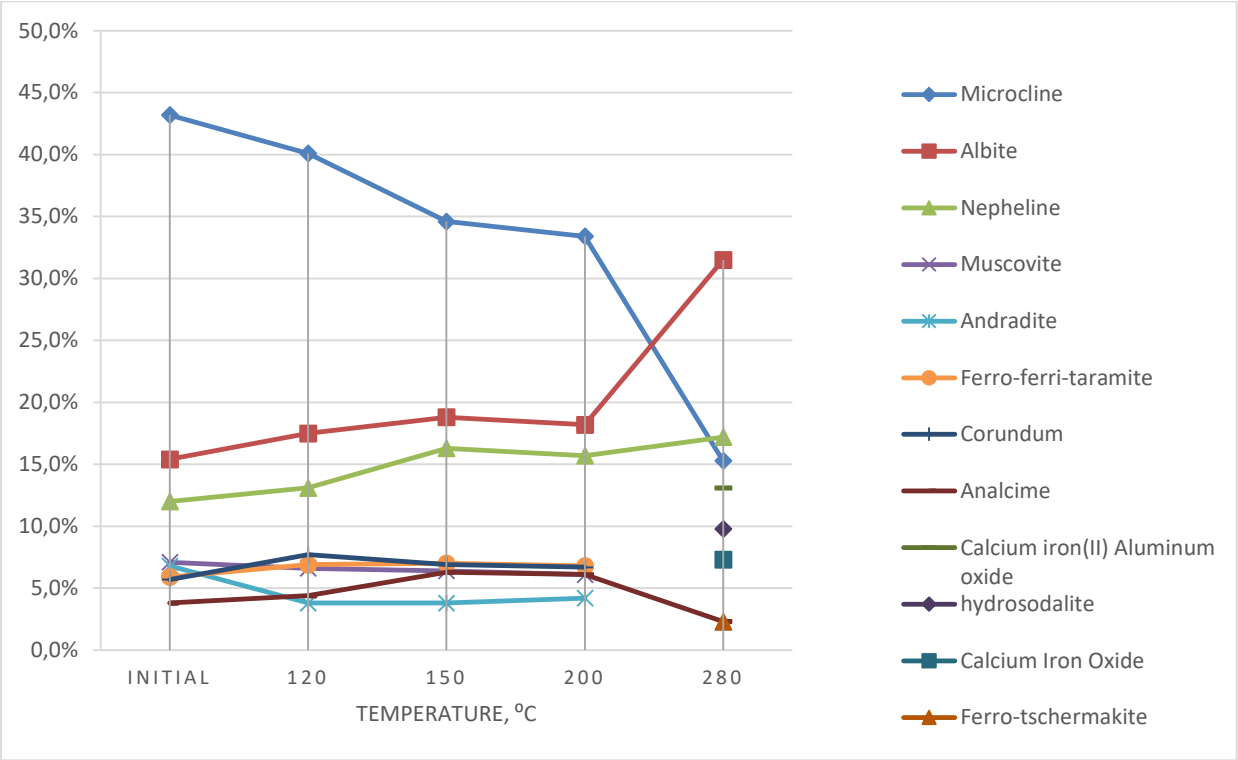

Figure 2 - Dependence of the change in the phase composition of nepheline syenites on the temperature of chemical activation

The influence of temperature of preliminary chemical activation of nepheline syenites on the degree of SiO_2 extraction at enrichment is investigated. It was shown that with increasing activation temperature the degree of extraction of silica in the solution increases (figure 3).

At an activation temperature of 280°C, the SiO_2 extraction rate during enrichment was 65.5 %. As a result of enrichment, the nepheline concentrate is received, composition wt.%: Al_2O_3 – 28.6; SiO_2 – 50.293; Fe_2O_3 – 5.08; CaO – 2.89; Na_2O – 6.79; K_2O – 4.74; MgO – 0.54.

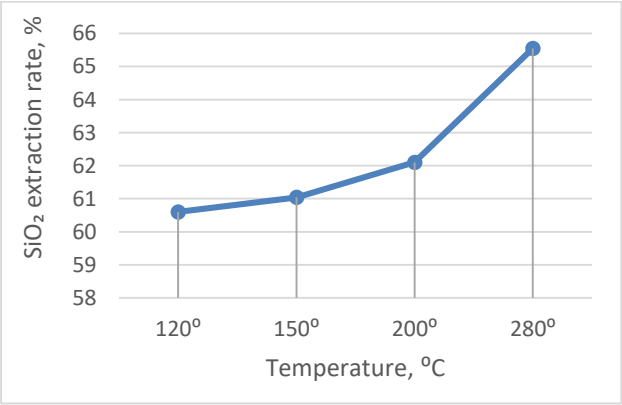

Figure 3 – SiO_2 extraction rate

Conclusions

Studies on the chemical activation of nepheline syenites of the Kubasadyr mine were conducted.

The obtained degree of enrichment of nepheline after preliminary chemical activation in a solution of sodium hydrogen carbonate is comparable with the degree of enrichment obtained after activation by pre-firing with the steam mixture at 500°C.

These results show the possibility in principle of obtaining high-quality nepheline concentrate, but require further research and refinement involving other techniques.

At chemical enrichment of nepheline syenites, the degree of extraction of silica is low (36%). As a result of pre-activation, the degree of extraction of silica in the solution reaches 65%.

During chemical activation depending on the temperature, there were changes in the phase composition of nepheline syenites: almost three times less microcline content; two times more albite content, hydro sodalite, calcium-iron oxide, and analcite phases were formed, and the andradite and corundum phases disappeared.

The results show the basic possibility ofobtaining high-quality nepheline concentrate, but

require further research and refinement involving other techniques.

Acknowledgement. This study was funded by the Science Committee of the Ministry of Science and Higher Education of the Republic of Kazakhstan (Grant No. AP14869579).

Conflict of interest. The corresponding author declares that there is no conflict of interest.

Cite this article as: Akhmadiyeva NK, Abdulvaliyev RA, Akcil A, Manapova AI. Pre-activation of nepheline before the enrichment. Kompleksnoe Ispolzovanie Mineralnogo Syra = Complex Use of Mineral Resources. 2023; 327(4):82-89. https://doi.org/10.31643/2023/6445.43

Нефелинді байытуға дейінгі алдын ала белсендіру

[1] Ахмадиева Н.К, [1] Абдулвалиева Р.А. [2] Акчил А., [1] Манапова А.И.

[1] Металлургия және кен байыту институты; Сәтбаев Университеті, Алматы, Қазақстан
[2] Сүлеймен Демирел университеті, Испарта, Туркия

Мақала келді: *20 желтоқсан 2022*
Сараптамадан өтті: *22 қаңтар 2023*
Қабылданды: *27 ақпан 2023*

ТҮЙІНДЕМЕ

Қазақстанда алюминий тотығын өнеркәсіптік өндіру саласындағы Байер бокситтерінің шектеулі қорларының салдарынан боксит емес шикізат-нефелиндерді пайдалануға болады. Неғұрлым перспективалы кен орны Кубасадыр кен орнының нефелинді сиениттері болып табылады. Қазіргі уақытта нефелин кендерін өңдеудің тиімді технологиясы жоқ. Жоғары энергия сыйымдылығы, капитал сыйымдылығы және атмосфераға елеулі шығарындылар нефелин кендерін пісіру тәсілімен өңдеудің жалпы қабылданған технологиясының негізгі кемшіліктері болып табылады. Нефелиндерді тиімді гидрохимиялық өңдеу үшін кремнеземнің бір бөлігін бөліп алу арқылы алдын ала байыту қажет. Қолданыстағы сілтілі ерітіндіде 280 ^{o}C температурада химиялық байыту технологиясына сәйкес кремнеземді алу дәрежесі 36 %-дан аспайды. Кремний тотығын алу дәрежесін арттыру үшін 500 ^{o}C температурада алдын ала күйдіруге қолданылады, және бұл экстракция дәрежесін 65 %-ға дейін арттыруға мүмкіндік береді. Мақалада натрий гидрокарбонатының ерітіндісіндегі нефелинді сиениттердің алдын ала химиялық белсенділігінің нәтижелері берілген. Белсендірудің оңтайлы шарттары анықталды. 280 ^{o}C температурасы кезіндегі белсенділік бастапқы шикізаттың фазалық құрамының өзгеруіне алып келді және 65,5 % байыту кезінде кремнезем алу дәрежесінде алды. Алынған нәтижелер алынған жоғары сапалы нефелинді концентраты үшін гидрохимиялық байыту технологиясын қолданудың және энергияны көп қажет ететін күйдіру процесін ауыстырудың түбегейлі мүмкіндігін көрсетті.

Түйін сөздер: нефелин, байыту, алдын ала белсендіру, кремний тотығы, алюминий тотығы

Ахмадиева Назым Қанатқызы — *Авторлар туралы ақпарат:*
PhD, Металлургия және Кен Байыту институтының глинозем және алюминий лабораториясының ғылыми қызметкері, Сатпаев Университет; Шевченко көшесі 29/133, 0500100, Алматы, Қазақстан. Email: n.akhmadiyeva@satbayev.university

Абдулвалиев Ринат Анварбекович — *Техникалық ғылымдарының кандидаты, Металлургия және Кен Байыту институтының глинозем және алюминий лабораториясының меңгерушісі, Сатпаев Университет; Шевченко көшесі 29/133, 0500100, Алматы, Қазақстан. Email: rin-abd@inbox.ru*

Ata Akcil — *PhD, профессор, Пайдалы қазбаларды және металдарды алу және өңдеуді зерттеу тобының (MMR&R) минералдық шикізатты өңдеу бөлімінің басшысы, Сулейман Демирел университетінің тау-кен факультеті, TR32260, Испарта, Турция. Email: ataakcil1@gmail.com*

Манапова Альфиям Ильяевна — *Техникалық ғылымдарының магистрі, Металлургия және Кен Байыту институтының глинозем және алюминий лабораториясының кіші ғылыми қызметкері, Сатпаев Университет; Шевченко көшесі 29/133, 0500100, Алматы, Қазақстан. Email: alfiya_0603@mail.ru*

Предварительная активация нефелинов перед обогащением

[1]Ахмадиева Н.К., [1]Абдулвалиев Р.А., [2]Акчил А., [1]Манапова А.И.

[1] Институт металлургии и обогащения; Сатпаев Университет, Алматы, Казахстан
[2] Университет Сулеймана Демиреля, Испарта, Турция

Поступила: *20 декабря 2022*
Рецензирование: *22 января 2023*
Принята в печать: *27 февраля 2023*

АННОТАЦИЯ

Вследствие ограниченных запасов байеровских бокситов в сферу промышленного производства глинозема в Казахстане возможно использование небокситового сырья – нефелинов. Наиболее перспективным месторождением является нефелиновые сиениты Кубасадырского месторождения. В настоящее время, не существует эффективной технологии переработки нефелиновых руд. Высокая энергоемкость, капиталоемкость и значительные выбросы в атмосферу являются основными недостатками общепринятой технологии переработки нефелиновых руд способом спекания. Для эффективной гидрохимической переработки нефелинов требуется предварительное обогащение с отделением части кремнезема. По существующей технологии химического обогащения в щелочном растворе при температуре 280^{o}C степень извлечения кремнезема составляет не более 36%. Для повышения степени извлечения кремнезема используют предварительный обжиг при 500^{o}C, который позволяет повысить степень извлечения до 65%. В статье представлены результаты предварительной химической активации нефелиновых сиенитов в растворе гидрокарбоната натрия. Определены оптимальные условия активации. Активация при температуре 280 ^{o}C привела к изменению фазового состава исходного сырья и получить степень извлечения кремнезема при обогащении 65,5%. Полученные результаты показали принципиальную возможность применения гидрохимической технологии обогащения для полученного качественного нефелинового концентрата и заменить энергоемкий процесс обжига.

Ключевые слова: нефелин, обогащение, предварительная активация, кремнезем, глинозем.

Информация об авторах:

Ахмадиева Назым Канатовна — *PhD, научный сотрудник лаборатории глинозема и алюминия Института металлургии и обогащения, Сатпаев Университет, ул.Шевченко 29/133, 050010, Алматы, Казахстан. Email: n.akhmadiyeva@satbayev.university*

Абдулвалиев Ринат Анварбекович — *Кандидат технических наук, заведующий лабораторией глинозема и алюминия Института металлургии и обогащения, Сатпаев Университет, ул.Шевченко 29/133, 050010, Алматы, Казахстан. Email: rin-abd@inbox.ru*

Ata Akcil — *PhD, профессор, руководитель исследовательской группы по восстановлению и переработке минералов и металлов (MMR&R), отдел обогащения полезных ископаемых, Факультет горного дела, Университет Сулеймана Демиреля, TR32260, Испарта, Турция. Email: ataakcil1@gmail.com*

Манапова Альфиям Ильяевна — *Магистр технических наук, младший научный сотрудник лаборатории глинозема и алюминия Института металлургии и обогащения, Сатпаев Университет, ул.Шевченко 29/133, 050010, Алматы, Казахстан. Email: alfiya_0603@mail.ru*

References

[1] Bauxite and alumina in the third quarter of 2022. Mineral Industry Surveys, USGS science for a changing world. https://d9-wret.s3.us-west-2.amazonaws.com/assets/palladium/production/s3fs-public/media/files/mis-2022q3-bauxi.pdf

[2] Komlossy G, Van Deursen C, Raahauge BE. Bauxite: Geology, Mineralogy, Resources, Reserves and Beneficiation. Springer Series in Materials Science. 2022; 320:19-132.

[3] Meyer FM. Availability of bauxite reserves. Natural Resources Research. 2004; 13:161-172. https://doi.org/10.1023/B:NARR.0000046918.50121.2e

[4] Kassa A, Shibeshi N, Tizazu B. Characterization and Optimization of Calcination Process Parameters for Extraction of Aluminum from Ethiopian Kaolinite. International Journal of Chemical Engineering. 2022, 1-18. https://doi.org/10.1155/2022/5072635

[5] Kyriakogona K, Giannopoulou I, Panias D. Extraction of Aluminium from Kaolin: a Comparative Study of Hydrometallurgical Processes. Proceedings of the 3rd World Congress on Mechanical, Chemical, and Material Engineering. 2017. Rome. https://doi.org/10.11159/mmme17.133

[6] ElDeeb AB, Brichkin VN, Kurtenkov RV, Bormotov IS. Extraction of alumina from kaolin by combination of pyro and hydo-metallurgical processes. Applied Clay Science. 2019; 172:146-154. https://doi.org/10.1016/j.clay.2019.03.008

[7] Kenzhaliyev BK, Imangaliyeva LM, Manapova AI, Azlan MN, Kaolinite clays as a source of raw materials for the aluminum industry of the Republic of Kazakhstan. Kompleksnoe Ispolzovanie Mineralnogo Syra = Complex Use of Mineral Resources. 2021; 319(4):5-12. https://doi.org/10.31643/2021/6445.34

[8] Al-Zahrani AA, Abdul-Majid MH. Extraction of alumina from local clays by hydrochloric acid process. Engineering science. 2009; 20(20:29-41.

[9] Bazin C, Quassiti KEl, Ouellet V. Sequential leaching for the recovery of alumina from a Canadian clay. Hydrometallurgy. 2007; 88(1-4):196-201. https://doi.org/10.1016/j.hydromet.2007.05.002

[10] Dissanayake DMSN, Manilaka MMMGPG, De Silva RT, De Silva RT, Pitawala HMTGA. Laterite and its potential as an alternative-bauxite. Cleaner Materials. 2021; 1:1000016. https://doi.org/10.1016/j.clema.2021.100016

[11] Padilla I, Lupez-Delgado A, Romero M. Kinetic study of the transformation of sodalite to nepheline. American Ceramic Society. 2022; 105:4336-4347. DOI: 10.1111/jace.18365

[12] Aluminium deposits in Kazakhstan. Handbook. Almaty. 1997, 94.

[13] Silva CM, Sorensen BE, Aasly K, Ellefmo SL. Geometrical approach to the element-to-mineral conversion for the Nabbaren Nephelin Syenite Deposit. Minerals. 2018; 8(8):325. https://doi.org/10.3390/min8080325

[14] Tan D, Ma H, Li G, Liu H, Zou D. Sintering reaction of pseudoleucite syenite: thermodynamic analysis and process evaluation. Earth Science Frontier. 2009; 16(4):269-279. https://doi.org/10.1016/S1872-5791(08)60084-6

[15] Bagani M, Balomenos E, Panias D. Naepheline syenite as an alternative source for aluminum production. Minerals. 2021; 11(7):734. https://doi.org/10.3390/min11070734

[16] Kovzalenko VA, Myltykbayeva LA, Tastanov EA, Beisembekova KO. Processing of aluminosilicate raw materials by hydrochemical method with preliminary chemical enrichment. Power Engineering and Resource Saving. 2009; 6:13-17

[17] Sadyralieva UJ, Tastanov EA, Ahmadieva NK, Ruzakhunova GS, Sultangazieva AN. Chemical enrichment of nepheline syenites of Sandyk deposit of Republic of Kyrgyzstan. Integrated use of raw materials. 2015; 1:3-8.

[18] Abdulvaliyev RA, Dyussenova SB, Manapova AI, Akcil A, Beisenbiyeva UZh. Modification of the phase composition of low grade gibbsite- kaolinite bauxites. Kompleksnoe Ispolzovanie Mineralnogo Syra = Complex Use of Mineral Resources. 2021; 317(2):94-102.

[19] Abdulvaliyev RA, Abdykirova GZ, Dyusenova SB, Imangalieva LM. Enrichment of chromite-containing sludge. Ore Enrichment. 2017; 327(6):15-19.

[20] Kenzhaliyev BK, Gladyshev SV, Abdulvaliyev RA, Omarova SA, Beisembekova KO, Manapova AI, Imangalieva LM. Activation of ash slag waste before chemical enrichment News of the national academy of sciences of the Republic of Kazakhstan series of geology and technical sciences. 2017; 422(2):143-148.

Crossref
DOI: 10.31643/2023/6445.44
Metallurgy

An Overview of the Current State and the Advantages of using acrylic resins as anticorrosive coatings

[1*]Muradova S.R., [1]Negim El-Sayed, [1]Makhmetova A.R., [1]Ainakulova D.T., [2]Mohamad N.M.I.

[1]School of Materials Science and Green Technologies, Kazakh-British Technical University, Almaty, Kazakhstan
[2]School of Chemical Sciences, Universiti Sains Malaysia, Pulau Pinang, Malaysia

** Corresponding author email: s_muradova@kbtu.kz*

Received: *December 16, 2022*
Peer-reviewed: *January 23, 2023*
Accepted: *March 02, 2023*

ABSTRACT
Corrosion protection coating is one of the most common ways of protecting structures against all kinds of negative external influences. Various types of anti-corrosion coatings can be used to successfully extend the service life of products. However, conventional paints are not water-resistant coatings, and small cracks always appear over time due to temperature fluctuations. Compared to other types of coatings, acrylic coatings are less expensive and just as durable. Acrylic resins have high anti-corrosion properties as well as water resistance, impact resistance, good adhesion to the substrate and overall durability. This powerful combination of cost and performance makes acrylic coatings such a popular and sensible solution for protecting structures against corrosion. The main purpose of this review is to describe the different types of acrylic resins and compare their properties, synthesis and drawbacks. It is expected that this work will be the cornerstone for the future development of acrylic resins.

Keywords: acrylic resins, corrosion, anti-corrosion coatings.

	Information about authors:
Muradova Sabina Rustamkyzy	*Bachelor's Degree in Materials Science and Technology of New Materials, 2nd year master student. Kazakh-British Technical University, School of Materials Science and Green Technologies, st. Tole bi, 59, 050000, Almaty, Kazakhstan. Email: s_muradova@kbtu.kz*
Negim Attia El-Sayed	*Doctor PhD of Chemistry, Professor. Kazakh-British Technical University, School of Materials Science and Green Technologies, st. Tole bi, 59, 050000, Almaty, Kazakhstan. Email: a.negim@kbtu.kz*
Makhmetova Alina Ruslanovna	*Bachelor's Degree in Materials Science and Technology of New Materials, 2nd year master student. Kazakh-British Technical University, School of Materials Science and Green Technologies, st. Tole bi, 59, 050000, Almaty, Kazakhstan. Email: al_makhmetova@kbtu.kz*
Ainakulova Dana Tulegenkyzy	*PhD Degree in Materials Science and Technology of New Materials, 2nd year PhD student. Kazakh-British Technical University, School of Materials Science and Green Technologies, st. Tole bi, 59, 050000, Almaty, Kazakhstan. Email: da_ainakulova@kbtu.kz*
Mohamad Nasir Mohamad Ibrahim	*Doctor PhD of Petroleum Engineering, Associate Professor, School of Chemical Sciences, Universiti Sains Malaysia, 11800 Pulau Pinang, Malaysia. Email: mnm@usm.my*

Introduction

Over the past decades, many effective methods have been developed to reduce or minimize various types of corrosion [1].

Coatings today are one of the most effective methods of corrosion protection for both metal and non-metal surfaces [[2], [3]].

For high anti-corrosion protection, coatings should be: with high mechanical characteristics, good adhesion, durability and low moisture permeability.

Acrylate polymers have high transparency [4], good adhesive properties [5], a number of monomer species [6] and high mechanical strength, and therefore have aroused great interest.

Acrylic resin coatings (ARCs) are a reliable anti-corrosion tool as they are resistant to adverse weather conditions and are therefore used to control atmospheric corrosion. Such coatings are oil resistant and have high mechanical strength [7].

Acrylic resin is made from water-based acrylic polymers by solution or suspension polymerization; therefore, when used, it may be liquid or solid. It has been designed to minimize the dispersion and release of hydrocarbons; thus, reducing the content of volatile organic substances. The ingredients used to crosslink the acrylic resin determine the

properties of the anti-corrosion agent used for the coating. The aim of the present review is to describe the best technology to protect metal from corrosion based on different acrylic resins to produce anticorrosion coating.

Properties, advantages and application of acrylic coatings

Acrylic coatings have the following protective properties:

- Transparent, glossy appearance and color stability;
- Relatively good resistance to weathering, chemicals, heat and solvents;
- Efficiency and flexibility;
- Excellent physical hardness and good adhesion;
- Fast drying and the ability to apply the pigment at ambient temperature.

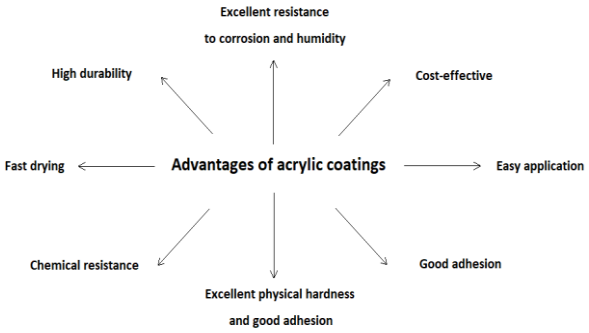

Figure 1 – Advantages of Acrylic coatings [[8], [9], [10], 11]].

Advantages of acrylic coating are illustrated in Figure 1. Acrylic resins have properties such as gloss retention [8], color retention [9], heat resistance [10] and corrosion resistance [11], so due to these properties, they are widely used in industry. They are used in automotive coatings and architectural coatings.

There is an acrylic urethane coating that has a high solids content and is used for auto repair work. This coating was made from acrylic and methacrylic and is a clear coat that cures at room temperature and exhibits very good overall performance [12].

Acrylic was also able to find application for the protection of museum items and monuments [13].

Acrylic resins are self-cleaning and therefore have found use in automobiles, buildings, and self-cleaning windows, which were synthesized to prevent or remove dirt by Yang et al [14].

In addition, acrylic resins are used as a protective material for paper, wood, ceramics, and glass [15].

But it is worth noting that its quality also depends on the composition of acrylic coatings. For example, if fillers are included in the composition of such coatings, this will increase their strength. If these fillers are properly dispersed in internal structures, they occupy micropores and this reduces the paths through which corrosive electrolytes pass through the coatings. Many coatings are compatible with fillers - barite, dolomite, silicon dioxide and others. But there are problems such as choosing the appropriate filler that is suitable for many inorganic and organic coatings.

Waterborne acrylic resins

Waterborne acrylic base coating as a single coat is used in various fields on account of its interesting properties such as high resistance to weather and different solvents as well as their excellent appearance [16].

Water-based acrylic resins in most cases copolymerize with acrylic, methacrylic acids and their esters, and their properties are adapted by adjusting the composition and ratios of different monomers as well as the structure of the starting materials.

There are several ways to synthesize water-based acrylic resin, which include emulsion, solution polymerization, bulk and suspension polymerization, emulsion polymerization being the most used. Synthesis occurs with monomers, water, emulsifiers and initiators [17].

Water-based acrylic resin, reacting with the appropriate filler, forms a solid mass, which in a short time reaches mechanical characteristics several times higher than classic water-based products. 50% mechanical performance is achieved after 15 hours at around 20°C. The acrylic system can be filled with iron oxide pigments, aluminum powder or various inert fillers to give the product the desired appearance. The addition of various fillers proportionally reduces the mechanical properties of the product.

Water-based coatings have greater advantages than coatings based on organic solvents [[18], [19],

[20], [21], [22], [23], [24], [25], [26]]. Such water-based coatings have low toxicity, are fire-resistant, and are environmentally friendly, which has attracted attention in the industry [[27], [28], [29], [30]]. Such coatings are increasingly used in the construction and paint industry, in metal and wooden coatings in order to reduce the emission of harmful substances [31].

But such coatings have a number of disadvantages, such as low chemical resistance and low water resistance, poor thermal stability, and low mechanical properties, despite this, water-based acrylic resins have become commercially available in recent years [32]. Applying modification and compounding can eliminate these shortcomings.

Water-based acrylic resins have a number of excellent characteristics and is applied in various aspects of production in connection with environmental protection. Such coatings are also used in the automotive industry, in the production of furniture and plastic parts, as well as in the anti-corrosion treatment of metals [17].

Acrylic coatings with various nanofillers

Nanoscale materials like TiO_2, SiO_2, ZnO and Fe_2O_3 are used to create hybrid organic coating systems [[33], [34], [35], [36], [37]]. When using mixed nanoparticles, it entails a synergistic effect and, in addition, improves some properties of the polymer. But, due to the high surface energy of nanoparticles, it allows easy agglomeration in some solutions [38]. In order to reduce the effect of the two-phase interface and to increase the stability and compatibility of nanoparticles in various media, modification of nanomaterials is required. Most researchers have found that the addition of nanoparticles can improve polymer characteristics [33-37], however, further research is needed on the synergistic effect of mixed nanoparticles and the improvement of polymer properties.

In studies of polymer and coatings, it was found that if such nanoparticles as TiO_2 [[39], [40]], ZnO [[41], [42]], Fe_3O_4 [43], SiO_2 [44], as well as their nanohybrids [[45], [46], [47]], then this, in addition to improving the various properties of the coating, also give new functions. For example, if a SiO_2 nanoparticle is added to the coating composition, this will improve the mechanical and thermal properties, as well as the anticorrosion properties of the organic coating [[48], [49], [50], [51], [52], [53]]. In addition, such nanoparticles were used for superhydrophobic [[54], [55], [56], [57], [58]] and hydrophilic coatings [59].

Acrylic polyurethane coating reinforced by sio_2 nanoparticles

SiO_2 nanoparticles are synthesized by such methods as the steam method, the sol–gel method, and the thermal decomposition method [[60], [61], [62]]. In such methods, tetraethoxysilane and tetramethoxysilane are used as precursors in order to obtain SiO_2 nanoparticles. Such precursors make it possible to control the size, shape, and purity of SiO_2 nanoparticles. However, the finished material has a high cost and is not an environmentally friendly process. Recent works have suggested more environmentally friendly approaches to obtain nano- SiO_2 using agricultural waste [[63], [64], [65], [66], [67]]. For example, rice husk is an agricultural waste that contains a large amount of silica (about 80–90 wt. %) [68]. Therefore, the use of rice husks to produce nanosilica has a high potential, since it is an environmentally friendly and cost-effective production, which, in addition, demonstrates rather high mechanical characteristics.

If the content of nanoparticles was increased from 0 to 2.5%, then this improved the mechanical performance as well. But, a higher addition of RHA-SiO_2 caused a decrease in mechanical properties. Many holes of different diameters from 20 nm to several microns appeared on the surface of the coatings and inside (without nano RHA- SiO_2), but the coating with 2.5 wt. % nano-GW- SiO_2 degraded less [69].

In the range of 200-400 nanometers, RHA- SiO_2 nanoparticles have high UV absorption. The nanocomposite coating is characterized by higher UV absorption compared to the pure one. Therefore, this suggests that if the nanocomposite contains nano-RHA- SiO_2, then this will scatter UV light and protect the half-dimensional matrix from the harmful effects of UV radiation. In acrylic polyurethane coatings, the photoprotective effect of RHA-SiO_2 nanoparticles is the same as in acryl melamine automotive varnishes [70].

The RHA- SiO_2 nanoparticle works like:

1) UV protector

2) as a nanofiller that screens and prevents the penetration of aging agents into the coating from the external environment.

This is evidence that such nanocomposite coatings are weather resistant.

Acrylic resin coating modified by functional graphene oxide

Carbon nanotubes (CNTs) are one of the most studied materials in recent years. CNTs are widely used in water treatment, biology, sensors, thin film transistors, and so on [71].

2 functional graphene oxide (FGO) was obtained by modifying the surface of graphene oxide (GO) with γ methacryloxypropyltrimethoxysilane (KN-570), then with acrylic nanocomposites with different loadings of GO and FGO. This is necessary in order to improve the dispersion and strength of the filler-matrix interface in acrylic resins [72].

To ensure that the coating effectively protects the substrate from the external environment and for good decorative properties, it is necessary that its adhesion to the given substrate is adequate. An adhesion tester is used to test the adhesion of a coating. It was maximum when the content of GO and FGO was 0.08 wt.%, since GO has a large specific surface area. With a small amount of GO, the surface energy of nanocomposites increases. Adhesion with FGO increased more than with GO. By adding FGO, the crosslink density increases, and the coating forms a 3-dimensional structure, and this leads to an increase in adhesion [73]. However, when adding GO and FGO more than 0.08 wt.%. adhesion is reduced. This manifestation may be due to the high agglomeration of nanoparticles, which led to the separation of the organic and inorganic phases and, therefore, GO and FGO do not play a significant role in adhesion [72].

Composites with both the addition of GO and the addition of FGO showed a high improvement in hardness. With the addition of 0.08 wt.% FGO and GO hardness increased by 64% and 41%. This phenomenon may be due to 2 reasons. The first reason is that GO has high mechanical properties. GO reduces the degree of surface deformation since it is well dispersed in the matrix resin. The second reason is that particles can be connected by different macromolecular chains and form physical / chemical crosslinks if a small amount of GO is added to the acrylic resin [74].

There was a comparison of the chemical resistance, water resistance, acid resistance, and alkali resistance of the nanocomposite coating. And a significant improvement in water resistance, acid resistance, and alkali resistance of coatings was found with the addition of FGO [72].

Characterization of anticorrosion zirconia/acrylic nanocomposite resin coatings

Using electrochemical methods, a study was made of the corrosion resistance of acrylic resin coatings that were modified with zirconium dioxide on steel substrates. Steel substrates coated with 3.5 wt.% NaCl were used for 1 and 7 days, at room temperature. From the impedance data, it was concluded that the corrosion resistance decreased as the ZrO_2NPs content increased. This was due to the oversaturation of the coating mesh and a decrease in the amount of base resin. If the concentrations are optimal, the modified zirconia particles act as a filler that reinforces the internal network of the coating and blocks the passage of the chloride ion that causes corrosion. But it should be noted that if the content of ZrO_2NPs in acrylic resin is more than 1 mg, the neutral electrolyte molecules will penetrate through the coatings due to the content of excess fillers, hence there is localized corrosion [75].

The content of modified ZrO_2NPs particles in the coatings of their acrylic resins blocks the penetration of corrosive chloride ions and water molecules through the coating to the metal surface, therefore it slows down local corrosion. Acrylic resin (10 g) contains the optimal concentration of ZrO_2NPs (1 mg) [76]. A change in the overall mechanical conductivity of the polymer coating was observed with the content of ZrO_2NPs nanoparticles. The average hardness value for the bare metal was 140 HV while the values for the coated samples were lower. This was due to the fact that nanoparticles act as inorganic fillers in the volume of acrylic resin coatings [75].

For each acrylic resin-coated substrate containing a ZrO_2NPs nanoparticle, the paths of corrosive ions and molecules that leaked onto the metal surface were blocked. Since the bulk porosity decreases due to particle dispersion, the protective

effect will depend on the density of the filler particles and their concentrations [75].

Using the experimental data of this study, it can be concluded that if the content of ZrO_2NPs nanoparticles increases and the content of the main resin decreases, this will lead to a decrease in corrosion resistance. ZrO_2NPs nanoparticles (1mg) show excellent anti-corrosion ability in acrylic resin coatings [75].

Conclusion

Acrylic polymers are used as the main binder in a wide variety of coatings. Acrylic polymers increase the strength of coatings.

If these fillers are correctly dispersed in the internal structure of the coating, they will occupy their inherent micropores and, as a result, will reduce the paths where corrosive electrolytes pass through the coatings.

Many coatings are compatible with fillers such as calcite, talc, and silica. But there are still problems in choosing the right filler that is suitable for most coatings. Compared to other types of chemicals, acrylic coating is less expensive but more durable. Acrylic resins are widely used in industry due to their great properties such as strength [26], colour retention [27], heat [28], and corrosion resistance [29].

Conflict of interest.

On behalf of all authors, the correspondent author declares that there is no conflict of interest.

Cite this article as: Muradova SR, Negim El-Sayed, Makhmetova AR, Ainakulova DT, Mohamad NMI. An Overview of the Current State and the Advantages of using acrylic resins as anticorrosive coatings . Kompleksnoe Ispolzovanie Mineralnogo Syra = Complex Use of Mineral Resources. 2023; 327(4):90-98. https://doi.org/10.31643/2023/6445.44

Акрил шайырларын коррозияға қарсы жабын ретінде пайдаланудың артықшылықтарына және оның қазіргі кездегі жай-күйіне шолу

[1*]Мурадова С.Р., [1]Негим Эльсайд, [1]Махметова А.Р., [1]Айнакулова Д.Т., [2]Мохамад Н.М.И.

[1]Қазақ-Британ техникалық университеті, Алматы, Қазақстан
[2]Сенс Малайзия университеті, Пулау Пинанг, Малайзия

Мақала келді: *16 желтоқсан 2022*
Сараптамадан өтті: *23 қаңтар 2023*
Қабылданды: *02 наурыз 2023*

ТҮЙІНДЕМЕ

Коррозияға қарсы жабын - құрылымдарды барлық жағымсыз сыртқы әсерлерден қорғаудың ең кең таралған әдістерінің бірі. Өнімдердің қызмет ету мерзімін ұзарту үшін коррозияға қарсы жабындардың әртүрлі түрлерін қолдануға болады. Дегенмен, әдеттегі бояулар суға төзімді жабындар емес, уақыт өте келе температураның өзгеруіне байланысты әрқашан кішкентай жарықшақтар пайда болады. Басқа жабын түрлерімен салыстырғанда, акрил жабындары арзанырақ және берік. Акрил шайырлары коррозияға қарсы жоғары қасиеттерге, сонымен қатар суға төзімділікке, соққыға төзімділікке, жақсы адгезияға ие және ұзаққа төзімді. Құны мен өнімділіктің бұлай сәйкес келуі акрил жабындарының құрылымдарды коррозиядан қорғау үшін өте жақсы таңдау екенін көрсетеді. Бұл шолудың негізгі мақсаты - акрилді шайырлардың әртүрлі түрлерін сипаттау және олардың қасиеттерін, синтезін және кемшіліктерін салыстыру. Бұл жұмыс акрилді шайырлар бойынша кейінгі зерттеулерді дамыту үшін өте маңызды кезең болады деп күтілуде.

Түйін сөздер: акрилді шайырлар, коррозия, коррозияға қарсы жабындар.

Авторлар туралы ақпарат:

Мурадова Сабина Рустамқызы — *Материалтану және жаңа материалдар технологиясы бакалавры, 2 курс магистранты. Қазақ-Британ техникалық университеті, Материалтану және жасыл технологиялар мектебі, Төле би, көш., 59, 050000, Алматы, Қазақстан. Email: s_muradova@kbtu.kz*

Негим Аттиа Эльсайд — *Химия ғылымдарының докторы, профессор. Қазақ-Британ техникалық университеті, Материалтану және жасыл технологиялар мектебі, көш. Төле би, 59, 050000, Алматы, Қазақстан. Email: a.negim@kbtu.kz*

Махметова Алина Руслановна	*Материалтану және жаңа материалдар технологиясы бакалавры, 2 курс магистранты. Қазақ-Британ техникалық университеті, Материалтану және жасыл технологиялар мектебі, көш. Төле би, 59, 050000, Алматы, Қазақстан. Email: al_makhmetova@kbtu.kz*
Айнакулова Дана Тулегенқызы	*Материалтану және жаңа материалдар технологиясы PhD докторантурасы, 2 курс PhD докторанты. Қазақ-Британ техникалық университеті, Материалтану және жасыл технологиялар мектебі, көш. Төле би, 59, 050000, Алматы, Қазақстан. Email: da_ainakulova@kbtu.kz*
Мохамад Насир Мохамад Ибрагим	*Мұнай инженері ғылымдарының докторы, доцент, Химия ғылымдары мектебі, Сенс Малайзия университеті, 11800 Пулау Пинанг, Малайзия. Email: mnm@usm.my*

Обзор современного состояния и преимущества использования акриловых смол в качестве антикоррозионных покрытий

[1*]Мурадова С.Р., [1]Эльсайд Негим, [1]Махметова А.Р., [1]Айнакулова Д.Т., [2]Мохамад Н.М.И.

[1]Казахстанско-Британский технический университет, Алматы, Казахстан
[2]Школа химических наук, Университет Сейнс Малайзия, 11800 Пулау Пинанг, Малайзия

Поступила: *16 декабря 2022*
Рецензирование: *23 января 2023*
Принята в печать: *02 марта 2023*

АННОТАЦИЯ

Антикоррозионное покрытие является одним из самых распространенных способов защиты конструкций от всевозможных негативных внешних воздействий. Для успешного продления срока службы изделий можно использовать различные виды антикоррозионных покрытий. Однако обычные краски не являются водостойкими покрытиями, и со временем всегда появляются небольшие трещинки из-за перепадов температур. По сравнению с другими видами покрытий, акриловые покрытия менее дорогие и такие же долговечные. Акриловые смолы обладают высокими антикоррозионными свойствами, а также водостойкостью, ударопрочностью, хорошей адгезией к основанию и общей долговечностью. Это мощное сочетание стоимости и производительности делает акриловые покрытия таким популярным и разумным решением для защиты конструкций от коррозии. Основной целью данного обзора является описание различных типов акриловых смол и сравнение их свойств, синтеза и недостатков. Ожидается, что эта работа станет краеугольным камнем для дальнейшего развития акриловых смол.

Ключевые слова: акриловые смолы, коррозия, антикоррозионные покрытия.

Мурадова Сабина Рустамқызы	***Информация об авторах:*** *Бакалавр материаловедения и технологии новых материалов, магистрант 2 курса. Казахстанско-Британский технический университет, Школа материаловедения и зеленых технологий, ул. Толе би, 59, 050000, Алматы, Казахстан. Email: s_muradova@kbtu.kz*
Негим Аттиа Эльсайд	*Доктор химических наук, профессор. Казахстанско-Британский технический университет, Школа материаловедения и зеленых технологий, ул. Толе би, 59, 050000, Алматы, Казахстан. Email: a.negim@kbtu.kz*
Махметова Алина Руслановна	*Бакалавр материаловедения и технологии новых материалов, магистрант 2 курса. Казахстанско-Британский технический университет, Школа материаловедения и зеленых технологий, ул. Толе би, 59, 050000, Алматы, Казахстан. Email: al_makhmetova@kbtu.kz*
Айнакулова Дана Тулегенкызы	*PhD материаловедения и технологии новых материалов, докторант 2 курса. Казахстанско-Британский технический университет, Школа материаловедения и зеленых технологий, ул. Толе би, 59, 050000, Алматы, Казахстан. Email: da_ainakulova@kbtu.kz*
Мохамад Насир Мохамад Ибрагим	*Доктор философии в области нефтяной инженерии, доцент, Школа химических наук, Университет Сейнс Малайзия, 11800 Пулау Пинанг, Малайзия. Email: mnm@usm.my*

References

[1] Ji G, Anjum S, Sundaram S, Prakash R. Musa paradisica peel extract as green corrosion inhibitor for mild steel in HCl solution, Corros. Sci. 2015; 90:107-117.

[2] Bera S, Rout TK, Udayabhanu G, Narayan R., Water-based & amp; eco-friendly epoxysilane hybrid coating for enhanced corrosion protection & amp; adhesion on galvanized steel, Prog. Org. Coat. 2016; 101:24-44.

[3] Liu M, Mao X, Zhu H, Lin A, Wang D. Water and corrosion resistance of epoxy– acrylic amine waterborne coatings: Effects of resin molecular weight, polar group and hydrophobic segment, Corros. Sci. 2013; 75:106-113.

[4] Kotlík P, Doubravová K, Horálek J, Kubáč L, Akrman J. Acrylic copolymer coatings for protection against UV rays, J. Cult. Herit. 2014; 15:44-48.

[5] Motamedi M, Ramezanzadeh M, Ramezanzadeh B, Mahdavian M. One-pot synthesis and construction of a high performance metal-organic structured nano pigment based on nanoceria decorated cerium (III)-imidazole network (NC/CIN) for effective epoxy composite coating anti-corrosion and thermo-mechanical properties improvement, Chem. Eng. J. 2020; 382:122820.

[6] Yu S, Zhou Y, Zhang T, He M. Preparation and Characterization of Acrylate Copolymers Modified by Fluorine and Silicon for Application in Release Films, Polym-Plast. Technol. 2014; 53:531-538.

[7] Morscha S, Lyona S, Gibbon SR. The degradation mechanism of an epoxy-phenolic can coating, Prog. Org. Coat. 2017; 102: 37-43.

[8] Zhou ZF, Xu WB, Fan JX, Ren FM, Xu CL. Synthesis and characterization of carboxyl group-containing acrylic resin for powder coatings. Prog. Org. Coat. 2008; 62:179-182.

[9] Natu AM, Mark MRVD. Synthesis and characterization of an acid catalyst for acrylic-melamine resin systems based on colloidal unimolecular polymer (CPU) particles of MMA-AMPS. Prog. Org. Coat. 2015; 81:35-46.

[10] Manfredi LB, Rodríguez ES, Przybylak MW, Vázquez A. Thermal degradation and fire resistance of unsaturated polyester, modified acrylic resins and their composites with natural fibers. Polym. Degrad. Stab. 2006; 91:255-261.

[11] Burja K, Šegedi U, Skale S, Berce P, Prosen P, Kukanja D. Improved anticorrosion properties of polyurethane coatings based high-solids acrylics synthesized in a high pressure reactor. Prog. Org. Coat. 2015; 78:275-286.

[12] Petit H, Henry N, Krebs A, Uytterhoeven G, Jong FD. Ambient cure high solids acrylic resins for automotive refinish clear coat applications. Prog. Org. Coat. 2000; 43:41-49.

[13] Khallaf MK, El-Midany AA, El-Mofty SE. Influence of acrylic coatings on the interfacial, physical, and mechanical properties of stone-based monuments. Prog. Org. Coat. 2011; 72:592-598.

[14] Yang X, Zhu LQ, Zhang Y, Chen YC, Bao BQ, Xu JL, Zhou WW. Surface properties and self-cleaning ability of the fluorinated acrylate coatings modified with dodecafluoroheptyl methacrylate through two adding ways. Appl. Surf. Sci. 2014; 295:44-49.
[15] Chiantore O, Lazzari M. Photo-oxidative stability of paraloid acrylic protective polymers. Polymer. 2001; 42:17-27.

[16] Calovi M, et al. Effect of functionalized graphene oxide concentration on the corrosion resistance properties provided by cataphoretic acrylic coatings, Mater. Chem. Phys. 2020; 239:121984.

[17] Cuiyan Jiao, Li Sun, Qian Shao, Jiyong Song, Qian Hu, Nithesh Naik, and Zhanhu Guo. Advances in Waterborne Acrylic Resins: Synthesis Principle, Modification Strategies, and Their Applications. ACS Omega. 2021; 6:2443-2449.

[18] Zheng Y, Wang X, Wu G. Chemical modification of carbon fiber with diethylenetriaminepentaacetic acid/halloysite nanotube as a multifunctional interfacial reinforcement for silicone resin composites, Polym. Adv. Technol. 2020; 31(3):527-535.

[19] He YX, Chen QY, Liu H, Zhang L, Wu DY, Lu C, OuYang W, Jiang DF, Wu MF, Zhang JX, Li YC, Fan JC, Liu CT, Guo ZH. Friction and wear of MoO3/graphene oxide modified glass fiber reinforced epoxy nanocomposites, Macromol. Mater. Eng. 2019; 304(8):1900166.

[20] He Y,Chen Q, Yang S, Lu C, Feng M, Jiang Y, Cao G, Zhang J, Liu C. Microcrack behavior of carbon fiber reinforced Fe3O4/graphene oxide modified epoxy composites for cryogenic application, Compos. 2018; 108(A):12-22.

[21] Koizhanova AK, Kenzhaliyev BK, Kamalov EM, Erdenova MB, Magomedov DR, Abdyldaev NN. Research of Gold Extraction Technology from Technogenic Raw Material. News of the National Academy of Sciences of the Republic of Kazakhstan: Series Chemistry and Technology. 2020; 439(1):95-101. https://doi.org/10.32014/2020.2518-1491.12

[22] Shahc N, Aslam S, Ul-Islam MU, Arain MB, Rehan T, Naeem M, Wajid Ullah MW, Yang G. Fabrication of thermally stable graphite-based poly (acrylonitrileco-acrylic acid) composite with impressive antimicrobial properties, Eng. Sci. 2019; 6:77-85. https://doi.org/10.30919/es8d758

[23] Hu W, Huang J, Zhang X, Zhao S, Pei L, Zhang C, Liu Y, Wang Z. A mechanically robust and reversibly wettable benzoxazine/epoxy/mesoporous TiO2 coating for oil/water separation, Appl. Surf. Sci. 2020; 507:145168.

[24] Zheng Y, Chen L, Wang X, Wu G. Modification of renewable cardanol onto carbon fiber for the improved interfacial properties of advanced polymer composites, Polymers. 2019; 12(1):45.

[25] Liu M, Li B, Zhou H, Chen C, Liu Y, Liu T. Extraordinary rate capability achieved by a 3D “skeleton/skin” carbon aerogel–polyaniline hybrid with vertically aligned pores, Chem. Commun. 2017; 53(19):2810-2813.

[26] Zheng Z, Olayinka O, Li B. 2S-Soy protein-based biopolymer as a non-covalent surfactant and its effects on electrical conduction and dielectric relaxation of polymer nanocomposites, Eng. Sci. 2018; 4:87-99. https://doi.org/10.30919/es8d766

[27] Sun K, Wang Z, Xin J, Wang Z, Xie P, Fan G, Murugadoss V, Fan R, Fan J, Guo Z. Hydrosoluble graphene/polyvinyl alcohol membranous composites with negative permittivity behavior, Macromol. Mater. Eng. 2020; 305(3):1900709.

[28] Lou C, Jing T, Zhou J, Tian J, Zheng Y, Wang C, Zhao Z, Lin J, Liu H, Zhao C, Guo Z. Laccase immobilized polyaniline/magnetic graphene composite electrode for detecting hydroquinone, Int. J. Biol. Macromol. 2020; 149:1130-1138.

[29] Shi X, Wang C, Zhang J, Guo L, Lin J, Pan D, Zhou J, Fan J, Ding T, Guo Z. Zwitterionic glycine modified Fe/Mg-layered double hydroxides for highly selective and efficient removal of oxyanions from polluted water, J. Mater. Sci. Technol. 2020; 51:8-15.

[30] Shi X, Wang C, Ma Y, Liu H, Wu S, Shao Q, He Z, Guo L, Ding T, Guo Z. Template-free microwave-assisted synthesis of FeTi coordination complex yolkshell microspheres for superior catalytic removal of arsenic and chemical degradation of methylene blue from polluted water, Powder Technol. 2019; 356:726-734.

[31] Huang S, Xiao J, Zhu Y, Qu J. Synthesis and properties of spray-applied high solid content two component polyurethane coatings based on polycaprolactone polyols, Prog. Org. Coating. 2017; 106:60-68.

[32] Yan L, Li Q, Chi H, Qiao Y, Zhang T, Zheng F. One-pot synthesis of acrylate resin and ZnO nanowires composite for enhancing oil absorption capacity and oilwater separation, Adv. Compos. Hybrid Mater. 2018; 1(3):567-576.

[33] Zhang J, Pan M, Luo C, Chen X, Kong J, Zhou T. A novel composite paint (TiO2 /fluorinated acrylic nanocomposite) for antifouling application in marine environments, J. Environ. Chem. Eng. 2016; 4:2545-2555.
[34] Ramezanzadeh B, Haeri Z., Ramezanzadeh M., A facile route of making silica nanoparticles-covered graphene oxide nanohybrids

(SiO2-GO); fabrication of SiO2-GO/epoxy composite coating with superior barrier and corrosion protection performance, Chem. Eng. J. 2016; 303:511-528.

[35] Haeri SZ, Ramezanzadeh B, Asghari M. A novel fabrication of a high performance SiO2-graphene oxide (GO) nanohybrids: Characterization of thermal properties of epoxy nanocomposites filled with SiO2-GO nanohybrids, J. Colloid Interf. Sci. 2017; 493:111-122.

[36] Sharifi Golru S, Attar MM, Ramezanzadeh B. Studying the influence of nano-Al2O3 particles on the corrosion performance and hydrolytic degradation resistance of an epoxy/polyamide coating on AA-1050, Prog. Org. Coat. 2014; 77:1391-1399.

[37] Javidparvar AA, Ramezanzadeh B, Ghasemi E. The effect of surface morphology and treatment of Fe3O4 nanoparticles on the corrosion resistance of epoxy coating, J. Taiwan Inst. Chem. E. 2016; 61:356-366.

[38] Zheng H, Gao F, Valtchev V. Nanosized inorganic porous materials: fabrication, modification and application, J. Mater. Chem. A. 2016; 4:16756-16770.

[39] Chen XD, Wang Z, Liao ZF, Mai YL, Zhang MQ. Roles of anatase and rutile TiO2 nanoparticles in photooxidation of polyurethane, Polym. Test. 2007; 26:202-208.

[40] Nguyen TV, Nguyen TP, Nguyen TD, Aidani R, Trinh VT, Decker C. Accelerated degradation of water borne acrylic nanocomposites used outdoor protective coatings, Polym. Degrad. Stab. 2016; 128:65-76.

[41] Nguyen TV, Dao PH, Duong KL, Duong QH, Vu QT, Nguyen AH, Mac VP, Le TL. Effect of R-TiO2 and ZnO nanoparticles on the UV-shielding efficiency of water-borne acrylic coating, Prog. Org. Coat. 2017; 110:114-121.

[42] To TXH, Ngo TD, Trinh TA, Nguyen TD, Bui VT, Pham GV, Thai H, Dinh TMT, Olivier MG. Effect of silane modified nano ZnO on UV degradation of polyurethane coatings, Prog. Org. Coat. 2015; 79:68-74.

[43] Maryam Jouyandeh, Negar Rahmati, Elnaz Movahedifar, Behzad Shirkavand Hadavand, Zohre Karami, Mehdi Ghaffari, Peyman Taheri, Ehsan Bakhshandeh, Henri Vahabi, Mohammad Reza Ganjali, Krzysztof Formela, Mohammad Reza Saeb, Properties of nano-Fe3O4 incorporated epoxy coatings from Cure Index perspective, Prog. Org. Coat. 2019; 133:220-228.

[44] Tuan Anh Nguyen, The Huyen Nguyen, Thien Vuong Nguyen, Hoang Thai, Xianming Shi, Effect of nanoparticles on the thermal and mechanical properties of epoxy coatings, J. Nanosci. Nanotechnol. 2016; 16:9874-9881.

[45] Phuong Nguyen Tri, Tuan Anh Nguyen, The Huu Nguyen, Pascal Carriere, Antibacterial behavior of hybrid nanoparticles (chapter 7), in: Satyabrata Mohapatra, Tuan Anh Nguyen, Phuong Nguyen-Tri (Eds.), Noble MetalMetal Oxide Hybrid Nanoparticles: Fundamentals and Applications. 2019, 141-155. https://doi.org/10.1016/B978-0-12-814134-2.00007-3

[46] Ngo TD, Le TMH, Nguyen TH, Nguyen TV, Nguyen TA, Le TL, Nguyen TT, Tran TTV, Le TBT. Antibacterial nanocomposites based on Fe3O4-Ag hybrid nanoparticles and natural rubber–polyethylene blends, Int. J. Polym. Sci. 2016, 9. Article ID 7478161.

[47] The Tam Le, Thien Vuong Nguyen, Tuan Anh Nguyen, Thi Thanh Huong Nguyen, Thai Hoang, Dai Lam Tran, Duc Anh Dinh, Thi Mai Nguyen, Trong Lu Le, Thermal, mechanical and antibacterial properties of water-based acrylic polymer/SiO2-Ag nanocomposite coating, J. Mater. Chem. Phys. 2019; 232:362-366.

[48] Allahverdi Ali, Morteza Ehsani, Hadi Janpour, Shervin Ahmadi, The effect of nanosilica on mechanical, thermal and morphological properties of epoxy coating, Prog. Org. Coat. 2012; 75(4):543-548.

[49] Shi X, Nguyen TA, Suo Z, Liu Y, Avci R. Effect of nanoparticles on the anticorrosion and mechanical properties of epoxy coating", Surf. Coat. Technol. 2009; 204(3):237-245.

[50] Ezio Amerio, Paola Fabbrib, Giulio Malucelli, Massimo Messorib, Marco Sangermano, Rosa Taurino, Scratch resistance of nano-silica reinforced acrylic coatings, Prog. Org. Coat. 2008; 62(2):129-133.

[51] Frank Bauer, Roman Flyunt, Konstanze Czihal, Helmut Langguth, Reiner Mehnert, Rolf Schubert, Michael R. Buchmeiser, UV curing and matting of acrylate coatings reinforced by nano-silica and micro-corundum particles, Prog. Org. Coat. 2007; 60(2):121-126.

[52] Maganty S, Roma MPC, Meschter SJ, Starkey D, Gomez M, Edwards DG, Elsken AEK, Cho J. Enhanced mechanical properties of polyurethane composite coatings through nanosilica addition, Prog. Org. Coat. 2016; 90:243-251.

[53] Yern Chee Ching, Nurehan Syamimie, Effect of nanosilica filled polyurethane composite coating on polypropylene substrate, J. Nanomater. 2013, 8. https:// doi.org/10.1155/2013/567908. Article ID 567908

[54] Junaidi MUM, Haji Azaman SA, Ahmad NNR, Leo CP, Lim GW, Chan DJC, Yee HM. Superhydrophobic coating of silica with photoluminescence properties synthesized from rice husk ash, Prog. Org. Coat. 2017; 111:29-37.

[55] Madhan Kumar A, Sanjay S Latthe, Sudhagar P, Obot IB, Zuhair M Gasem. Insitu synthesis of hydrophobic SiO2-PMMA composite for surface protective coatings: experimental and quantum chemical analysis, Polymer. 2015; 77:79-86.

[56] Guomin Wu, Di Liu, Jian Chen, Guifeng Liu, Zhenwu Kong, Preparation and properties of super hydrophobic films from siloxane-modified two-component waterborne polyurethane and hydrophobic nano SiO2, Prog. Org. Coat. 2019; 127:80-87.

[57] Ammar Sh, Ramesh K, Ma IAW, Farah Z, Arof AK. Studies on SiO2-hybrid polymeric nanocomposite coatings with superior corrosion protection and hydrophobicity, Surf. Coat. Technol. 2017; 324:536-545.

[58] Hengzhen Chen, Xia Zhang, Pingyu Zhang, Zhijun Zhang. Facile approach in fabricating superhydrophobic SiO2/polymer nanocomposite coating, Appl. Surf. Sci. 2012; 261:628-632.

[59] Baozhong Lin, Shuxue Zhou, Poly (ethylene glycol)-grafted silica nanoparticles for highly hydrophilic acrylic-based polyurethane coatings, Prog. Org. Coat. 2017; 106:145-154.

[60] Tomozawa M, Kim DL, Lou V. Preparation of high purity, low water content fused silica glass, J. Non-Cryst. Solids. 2001; 296:102-106.

[61] Wu G, Wang J, Shen J, Yang T, Zhang Q, Zhou B, Deng Z, Bin F, Zhou D, Zhang F. Properties of sol-gel derived scratch-resistant nano-pourous silica films by mixed atmosphere treatment, J. Non-Cryst. Solids. 2000; 275:169-174.

[62] Bogush GH, Tracy MA, Zukoski CF. Preparation of monodisperse silica particles: control of size and mass fraction, Non-Cryst. Solids. 1988; 104:95-106.

[63] Patel KG, Shettigar RR, Misra NM. Recent advance in silica production technology from agriculture waste straw - Review, J. Adv. Agric. Technol. 2017; 4:274-279.

[64] Ragini P, Dongre R, Meshram J. Preparation of silica powder from rice husk, J. Appl. Chem. 2014, 26-29.

[65] Ghorbani F, Sanati A, Maleki M. Production of silica nanoparticals from rice husk as agricultural waste by environmentaly friendly technique, Environ. Stud. Persian Gulf. 2015; 2:56-65.

[66] Kalapathy U, Proctor A, Shultz J. An improved method for production of silica from rice hull ash, Bioresour. Technol. 2002; 82:285-289.

[67] Yuvakkumara R, Elangoa V, Rajendrana V, Kannan N. High-purity nano silica powder from rice husk using a simple chemical method, J. Exp. Nanosci. 2014; 9:272-281.

[68] Kaupp A, Goss JR. Technical and economical problems in the gasification of rice hulls, Phys. Chem. Prop. Energy Agric. 1981-1982; 1:201–234. https://doi.org/10.1016/0167-5826(81)90019-X

[69] Thi Mai Anh Bui, Thien Vuong Nguyen, Thi Mai Nguyen, Thu Ha Hoang, Thi Thanh Huong Nguyen, Thi Hoan Lai, Thuy Nga Tran, Van Hau Nguyen, Viet Hai Hoang, Trong Lu Le, Dai Lam Tran, Tran Chien Dang, Quoc Trung Vu, Phuong Nguyen-Tri. Investigation of crosslinking, mechanical properties and weathering stability of acrylic polyurethane coating reinforced by SiO2 nanoparticles issued from rice husk ash. Materials Chemistry and Physics. 2020; 241:122445.

[70] Yari H, Moradian S, Tahmasebi N. The weathering performance of acrylic melamine automotive clearcoats containing hydrophobic nanosilica, J. Coat. Technol. Res. 2014; 11(3):351-360.

[71] Saha A, Jiang CM, Martí AA. Carbon nanotube networks on different platforms. Carbon. 2014; 79:1-18.

[72] Rui Dong Lili Liu, Preparation and properties of acrylic resin coating modified by functional graphene oxide. PII: S0169-4332(16)30136-2, Reference: APSUSC 32507, http://dx.doi.org/doi:10.1016/j.apsusc.2016.01.275

[73] Gao SL, Mäder E, Plonka R. Nanocomposite coatings for healing surface defects of glass fibers and improving interfacial adhesion. Compos. Sci. Technol. 2008; 68:2892-2901.

[74] Dashtizadeh A, Abdouss M, Mahdavi H. Acrylic coating exhibiting improved hardness, solvent resistance and glossiness by silica nano-composites. Appl. Surf. Sci. 2011; 257:2118-2125.

[75] Ubong Eduoka, Jerzy Szpunara, Eno Ebenso. Synthesis and characterization of anticorrosion zirconia/acrylic nanocomposite resin coatings for steel. Progress in Organic Coatings. 2019; 137:105337.

[76] Shi X, Nguyen TA, Suo Z, Liu Y, Avci R. Effect of nanoparticles on the anticorrosion and mechanical properties of epoxy coating, Surf. Coat. Technol. 2009; 204:237-245.

Crossref
DOI: 10.31643/2023/6445.45
Metallurgy

Microstructure and tribological study of TiAlCN and TiTaCN coatings

[*1]Bakhytuly N., [1]Kenzhegulov A.K., [2]Nurtanto M., [3]Aliev A.E., [1]Kuldeev E.I.

[1]JSC Institute of Metallurgy and Ore Beneficiation, Satbayev University, Almaty, Kazakhstan
[2]University of Sultan Ageng Tirtayasa, Banten, Indonesia
[3]University of Texas at Dallas, state Texas, USA

[*]Corresponding author email: Nauka-PhD@mail.ru

Received: *January 9, 2023*
Peer-reviewed: *February 13, 2023*
Accepted: *March 24, 2023*

ABSTRACT

The low coefficients of friction and wear rates of transition metal carbonitride make them excellent candidates for friction and wear applications. Coatings based on titanium carbonitride alloyed with Ta and Al were deposited using reactive magnetron sputtering on the surface of titanium VT1-0 and steel AISI 304. The effect of alloying titanium carbonitrides with Ta and Al and acetylene flow during deposition on the structure, composition, and tribological properties of the coating was studied. TiAlCN and TiTaCN coatings were deposited in various acetylene flows along with stable argon and nitrogen flows. Scanning electron microscopy, optical microscopy, X-ray phase analysis, and sliding wear test (ball-on-disk method) in two media were used to study the resulting coatings. The average coefficient of friction of the coating under friction without lubrication varied in the range of 0.13-0.85 and under friction with lubrication in the range of 0.0015-0.081. From the point of view of wear rate, it is shown that the most wear-resistant coating under friction conditions with and without lubrication is TiAlCN-2. The resulting coatings can be useful as protection for machine parts or tools that are subject to friction and wear.

Keywords: titanium carbonitride, magnetron sputtering, alloying, coefficient of friction, wear rate, wear resistance.

Information about authors:

Bakhytuly Nauryzbek — *Ph.D., Researcher, JSC "Institute of Metallurgy and Ore Beneficiation", Satbayev University, st. Shevchenko, 29/133, 050010, Almaty, Kazakhstan. Email: n.bakhytuly@satbayev.university*

Kenzhegulov Aidar Karaulovich — *Ph.D., Researcher, JSC "Institute of Metallurgy and Ore Beneficiation", Satbayev University, st. Shevchenko, 29/133, 050010, Almaty, Kazakhstan. Email: a.kenzhegulov@satbayev.university*

Nurtanto Muhammad — *Ph.D., Researcher, JSC Department of Mechanical Engineering Vocational Education, Faculty of Teacher and Training Education, Sultan Agung Tirtayasa University, Banten, Indonesia, Email: mnurtanto23@untirta.ac.id*

Aliev Ali Enverovich — *Researcher Professor, "Alan MacDiarmid NanoTech Institute", University of Texas at Dallas, state Texas, USA. Email:Ali.Aliev@utdallas.edu*

Kuldeev Erzhan Itemenovich — *Candidate of Geological and Mineralogical Sciences, Vice-Rector for Corporate Development and Strategic Planning, JSC "Institute of Metallurgy and Ore Beneficiation", Satbayev University, st. Shevchenko, 29/133, 050010, Almaty, Kazakhstan. Email: e.kuldeyev@satbayev.university*

Introduction

Hard protective coatings greatly contribute to increasing wear resistance and increasing the service life of components and machine structures that are constantly subjected to mechanical and chemical degradation due to wear processes [[1],[2], [3]]. The use of hard protective coatings such as TiC [4], TiN [5], TiCN [6], TiAlN [7], TiSiC [8], thin multi-layer coatings [9], diamond-like films [[10], [11]], and others are a suitable way to protect machine parts or tools from environmental hazards and wear. In these works, it is noted that coatings based on titanium carbides and nitrides provide good wear resistance due to a combination of ductility and hardness, and high adhesion to the substrate.

To date, various physical and chemical deposition technologies are used to obtain solid protective coatings. There are such methods as magnetron sputtering (MS) [12], cathode sputtering [13], plasma deposition [14], laser methods [15], CVD-based methods [16], and others. Among them, MS is very often used for applying various hard tribological coating based on titanium carbonitride (TiCN) with increased wear resistance. MS provides a low level of impurities and allows easy control of the deposition rate. Several studies of TiCN [[13, [17], [18], [19]] have been carried out to study the tribological properties coatings obtaining by

magnetron sputtering. The advantages of these coatings over other coating materials are associated with their excellent friction characteristics in contact with steel, high hardness, and residual stress [[20], [21]].

To meet the increased requirements for wear-resistant coatings, it is necessary to complicate the composition of the coating more and more, using metal alloying additives. To improve the tribological properties of TiCN coatings, alloying with such metals as Al, Ag, O, Zr, Cr, etc. is carried out [[7], [22], [23]]. Srinath M.K. and colleagues [1] reported that TiCN-coated Al-7075 heat-treated at 500°C for 1 hour gives good results in terms of wear resistance and corrosion resistance. Recently, in [22], the authors reported that the addition of Ag to the TiCN coating can improve friction and wear resistance at room and elevated temperatures. In [20], the surface and tribological parameters of Ti(C,O,N) coatings were analyzed and discussed depending on the composition and structural features of the films, as well as their thickness. In our previous work [23], the tribological and corrosion properties of TiCN coatings doped with Cr and Zr were studied. The combined results of this work showed the most preferable composition, the $Ti_{21}Zr_{12}C_{35}N_{32}$ (TiZrCN-1) coating, which is resistant to wear and corrosion damage.

To date, a lot of data has been published on the efficient use of magnetron sputtering for the deposition of wear-resistant alloyed TiCN coatings. At the same time, information on the analysis of the wear characteristics of TiAlCN and TiTaCN coatings is very limited. Only a few works are devoted to the analysis of TiAlCN coatings, and there is even no work on the analysis of TiTaCN coatings. In this regard, it seems interesting to study the effect of doping with Al and Ta on the tribological characteristics of TiAlCN and TiTaCN coatings.

Materials and methods

Substrate preparation and coating process

The TiAlCN and TiTaCN coatings were deposited in a 100 kHz pulsed DC MS system. The distance between the target and the substrate holder was kept constant and equal to 30 cm. Composite targets were fabricated for the deposition of TiAlCN and TiTaCN coatings. To do this, an alloying element in the form of 3 disks of aluminum and tantalum was welded onto the sputtered surface of a VT1-0 titanium target. Three disks of aluminum and tantalum were welded onto the surface of the titanium target. Well-polished disks (Ø 58 mm) made of VT1-0 titanium and AISI 304 steel were used as substrates. When preparing the surface of the substrates for deposition, grinding with sandpaper, four-stage polishing with diamond paste and ion cleaning in a vacuum were used, which is described in detail. in [[19], [23]]. Before deposition, the chamber was evacuated to a base pressure below $3 \cdot 10^{-3}$ Pa. Scheme of the process of preparing the substrate and coating deposition shows in figure 1. The MS facility is equipped with an APEL-IS-21CELL ion source (Applied Electronics, Tomsk, Russia) and APELMRE100 magnetrons (Applied Electronics, Tomsk, Russia). The potential shift to the substrate was fixed at -70 V, which was supplied using an APEL-M-5PDC power supply (Applied Electronics, Tomsk, Russia). This potential value was chosen based on the results described in our earlier published work [19]. The flow rate of the inert and reactive gas was controlled using RRG-12 flowmeters (Eltochpribor, Moscow, Russia). Previously, composite targets were worked out to clean the surface from unwanted contaminants. The deposition parameters of all obtained coatings are presented in Table 1.

Table 1 - Magnetron sputtering parameters for the obtained coatings

Coating	Coating deposition parameters				
	Chamber pressure, Pa	Plasma current, A	Flow of inert and reactive gas, sccm	Substrate bias, V	Deposition time, min
TiAlCN-1	0.45	2	Ar = 18; C_2H_2 = 3.4; N_2 = 3	-70 V	120
TiAlCN-2	0.45	2	Ar = 18; C_2H_2 = 4.6; N_2 = 3	-70 V	120
TiTaCN-1	0.45	2	Ar = 18; C_2H_2 = 3.4; N_2 = 3	-70 V	120
TiTaCN-2	0.45	2	Ar = 18; C_2H_2 = 4.6; N_2 = 3	-70 V	120

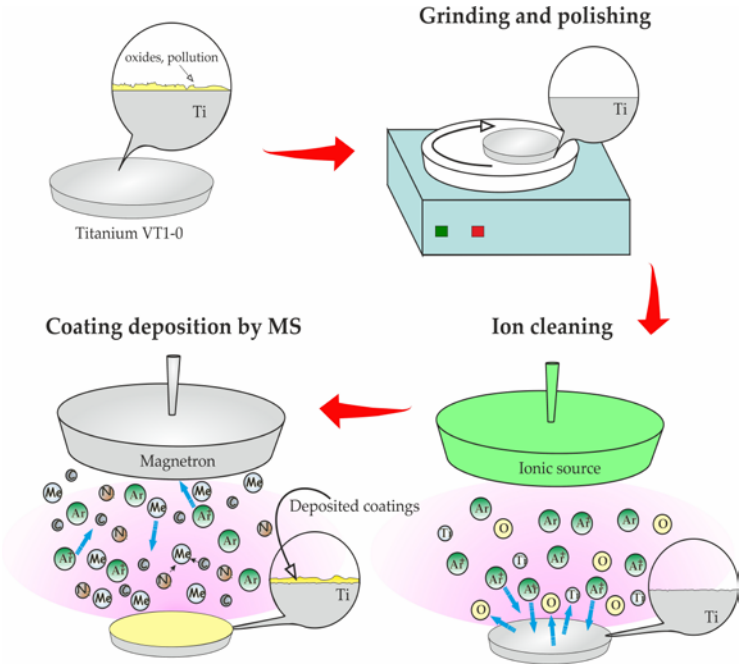

Figure 1 – Scheme of the process of preparing the substrate and coating deposition.

Morphology and composition of coatings

The surface morphology of the coating was studied by scanning electron microscopy (SEM). For these purposes, an electron microscope model JXA-8230 (JEOL, Tokyo, Japan) with an accelerating voltage of 25 kV and an electron beam current of up to 7 nA was used. All selected coatings were studied in the backscattered electron mode (COMPO). The elemental composition of the coating was analyzed by energy dispersive X-ray analysis (EDX) over the surface area of the coating 40 × 40 μm^2 at ×2000 magnification.

Optical microscopy was used to check the coating thickness. Micrographs were taken with a Leica DM IRM optical microscope (Leica, Wetzlar, Germany). The thickness of the coatings was measured in several areas at least 20 times. In the work, the average thickness of each coating was given.

The phase composition and crystal structure of the coating were determined on a D8 Advance diffractometer (BRUKER, Karlsruhe, Germany) with α-Cu radiation (λ ≈ 1.54 Å). Radiography was performed with focusing according to the Bragg–Brentano method. The diffraction patterns were recorded in the range of angles 2θ: 20–90° with a step of 0.05°, a shooting rate of 2 deg/min at a voltage of 35 kV and a current of 20 mA. The PDF 2 database was used for phase analysis.

Tribological tests

To measure the tribological characteristics of TiAlCN and TiTaCN, coatings were deposited on the surface of a substrate made of VT1-0 titanium and AISI 304 steel with a diameter of 58 mm. The tribological characteristics of the coatings were measured in the ball-on-disk sliding friction mode on a TRB^3 tribometer (CSM Instruments, Pese, Switzerland) at room temperature in friction conditions with and without lubrication. Test parameters in friction without lubrication: speed of movement of the sample surface relative to the counterbody – 1 cm/s, load – 2 N, the radius of the wear track – 4 mm, friction path – 300 m, data acquisition rate – 50 Hz, a ball of Si_3N_4 was used as a counterbody 6 mm in diameter.

Under lubricated friction conditions, TM-5-18 API GL-5 gear oil was used. Test parameters in friction with lubrication: speed of movement of the sample surface relative to the counterbody – 1 cm/s, load – 5 N, the radius of the wear track – 27 mm, friction path – 17500 m (200000 cycles), data acquisition rate – 50 Hz, as a counterbody a ball made of steel grade ShH15 (SUJ2) with a diameter of 3 mm was used. Test conditions are following international standards ASTM G99-959. The wear given in the work was calculated from the volumetric wear of the coatings during tribological tests. To do this, using a profilometer brand 130

(Proton, Zelenograd, Russia) measured the cross-sectional area of the wear track. Next, the wear rate was calculated according to formulas 1 and 2. Quantitatively, the loss of volume during wear is carried out according to the formula:

• sample volume loss, (mm^3)

$$\Delta V = S \cdot l \quad (1)$$

The wear I given in the work was calculated using the volume loss during the test ΔV for the values of the run N and the applied load P:

$$I = \Delta V / N \cdot P \quad (2)$$

Optical microscopy was used to take pictures of the wear tracks after the tribological test.

Research results

Morphology and composition of coatings

The surface morphology of the coating and the thickness of the coatings was measured by SEM and optical microscopy, respectively. Figure 2 shows that the coating material was evenly distributed over the surface of the steel substrate. The morphology of the coatings has a smooth and dense structure without visible chips and cracks. It can be seen from the image that dome-shaped nuclei are locally located on the surface of the samples. All deposited MS coatings showed a similar surface structure, and no significant changes were observed after alloying with aluminum and tantalum. According to the results of optical microscopy, it was determined that the TiAlCN-1, TiAlCN-2, TiTaCN-1, TiTaCN-2 coatings have an average thickness of 2.30, 1.40, 2.56, and 2.23 µm, respectively. When coatings are deposited in an acetylene flow of 3.4 sccm, the thicknesses of the coatings are approximately similar in both cases (2.30 and 2.56 µm), while at a flow of 4.6 sccm, the difference is noticeably greater (1.40 and 2.23 µm). One of the reasons for these changes in thickness is the sputtering coefficients of aluminum and tantalum under the action of working gas ions.

Table 2 shows the composition of the TiAlCN and TiTaCN coatings deposited at different flows of the reaction gases of acetylene and nitrogen. The concentration of Al and Ta in the deposited coatings undergoes insignificant changes in the range from ~ 4.8 to 6.7 at. %. Also, titanium in all coatings

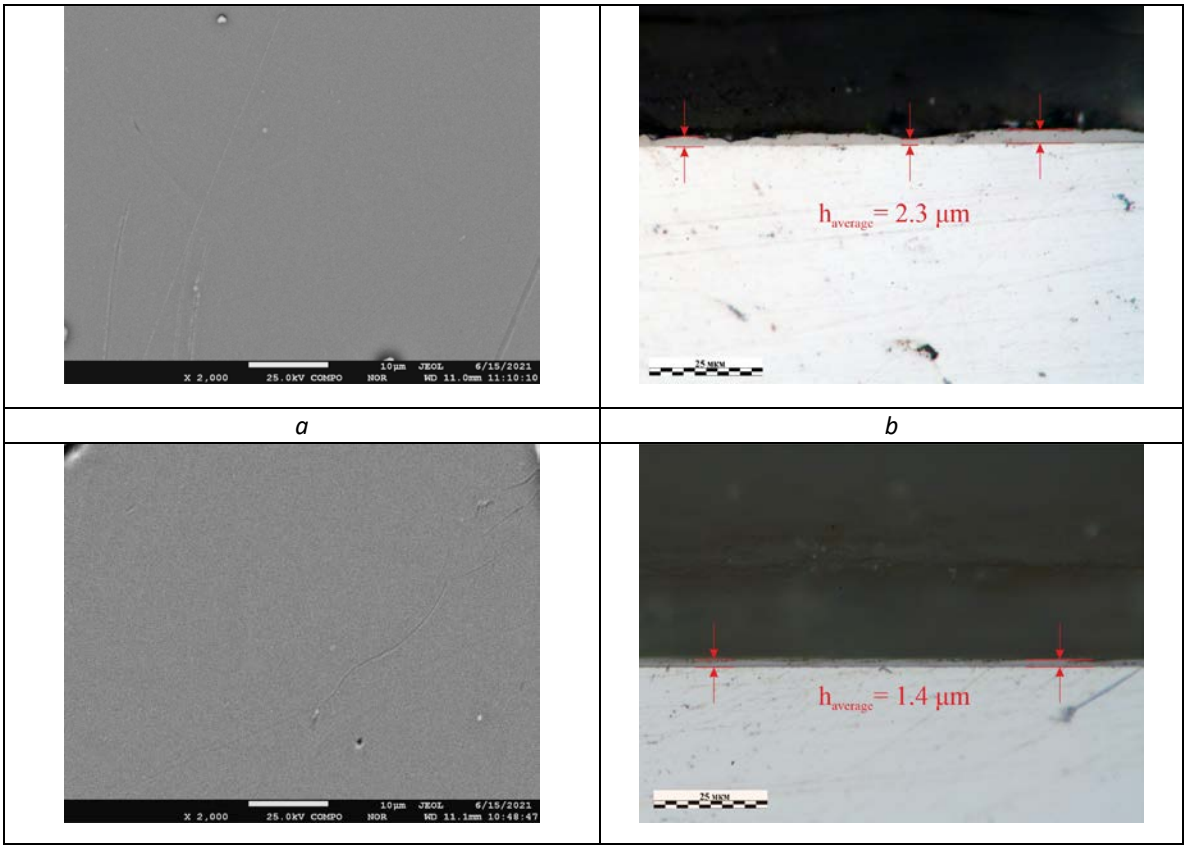

a *b*

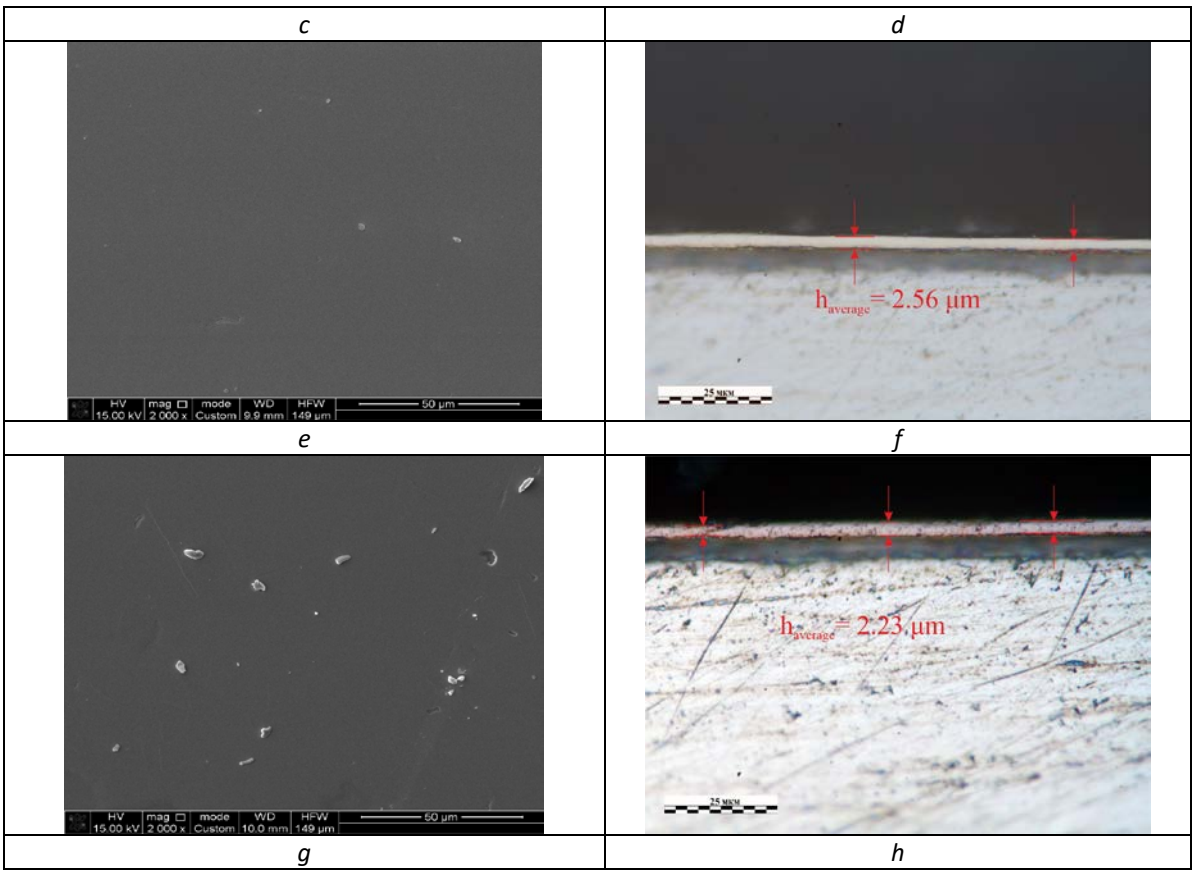

Figure 2 – SEM images of the morphology and optical images of the thickness of the cross sections of samples: (a) TiAlCN-1 surface, (b) TiAlCN-1 thickness, (c) TiAlCN-2 surface, (d) TiAlCN-2 thickness, (e) surface TiTaCN-1, (f) TiTaCN-1 thickness, (g) TiTaCN-2 surface, (h) TiTaCN-2 thickness

Table 2 - Elemental composition and (C+N)/(sum of metals) of deposited coatings

Coating	Elemental composition of deposited coatings, at.%					(C+N)/(sum of metals)
	Ti	Al	Ta	C	N	
TiAlCN-1	31.6	4.8	–	21.1	42.5	1.75
TiAlCN-2	36.7	5.5	–	29.9	27.9	1.37
TiTaCN-1	32.9		6.7	19.5	40.9	1.84
TiTaCN-2	31.5		6.4	24.5	37.6	1.97

showed only small changes in the region of 31-37 at. %. It is interesting to note that carbon content only in the TiAlCN-2 coating is closer to 30 at. %, in other coatings it is stable within 19-24 at. %, this in turn has the opposite effect on nitrogen. The ratio (C+N)/(sum of metals) for TiAlCN coatings decreases from 1.75 to 1.37 with increasing acetylene flow, and in the case of TiTaCN coating, it increases from 1.84 to 1.97.

The phase composition of the deposited coatings was analyzed using X-ray phase analysis. Figure 3 shows the results of the analysis of all obtained coatings. As shown in the X-ray diffraction patterns, the TiAlCN coatings consist of several phases with preferred orientations in the [100] and [200] directions, and in the case of TiTaCN coatings, in the direction [111] and [200]. In TiAlCN coatings, X-ray diffraction patterns show peaks of carbonitride and nitride phases, such as Ti_2CN, $TiC_{0.5}N_{0.12}$, $(TiN)_{0.96}$, $Ti_2Al(N_{0.5}C_{0.5})$ and $Ti(C_{0.25}N_{0.75})$. In the TiTaCN coatings, phases consisting of $Ta_{0.47}Ti_{0.53}N_{0.47}C_{0.53}$, $TiC_{0.496}N_{0.502}$, $TaTiN_2$, $(TaTi)C_2$ and $TaC_{0.7}N_{0.3}$were identified in the X-ray diffraction patterns. As the rate of C_2H_2 flow into the TiTaCN-2 coating increases, an additional peak appears, indicating the presence of the $(TaTi)C_2$ phase.

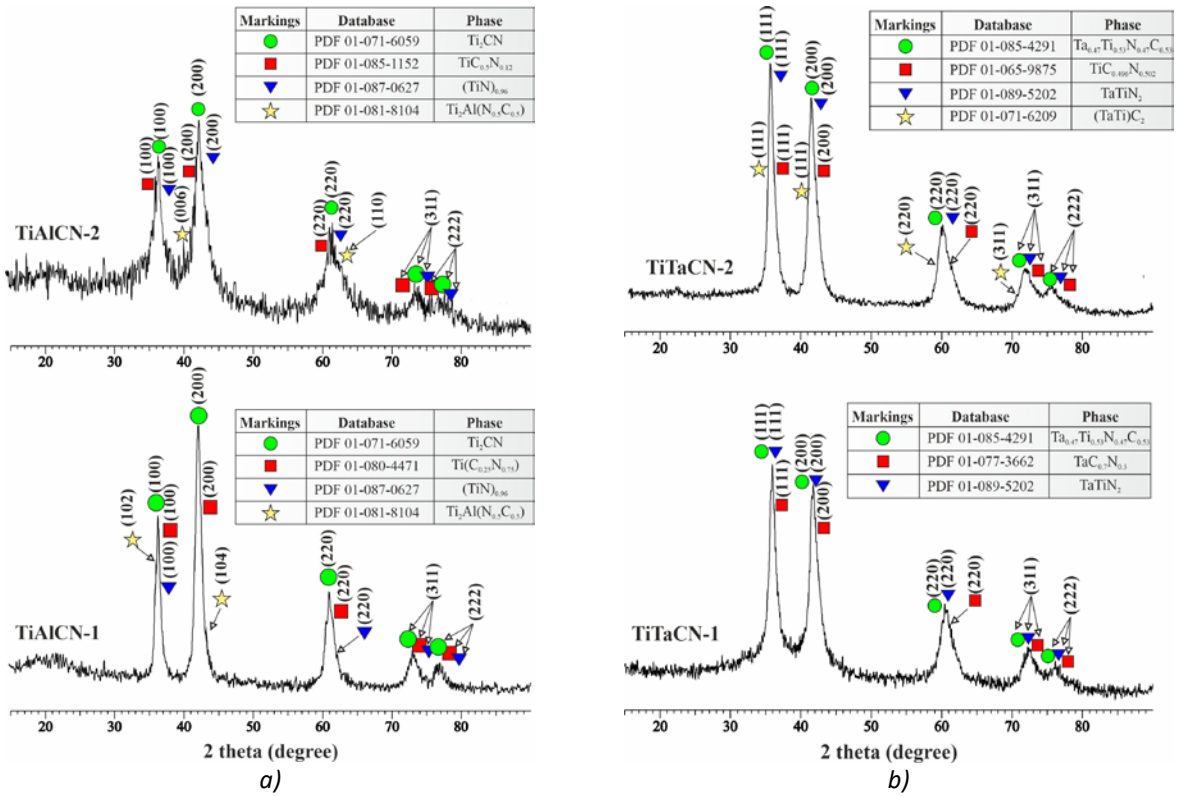

Figure 3 - Results of phase analysis of coatings: (*a*) TiAlCN, (*b*) TiTaCN

Tribological testing of coatings

The friction wear test was performed under friction conditions with and without lubrication. According to friction conditions without lubrication, where the coatings were tested on the surface of a titanium substrate with a diameter of 58 mm. Figure 4 shows the coefficient of friction (CoF) plots with the averaged value of all deposited TiAlCN and TiTaCN coatings obtained at different flows of carbon-containing gas. The TiAlCN-2 coating shows the lowest and most stable CoF compared to other coatings. TiAlCN-1 and TiTaCN-2 coatings in the friction area from 0 to 150 m are characterized by an increase in CoF and then CoF becomes stable.

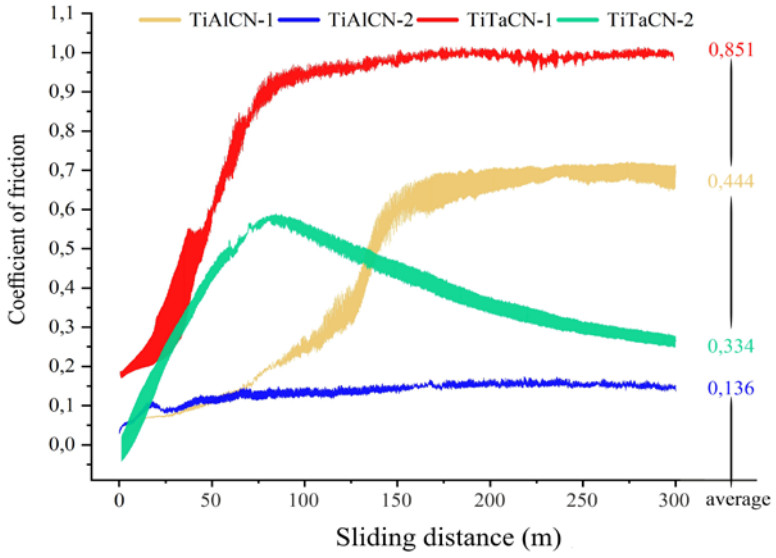

Figure 4 - CoF coatings with an average value obtained under friction conditions without lubrication

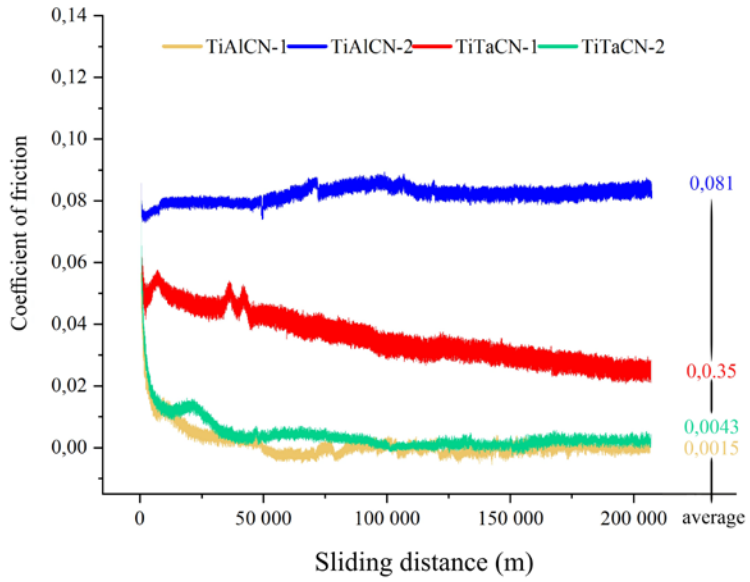

Figure 5 - CoF coatings with an average value obtained under friction conditions with lubrication

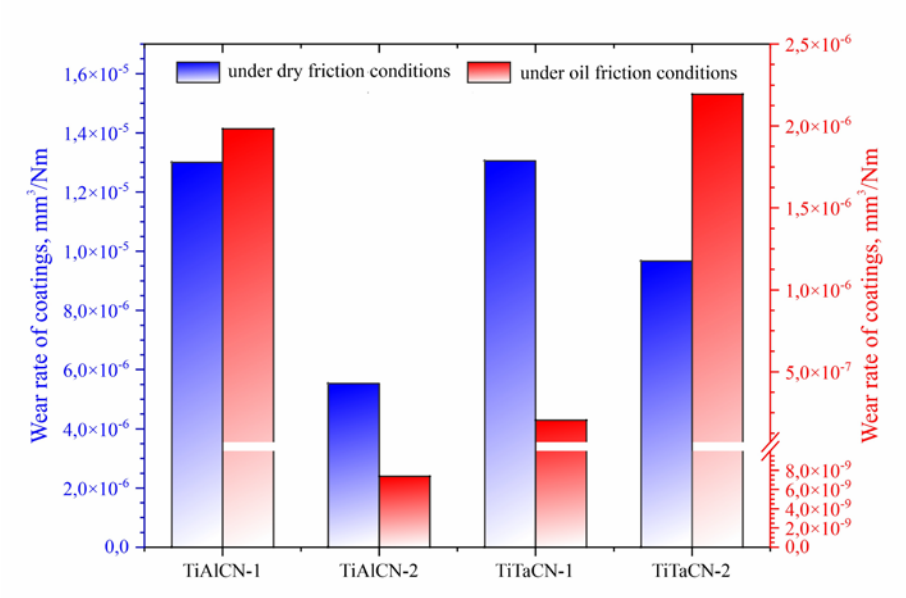

Figure 6 - Wear rates of the studied coatings in two friction conditions

In the case of testing under lubricated friction conditions, very low CoFs were recorded. The results of these tests are presented in Figure 5, where the coatings were tested on the surface of a steel substrate with a diameter of 58 mm. TiAlCN-1 and TiTaCN-2, which had CoF of 0.0015 and 0.0043, had the smallest CoF among the studied coatings. After them, there is a coating of TiTaCN-1. The TiAlCN-2 coating had the highest CoF value of 0.081, although this coating under friction condition without lubrication showed the best result with a low CoF. In general, when the friction test enters a relatively stable stage, all coatings show a stable CoF value with rare small fluctuations.

Figure 6 shows the wear rates of all coatings under frictional wear conditions with and without lubrication. To compare the results, the wear test of the coatings in each medium was carried out under the same conditions in the ball-on-disk system. The results under friction conditions without lubrication show a spread in wear rate (WR) from 5.5×10^{-6} to 1.3×10^{-5} mm^3/Nm. When tested under friction conditions with lubrication, the coatings wore out much lower due to the lubricating medium with WR

from 7.4×10^{-9} to 2.2×10^{-6} mm^3/Nm. In the case of the TiAlCN coating, WR decreases with an increase in the carbon content in the TiAlCN coatings due to an increase in the C_2H_2 flux during the deposition process and reaches the lowest value among the studied coatings (7.4×10^{-9} mm^3/Nm). With respect to TiTaCN coatings, WR increases with an increase in the carbon content in the composition. This was probably caused by the low hardness of the TiTaCN-2 coating.

Research discussions

An increase in the acetylene flow from 3.4 to 4.6 sccm leads to an increase in the carbon concentration and a change in nitrogen composition in the deposited coatings. The interaction between C and N atoms can also contribute to a nonlinear change in the C content, as described in [[24], [25]]. It is known that the ratio (C + N)/(sum of metals) should tend to 1, however, there are works where the ratio is higher than unity. In particular, in our previous work [23], a TiZrCN coating with a (C+N)/(Ti+Zr) ratio of 2.04 characterized by the highest wear resistance among the studied coatings. Also, other works show high abrasion resistance of coatings with a ratio greater than one: (C+N)/(Ti+Al) up to 1.75 [26], (C+N)/(Zr+Hf) [27] up to 3.1.

The phase composition of the TiAlCN-1 and TiAlCN-2 coatings differs in that $Ti(C_{0.25}N_{0.75})$ transforms into $TiC_{0.5}N_{0.12}$ as the C_2H_2 flow rate increases due to the difference in the elemental composition. In addition, the half-width of the peaks shows that with an increase in the carbon content, the probability of the formation of an amorphous phase increases, which contributes to a decrease in crystallinity. If the concentration of C exceeds its solid state solubility in the crystalline phase, excess C will begin to form a carbon-rich amorphous phase [28]. In the case of TiTaCN, no broadening of the half-width of the peaks is observed, i.e., there is no decrease in the crystallinity of the coating, as in TiAlCN-2. Apparently, the carbon content was not excessive (24.5 at %) for the formation of a carbon-rich amorphous phase.

As can be seen from the friction results without lubrication, the TiAlCN-2 coating has the lowest and most stable CoF compared to the other coatings, indicating that this coating has low friction resistance [[29-32]]. In addition, low CoF can be associated with the formation of debris in the wear track, which leads to the subsequent formation of a lubricating transition layer, mainly due to an increase in carbon sp^2 [33]. Moreover, the elemental and phase composition of this coating has the highest carbon content. With the TiTaCN-2 coating, one can observe a significant increase at the beginning of the test and a subsequent gradual drop in CoF, which is related to the run-in period. The running-in period can be characterized by grinding of the roughness peaks on the coating surfaces [[34], [35]]. A possible reason for the sharp increase in CoF for TiAlCN-1 and TiTaCN-2 coatings may be related to the onset of the degradation process, although no serious damage to the coating was observed after testing. Summarizing the results of CoF, we can say that an increase in the acetylene flow during the deposition of carbonitride films leads at least to a decrease in CoF in friction without lubrication. The presence of amorphous carbon in composite films can significantly reduce the friction coefficient [36].

In the case of testing under friction conditions with lubrication, CoF has significantly lower values compared to the results of CoF in conditions without lubrication. Such a difference in the results depends on many factors: tribochemical processes during abrasion, counterbody material, lubricating medium, load, etc. As a rule, the friction parameters on the contact surface is largely determined by the physical state of the contact surface and the chemical interactions between the sliding surfaces and the environment. medium [37]. As can be seen in Figures 4 and 5, the frictional behavior of the deposited coatings under friction conditions without lubrication was more unstable with sharp jumps or a decrease in CoF after running in, and under friction conditions with lubrication, CoF of tribo-pairs showed the most stable performance with small jumps.

It has been determined that an increase in the C_2H_2 flow during MS deposition leads to a decrease in the WR of the coating. Since, according to the graph in Figure 6, it can be seen that the TiAlCN-2 and TiTaCN-2 coatings have low WR in friction without lubrication compared to the results of the TiAlCN-1 and TiTaCN-1 coatings. One of the reasons for the decrease in WR with an increase in the carbon content in the coatings can be associated with formation of a thin lubricating tribolayer formed upon contact of friction bodies. This is

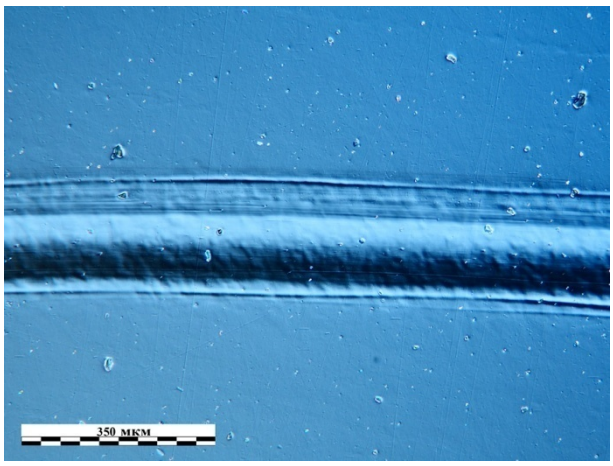

Figure 7 - Deformation of the surface of the substrate coated with TiAlCN-2 after a friction test with lubrication

mainly due to the increase in carbon sp^2 [33]. In a tribological test with respect to steel ShKh15 (SUJ2) under lubricated friction conditions, the deposited coatings showed completely different WR results compared to the test without lubrication. When sliding along a steel ball-coating scheme, the change in the tribological characteristics of the coatings was strongly influenced by the difference in hardness between the ball and the coating. In most cases, in the wear track, the coating was "punched" along with the surface of the substrate material. Figure 7 shows the local deformation caused by the action of the counterbody on the surface of the substrate through the coating, which occurred when testing the TiAlCN-2 coating with lubrication.

Summarizing the results of tribological testing in the two studied mediums, we can say that after the completion of the tests, no obvious destruction of the deposited coatings was observed. The clear favorite among all obtained coatings is the TiAlCN-2 coating with WR 7.4×10^{-9} mm^3/Nm under friction conditions with lubrication and 5.5×10^{-6} mm^3/Nm under friction conditions without lubrication. The difference and scatter of all wear rate results can also be related to the thickness of the coating. As is known that with an increase in the thickness of the coating of the resulting MS, the adhesion strength to the substrate decreases, which negatively affects the tribological characteristics. But the residual stress of the resulting coatings can also be of great importance, even if they cannot be quantified for the studies given. Thus, Al alloying of titanium carbonitride coatings can increase the service life of machine parts and mechanisms operating under friction and wear conditions than Ta alloying. Although it should be noted that the TiTaCN-1 coating also had good wear resistance.

Conclusions

In this work, TiAlCN and TiTaCN coatings were deposited by reactive magnetron sputtering in an argon-acetylene-nitrogen atmosphere. The carbon content of the coatings varied with the acetylene flow, which in turn affected the nitrogen content. The resulting coatings had a dense structure with thicknesses from 1.4 to 2.5 μm with a stoichiometric ratio (C+N)/(sum of metals) from 1.37 to 1.97. It has been determined that carbonitride phases are formed in TiAlCN coatings with preferential orientation in the [100] and [200] directions and the case of TiTaCN coatings [111] and [200] directions. The average coefficient of friction of the coating under friction without lubrication varied in the range of 0.13-0.85 and under friction with lubrication in the range of 0.0015-0.081. It has been established that an increase in the flow of acetylene during the deposition of TiAlCN and TiTaCN coatings leads at least to a decrease in CoF and WR during friction without lubrication. In the case of tribological testing under lubricated friction conditions, it was found that an increase in the carbon content in the TiAlCN coatings due to an increase in the C_2H_2 flux during the deposition process contributes to a decrease in WR. In relation to TiTaCN coatings, WR increases, probably due to the low hardness of the coating and insufficient content of carbon amorphous phases.

Thus, alloying titanium carbonitride (TiAlCN-2) coatings with aluminum can increase the service life of parts of machines and mechanisms operating under friction conditions, since such coatings

showed the least result in terms of wear rate (7.4 × 10^{-9} mm^3/Nm under lubricated friction conditions and 5.5 × 10^{-6} mm^3/Nm under friction conditions without lubrication) and low coefficients of friction.

Funding: This research was funded by the Science Committee of the Ministry of Education and Science of the Republic of Kazakhstan, Grant No. AP19576642.

Cite this article as: Bakhytuly N, Kenzhegulov AK, Nurtanto M, Aliev AE, Kuldeev EI. Microstructure and tribological study of TiAlCN and TiTaCN coatings. Kompleksnoe Ispolzovanie Mineralnogo Syra = Complex Use of Mineral Resources. 2023; 327(4):99-110. https://doi.org/10.31643/2023/6445.45

TiAlCN және TiTaCN жабындарының микроқұрылымы мен трибологиялық зерттеуі

[1]Бахытулы Н., [1]Кенжегулов А.К., [2]Нуртанто М., [3]Алиев А.Э., [1]Кульдеев Е.И.

[1]Металлургия және кен байыту институты АҚ, Сәтбаев университеті, Алматы, Қазақстан
[2]Султан Агунг Тиртаяса университеті, Бантен, Индонезия
[3]Техас университеті Даллас қаласындағы, штат Техас, АҚШ

Мақала келді: *9 қаңтар 2023*
Сараптамадан өтті: *13 ақпан 2023*
Қабылданды: *24 наурыз 2023*

ТҮЙІНДЕМЕ

Өтпелі металл карбонитридтерінің үйкеліс пен тозу жылдамдығы коэффициенттерінің төмен болуы, оларды механикалық үйкеліс пен тозу саласында қолдануда таптырмас материал етеді. Та және Al легірленген титан карбонитридіне негізделген жабындар титан VT1-0 және AISI 304 бетінде реактивті магнетронды шашырату арқылы тозаңдатылды. Жабындының құрылымына және құрамына, трибологиялық қасиеттеріне титан карбонитридін Та және Al қоспаларымен легірлеу және тозаңдату кезінде ацетилен ағынының әсерлері зерттелді. TiAlCN және TiTaCN жабындары тұрақты аргон және азот ағындарымен бірге әртүрлі ацетилен ағындарында тозаңдатылды. Алынған жабындарды зерттеу үшін сканерлеуші электронды микроскопия, оптикалық микроскопия, рентгендік фазалық талдау және екі ортадағы сырғымалы тозу сынағы (дисктегі шар әдісі) қолданылды. Құрғақ үйкеліс жағдайында жабынның орташа үйкеліс коэффициенті 0,13-0,85 және майлы үйкеліс жағдайында 0,0015-0,081 аралығында өзгерді. Тозу жылдамдығы тұрғысынан TiAlCN-2 ауада және майлы ортада тозуға ең төзімді жабын екені анықталды. Алынған жабындар үйкеліс пен тозуға ұшырайтын машина бөлшектерінің немесе құралдардың қорғанышы ретінде пайдалы болуы мүмкін.

Түйін сөздер: титан карбонитриді, магнетронды шашырату, легірлеу, үйкеліс коэффициенті, тозу жылдамдығы, тозуға төзімділік.

Информация об авторах:

Бахытұлы Наурызбек *Ғылыми қызметкер, «Металлургия және кен байыту институты» АҚ, Сәтбаев университеті, Алматы, Қазақстан. Email: n.bakhytuly@satbayev.university*

Кенжегулов Айдар Караулович *PhD, Ғылыми қызметкер, «Металлургия және кен байыту институты» АҚ, Сәтбаев университеті, Алматы, Қазақстан. Email: a.kenzhegulov@satbayev.university*

Нуртанто Мухаммад *Ph.D., Ғылыми қызметкер, Машина жасау кәсіптік білім беру департаменті АҚ, Педагогикалық және біліктілікті арттыру факультеті, Султан Агунг Тиртаяса университеті, Бантен, Индонезия. Email: mnurtanto23@untirta.ac.id*

Алиев Али Энверович *Зерттеуші Профессор, «Алан МакДиармид атындағы Нанотех Институты», Техас университеті Даллас қаласындағы, штат Техас, АҚШ. Email: Ali.Aliev@utdallas.edu*

Кульдеев Ержан Итеменович *Геология-минералогия ғылымдарының кандидаты, Корпоративтік даму және стратегиялық жоспарлау жөніндегі проректоры, «Металлургия және кен байыту институты» АҚ, Сәтбаев университеті, Алматы, Қазақстан. Email: e.kuldeyev@satbayev.university*

Микроструктура и трибологическое исследование покрытий TiAlCN и TiTaCN

[1]Бахытулы Н., [1]Кенжегулов А.К., [2]Нуртанто М., [3]Алиев А.Э., [1]Кульдеев Е.И.

[1]АО «Институт металлургии и обогащения», Satbayev University, Алматы, Казахстан
[2]Университет Султана Агунг Тиртаяса, Бантен, Индонезия
[3]Техасский Университет в Далласе, штат Техас, США

Поступила: *9 января 2023*
Рецензирование: *13 февраля 2023*
Принята в печать: *24 марта 2023*

АННОТАЦИЯ

Низкие коэффициенты трения и скорости износа карбонитридов переходных металлов делают их отличными кандидатами для применения в областях трения и износа. Покрытия на основе карбонитрида титана легированные Ta и Al были нанесены с использованием метода реактивного магнетронного распыления на поверхность титана ВТ1-0 и AISI 304. Исследовано влияние легирования карбонитрида титана Ta и Al и потока ацетилена в процессе осаждения на структуру, состав и трибологические свойства покрытия. Осаждались TiAlCN и TiTaCN покрытия в разных потоках ацетилена наряду со стабильными потоками аргона и азота. Для исследования полученных покрытий использовались сканирующая электронная микроскопия, оптическая микроскопия, рентгенофазовый анализ и испытание на износ при скольжении (метод шар на диске) в двух средах. Средний коэффициент трения покрытия в условиях сухого трения варьировалась в диапазоне 0.13-0.85 и в условиях маслянного трения в диапазоне 0.0015-0.081. С точки зрения скорости износа показано, что наиболее износостойким покрытием на воздухе и в масленной среде является TiAlCN-2. Полученные покрытия могут быть полезны в качестве защиты для деталей машин или инструментов, которые подвергаются к трению и износу.

Ключевые слова: карбонитрид титана, магнетронное распыление, легирование, коэффициент трения, скорость износа, износостойкость.

Информация об авторах:

Бахытулы Наурызбек
PhD, Научный сотрудник, АО «Институт металлургии и обогащения», Satbayev University, Алматы, Казахстан. Email: n.bakhytuly@satbayev.university

Кенжегулов Айдар Караулович
PhD, Научный сотрудник, АО «Институт металлургии и обогащения», Satbayev University, Алматы, Казахстан. Email: a.kenzhegulov@satbayev.university

Нуртанто Мухаммад
PhD, Научный сотрудник, АО Департамент профессионального образования в области машиностроения, факультет педагогического и профессианольного образования, Университет Султана Агунг Тиртаяса, Бантен, Индонезия. Email: mnurtanto23@untirta.ac.id

Алиев Али Энверович
Исследователь Профессор, «Институт НаноТех им. Алан МакДиармид», Техасский Университет в Далласе, штат Техас, США. Email: Ali.Aliev@utdallas.edu

Кульдеев Ержан Итеменович
Кандидат геолого-минералогических наук, Проректор по корпоративному развитию и стратегическому планированию, АО «Институт металлургии и обогащения», Satbayev University, Алматы, Казахстан. Email: e.kuldeyev@satbayev.university

References

[1] Srinath MK, Ganesha MSP. Wear and corrosion resistance of titanium carbo-nitride coated Al-7075 produced through PVD. Bulletin of Material Science. 2020; 43:1-11. https://doi.org/10.1007/s12034-020-2069-9

[2] Ramazanova JM, Zamalitdinova MG. Physical and mechanical properties investigation of oxide coatings on titanium. Kompleksnoe Ispolzovanie Mineralnogo Syra = Complex Use Mineral Resources. 2019; 2:34-41. https://doi.org/10.31643/2019/6445.14

[3] Yeshmanova GB, Smagulov DU, Blawert C. Plasma electrolytic oxidation technology for producing protective coatings of aluminum alloys. Kompleksnoe Ispolzovanie Mineralnogo Syra = Complex Use of Mineral Resources. 2021; 317(2):78-93. https://doi.org/10.31643/2021/6445.21

[4] Kopf A, Haubner R, Lux B. Double-layer coatings on WC-Co hard metals containing diamond and titanium carbide/nitride. Diamond and Related Materials 2000; 9:494-501. doi:10.1016/s0925-9635(00)00214-4

[5] Matei AA, Pencea I, Branzei M, Tranca DE, et all. Corrosion resistance appraisal of TiN, TiCN and TiAlN coatings deposited by CAE-PVD method on WC-Co cutting tools exposed to artificial sea water. Applied Surface Science. 2015; 358:572-578. doi:10.1016/j.apsusc.2015.08.041

[6] Su JF, Yu D, Nie X, Hu H. Inclined impact-sliding wear tests of TiN/Al2O3/TiCN coatings on cemented carbide substrates. Surface and Coatings Technology. 2011; 206:1998-2004. doi:10.1016/j.surfcoat.2011.09.067

[7] Gil LE, Liscano S, Goudeau P, Le Bourhis E, et all. Effect of TiAlN PVD coatings on corrosion performance of WC–6%Co. Surface Engineering. 2010; 26:562-566. doi:10.1179/174329408x326399

[8] Rakhadilov B, Buitkenov D, Idrisheva Z, Zhamanbayeva M, Pazylbek S, Baizhan D. Effect of Pulsed-Plasma Treatment on the Structural-Phase Composition and Tribological Properties of Detonation Coatings Based on Ti-Si-C. Coatings. 2021; 11:795-806. doi:10.3390/coatings11070795

[9] Iwai Y, Nanjo Y, Okazaki K, Tao M, Sentoku E. Application of Micro Slurry-Jet Erosion (MSE) for the Evaluation of Surface Properties of PVD TiN / TiCN Two-Layer Coatings. Tribology Online. 2017; 12(2):49-57.

[10] Zhang D, Shen B, Sun F. Study on tribological behavior and cutting performance of CVD diamond and DLC films on Co-cemented tungsten carbide substrates. Applied Surface Science. 2010; 256:2479-2489. doi:10.1016/j.apsusc.2009.10.092

[11] Mansurov B, Medyanova B, Kenzhegulov A, Partizan G, Zhumadilov B, Mansurova M, Koztayeva U, Lesbayev B. Investigation of microdiamonds obtained by the oxygen-acetylene torch method. Eurasian Chemico-Technological Journal. 2017; 19:163-167. doi:10.18321/ectj647

[12] Razmi A, Yesildal R. Microstructure and mechanical properties of TiN/TiCN/TiC multilayer thin films deposited by magnetron sputtering. International Journal of Innovative Research and Reviews. 2021; 5:15-20. doi: 10.20944/preprints201807.0127.v1

[13] Matei AA, Pencea I, Stanciu SG, Hristu R, Antoniac I, Ciovica (Coman) E, Sfat CE, Stanciu GA. Structural characterization and adhesion appraisal of TiN and TiCN coatings deposited by CAE-PVD technique on a new carbide composite cutting tool. Journal of Adhesion Science and Technology. 2015; 29:2576-2589. doi:10.1080/01694243.2015.1075857

[14] Zhu L, He J, Yan D, Liao H, Zhang N. Oxidation behavior of titanium carbonitride coating deposited by atmospheric plasma spray synthesis. Journal of Thermal Spray Technology. 2017; 26(7):1701-1707. doi:10.1007/s11666-017-0620-z

[15] Yang Y, Guo N, Li J. Synthesizing, microstructure and microhardness distribution of Ti–Si–C–N/TiCN composite coating on Ti–6Al–4V by laser cladding. Surface and Coatings Technology. 2013; 219(12):1-7. doi:10.1016/j.surfcoat.2012.12.038

[16] Zhang J, Xue Q, Li S. Microstructure and corrosion behavior of TiC/Ti(CN)/TiN multilayer CVD coatings on high strength steels. Applied Surface Science. 2013; 280:626-631. doi:10.1016/j.apsusc.2013.05.037

[17] Lou J, Gao Z, Zhang J, He H, Wang X. Comparative investigation on corrosion resistance of stainless steels coated with titanium nitride, nitrogen titanium carbide and titanium-diamond-like carbon films. Coatings. 2021; 11:1543. doi:10.3390/coatings11121543

[18] Mamaeva AA, Kenzhegulov AK, Panichkin AV, Kshibekova BB, Bakhytuly N. Deposition of carbonitride titanium coatings by magnetron sputtering and its effect on tribo-mechanical properties. Kompleksnoe Ispolzovanie Mineralnogo Syra = Complex Use of Mineral Resources. 2022; 321(2):65-78. https://doi.org/10.31643/2022/6445.19

[19] Mamaeva A, Kenzhegulov A, Panichkin A, Alibekov Z, Wieleba W. Effect of Magnetron Sputtering Deposition Conditions on the Mechanical and Tribological Properties of Wear-Resistant Titanium Carbonitride Coatings. Coatings. 2022; 12(2):193. doi:10.3390/coatings12020193

[20] Olteanu C, Munteanu D, Ionescu C, Munteanu A. Tribological characterisation of magnetron sputtered Ti(C, O, N) thin films. International Journal of Materials and Product Technology. 2010; 39:186-194. https://doi.org/10.1504/ijmpt.2010.034270

[21] Azlan MN, Hajer SS, Halimah MK, et al. Comprehensive comparison on optical properties of samarium oxide (micro/nano) particles doped tellurite glass for optoelectronics applications. J Mater Sci: Mater Electron. 2021; 32:14174-14185. https://doi.org/10.1007/s10854-021-05961-z

[22] Zhou R, Ju H, Liu Sh, Zhao Z, Xu J, etc all. The influences of Ag content on the friction and wear properties of TiCN–Ag films. Vacuum. 2022, 110719. https://doi.org/10.1016/j.vacuum.2021.110719

[23] Kenzhegulov A, Mamaeva A, Panichkin A, Alibekov Z, Kshibekova B, Bakhytuly N, Wieleba W. Comparative Study of Tribological and Corrosion Characteristics of TiCN, TiCrCN, and TiZrCN Coatings. Coatings. 2022; 12:564. https://doi.org/10.3390/coatings12050564

[24] Charitidis CA. Nanomechanical and nanotribological properties of carbon-based thin films: a review. International Journal of Refractory Metals and Hard Materials. 2010; 28(1):51-70.

[25] Zeng Y, Qiu Y, Mao X, et al. Superhard TiAlCN coatings prepared by radio frequency magnetron sputtering, Thin Solid Films. 2015; 584:283-288. http://dx.doi.org/10.1016/j.tsf.2015.02.068

[26] Stueber M, Barna PB, Simmonds MC, Albers U, etc all. Constitution and microstructure of magnetron sputtered nanocomposite coatings in the system Ti-Al-N-C. Thin Solid Films. 2005; 493:104-112. doi:10.1016/j.tsf.2005.07.290

[27] Braic M, Balaceanu M, Vladescu A, Zoita CN, Braic V. Study of (Zr,Ti)CN, (Zr,Hf)CN and (Zr,Nb)CN films prepared by reactive magnetron sputtering. Thin Solid Films. 2011; 519:4092-4096. doi:10.1016/j.tsf.2011.01.375

[28] Zhang X, Jianqing J, Zeng Y, et al. Effect of carbon on TiAlCN coatings deposited by reactive magnetron sputtering. Surface & Coatings Technology. 2008; 203:594-597.

[29] Kenzhegulov AK, Mamayeva AA, Panichkin AV. Adhesion properties of calcium phosphate coatings on titanium. Kompleksnoe Ispolzovanie Mineralnogo Syra = Complex Use of Mineral Resources. 2017; 3:35-41.

[30] Kenzhegulov AK. et al. Investigation of the adhesion properties of calcium-phosphate coating to titanium substrate with regards to the parameters of high-frequency magnetron sputtering. Acta Bioeng. Biomech. 2020; 22:111-120.

[31] Mamaeva AA, Kenzhegulov AK, Panichkin AV. A Study of the Influence of Thermal Treatment on Hydroxyapatite Coating. Protection of Metals and Physical Chemistry of Surfaces. 2018; 54(3):448-452.

[32] Mamaeva AA, Kenzhegulov AK, Panichkin AV, Shah A. Obtaining hydroxyapatite coatings by mechanochemical interaction. Kompleksnoe Ispolzovanie Mineralnogo Syra = Complex Use of Mineral Resources. 2020; 314(3)76-83.

[33] Mahdipoor M, Mahboubi F, Ahangarani S, Raoufi M, Elmkhah H. The Influence of Plasma Nitriding Pre-Treatment on Tribological Properties of TiN Coatings Deposited by PACVD. Journal of Materials Engineering and Performance. 2011; 20:1-7. doi: 10.1007/s11665-011-9971-7

[34] Lackner JM, Waldhause W, Ebner R, Keckes J, Schoberl T. Room temperature deposition of (Ti, Al)N and (Ti, Al)(C, N) coatings by pulsed laser deposition for tribological applications, Surface & Coatings Technology. 2004; 177,178:447-452.

[35] Zhang X, Qiu Y, Tan Zh, Lin J, Xu A, Zeng Y, Moore JJ, Jiang J. Effect of Al content on structure and properties of TiAlCN coatings prepared by magnetron sputtering. Journal of Alloys and Compounds. 2014; 617:81-85.

[36] Zheng XH, Tu JP, Gu B, Hu SB. Preparation and tribological behavior of TiN/a-C composite films deposited by DC magnetron sputtering. Wear. 2008; 26:261-265.

[37] Wang Q, Zhou F, Chen K, Wang M, Qian T. Friction and wear properties of TiCN coatings sliding against SiC and steel balls in air and water. Thin Solid Films. 2011; 519:4830-4841.

МАЗМҰНЫ
СОДЕРЖАНИЕ
CONTENTS

ENGINEERING AND TECHNOLOGY

Altynbekova A.D., Lukpanov R.E., Dyussembinov D.S., Askerbekova A.M., Gunasekaran M. EFFECT OF A COMPLEX MODIFIED ADDITIVE BASED ON POST-ALCOHOL BARD ON THE STRENGTH BEHAVIOR OF CONCRETE…….. 5

Mussabekov N., Mukhanov B.K. DEVELOPMENT OF A MATHEMATICAL MODEL FOR A COMPOUND TECHNOLOGICAL COMPLEX OF VANYUKOV MELTING IN ORDER TO CONTROL THE MATERIAL AND THERMAL REGIME……. 22

Andirov M.Y., Assan Zh.Zh., Nopembri S., Seilkhan A.M., Myrzakhmetov D.E. CLASSIFICATION OF TEXTS ON EMERGENCY SITUATIONS IN ALMATY….. 25

Ablakatov I., Ismailov M., Mustafa L.M., Sanin A.F. INVESTIGATION OF THE TECHNOLOGY OF INTRODUCING LI, MG AND ZR ALLOYS INTO ALUMINUM ALLOY…….. 32

Kosparmakova S., Azlan M., Fischer D. A STUDY OF SUPERPAVE DESIGN GYRATIONS FOR HIGH TRAFFIC SURFACE MIXTURES …… 41

EARTH SCIENCES

Tyo S., Zeitinova Sh. OPTIMIZING THE CONTOURS OF OPEN PIT MINING WITH THE USE OF MINING AND GEOLOGICAL INFORMATION SYSTEMS AND TECHNOLOGIES ……. 50

Baisanov A., Vorobkalo N., Makhambetov Y., Mynzhasar Y., Zulhan Z. STUDIES OF THE THERMAL STABILITY OF BRIQUETTES BASED ON MICROSILICA …….. 57

METALLURGY

Toishybek A.M., Baigenzhenov O.S., Turan M.D., Kurbanova B., Merkibayev Y.S. A REVIEW OF RECOVERY TECHNOLOGIES OF RARE AND RARE EARTH METALS FROM WASTES GENERATED IN TITANIUM AND MAGNESIUM PRODUCTION ……. 64

Akylbekov Y., Shevko V.M., Aitkulov D., Karatayeva G. ELECTROTHERMAL PROCESSING OF CHRYSOTILE-ASBESTOS WASTES WITH PRODUCTION OF FERROALLOY AND EXTRACTION OF MAGNESIUM INTO THE GAS PHASE…. 74

Akhmadiyeva N., Abdulvaliyev R.A., Akcil A., Manapova A.I. PRE-ACTIVATION OF NEPHELINE BEFORE THE ENRICHMENT ……. 82

Muradova S., Negim El-Sayed, Makhmetova A., Ainakulova D., Mohamad N.M.I. AN OVERVIEW OF THE CURRENT STATE AND THE ADVANTAGES OF USING ACRYLIC RESINS AS ANTICORROSIVE COATINGS ……... 90

Bakhytuly N., Kenzhegulov A.K., Nurtanto M., Aliev A.E., Kuldeev E.I. MICROSTRUCTURE AND TRIBOLOGICAL STUDY OF TIALCN AND TITACN COATINGS …….. 99

Техникалық редакторлар:
Г.К. Қасымова, Н.М.Айтжанова, Т.И. Қожахметов

Компьютердегі макет:
Г.К. Қасымова

Дизайнер:
Г.К. Қасымова, Н.М.Айтжанова

Металлургия және кен байыту институты; Сәтбаев Университеті
050010, Қазақстан Республикасы, Алматы қаласы, Шевченко к-сі, 29/133

Жариялауға 24.03.2023 жылы қол қойылды

Технические редакторы:
Г.К. Касымова, Н.М. Айтжанова, Т.И. Кожахметов

Верстка на компьютере:
Г.К. Касымова

Дизайнер:
Г.К. Касымова, Н.М.Айтжанова

Институт металлургии и обогащения; Сатпаев Университет
050010, г. Алматы, Республика Казахстан. ул. Шевченко, 29/133

Подписано в печать 24.03.2023г.

Technical editors:
G.K. Kassymova, N.M. Aitzhanova, T.I. Kozhakhmetov

The layout on a computer:
G.K. Kassymova

Designer:
G.K. Kassymova, N.M. Aitzhanova

Institute of Metallurgy and Ore Benficiation; Satbayev University,
050010, Almaty city, the Republic of Kazakhstan. Shevchenko str., 29/133

Signed for publication on 24.03.2023